Defining the critical characteristics of Natural Killer cell memory

Helena Arellano Ballestero

A thesis submitted to University College London for the Degree of Doctor of Philosophy in the Faculty of Medicine

March 2024

To my parents

Statement of Originality

I, Helena Arellano Ballestero, confirm that the work presented in this thesis is my own. Where information has been derived from other sources, I confirm that this has been indicated in the thesis.

Abstract

Natural killer (NK) cells are cytotoxic lymphocytes capable of rapidly eliminating viral- and tumour-transformed cells. Fascinating earlier evidence suggests an intrinsic capacity of natural killer (NK) cells to acquire features of immunological memory in the context of cytomegalovirus (CMV) infection or pro-inflammatory cytokine stimulation (CIML-NK). We and others have identified that priming NK cells with specific cancer cell lines induces tumour-primed NK (TpNK) cells, which are capable of lysing previous resistant cancer cells and acquire features that resemble immunological memory. However, tumour-memory NK cells remain far less studied.

Here, I generated memory-NK cells by cytokine and tumour-priming to find commonalities, and better define the nature of NK cell "memory" *in vitro* and, for the first time, *in vivo*. TpNK cells showed increased cytotoxicity against multiple tumour cell lines *in vitro*, analogous to CIML-NK cells. Multidimensional cytometry identified distinct memory-like profiles of subsets of cells with memory-like characteristics; upregulation of CD57, CD69, CD25 and ICAM1. Proteomic profiling identified 170 proteins restricted to TpNK cells, including proteins involved in mitochondrial survival, which translated into enhanced metabolic function. NK cell homotypic interactions were studied as a potential mechanism of activation, providing preliminary evidence that TpNK cells engage in homotypic interactions with autologous NK cells and potentially activate NK cells in a homotypical manner.

Finally, I provide evidence of the generation of tumour-memory NK cells in patients with myeloid leukaemias both *in vitro* and *in vivo* as part of a clinical trial (NCT05933070). The patients' NK cells present a phenotype akin to the one described in healthy donors previously and display enhanced cytotoxic capacity and persistence over time, all in keeping with the characteristics of tumour-memory NK cells.

To my knowledge, an in-depth characterisation of the effects of tumour-priming in the generation of tumour-memory NK cells has not been done and highlights the importance of further understanding tumour-memory NK cells for their important implications in the context of cancer immunotherapy.

Popular science abstract

Natural killer (NK) cells are a specific cell type of the immune system specialised in killing cancerous cells and cells infected by viruses. They are characterised by their ability to quickly kill target cells. This is because they do not need to go through a learning process like other immune cells; their ability to kill target cells is “innate” to them.

In the context of cancer, the immune system appears dysregulated, as cancerous cells induce changes in their surroundings that confuse immune cells into believing they are unnecessary. Despite that, these changes are reversible, and scientists are constantly developing new techniques and therapies that restore and aid the immune system so that it is effective again in attacking cancer cells. This is called cancer immunotherapy.

The Lowdell lab has been focused on studying the interaction of NK cells with cancer cells. They identified a cancer cell line called INB16 that had specific properties; when INB16 is incubated with NK cells, these NK cells achieve an intermediate state of activation that can be used for immunotherapy. These NK cells are called tumour-primed NK cells (TpNK) and are currently used as an experimental therapy for cancer patients.

In this thesis, I have further characterised TpNK cells by looking at what makes them a good option for immunotherapy. This included looking at changes in their proteins, as well as different experiments to test how they perform their functions. I identified that these cells have indeed multiple benefits, which provide them with an advantage in killing cancer cells. Furthermore, in this thesis, we have also tested TpNK cells in a clinical trial in patients with blood cancers and have shown that this treatment is safe and can be beneficial to some patients.

Ultimately, understanding more about TpNK cells and how we can use them to our advantage will help us develop better therapies for cancer patients.

Impact statement

Immunological memory has been extensively studied in various types of NK cells, yet the characteristics of tumour-memory NK cells remain largely undefined. This thesis presents valuable insights into the generation of tumour-primed NK cells with features of immunological memory.

This work highlights similarities and differences between tumour- and cytokine-memory NK cells, providing important understanding into defining commonalities in NK cell memory. This comparison is novel and contributes to the understanding of the basic biology of the innate immune system.

The culmination of this research is the successful generation of tumour-memory NK cells in patients with myeloid leukaemias in a clinical trial. The evidence indicates that this approach is safe and well-tolerated, setting the precedent for future clinical trials with similar protocols.

The findings of this research have important implications for both basic and translational research, offering significant revelations into the biology of tumour-memory NK cells.

Acknowledgements

I would like to express my most heartfelt gratitude to Professor Mark Lowdell for giving me the opportunity to pursue a PhD and for your supervision in the past years. I have truly enjoyed our NK cell discussions and seeing science through your eyes.

Thank you to Dr. Dimitra Peppa for your supervision and for welcoming me into your lab. I am grateful for all the opportunities you granted me and for your guidance and support.

Thank you to the Royal Free Charity and InmuneBio Inc. for the scholarship which made this work possible.

Thank you to May Sabry for your mentorship and guidance both in and outside the lab. I am grateful for your friendship and for the faith you showed in me.

Thank you to Aga Zubiak for your endless patience and support. Your guidance in the lab has been key in this work. I am grateful for our conversations and for your friendship. I owe you so much.

Thank you to my thesis committee, Dr. Beth Payne and Dr. Sergio Quezada, for your valuable advice and guidance during my PhD.

Thank you to all the blood donors and patients for their generous blood donations, without whom no science would be possible.

Thank you to everyone at the CCGTT and Room 1/458 for creating such a nice work environment. Thank you to Maria Rodriguez-Giraldez for your friendship throughout the years and your endless support. Thank you to Xenia Charalambous and Shaun Haran, you made the time in the lab much more enjoyable. Thank you to Melina Michael for your help, guidance and friendship. Thank you to the guys at INmuneBio, Jorge Salazar, Nikita Patel, Segun Abiola, Ella Kline, Margarida Faria, Ben Hammond and Ben Weil, for always being there whenever I needed. Thank you to Francesca Semplici for your endless help throughout the years. Thank you to the rest of the staff at the CCGTT, present and past members: Owen Bain, Janet North, Carla Carvalho, Toby Proctor, Fahim Ghourbandi, Sufia Khatun, Sian Smalley, Matt Wright,

Kenny Moya, the Pule team… For being so nice and for your help when I needed it, I truly appreciate it.

Thank you to the members of the Peppa team, Jonida Kokici, Aljawharah Alrubayyi, Kelly Da Costa, Neha Khawaja and Eddy Arbe-Barnes, for your endless help and for being such a lovely bunch.

Thank you to Sam Jide-Banwo for your help with phlebotomy and running coaching. To Claire Beesley for our lunch breaks and coffee walks around the Heath. Thank you to Catherine Zhu for your help collecting the MDS samples.

To my friends from Begues: Nuria Benaiges, Georgina Boixereu, Anna Escala, Julia Huerta, Sara Lujan, Carlota Morales and Carlos Moreno. Thank you for always being there for me despite the distance. To Clara Domingo, for your friendship and for the time spent in London, which I hold dear to my heart. To Ariadna Chueca, for your friendship and for always being there for me no matter what. To Marcel Buen, no matter how long it has been, we keep making time for each other. To Zuzanna Wilk for always being there for me and making London a better place.

To Johannes Wiebe, no words can describe how much I owe you. Thank you for your endless support during this journey, you have truly always been there for me. Thank you for your generosity and good heart. Thank you for making me a better person.

Finally, I am grateful to my family. To my grandparents, for their love and support: Daniel Ballestero, Josefina Belio, Pere Arellano, and my late grandmother Barbara Ortiz. To my brothers Jordi and Marc Arellano, for being my favourite people in the world and for always making me laugh. I am so lucky to have you. To my parents, Maria Jose Ballestero and Jordi Arellano, for the support you have shown throughout all chapters of my life. Thank you for providing me with countless opportunities, without which I would not be here today. Thank you for teaching me your work ethic and for always reminding me that being a good person is what I should strive for, beyond any academic or professional achievements. This thesis is for you.

List of scientific papers

Scientific papers included in this thesis

Arellano-Ballestero H, Zubiak A, Dally C, Orchard K, Michael M, Charalambous X, et al. (2023) Proteomic and phenotypic characteristics of memory-like Natural Killer cells for cancer immunotherapy. Journal for Immunotherapy of Cancer. Manuscript under revision.

Arellano-Ballestero H, Sabry M, Lowdell MW. A Killer Disarmed: Natural Killer Cell Impairment in Myelodysplastic Syndrome. *Cells*. 2023; 12(4):633. https://doi.org/10.3390/cells12040633

Scientific papers not included in this thesis

Sabry M, Zubiak A, Hood SP, Simmonds P, **Arellano-Ballestero H**, Cournoyer E, et al. (2019) Tumor- and cytokine-primed human natural killer cells exhibit distinct phenotypic and transcriptional signatures. PLoS ONE 14(6): e0218674. https://doi.org/10.1371/journal.pone.0218674

UCL Research Paper Declaration Form (1)

referencing the doctoral candidate's own published work(s)

For a research manuscript that has already been published

a) **What is the title of the manuscript?** A Killer Disarmed: Natural Killer Cell Impairment in Myelodysplastic Syndrome
b) **Please include a link to or doi for the work** 10.3390/cells12040633
c) **Where was the work published?** Cells
d) **Who published the work?** MDPI
e) **When was the work published?** 2023
f) **List the manuscript's authors in the order they appear on the publication** Helena Arellano-Ballestero, May Sabry, Mark W. Lowdell
g) **Was the work peer reviewed?** Yes
h) **Have you retained the copyright?** No
i) **Was an earlier form of the manuscript uploaded to a preprint server?** No

   If 'No', please seek permission from the relevant publisher and check the box next to the below statement:

   ☒

   *I acknowledge permission of the publisher named under **d** to include in this thesis portions of the publication named as included in **c**.*

For multi-authored work, please give a statement of contribution covering all authors. H.A.B. and M.S.—writing and original draft preparation; M.W.L.—writing, review and editing.

In which chapter(s) of your thesis can this material be found? Chapter 1, chapters 3-7

e-Signatures confirming that the information above is accurate

Candidate: Helena Arellano Ballestero *Date:* 05/02/2024

Supervisor/Senior Author: Professor Mark Lowdell *Date:* 05/Feb/2024

UCL Research Paper Declaration Form (2)

referencing the doctoral candidate's own published work(s)

For a research manuscript prepared for publication but that has not yet been published

a) **What is the current title of the manuscript?** Proteomic and phenotypic characteristics of memory-like Natural Killer cells for cancer immunotherapy
b) **Has the manuscript been uploaded to a preprint server?** No
c) **Where is the work intended to be published?** Journal for Immunotherapy of Cancer
d) **List the manuscript's authors in the intended authorship order.** Helena Arellano-Ballestero, Agnieszka Zubiak, Chris Dally, Kim Orchard, Melina Michael, Xenia Charalambous, Aljawharah Alrubayyi, Robert Torrance, Trinity Eales, Kushal Das, Maxine G. B. Tran, May Sabry, Dimitra Peppa and Mark W. Lowdell
e) **Stage of publication** Manuscript under revision

For multi-authored work, please give a statement of contribution covering all authors. Conceptualization: MWL, MS, DP; Methodology: MWL, DP, HAB; Investigation: HAB, AZ, MM, XB, AA, RT, TE, KD; Clinical aspects: CD, KO, MT; Funding acquisition: MWL; Project administration: MWL, MS; Supervision: MWL, MS, DP; Writing – original draft: MWL, HAB, MS; Writing – review & editing: MWL, HAB, DP.

In which chapter(s) of your thesis can this material be found? Chapter 1, chapter 3-7

e-Signatures confirming that the information above is accurate

Candidate: Helena Arellano Ballestero *Date:* 05/02/2024

Supervisor/Senior Author: Professor Mark Lowdell *Date:* 05/Feb/2024

Table of contents

List of figures

List of tables

Abbreviations

2-DG – 2-deoxy-glucose

AA – antimycin A

ADCC – antibody-depended cell cytotoxicity

aKIR – activating KIR

ALL – acute lymphoblastic leukaemia

AML – acute myeloid leukaemia

AUC – area under the curve

BiKE – bispecific killer cell engager

CB – coord blood

CIML – cytokine-induced memory-like

CMV – cytomegalovirus

CLP – common lymphoid progenitor

CR – complete remission

DC – dendritic cell

DMSO – dimethyl sulfoxide

ECAR – extracellular acidification rate

ETC – electron transport chain

FasL – Fas ligand

FBS – foetal bovine serum

FCCP – carbonyl cyanide-4 (trifluoromethoxy) phenylhydrazone

FDA – Food and Drug Administration

FSC – forward scatter

Gal – Galectin

GM-CSF – granulocyte/ monocyte colony-stimulating factor

GO – gene ontology

GVHD – graft-versus-host disease

hCMV – human cytomegalovirus

mCMV – murine cytomegalovirus

hESC – human embryonic stem cells

HD- healthy donor

HLA – Human Leukocyte Antigen

HSC – haematopoietic stem cell

HSCP – hematopoietic stem and progenitor cells

HSCT – haematopoietic stem cell transplant

IFNγ – interferon-γ

Ig – immunoglobulin

IL – interleukin

IL2-R – IL2 receptor

ILCs – innate lymphoid cells

iKIR – inhibitory KIR

iPSC – induced-pluripotent stem cell

IPSS – International Prognostic Scoring System

IPSS-M – molecular IPSS

IPSS-R – revised IPSS

KIR – Killer cell Immunoglobulin-like Receptors

KO - knockout

LAK – lymphokine-activated killer cell

LMPP – lymphoid-primed multipotential progenitors

MCMV – murine cytomegalovirus

MDS – myelodysplastic syndrome

MDSC – myeloid-derived suppressor cell

MeFI – median fluorescence intensity

MHC – major histocompatibility complex

MPN – myeloproliferative neoplasm

MSC – mesenchymal stromal cell

MTOC – microtubule organizing centre

NCAM – neural cell adhesion molecule

NCR – Natural Cytotoxicity Receptor

NK – Natural Killer

NKP – NK cell progenitor

NS – non-significant

OCR – oxygen consumption rate

Oxphos – oxidative phosphorylation

PBMC – peripheral blood mononuclear cell

PBS – phosphate buffer saline

PR – partial remission

scRNA-seq – single-cell RNA sequencing

SD – standard deviation

SSC – side scatter

TIML – tumour-induced memory-like

TME – tumour microenvironment

TMRM – tetramethylrhodamine methyl ester

TNF – tumour necrosis factor

TRAIL – Tumour necrosis factor–related apoptosis-inducing ligand

Treg – T regulatory cell

TriKE – trispecific killer cell engager

trNK cell – tissue resident NK cell

TpNK – tumour-primed NK cell

tSNE – t-Distributed Stochastic Neighbour Embedding

rNK – resting NK cell

ROS – reactive oxygen species

Rot – rotetone

RT – room temperature

VEGF – vascular endothelial growth factor

viSNE – visual interactive Stochastic Neighbour Embedding

WT – wild type

Chapter 1 Introduction

1.1 Basic Biology and Functions of Natural Killer Cells

Natural Killer (NK) cells were first identified in the 1970s and were characterized by the presence of large granules in the cytoplasm and their ability to “spontaneously” lyse tumour cells (Herberman, Nunn, & Lavrin, 1975; Herberman, Nunn, Holden, et al., 1975; Kiessling, Klein, & Wigzell, 1975; Kiessling, Klein, Pross, et al., 1975). They belong to the family of group 1 innate lymphoid cells (ILCs) and, in humans, form between 5 to 15% of the total population of circulating lymphocytes, where they display a critical role in infection, autoimmunity, transplantation, reproduction and tumour immune surveillance (Spits et al., 2013). Once activated, NK cells exhibit direct cytotoxicity against stressed cells and secrete cytokines like tumour necrosis factor α (TNFα) and interferon γ (IFNγ) to modulate the functions of other immune cells (Fauriat et al., 2010). NK cells share many characteristics with T cells, including a common lymphocyte progenitor and their ability to mount robust cytotoxic responses and cytokine secretion. Still, they remain distinct in their ability to kill target cells without prior sensitization or major histocompatibility complex (MHC) restriction (Narni-Mancinelli et al., 2011; J. C. Sun & Lanier, 2011).

The importance of NK cells is illustrated by studies showing that the impairment of these cells results in increased viral infections (Biron et al., 1989; Eidenschenk et al., 2006), where complete NK cell deficiencies in humans result in fatal infections during childhood (Orange, 2006). Impairment of NK cells also increases susceptibility to developing tumours (Waldhauer & Steinle, 2008), where individuals with less cytotoxic NK cells have an increased risk of developing cancer (K. Imai et al., 2000).

1.1.1 NK cell subsets and development

Human NK cells are defined phenotypically by their expression of the neural cell adhesion molecule (NCAM) CD56 and the lack of expression of the T cell receptor CD3. According to the surface cell density of CD56, NK cells can be

sub-categorised into $CD56^{dim}$ and $CD56^{bright}$, which have different characteristics and display different functions.

$CD56^{dim}$ NK cells are the more mature subset and comprise approximately 90% of circulating NK cells (Cooper et al., 2001). These cells express lower levels of CD56 and the low-affinity IgG receptor CD16 and express high levels of perforin and granzymes, making them primarily responsible for cytotoxicity. They are highly efficient at forming conjugates with target cells and can induce both direct cytotoxicity and antibody-dependent cell cytotoxicity (ADCC) (Cooper et al., 2001). However, they have less ability to produce immunoregulatory cytokines (Cooper et al., 2001; Jacobs et al., 2001).

$CD56^{bright}$ NK cells account for 10% of peripheral blood NK cells and are more immature than $CD56^{dim}$ NK cells. $CD56^{bright}$ NK cells express high levels of CD56 and little to no expression of CD16. They lack perforin and display reduced cytotoxicity upon contact with target cells; instead, $CD56^{bright}$ NK cells are the predominant source of immunoregulatory cytokines like TNFα and IFNγ (Cooper et al., 2001).

Despite this classification, it is well known that NK cells are a very heterogeneous cell type (C. Yang et al., 2019), which include subsets of tissue resident NK cells (trNK). These are NK cells found in the liver, lungs, spleen and uterus among other organs, that have unique tissue-specific markers and are lineage distinct, requiring different transcription factors for their differentiation (Hashemi & Malarkannan, 2020). While both conventional NK cells and trNK cells share similar effector functions, studies indicate that trNK cells are more specialised depending on the tissue where they reside (Hashemi & Malarkannan, 2020). For example, uterine trNK cells have a role in placental vascular remodelling, foetal growth and memory of pregnancy (Lash et al., 2006; Matson & Caron, 2014). In the liver, their importance is highlighted by the fact that liver trNK cells represent up to 30–50% of all hepatic lymphocytes in contrast to 5–16% in PBMC (Racanelli & Rehermann, 2006). Functionally, it appears that liver NK cells are non-cytotoxic but produce high levels of pro-inflammatory cytokines, suggesting they have different functional characteristics and might contribute to liver inflammation and

fibrosis (Martrus et al., 2017). While more studies are looking into trNK cells, they remain far less studied than peripheral blood NK cells.

1.1.1.1 Stages of development

Initially thought to originate only in the bone marrow, it is now known that NK cells can also develop from common lymphoid progenitors and mature in secondary lymphoid tissues like the tonsils, spleen, and lymph nodes (Scoville et al., 2017).

Freud and Caliguiri described a stepwise model for the development and maturation of human NK cells, based on the expression of CD34, CD117, CD94 and CD16 (Freud & Caligiuri, 2006). However, this model could not explain the exclusive identity of progenitors committed only to NK cell development.

The different stages of NK cell development are summarised in Figure 1.1. Haematopoietic stem cells (HSCs) that are $Lin^{-}CD34^{+}CD133^{+}CD244^{+}$ give rise to the lymphoid-primed multipotential progenitors (LMPP); LMPP retain CD34 expression and express CD45RA and CD10. The next stage gives rise to the common lymphoid progenitor (CLP), important markers in this stage are CD10 and CD7 (Sathe et al., 2017). Next, these cells lose CD34 expression and acquire LFA1, which will give rise to the NK cell progenitor (NKP). Another important marker in the distinction between CLPs and NKPs is CD127 (Renoux et al., 2015). NKPs express CD122, which is the IL2/15 receptor β chain, allowing the NK cells to become responsive to IL15 which will enhance their development, maturation and function (Cichocki et al., 2019). The acquisition of CD94 characterises the next stage, representing the $CD56^{bright}$ NK cell subset. Finally, the loss of CD94 and the acquisition of CD16 and KIR gives rise to the $CD56^{dim}$ NK cell subset (Briercheck et al., 2009; Cichocki et al., 2019).

The $CD56^{dim}$ subset of NK cells is a very heterogeneous mix of different populations based on the expression of several markers, such as Killer cell Immunoglobulin-like Receptors (KIR), CD94, NKG2A, CD62L, and CD57, which indicate the maturation status of NK cells. Mature NK cells will

downregulate NKG2A and CD62L and express KIR and CD57 (Björkström et al., 2010; Lopez-Vergès et al., 2010).

There is an ongoing debate on whether the linear model of NK cell development is accurate, as it is unlikely to explain the vast heterogeneity found in NK cells. Horowitz and colleagues have estimated that there are between 6,000 and 30,000 distinct phenotypic populations within an individual (Horowitz et al., 2013), which raises questions about the origin of these populations, but no studies have been conducted so far.

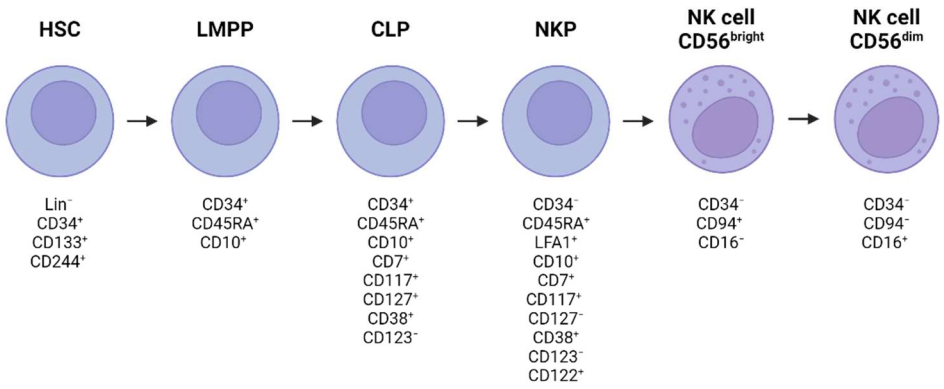

Figure 1.1. Stages of NK cell development

NK cells exhibit different maturational stages with distinct NK cell populations. HSC, haematopoietic stem cells; LMPP, lymphoid-primed multipotential progenitors; CLP, common lymphoid progenitor; NKP, NK cell progenitor. Created with Biorender.

1.1.2 NK cell recognition

NK cells were discovered in the mid-70s, but the mechanisms by which they exerted cytotoxicity remained unknown for a long time. The first studies regarding NK cell cytotoxicity came in the late 80s from Karre and Ljunggren, when they observed that murine NK cells could kill targets with reduced or absent MHC class I molecules and thus proposed the “missing-self” hypothesis (Kärre et al., 1986; Ljunggren & Kärre, 1990). The search for the intricacies of this mechanism led to the discovery of inhibitory KIRs, which supported their hypothesis (Colonna & Samaridis, 1995; D’Andrea et al., 1995; Karlhofer et al., 1992; Wagtmann et al., 1995).

With more advances in the NK cell field, studies showed that the absence of MHC class I was insufficient to trigger NK cell cytotoxicity (Costello et al., 2002; Ruggeri et al., 2002); this was at a time when many NK cell activating receptors were discovered and led to the formulation of the “dynamic equilibrium” hypothesis, which explains that the balance of activating and inhibitory receptors is what determines the final outcome (Brumbaugh et al., 1998).

When the minimal requirements for NK cell cytotoxicity are met, lysis can occur irrespective of strong inhibitory signals (Bryceson et al., 2006; North et al., 2007). It is well established that pre-activating NK cells with a cytokine such as interleukin (IL) IL2 results in the generation of lymphokine-activated killer cells (LAKs) that can exert cytotoxicity against previously resistant target tumours (Frederick et al., 1997; Hoskin et al., 1989; Storkus et al., 1989). Thus, if the NK cell meets the right combination of activating stimuli, it can exert cytotoxicity even in the presence of inhibitory signalling.

NK cell receptors, including activating, maturation/differentiation, homing, and inhibitory receptors, as well as their ligands, are summarised below (Figure 1.2).

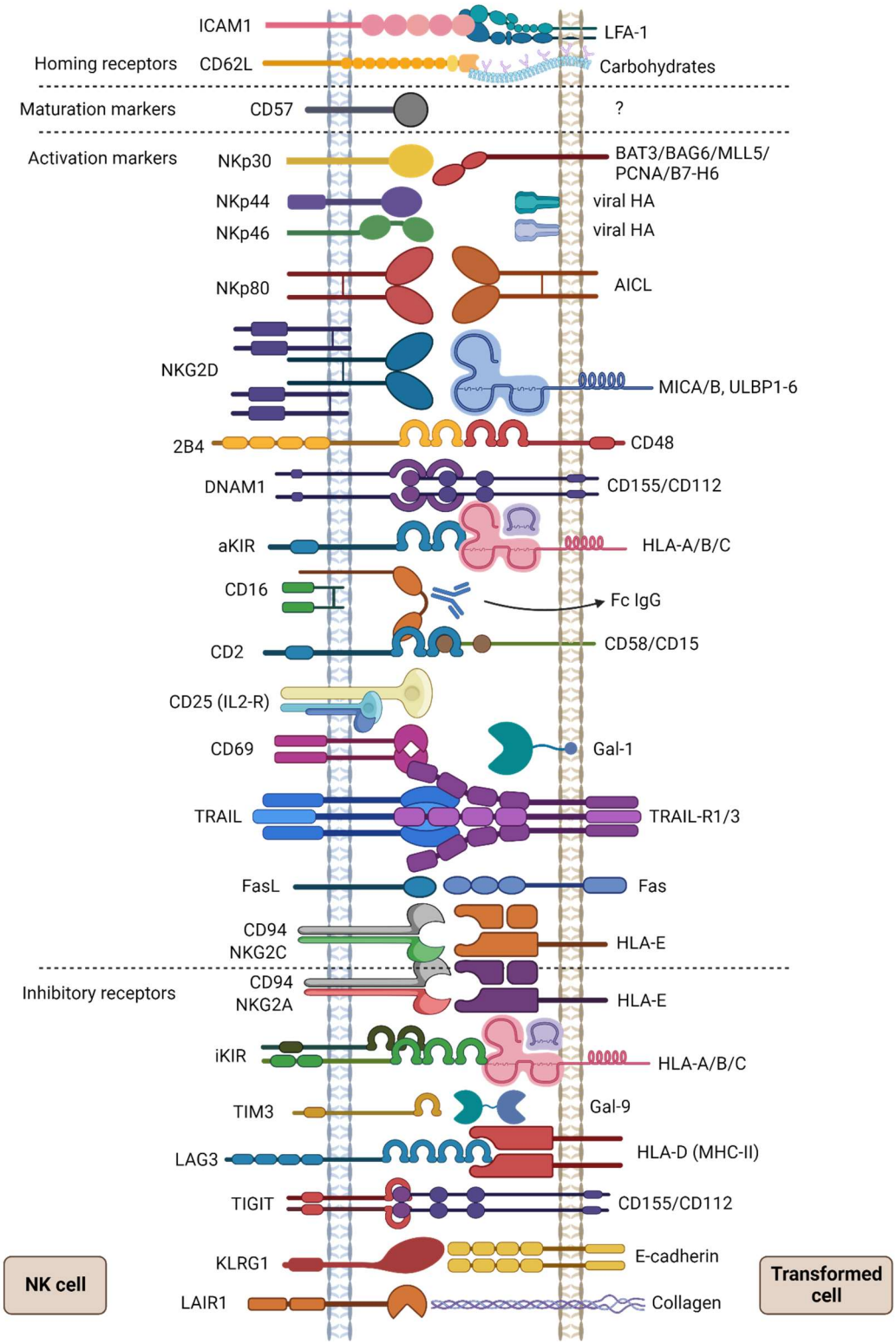

Figure 1.2. NK cell receptors and their ligands

NK cell receptors are represented on the left hand side; the right hand side represents a transformed cell expressing NK cell ligands. Created with Biorender.

1.1.2.1 Activating receptors

The Natural cytotoxicity receptors (NCRs) are amongst the major activating NK cell receptors and comprise NKp46, NKp44 and NKp30. NKp46 and NKp30 are expressed in resting NK (rNK) cells and are upregulated in activated NK cells; NKp44 is only expressed constitutively in $CD56^{bright}$ NK cells and is upregulated in all NK cells when activated. Various ligands interact with the NCRs; some are virus-derived and interact with viral-infected cells like the influenza virus-derived HA recognized by NKp46 or NKp44. Others like BAT3/BAG6, MLL5, and PCNA are expressed in cells in response to stress or during tumour transformation (Sivori et al., 2019). B7-H6 is another NKp30 ligand expressed on the surface of tumour cells (Brandt et al., 2009).

Another important activating receptor on NK cells is NKG2D, a type II transmembrane and C-type lectin-like receptor expressed constitutively on NK cells; its ligands are ULBP1-6 and MICA/B, which are Human Leukocyte Antigen (HLA) class I structural homologs that are upregulated in infected, stressed, and cancer cells (Bauer et al., 1999).

NKG2C is an HLA-specific activating receptor that forms a heterodimer with CD94 and binds to HLA-E with low affinity (Valés-Gómez et al., 1999). CD94/NKG2C is involved in the response to human cytomegalovirus (HCMV) and is highly expressed in these individuals (Gumá et al., 2006; Lopez-Vergès et al., 2011a).

CD69 is a membrane-bound, type II C-lectin receptor; it is a classical early marker of lymphocyte activation and is rapidly induced in NK cells shortly after activation (Borrego et al., 1999). The ligand for CD69 was unknown for a long time, but is now known to interact with Galectin (Gal)-1 (de la Fuente et al., 2014); Gal-1 is a carbohydrate-binding protein expressed in dendritic cells and macrophages.

Other NK cell activation markers include the IL2Rα chain or CD25, which, together with the IL2/15Rβ-chain (CD122) and the common γ-chain (CD132), form the high-affinity IL2 receptor. This increases the affinity for IL2, which

drives proliferation and enhanced cytotoxicity (Caligiuri et al., 1990, 1993; S.-H. Lee et al., 2012; Minami et al., 1993).

Other molecules, including 2B4 (Sivori et al., 2000), DNAM-1 (Shibuya et al., 1996), NKp80 (Vitale et al., 2001), and CD2 (Selvaraj et al., 1987), act as co-stimulatory molecules amplifying the NK cell triggering induced by NCRs or NKG2D.

The Fcγ receptor CD16, is the only receptor that can mediate direct cytotoxicity without the need for other molecules (Bryceson et al., 2006). It recognises the Fc portion of Immunoglobulin (Ig) G-coated target cells and induces ADCC (Ochoa et al., 2017). High expression of CD16 is also a marker for NK cell terminal differentiation and is restricted to $CD56^{dim}$ KIR^{+} NK cells.

The NK cell death receptors include Tumour necrosis factor–related apoptosis-inducing ligand (TRAIL) and its receptors TRAIL-R1/2/3 (Falschlehner et al., 2009; Wiley et al., 1995); and Fas ligand (FasL) in the NK cell and its receptor Fas in the target cell (Ashkenazi & Dixit, 1998). Ligation via death cell receptors induces caspase-mediated apoptosis in the target cell.

1.1.2.2 Inhibitory receptors

Inhibitory KIRs (iKIR) are HLA class I-specific inhibitory receptors with type I transmembrane receptors specific for polymorphic HLA-A, B and C molecules (Moretta et al., 1996). To transduce the inhibitory signals, they contain ITIM motifs in their cytoplasmatic tails (Moretta et al., 1996). Activating KIRs (aKIR) have also been described, but there is limited knowledge about them (Moretta et al., 1995). Inhibitory KIRs contain long cytoplasmic tails, whereas activating KIRs have short cytoplasmic tails (“L” or “S” in the nomenclature, respectively).

Another HLA-class I-specific inhibitory receptor is NKG2A, which heterodimerises with CD94. NKG2A is a type II transmembrane receptor that recognizes HLA-E, a non-classical HLA molecule. Like KIR molecules, it contains ITIM motifs in its cytoplasmic tail to transduce inhibitory signals (Braud et al., 1998; Moretta et al., 1996).

Besides the HLA class I specific inhibitory receptors, NK cells contain various other inhibitory receptors. Some of those are absent in healthy cells but can

be induced in the context of disease to facilitate immune escape. These include receptors like TIM3 (Golden-Mason et al., 2013), TIGIT (X.-M. Zhou et al., 2018), LAG3 (Miyazaki et al., 1996), KLRG1 (Huntington et al., 2007), and LAIR1 (Meyaard et al., 1997).

1.1.2.3 Homing receptors

The regulation of NK cell trafficking throughout the body relies on a complex interplay of chemokines, chemokine receptors, and adhesion molecules. Among these adhesion molecules, ICAM1 is a key facilitator of leukocyte migration by binding to LFA1 (Barber et al., 2004; Chong et al., 1994; Wee et al., 2009). CD62L is another important receptor belonging to the adhesion molecule family, which enables lymphocyte trafficking in and out of the bloodstream by promoting rolling and adhesion to the blood vessel wall (Bevilacqua, 1993).

1.1.2.4 Maturation/differentiation markers

The significance of the CD57 expression on NK cells remained elusive for a long time. In CD8+ T cells, CD57 was regarded as both a marker of terminal differentiation and a marker of senescence (Kern et al., 1996), which is why its role in NK cells remained unclear. Nowadays, it has been well established that CD57 is a marker of terminally differentiated NK cells. Studies have shown that $CD57^{+}$ NK cells have a receptor repertoire that suggests maturation; these NK cells are $CD56^{dim}$, KIR^{+} and $CD16^{+}$. Furthermore, $CD57^{+}$ NK cells proliferate less and have an enhanced capacity to secrete IFNγ and induce lytic potential, all in keeping with a phenotype of terminal differentiation (Björkström et al., 2010; Lopez-Vergès et al., 2010). This is further supported by observations that 30-60% of $CD56^{dim}$ $CD16^{bright}$ NK cells express CD57, which is not observed in immature $CD56^{birght}$ NK cells (Lanier et al., 1983; Nagler et al., 1989). Furthermore, foetal and newborn NK cells do not express CD57 (Abo et al., 1984), and CD57 expression in NK cells increases with age (J. Merino et al., 1998; Tilden et al., 1986).

1.1.3 NK cell cytotoxicity

NK cells can lyse cancerous or virus-transformed cells by recognising different ligands on the surface of these cells. Once the NK cell has committed to eliminate a viral infected or transformed cell, there are three main mechanisms to induce cell death: the release of cytotoxic granules containing perforin and granzymes; the induction of death receptor-mediated apoptosis by expressing TRAIL or FasL and via ADCC. In addition, NK cells will secrete an array of cytokines like TNFα and IFNγ that will modulate other immune cell responses (Figure 1.3).

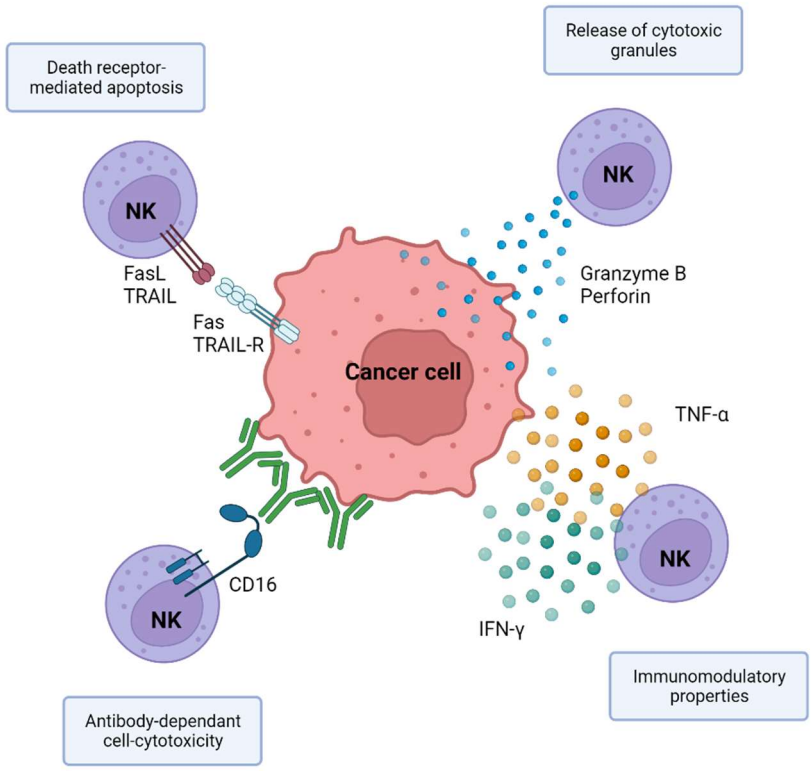

Figure 1.3. NK cell cytotoxicity

NK cells can exert direct cytotoxicity against target cells through the release of cytotoxic granules like perforin and granzyme B, through the engagement of death-cell receptors in the surface of cancer cells, and via antibody-dependent cell cytotoxicity through the recognition of the Fc portion of IgG with CD16. NK cells can also exert indirect cytotoxicity via the release of TNFα and IFNγ, which will have anti-tumour functions and modulate other immune responses. Created with Biorender.

1.1.3.1 Direct cytotoxicity

1.1.3.1.1 Release of cytotoxic granules

NK cells exert their cytotoxic effect mainly through the targeted release of lytic granules containing granzymes and perforin, which are synthesized under tight regulation. Granzyme B has been the most extensively studied in relation to NK cells, despite the existence of other granzymes. Granzyme B is a serine protease whose substrates are caspase-3 and caspase-7 in the target cell, inducing caspase-dependent cell death; they can also kill by cleavage of Bid, which relocates to the mitochondria and cause a series of events that lead to cell apoptosis (Fischer et al., 2003; Krzewski & Coligan, 2012; Salcedo et al., 1993; Sutton et al., 2000).

NK cells follow different steps to recognise the target, where the formation of the immunological synapse is considered the main event, culminating with the secretion of preformed lytic granules. This requires the coordination of different elements, including cytoskeleton reorganisation (Mace et al., 2014). A crucial step is the ligation of LFA1 on the NK cell, leading to F-actin reorganisation (Mace et al., 2009, 2010). The next step begins with the preformed lytic granules moving along microtubules and converging in the microtubule organizing centre (MTOC) (Mentlik et al., 2010). At the synapse, perforin monomers will aggregate and form pores in the membrane, allowing granzyme B to travel inside the cell and trigger apoptosis (Leung et al., 2017; Lopez et al., 2013). As an alternative mechanism, it has been proposed that granzymes are taken up by the target cell via endocytosis, which is facilitated by the binding of granzyme B to the mannose 6-phosphate receptor. Once inside the target cell, perforin facilitates the breakage of the endocytic vesicle so that granzyme B can be released (Froelich et al., 1996; Thiery et al., 2011).

1.1.3.1.2 Death receptor-mediated apoptosis

NK cells can also induce death via the expression of FasL or TRAIL on their surface. FasL (CD95L) is a transmembrane protein which, upon expression, links to Fas (CD95) on the target cell and thus activate the apoptotic cascade. FasL is stored in secretory granules distinct from the ones containing perforin

and granzymes, and its expression relies on NK cell degranulation (Bossi & Griffiths, 1999; Peter & Krammer, 2003). TRAIL is also a transmembrane protein, which binds to different TRAIL receptors; TRAIL-R1 and TRAIL-R2 induce apoptosis on the target cell, TRAIL-R3, TRAIL-R4, and osteoprotegerin induce NF-κB signalling (von Karstedt et al., 2017). However, how TRAIL is stored in NK cells or under what conditions it is induced onto the NK cell surface is unknown. It is also unknown how a target cell can induce surface expression of TRAIL in the synapse.

1.1.3.1.3 Antibody-dependant cell-cytotoxicity

ADCC is a granule-mediated form of NK cell killing. Its ability to function without requiring multiple receptor/ligand interactions between the NK and target cells sets it apart. Rather, it depends on recognising the Fc portion of an IgG on a coated target cell. This is achieved via the Fc receptor expressed by NK cells (FcγRIII or CD16) binding to the Fc portion of the antibody, which will precede the release of perforin and granzyme by the NK cell (Romee et al., 2013).

1.1.3.2 Immunomodulatory properties of NK cells

NK cells are potent producers of pro-inflammatory and immunosuppressive cytokines, which modulate various other immune responses. Although they can produce a wide range of cytokines, they primarily secrete Th1-type cytokines, which include IFNγ, TNFα and granulocyte/ monocyte colony-stimulating factor (GM-CSF). NK cells also produce chemotactic cytokines called chemokines, including CCL3 (MIP-1α), CCL4 (MIP-1β), CCL5 (RANTES), and CXCL8 (IL8), which attract effector cells to inflamed tissues. These secreted cytokines will have anti-tumour and anti-viral functions but will also modulate other immune cells like neutrophils, T cells, B cells, and monocytes (Abel et al., 2018; Cichicki et al., 2016; van den Bosch et al., 1995).

1.2 Natural Killer Cell Priming

Although it was once believed that resting NK cells were capable of "spontaneous" lysis of tumour cells, it is now known that NK cells need to be primed to exert cytotoxicity fully, which can be achieved through various mechanisms (Figure 1.4).

Pro-inflammatory cytokines remain among the most used mechanisms to prime NK cells *ex vivo*. This is achieved by exposure to cytokines like IL2 or IL15, generating LAK cells which exhibit enhanced killing of tumour target cells or the secretion of pro-inflammatory cytokines (Bryceson et al., 2006; Ferrini et al., 1987; Rosenberg et al., 1987).

Alternatively, we and others have shown that NK cells can be primed by interacting with certain tumour cells; the Lowdell group described that when an NK cell that comes into contact with the acute lymphoblastic leukaemia (ALL) cell line CTV-1 or its cloned daughter cell line INB16, this generates tumour-primed NK cells (TpNK) that are capable of killing NK-resistant tumour cell lines, primary leukaemias and solid tumours, in HLA-matched, allogeneic or autologous settings (North et al., 2007). The priming cell presents an appropriate ligand combination to prime the NK cells without triggering its cytotoxicity. A critical receptor/ligand combination identified for tumour-mediated NK cell priming is via CD2 binding on the NK cell to CD15 on INB16 (North et al., 2007; Sabry et al., 2011). In this interaction, CD16 is shed, leading to the release of CD3ζ. Subsequently, CD3ζ binds to the intracellular domain of CD2 in the NK cells, forming a complex with CD15 in INB16. This interaction results in the phosphorylation of CD3ζ, LAT, and STAT5, ultimately reducing the threshold signalling required for NK cells to exert cytotoxicity (Sabry et al., 2011). Others have also determined how NK cells can be activated by cancer cell lines. Dufva and colleagues uncovered distinct NK cell activation patterns and molecular phenotypes on NK cells primed with cell lines from haematological cancers, ranging from more sensitive myeloid to less sensitive B-lymphoid cancers (Dufva et al., 2023).

NK cells can also be primed by interacting with other cells from the immune system cells, mainly DCs. DCs trans-present cytokines like IL15 or IL2 to NK cells to activate them, in turn inducing DCs maturation (Moretta, 2002).

NK cell priming has also been described in the context of NK-to-NK cell homotypic interactions. NK cells have been seen to trans-present IL2 to neighbouring NK cells in a homotypical manner to ensure IL2 availability in a challenging tumour microenvironment (TME) (M. Kim et al., 2017; T.-J. Kim et al., 2014), but these interactions have been very ill-defined. Our group has provided some evidence where, in the context of tumour-priming, patients with acute myeloid leukaemia (AML) who received allogeneic tumour-primed NK cells displayed primed autologous NK cells after treatment, which could only be explained by the donor NK cells priming the patient's NK cells (Fehniger et al., 2018; Kottaridis et al., 2015). In this thesis, I further explore this phenomenon by providing evidence of NK-NK homotypic interactions in the context of tumour-priming.

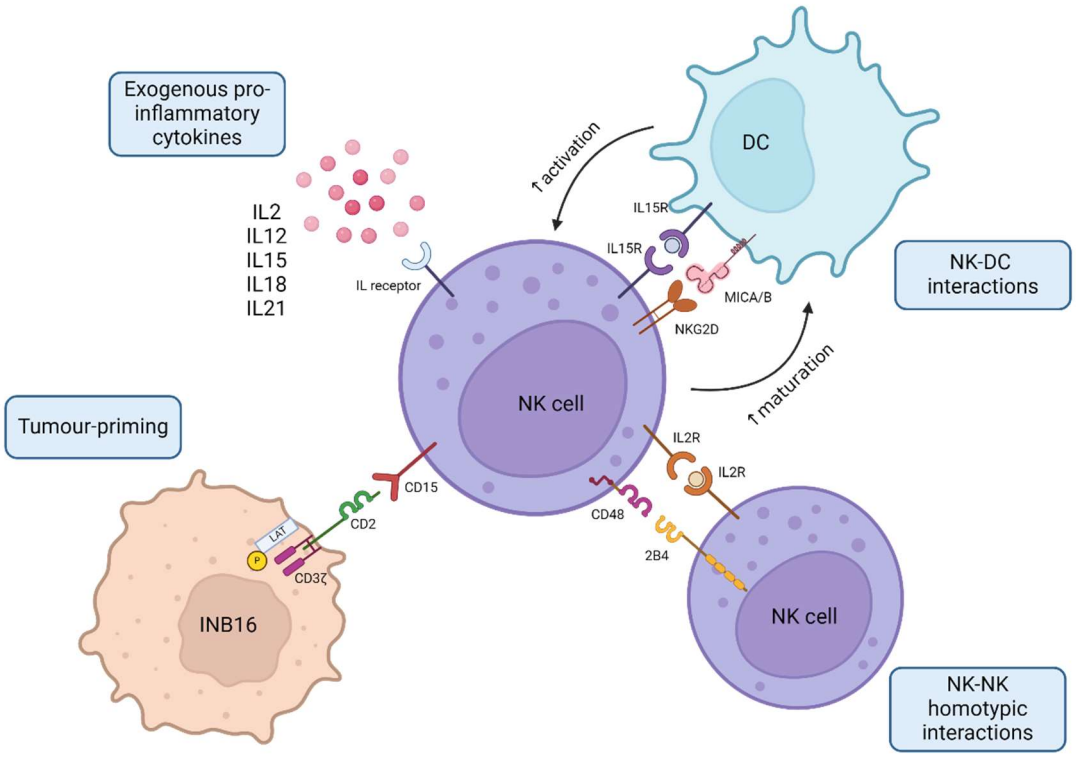

Figure 1.4 Mechanisms of NK cell priming

NK cells can be primed through various mechanisms. Exogenous pro-inflammatory cytokines like IL2/12/15/18/21 can prime NK cells *ex vivo* and generate NK cells with enhanced cytotoxic capacity. Tumour-priming is achieved by the interaction of specific receptor-ligand interactions between the cancer cell and the NK cell. DCs prime NK cells by trans-presenting IL2 or IL15 which in turn induces DC maturation. NK-NK homotypic priming occur by an activated NK cell trans-presenting IL2 to a neighbouring NK cells. Created with Biorender.

1.3 Natural Killer Cell Memory

New evidence has emerged in the past decade demonstrating that specific populations of NK cells exhibit properties similar to immunological memory, formerly only attributed to the adaptive immune system.

In the adaptive immune system, specific naïve T cells are stimulated when they recognise an antigen and expand to generate daughter cells with effector functions. Most of these expanded T cells undergo apoptosis leaving behind an array of memory cell subsets, which reside in tissues and patrol through the body to identify the same antigen in the future. If that happens, the recall phase starts, in which the T cell robustly expands to fight the same antigen again (Pennock et al., 2013).

Until recently, the memory and recall phases characteristic of the adaptive immune system had not been described in NK cells; however, there is mounting evidence that some subsets of NK cells display an array of responses corresponding to these phases. The first evidence on NK cell memory was described in response to various haptens. Mice lacking T and B cells but not NK cells developed contact hypersensitivity responses to haptens that persisted for several weeks. The transfer of NK cells from sensitised mice to unexposed mice resulted in contact hypersensitivity responses upon a second exposure to the same hapten (O'Leary et al., 2006; Paust et al., 2010). Since then, NK cells with characteristics of immunological memory have been described under different conditions, which are covered next (Table 1.1).

	Adaptive NK cells	CIML-NK cells	Tumour-memory NK cells
Mode of generation	Viral infection	Exposure to IL12/15/18	Priming with tumour specimen
Phenotype	NKG2C^{+} CD57^{hi} CD25^{hi} NKG2A^{-} FCεRγ^{-}	CD25^{hi} CD94^{hi} NKG2A^{hi} CD69^{hi} NKp46^{hi}	Depending on priming agent
Functional characteristics	↑IFNγ production ↑ADCC	↑ IFNγ production ↑ anti-tumour cytotoxicity	↑ IFNγ production ↑ anti-tumour cytotoxicity
Antigen dependence	Viral-encoded proteins	Unlikely	?
Epigenetic modulation	Yes	Yes	?

Table 1.1. Overview of various forms of human memory NK cells

Table shows the differences between adaptive NK cells, cytokine-induced memory-like NK cells and tumour-memory NK cells.

1.3.1 Adaptive NK cells

The first evidence of memory properties in NK cells came from studies in murine cytomegalovirus (mCMV) infections. Sun and colleagues observed that NK cells bearing the virus-specific Ly49H receptor proliferated and showed antigen specificity towards the mCMV-encoded glycoprotein m157, resembling characteristics of immune memory. Furthermore, the infection with an mCMV strain lacking m157 did not induce the expansion or development of memory NK cells. These NK cells also persisted over time and showed enhanced responses upon a secondary mCMV exposure (J. C. Sun et al., 2009). These NK cells were termed “adaptive” NK cells.

Similar observations were made in humans, where CMV^{+} individuals present enriched NKG2C^{+} populations of NK cells that are long-lived and show enhanced secondary responses against CMV-infected target cells compared

to “naïve” NK cells (Béziat et al., 2013; Foley et al., 2012; Lopez-Vergès et al., 2011a).

Adaptive memory-like NK cells are mainly characterised by their high expression of NKG2C; other surface markers identified include $CD57^{hi}$ $CD25^{hi}$ and $NKG2A^{-}$ (Béziat et al., 2013; Foley et al., 2012; Lopez-Vergès et al., 2011b; J. C. Sun et al., 2009).

These adaptive NK cells are potent secretors of IFNγ, and show enhanced cytotoxicity in secondary responses to viral infected cells but only in an antibody-dependent manner (J. Lee et al., 2015).

There is evidence that adaptive NK cells are imprinted at the epigenetic level. In the setting of transplantation, patients who received $NKG2C^{+}$ NK cells from CMV-seropositive donors showed heightened function in response to primary CMV infections compared to patients who received $NKG2C^{+}$ NK cells from seronegative donors (Foley et al., 2012). In CMV-seropositive donors, specific populations of expanded NK cells display an imprinted KIR repertoire expressing self-specific iKIRs, contrary to a random expression of KIR molecules in CMV-seronegative donors (Béziat et al., 2013). Other observations point to epigenetic imprinting of the CNS1 region of the IFNG locus in NKG2C expanded adaptive NK cells, which leads to consistent IFNγ production (Luetke-Eversloh et al., 2014), as well as lack of the signalling proteins FcεRIγ, SYK and EAT-2, because of promoter DNA hypermethylation. This was associated with a reduction of the transcription factor PLZF (J. Lee et al., 2015; Schlums et al., 2015). These epigenetic changes might explain why adaptive NK cells can persist in the body, as these characteristics might be passed onto the progeny.

More characteristics of adaptive NK cells confirming immunological memory have been unravelled in recent years. The Romagnani group recently elucidated the mechanism by which adaptive NK cells are capable of antigen-induced expansion; the binding of the human CMV (hCMV) UL-40-derived peptide to HLA-E stabilises HLA-E onto the surface of hCMV infected cells, which is recognised by NK cells to drive their expansion. This did not occur with other hCMV-derived peptides since HLA-E was not stabilised onto the

surface with the same capacity, and thus, NK cell recognition was hampered (Hammer et al., 2018). These findings partly resolve the mystery of how adaptive NK cells recognise infected cells independent of antigen-receptor diversification. Furthermore, work from the same group demonstrated clonal expansion of adaptive NK cells in hCMV^{+} individuals, where adaptive NK cells clonally persist in a memory state (Rückert et al., 2022).

1.3.2 Cytokine-induced memory-like NK cells

Memory NK cells can be generated in the context of cytokine priming. This phenomenon was first observed in mouse NK cells activated *ex vivo* with the triple cytokine cocktail IL12/15/18. These NK cells persisted for several weeks after being transferred back into the mice and showed enhanced IFNγ secretion after restimulation *ex vivo* (Cooper et al., 2009). These cells were termed cytokine-induced memory-like (CIML) NK cells.

Similar experiments have been performed in humans where NK cells were activated *in vitro* with IL12/15/18 and rested for one week in low-dose IL15 to allow for differentiation. After this rest period, these CIML-NK cells show enhanced cytotoxicity and IFNγ secretion upon cytokine restimulation compared to control NK cells, both against cancer cell lines and primary leukemic blasts (Romee et al., 2012, 2016).

CIML-NK cells have been characterised by their surface marker expression as CD25^{hi} CD94^{hi} NKG2A^{hi} CD69^{hi} NKp46^{hi} (Cooper et al., 2009; Romee et al., 2012, 2016).

A potential mechanism involved in this enhanced function is through the increased expression of CD25 and increased STAT5 phosphorylation that CIML-NK cells show over time, allowing these cells to respond to picomolar concentrations of IL2, which translates to enhanced functional responses (Leong et al., 2014). Epigenetic imprinting, akin to adaptive NK cells, has been observed in CIML-NK cells, elucidating their augmented functionality. Specifically, demethylation of the CNS1 region of the IFNG gene has been identified as a critical contributor to the stabilization of the IFNγ-producing phenotype (Luetke-Eversloh et al., 2014; Ni et al., 2016).

1.3.3 Tumour-memory NK cells

The generation of tumour-primed NK cells has been defined by the Lowdell group and others (Dufva et al., 2023; North et al., 2007), and it has become evident that TpNK cells exhibit characteristics of immunological memory (Pal et al., 2017). As described by the Lowdell group, upon exposure to certain cancer cell lines, NK cells become primed so that if exposed to a second cell line, they display enhanced cytotoxicity and cytokine secretion resembling memory properties (Sabry et al., 2019). These NK cells retain enhanced cytotoxic properties even after cryopreservation (North et al., 2007). Pal and colleagues generated tumour-memory NK cells by exposing NK cells to ALL cell lines or primary specimens, which, after a period of rest, exhibited enhanced cytotoxicity and cytokine production. This was only evident after the NK cells were exposed to the same cells used at the priming stage, showing some degree of specificity (Pal et al., 2017).

Tumour-memory NK cells exhibit a distinct phenotypic signature, dependent upon the priming agent utilised (Dufva et al., 2023). However, commonalities are identified, and these cells have a phenotype reminiscent of highly activated NK cells, marked by $CD69^{high}$ and $CD25^{high}$ expression (Pal et al., 2017; Sabry et al., 2019). When NK cells come into contact with a cancer cell, they are differentially “imprinted” according to the cancer target cells used for priming. Common genes reported overexpressed are associated with enhanced NK cell cytotoxicity and immunomodulatory functions, in keeping with their phenotype of activated NK cells and their superior cytotoxic capacity (Dufva et al., 2023; Pal et al., 2017; Sabry et al., 2019). Despite changes in the genome, it is currently unknown whether the exposure of NK cells to cancer cells induces epigenetic changes similar to what has been described in other types of memory-NK cells.

Contrary to adaptive and CIML-NK cells, the effects of tumour-priming on NK cells and how this leads to NK cell memory have been ill-defined. The primary focus of this thesis is to provide more insights into the generation of tumour-memory NK cells and how it compares to other types of NK cell memory.

1.4 Natural Killer cells and Cancer

1.4.1 Cancer immunosurveillance by NK cells

The theory of cancer immunosurveillance, postulated by Burnet in 1970, proposed that immune cells constantly survey the body in search of newly transformed cells (Burnet, 1970). However, it soon became apparent that cancer immunosurveillance was only one dimension of the complex relationship between the immune system and cancer. This led to the cancer immunoediting hypothesis, postulated by Dunn and colleagues (Dunn et al., 2004), which states a dynamic interaction between immune cells and cancer cells. They defined cancer immunoediting as a process consisting of three phases: elimination, equilibrium and escape. In the elimination phase, the immune system cells that carry out immune surveillance may eradicate the tumour and protect the host. If this fails, the tumour enters an equilibrium stage, which is either maintained chronically or sculpted by immune “editors”. This is due to new mutations arising that confer cancer cells with increased resistance to the immune system. These new cancer variants eventually evade the immune system and escape (Dunn et al., 2004).

To identify viral- or tumour-transformed cells, NK cells sense changes in the surface of target cells, such as the downregulation of MHC class I molecules, as well as the recognition of non-MHC class I molecules like collagen and glycans, which are also crucial for NK cell discrimination of self (Boudreau & Hsu, 2018). Other ligands associated with aberrant cells include the expression of MICA/B proteins and the UL16-binding proteins which are recognised by NKG2D (Mistry & O’Callaghan, 2007).

The increased tumour incidence in humans and experimental models that show impaired NK cell function highlight the importance of NK cells in cancer immunosurveillance (Dewan et al., 2007). A prospective 11-year follow-up study on a cohort of 3,625 individuals demonstrated that high cytotoxic NK cell function was associated with reduced cancer risk, whereas low NK cell activity was associated with increased cancer incidence (K. Imai et al., 2000).

While NK cells have been proven very successful in eliminating haematological malignancies, the infiltration into solid tumours remains poor. Intratumoral accumulation and persistence in an activated state are two key parameters for NK cell efficacy in solid tumours, which are usually challenged due to impaired trafficking into tumour sites and a suppressive TME (Tong et al., 2022).

1.4.2 Tumour evasion of NK cells in haematological malignancies

In the 2011 version of *Hallmarks of Cancer* (Hanahan & Weinberg, 2011), 'evasion of the immune system' was included for the first time as an 'emerging hallmark of cancer'; in the 2022 edition, it was reclassified to 'core hallmark', which underscores the critical role of immune dysfunction in the development and progression of cancer (Hanahan, 2022).

To hamper recognition, cancer cells downregulate the expression of NK cell ligands such as MICA/B, affecting NK cell recognition (Deng et al., 2015; Vetter et al., 2004). Furthermore, the shedding of MICA/B creates a soluble ligand that blocks NK cell cognate receptors (Bauer et al., 1999; Raulet et al., 2013). Another mechanism includes upregulating MHC class I molecules to increase NK cell inhibitory signals (Costello et al., 2002). The upregulation of inhibitory molecules is also a common occurrence, including the non-classical HLA class I molecules HLA-G and -E; Nectin-4; PVR; and immune checkpoint ligands, which will impede NK cell recognition (Sivori et al., 2019, 2020).

Indirect mechanisms of cancer evasion include shaping the TME (Figure 1.5), a key element in NK cell dysfunction and cancer progression in patients with haematological malignancies (Arellano-Ballestero et al., 2023).

NK cell-DC interaction is crucial for NK cell activation. DCs are impaired in cancer (Xiao et al., 2023), which have a negative effect on DC-NK cell crosstalk and the release of activating soluble factors like IL12, IL18 and type-I IFN, that prime NK cells for tumour lysis (Ferlazzo & Moretta, 2014).

Increased levels of vascular endothelial growth factor (VEGF) were found in the serum of cancer patients, contributing to the immunosuppressive role of the TME (Invernizzi et al., 2017; Olson et al., 1994). Increased VEGF inhibits

DC maturation (Gabrilovich et al., 1996; Terme et al., 2013) and induces T regulatory cell (Treg) activation (Gabrilovich et al., 1996; Terme et al., 2013), which is associated with an unfavourable disease prognosis (Dąbrowska et al., 2023). Tregs are well known to suppress NK cell function via cell-to-cell contact or through the secretion of soluble factors like IL10 or TGFβ (Ghiringhelli et al., 2005; Szczepanski et al., 2009).

Another source of VEGF is from myeloid-derived suppressor cells (MDSCs) (Chen et al., 2013; Horikawa et al., 2017), which are expanded in the bone marrow of patients with haematological malignancies and correlate with high-risk disease (Jiang et al., 2013; Kalathil & Thanavala, 2021). MDSCs secrete a plethora of immunosuppressive cytokines like IL10, TGFβ and reactive oxygen species (ROS) which ultimately impair NK cells (Lv et al., 2019; Palumbo et al., 2019). In some haematologic malignancies, ROS triggers NK cell apoptosis and induces downregulation of activating receptors, leading to NK cell dysfunction (Aurelius et al., 2013, 2017; Mellqvist et al., 2000).

Mesenchymal stromal cells (MSCs) are another cell type reportedly impaired in patients with haematological malignancies. These cells exhibit reduced proliferative capacity and poor ability to differentiate into other cell types, altered morphology, and alteration of molecules and cytokines involved in hematopoietic stem and progenitor cells (HSCPs)-MSCs interactions (Corradi et al., 2018; Geyh et al., 2013). MSCs have a very important role in supporting HSCPs in their renewal and differentiation, which will allow the production of mature blood cells, including NK cells (Frias et al., 2008; Zhao et al., 2018). In myelodysplastic syndrome (MDS), it has been argued that the absence of stromal support leads to a lack of fully mature NK cells, as it is known that fully mature KIR-expressing NK cells require the presence of stromal cells (Hejazi et al., 2015; Miller & McCullar, 2001). The increased secretion of the pro-inflammatory cytokine IL6 by MSCs has also been reported in some cancers (Antoon et al., 2022; Lopes et al., 2017), contributing to general inflammation.

An inflammatory state has been described in the bone marrow of patients, described by increased levels of pro-inflammatory cytokines like IFNγ and TNFα, which induce apoptosis on CD34 cells and bone marrow failure, helping

in the selection of malignant CD34 cells (Kerbauy & Deeg, 2007; Zeng et al., 2006). Importantly, TNFα activates the transcription factor NF-$\kappa\beta$, which regulates cell signalling, proliferation and differentiation (Hayden & Ghosh, 2014). Furthermore, some studies have shown that NF-$\kappa\beta$ signalling contributes to leukaemia progression (Kagoya et al., 2014).

Hypoxia also plays an important role in the TME by inhibiting the PI3K/mTOR signalling pathway, hampering NK cell function (Chouaib et al., 2017). In hematologic malignancies, hypoxic conditions select CD34 malignant cells with stem cell potential in patients (Masala et al., 2018). Expanded CD34 malignant blasts will further contribute to inflammation in the bone marrow by secreting pro-inflammatory cytokines like IL8 and TGFβ (Geyh et al., 2018; Kuett et al., 2015; Schinke et al., 2015; L. Zhou et al., 2008) and increasing levels of ROS (Gonçalves et al., 2015; Peddie et al., 1997; Picou et al., 2019), ultimately affecting NK cells. Furthermore, hypoxia reduces MICA/B expression in tumours, hindering cancer cell recognition by NK cells (Torres et al., 2020).

Understanding the role of the TME and its contribution to NK cell impairment is crucial to developing successful anti-cancer therapies that could include combination strategies targeting different elements of the TME and thus enhancing NK cell activity for the successful killing of malignant blasts.

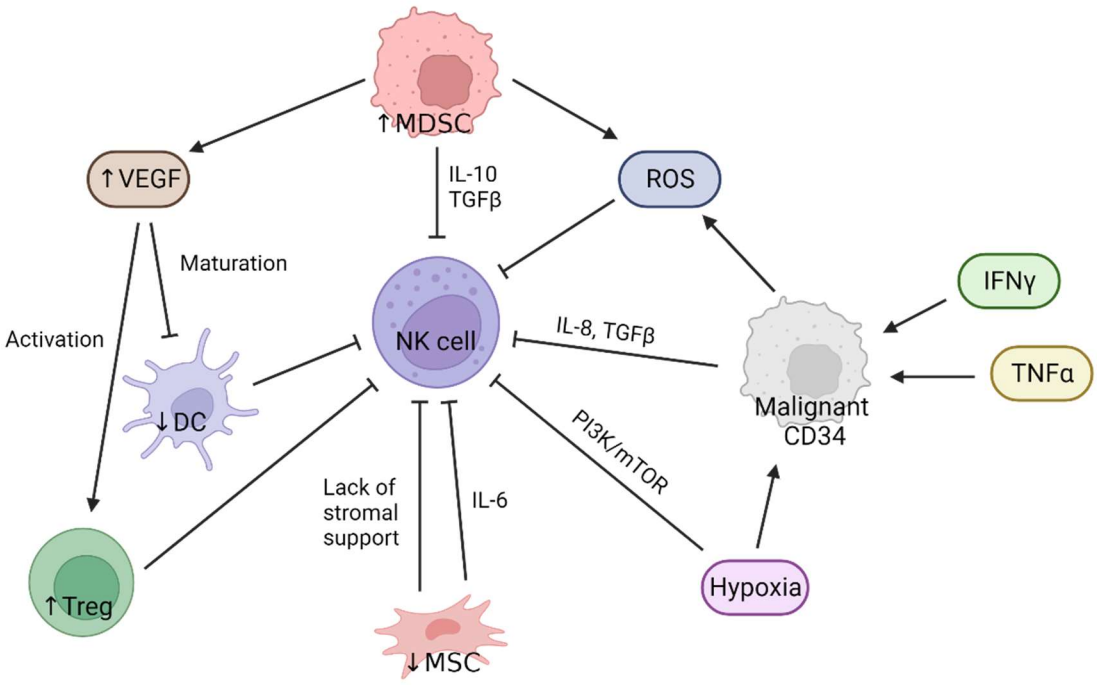

Figure 1.5. NK cell impairment by the tumour microenvironment.

The presence of immature DCs directly affects NK cell activation. Increased levels of VEGF contribute to DC immaturity and also Treg expansion. Increased levels of hyperactive Tregs secrete IL10 and TGFβ into the TME, suppressing NK cell activation. A source of VEGF in cancer are MDSCs, which are expanded and hyperactive and contribute to NK cell impairment by secreting IL10, TGFβ and ROS into the TME. MSCs are also reported to be reduced in numbers and have an impaired phenotype in cancer; impaired MSCs cannot support NK cell maturation and contribute to general inflammation by secreting pro-inflammatory cytokines like IL6. Hypoxia will inhibit NK cells by impairing the PI3K/mTOR signalling pathway. In haematological malignancies, the general inflammatory state in the bone marrow is characterized by an increase of IFNγ, TNFα and increased hypoxia, inducing bone marrow apoptosis that helps select malignant CD34 cells. Those cells further secrete ROS and pro-inflammatory cytokines like IL8 and TGFβ, impairing directly or indirectly NK cell function and activation. Created with Biorender.

1.4.3 NK cell modulation for therapy

The use of NK cells for cancer immunotherapy presents a variety of advantages compared to other immune cells. Allogeneic NK cells do not cause graft-versus-host disease (GVHD), cytokine release syndrome or neurotoxicity. Furthermore, they can be prepared to be used off the shelf, making them immediately available and at reduced costs. Despite having shown some clinical benefit in a variety of clinical trials, one of the main challenges continues to be the generation of large numbers of NK cells *ex vivo*, as well as their short lifespan *in vivo* (Arellano-Ballestero et al., 2023; Berrien-Elliott et al., 2023; Sabry & Lowdell, 2020).

NK cells can come from a variety of sources. Allogeneic donors are the most common source of NK cells in clinical trials, as they induce potent responses against cancer cells and are relatively easy to obtain. Despite being widely used, allogeneic NK cells from peripheral blood present some challenges, like donor-to-donor variability and the limited number of cells you can obtain from each apheresis (Cooper et al., 2001). Other sources of NK cells include cord blood (Dalle et al., 2005), CD34+ human pluripotent stem cells (hPSCs) (Miller et al., 1992; Spanholtz et al., 2010; H. Yu et al., 1998) and induced pluripotent stem cell (iPSCs) (Lupo et al., 2021; H. Zhu & Kaufman, 2019).

Several approaches are being considered to improve NK cell therapies; these include the enhancement of effector responses, the blockade of inhibitory signals, the enhancement of target cell recognition, and the improvement of NK cell persistence *in vivo*.

1.4.3.1 Enhancement of effector responses

Initial trials in allogeneic NK cell therapy included NK cell priming with pro-inflammatory cytokines like IL2, which remains one of the most used strategies in NK cell clinical trials in cancer patients (Curti et al., 2011; Miller et al., 2005; Rosenberg et al., 1987; Rubnitz et al., 2010; Szmania et al., 2015). In the first trial utilising IL2-activated NK cells in patients with metastatic cancers, authors reported clinical responses with minimal side effects (Rosenberg et al., 1987), paving the way to modern NK cell therapies.

The use of CIML-NK cells for clinical trials has been gaining more popularity in recent years. NK cells from allogeneic donors are activated overnight with a combination of IL12/15/18 and infused on the patient the next day. This has shown no toxicities related to the product, with complete remissions seen in 47% of patients (Berrien-Elliott et al., 2020, 2022). It has also been trialled in leukaemia patients post-hematopoietic stem cell transplant (HSCT), where CIML-NK cells were shown to expand and persist (Bednarski et al., 2022; Shapiro et al., 2022).

Tumour-primed NK cells have also been used in clinical trials for AML/MDS, with little toxicity and some sustained clinical responses. This is of particular note since these were the first clinical trials of an adoptive NK therapy in the absence of cytokine support. Allogeneic NK cells from related, haploidentical donors were incubated overnight with a lysate of INB16 that was then removed and the tumour-primed NK cells were cryopreserved, shipped and infused into the patients one day after completion of lymphoreductive chemotherapy (Kottaridis et al., 2015). Four of the seven patients who completed treatment showed clinical responses, with one patient with chemo-resistant AML achieving complete remission (CR), which was sustained for over 11 months. In a second trial, 12 AML patients at high risk of recurrence were treated following the same protocol, where 2 patients remained relapse-free in post-trial follow-up and 3 patients remained in complete remissions for 32.6 to 47.6+ months (Fehniger et al., 2018). Tumour-priming of endogenous NK cells *in vivo* is currently trialled in high-risk MDS and AML patients (NCT05933070) who receive three weekly infusions of a replication-incompetent preparation of the INB16 cell line. These patients receive no lymphoreductive conditioning chemotherapy and no cytokine support, resulting in a treatment that is well tolerated and compatible with an elderly patient cohort. The results of the patients treated in this trial are reported in this thesis.

1.4.3.2 Blockade of inhibitory signals

The blockade of inhibitory signals on NK cells has been explored to unleash their triggering.

Monoclonal antibodies (mAbs) have been developed to target inhibitory KIR2D (lirilumab) to trigger NK cell cytotoxicity. Two phase 1 clinical trials were conducted with lirilumab, demonstrating safety and some responses in patients with leukaemia and myeloma (Benson et al., 2015; Vey et al., 2012). However, randomised phase 2 trials failed to show clinical improvement (Vey et al., 2017).

Another monoclonal antibody explored is monalizumab, which blocks the inhibitory receptor NKG2A from binding to HLA-E/G ligands. Monalizumab has been tested in clinical trials in solid tumours and demonstrated safety and some clinical responses (André et al., 2018); however, a randomised phase 3 clinical trial in solid tumours did not demonstrate clinical improvements (INTERLINK-1 study; NCT04590963).

Other mAbs evaluated preclinically to block NK cell inhibitory receptors include TIM3, TIGIT, LAG3, PD1, CD161 and CD96 (Blake et al., 2016; Hsu et al., 2018; Q. Zhang et al., 2018), but no clinical data is available at present.

1.4.3.3 Enhancement of target cell recognition

Multiple clinical studies are currently being conducted to explore different mechanisms that can enhance the ability of NK cells to target and attack tumours.

Monoclonal antibodies have been utilised to recruit NK cells expressing CD16 that will induce ADCC against cancer cells (Capuano et al., 2021).

Bispecific and trispecific killer cell engagers (BiKE and TriKE) are single-chain variable fragment recombinant reagents that contain an anti-CD16 expressed on effector NK cells and other antigens of interest in cancer cells. In hematologic malignancies, BiKEs have been designed to target CD33, engaging myeloid cells (Gleason et al., 2014). TriKEs containing anti-CD16, anti-CD33, and a modified IL15 linker to induce NK cell proliferation have been tested in an MDS/AML clinical trial, where they were reported to be safe and induce expansions of endogenous NK cells with anti-tumour activity (Miller et al., 2021).

Chimeric Antigen Receptor (CAR)-NK cells are currently developing to broaden target cell specificity. Multiple targets have been developed and tested in clinical trials in various cancers with some encouraging results (Marin et al., 2024). However, major limitations include large-scale manufacturing, *in vivo* activation, and durability (L. Zhang et al., 2022).

1.4.3.4 Improvement of NK cell persistence

The insufficient persistence of NK cells *in vivo* remains a major challenge in the field of NK cell immunotherapy. Several strategies are currently under development to overcome this obstacle.

The infusion of NK cells into patients usually requires cytokine support. The most used strategy is the infusion of IL2 after NK cell transfer, which is generally considered safe and helps with NK cell persistence *in vivo* (Bachanova et al., 2014; Miller et al., 2005).

Synthetic IL15-receptor agonists have also been tested as an alternative to IL2 infusions (Ma et al., 2022). However, in some clinical trials it induced reduced clinical activity compared with IL2, due to promoting recipient CD8 T-cell activation that caused donor NK cell rejection (Berrien-Elliott et al., 2022; Cooley et al., 2019).

Low NK cell numbers are also one of the main challenges for NK cell persistence *in vivo.* To overcome that, feeder cells have been utilised in order to expand NK cells with the use of K562-mbIL15-41BBL, which resulted in enhanced expansion and cytotoxicity in *in vitro* and *in vivo* models (Fujisaki, Kakuda, Shimasaki, et al., 2009a). In clinical trials, K562-mbIL15-41BBL has been utilised in order to expand CAR-NK cells with anti-NKG2D and anti-CD19, showing benefits *in vitro* (Morisot et al., 2020) and are currently tested in clinical trials in patients with haematological malignancies (Bachier et al., 2020; Dickinson et al., 2021). Alternatively, K562-mbIL21-41BBL feeder cells have also been developed, as they increase the fold expansion of NK cells compared to mbIL15 (Dickinson et al., 2021).

To summarise, NK cell immunotherapy in cancer offers a wide range of options that show exciting opportunities and appear to be safe for treating this disease. Despite that, relapse rates are still high, and side effects of concurrent cytokine treatment are common. Cytokine administration is usually required to sustain adoptively transferred NK cells, especially those generated by extensive *ex vivo* expansion. As seen here, the field of NK cell immunotherapy is rapidly evolving and has been very popular in the past years; for it to be successful, developing better strategies for NK cell expansion and persistence post-infusion remains a central tenet of research.

1.5 Thesis Aims

While adaptive and cytokine-induced memory-like NK cells have been thoroughly studied in the past 10 years, the effects of tumour interactions with NK cells and whether this generates NK cells with memory properties remains in its infancy.

The aim of this thesis is to provide a better understanding of how tumour-priming of NK cells generates memory NK cells and to evaluate tumour-primed NK cells as an immunotherapeutic agent for patients with hematologic malignancies. The experimental aims of the thesis are as follows:

1. To characterise the phenotype and proteomic profile of TpNK and CIML-NK cells to define the initial events leading to the generation of tumour- and cytokine-memory NK cells (Chapter 3)

2. To characterise the cytotoxic capacity and metabolic function of TpNK and compare them to CIML-NK cells (Chapter 4)

3. To investigate interactions between NK cells and define whether TpNK cells can induce activation of rNK cells in a homotypical manner (Chapter 5)

4. To characterise NK cells from patients with MDS and to evaluate if TpNK cells can be generated *in vitro* from the NK cells of these patients (Chapter 6)

5. To evaluate if tumour-memory NK cells can be generated *in vivo* with an immunotherapeutic drug at the clinical trial stage in patients with MDS and AML (Chapter 6)

Chapter 2 Methods

2.1 Cell lines and cell culture

2.1.1 Cell lines

Cell lines were purchased from the American Type Culture Collection (ATCC) or donated as indicated and were maintained in culture according to manufacturer instructions. The main cell lines used for this thesis are described below:

INB16: T-cell acute lymphoblastic leukaemia (T-ALL) cell line derived from a distinct clone of the CTV-1 leukemic cell line. These cells are round or multiform and are single cells or clustered in suspension.

K562: chronic myelogenous leukaemia (CML) cell line used as the prototypical NK-sensitive target cell, which lacks expression of HLA molecules. These cells are round and are single cells in suspension.

Raji: Burkitt lymphoma cell line that is one of the prototypical NK-resistant target cell, which expresses HLA molecules. These cells are round and single cells in suspension with a tendency to form clumps.

MDS-L: MDS cell line kindly provided by Kaoru Tohyama. These cells are round and are single cells in suspension.

2.1.2 Culture medium and cell culture

Cell cultures were performed in complete growth medium (CM) RPMI 1640 GlutaMax™ (Gibco) supplemented with 10% v/v foetal bovine serum (FBS, Gibco) and 1% antibiotic-antimycotic (Gibco). MDS-L was maintained in CM and 50ng/mL IL-3 (R&D). Cells were passaged every 2-3 days at 1:1 ratio. Cells were cultured in T75 flasks for 3 months and after that new cultures were started and cell vial stocks were stored in liquid nitrogen phase. Cells were incubated at 37°C in a humidified standard cell culture incubator with 5% CO2 and 21% O2.

2.1.3 Cell counting and viability

Two methods were used to count cells and assess viability:

In the first one, cells were assessed using the Trypan blue exclusion method under a brightfield microscope. An aliquot of cell suspension was diluted with 0.4% Trypan Blue solution (Sigma-Aldrich), which is taken up by non-viable cells and appear in blue colour. After mixing, 10µL of cell suspension was loaded onto a haemocytometer counting chamber (Labtech), which was placed under a brightfield microscope (Nikon) for cell counting. The average number of cells counted in the four sets of 16 squares ($1mm^2$) is then multiplied by the dilution factor in Trypan blue. After that, cell concentration was multiplied by $x10^4$ to account for the volume of the haemocytometer, obtaining the cell concentration ($x10^6$ cells/mL).

The second method for cell counting was done by staining cells with a viability dye and acquiring in a flow cytometry instrument (Novocyte, Agilent). Cells were appropriately diluted in a final volume of 100µL. After that, 10µL (10% of final volume) of TOPRO3 stain (ThermoFischer) was added to the sample. TOPRO3 is a nuclear dye that penetrates compromised membranes, where dead cells will appear as positive. A minimum of 10,000 events were acquired after the gating of cells using forward scatter (FSC) and side scatter (SSC) signals (Figure 2.1). Cell concentration was obtained after analysing the data using NovoExpress software (Agilent) and multiplied by the cell dilution and by x1.1 to account for the addition of 10% TOPRO3, obtaining the final cell concentration (cells/mL).

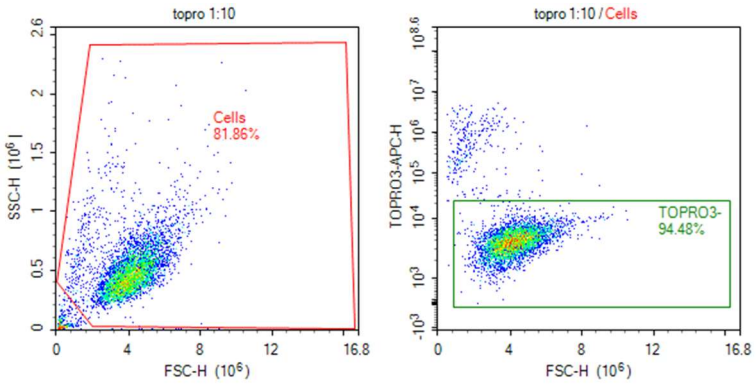

Figure 2.1. Basic gating strategy for cell counting in flow cytometer

A FSC versus SSC plot was created around the cell population of interest (excluding debris). After that, the gate was projected onto a second dot plot of FSC versus TOPRO3-APC and a second gate drawn to identify TORPO3 negative cells.

2.1.4 Cell cryopreservation

A minimum of $1x10^6$ cells and a maximum of $20x10^6$ cells were cryopreserved each time. A cryomix solution was made up of 80% FBS and 20% dimethyl sulfoxide (DMSO, Merck) and allowed to cool down. Cells were pelleted and resuspended at double the concentration of interest in CM, and 0.5mL of cell suspension was added into a 2mL cryogenic vial (Corning) followed by 0.5mL of cryomix, resulting in a vial at the desired cell concentration in 10% DMSO/FBS cryomix. After that, the vials were quickly placed inside a freezing container (CoolCell, Corning) and stored at -80°C for 24 hours. The vials were then transferred for storage in liquid nitrogen at -196°C or vapour phase nitrogen at -152°C.

2.1.5 Cell thawing

Cryopreserved cells were gently thawed into a 37°C water bath by partially immersing the vials until cells were partly thawed. The cells were then pipetted into a 15mL Falcon tube containing 10mL of CM and centrifuged at 300xg for 5 minutes (all centrifugations were done at 300xg for 5 minutes unless otherwise stated). The supernatant was discarded, and cell pellets were

resuspended in CM for future use and allowed to recover for a minimum of 1 hour before cell count. After that, cells were cultured or used for experiments.

2.2 Blood donors

Healthy donor blood samples were obtained from leukocyte cones from NHS UK Blood and Transplant or by directly using a needle and syringe tube with 1,000IU/mL heparin (Wockhardt) by phlebotomist staff at the Royal Free Hospital. Blood samples from patients were taken by using a needle and Vacutainer tubes (BD biosciences) containing lithium heparin by phlebotomist staff at UCL Hospital. Patient samples were acquired after informed consent and following ethical approval by the RFH/UCL Research Tissue Bank (UK National Research Ethics IRAS 63407- project codes NC2020.15, NC2021.03). Obtaining blood from healthy donors was approved by the University College London- Royal Free Hospital Biobank Ethical Review Committee (NC.2015.019). The clinical trial monitoring samples (MDS#01) were taken as part of an ethically approved UK national trial of INKmune™ in MDS/AML (NCT05933070) whilst the samples from patients with multiply relapsed AML were from patients treated compassionately after local institutional ethical approval.

2.3 Isolation of peripheral blood mononuclear cells

All peripheral blood mononuclear cells (PBMCs) isolations were carried out in a microbiological safety cabinet class II. Heparinised blood samples were diluted at a 1:1 ratio with Hanks Balanced Salt Solution (HBSS) modified without Ca^{2+} and Mg^{2+} (Gibco). Lympholite solution (Cedarlane) was used to isolate the PBMCs by density gradient centrifugation. In all cases, 25mL of Lympholite was placed in a 50mL Falcon tube, and then 20mL of diluted blood was layered slowly on top. The tubes were then centrifuged at 800xg for 20 minutes at brake 0, allowing for the layer of PBMCs to form. The PBMCs layer was collected using a Pasteur pipette and placed into a new 50mL Falcon tube, which was subsequently washed with HBSS and centrifuged at 800xg for 10 minutes at brake 3. The resulting pellet was resuspended in CM, and PBMCs were counted and checked for viability.

2.4 Isolation of NK cells

Human NK cells were isolated from PBMCs using the negative selection sort method. Negative selection of NK cells relies on the depletion of non-NK cells through a tetrameric antibody complex and magnetic particles, allowing the sorted NK cells to be “untouched”. The EasySep NK Enrichment Kit (StemCell Technologies) was used per the manufacturer’s protocol.

Accordingly, the desired amount of PBMCs to sort was centrifuged, and pelleted cells were resuspended in EasySep Buffer at a final concentration of $50x10^6$ cells/mL. Depending on the volume to work with, cells were transferred to a 5mL round-bottom tube for volumes between 0.25mL – 2.5mL or to a 13mL round-bottom tube for volumes between 2.5mL – 8.5mL. The enrichment cocktail (50µL/mL) was added and resuspended to the tube and samples were incubated at room temperature (RT) for 10 minutes. In the meantime, magnetic particles (100µL/mL) were then vigorously vortexed for 30 seconds. After the incubation time was finished, they were added and resuspended to the sample, and incubated at RT for 5 minutes. After that, the samples were topped up, if needed, with EasySep buffer to 2.5mL for the 5mL tubes or to 8.5mL for the 13mL tubes. Finally, the sample was placed into the EasySep magnet and incubated for 2.5 minutes at room temperature. After incubation, the sample was carefully poured into a fresh Falcon tube by continuous inverted motion and centrifuged in CM. Once cells were pelleted, they were resuspended in fresh CM. All selected cells were counted and confirmed for purity by phenotyping for $CD56^+$ $CD3^-$ markers using flow cytometry, where only sorted NK cells that were >90% pure were used for subsequent experiments.

2.5 Immunophenotyping of NK cells to check purity

After isolation, NK cells were routinely phenotyped to determine sort purity and yield. Surface staining was carried out in polycarbonate tubes, where a total of 10^5 cells were incubated with saturating concentrations of CD56 and CD3 monoclonal antibodies, as described below. Cells were washed in staining buffer (phosphate buffer saline (PBS, Thermo Fischer scientific) + 2% FBS) by centrifuging, and the pellet was resuspended in 100uL of staining buffer and

the fluorochrome-conjugated monoclonal antibodies. To check the purity of the sort, NK cells were labelled using 5uL of CD56 (HCD56 clone) APC/Cy7 (BioLegend) and 2µL of CD3 (BW264/56) VioBlue (Miltenyi Biotec), and incubated for 15 minutes in the dark at 4ºC. After that, cells were washed with staining buffer by centrifuging, and the pellet was resuspended in 100µL of staining buffer before acquisition on a Novocyte flow cytometer (Agilent). A minimum of 10,000 $CD56^+$ $CD3^-$ events were acquired after gating cells using FSC and SSC signals in NovoExpress software (Agilent).

2.6 *In vitro* stimulation of NK cells

2.6.1 Tumour-priming of NK cells

Tumour-priming of NK cells was achieved by co-incubating isolated NK cells ($1x10^6$ cells/mL) with INB16-mitomycin C treated ($2x10^6$ cells/mL) at a ratio 2:1 stimulator:responder; for 16 hours at 37ºC, 5% CO_2 in CM in a round-bottom tube.

To mimic the drug given to the patients, INB16 cells were pre-treated with Mitomycin C for all experiments. Mitomycin C is a chemotherapy drug that induces replication incompetence in the INB16 cells.

Mitomycin C (Sigma-Aldrich) was resuspended with saline solution at the concentration of 1,000µg/mL. INB16 cells were harvested and washed by centrifugation with HBSS; the cell pellet was resuspended in CM at $5x10^6$ cells/mL. Cells were treated with 10µg/mL of Mitomycin C for 2 hours at 37ºC, 5% CO_2 in CM in T-25 flask. After that, cells were washed 3 times by centrifugation with HBSS. INB16 cells were counted and put at the right concentration in CM.

From now on, Mitomycin C treated INB16 will be referred to as just INB16.

2.6.2 Cytokine stimulation of NK cells

For cytokine priming, NK cells were co-incubated with the exogenous cytokine IL15 (1ng/mL, R&D systems). For the generation of cytokine-induced memory-like (CIML), NK cells were co-incubated with IL15 (1ng/mL, R&D systems), IL12 (10ng/mL, R&D systems) and IL18 (50ng/mL, R&D systems) in CM

(Romee et al., 2012). Cells were at the concentration of $1x10^6$ cells/mL and primed for 16 hours at 37°C, 5% CO_2 in a round-bottom tube.

2.6.3 Lysate-priming of NK cells

To generate INB16 lysates, INB16 cells were transferred to a 50mL Falcon tube with HBSS and spun at 250xg for 10 minutes. Cells were then put at the concentration of $5x10^6$ cells/mL and were transferred to a 15mL Falcon tube. To disrupt the cell membrane, the tube containing INB16 was placed at -80°C for 30 minutes and then thawed at 37°C in a water bath; this process was repeated twice. After that, 50µL of DNAase (2,500 units/ml) was added for every mL of cell suspension; cells were incubated for 30 minutes at 37°C. Finally, cells were spun for 10 minutes at 600xg, and the lysate pellet was resuspended in CM to a final concentration of $2x10^6$ cells/mL.

To prime NK cells with INB16 lysates, isolated NK cells at $1x10^6$ cells/mL with INB16 lysates at a calculated $2x10^6$ cells/mL and at a ratio 2:1 stimulator:responder were co-incubated for 16 hours at 37ºC, 5% CO_2 in CM in a round-bottom tube.

2.7 Labelling of cells

2.7.1 PKH dyes

PKH26 and PKH67 are cell linkers that bind to lipid regions of the cell membrane and were used to identify cell populations. Both are fluorochromes excited by the 488nm laser line; PKH26 emits red fluorescence (567nm), and PKH67 emits green fluorescence (502nm). For labelling, cells were washed with HBSS and pelleted by centrifuging. In a separate 50mL Falcon tube, 500µL of Diluent C was mixed with 4µL of PKH dye, all from the PKH Fluorescent Cell Linker Kit (Sigma-Aldrich), and kept in the dark. After the cells were washed, 500µL of Diluent C was used to resuspend the pellet and the cell suspension was then transferred to the solution containing the dye in one continuous motion. Cells were incubated in the dark for 3 minutes at room temperature, and after that, an equal volume of neat FCS was added to stop the reaction for 1 minute. Cells were then washed with HBSS by centrifugation. The resulting pellet was resuspended in 10mL of CM and transferred to a new

15mL Falcon tube to be centrifuged again. Finally, the labelled cells were resuspended in an appropriate volume of CM, and the cell concentration, viability and efficacy of the labelling were evaluated using flow cytometry (Novocyte, Agilent).

2.7.2 CellTrace™ dyes

Both CellTrace™ Violet and CellTrace™ CFSE (Thermo Fischer) were used in this project to label cells. CellTrace™ dyes are non-fluorescent molecules that enter cells by diffusion through the membrane. Once inside the cell, the non-fluorescence molecule is converted to a fluorescent derivative by cellular estearases, which will bind to proteins and result in long-term dye retention inside the cell. CellTrace™ dyes can be used to study cell proliferation as through every cell division, daughter cells receive half of the fluorescent label of the parent cell, allowing analysis by flow cytometry. CellTrace™ Violet excitation/emission is 405/450nm, and CellTrace™ CFSE is 495/519nm.

Before staining, dyes were reconstituted to a working concentration of 5μM in DMSO. CellTrace™ dyes are optimised by the manufacturer for a cell concentration of 10^6 cells/mL in PBS . To stain cells, 1μL of working solution was added for every mL of cell suspension. Cells then were incubated for 20 minutes at 37^{o}C. After the incubation, 5 times the original staining volume of CM was added and incubated for 5 minutes to remove any remaining free dye. Cells were then pelleted by centrifugation and resuspended in fresh CM; before proceeding to any experiment, cells were allowed to rest for 5 minutes.

2.8 INB16 whole cell/lysate depletion from TpNK cells

Some experiments required the depletion of INB16 whole cell or lysate after the co-incubation with NK. To deplete INB16 whole cell, a 2-step protocol was followed by first removing dead cells and second by isolating NK cells using positive selection. For the removal of INB16 lysates, only the removal of dead cells was performed.

2.8.1 Dead cell removal

Dead cells were removed using a Dead Cell Removal Kit (Miltenyi Biotec). This kit contains microbeads that recognise a fraction in the membrane of apoptotic and dead cells, which will be magnetically labelled and separated through a separation column. The magnetically labelled cells will be retained in the column, only allowing live cells to flow through.

NK cells were counted, and a separator column was selected depending on the number of cells to be sorted, with a maximum of $2x10^8$ for an MS MACS column and a maximum of $2x10^9$ for an LS MACS column. After that, 20x binding buffer was diluted to x1 with double-sterile water. The cell suspension was pelleted by centrifuging at 300xg for 10 minutes, and the pellet was resuspended in 100µL of Dead Cell removal MicroBeads per 10^7 total cells and incubated for 15 minutes at room temperature. If needed, 1x Binding Buffer was added to the cell suspension to reach a volume of 500µL. An appropriate MACS column was placed into the MACS separator and rinsed with 1x Binding Buffer (500µL for an MS column or 3mL for an LS column). Cell suspension was then applied to the column, and flow-through was collected. The column was then rinsed 4 times with 1x Binding Buffer (500µL for an MS MACS column or 3mL for an LS MACS column), collecting unlabelled cells (live cells). Finally, cells were washed with CM by centrifuging at 300xg for 10 minutes and resuspended in fresh CM for further experiments.

If NK cells were depleted from INB16 lysates, the sorted NK cells were checked for purity and yield and used for consecutive experiments. If NK cells were depleted from INB16 whole cells, NK cells were counted and then proceeded to NK cell positive selection.

2.8.2 Positive selection

For positive selection of NK cells, cells are separated using magnetic-activated cell sorting (MACS, Miltenyi Biotec) to a CD56 antibody that will bind to NK cells. Cells were counted and washed with MACS buffer (PBS +2mM EDTA + 0.5% FBS) by centrifuging. The recommended range for lymphocyte separation is $10^5 – 10^8$ labelled cells in $10^7 – 2x10^9$ total cells. The cell pellet

was resuspended in MACS buffer (80µL per 1x10^7 cells) and with CD56 MicroBeads (Miltenyi Biotec) (20µL per 1x10^7 cells) and was incubated for 15 minutes at 4^{o}C. In the meantime, an LS MACS magnetic column was used and placed into a MACS separator. The column was prepared by rinsing it with 3mL of MACS buffer, letting it run through, and discarding the effluent. After incubation, the cells with the beads were topped up to 5mL with MACS buffer and run through the column, pipetting slowly to the side of the column. Once all the sample passed through, the column was rinsed 3 times with 3mL of MACS buffer. After that, the column was removed from the magnetic separator and placed into a new Falcon tube. Five mL of MACS buffer were pipetted into the reservoir and firmly applied the plunger to collect the cells (positive fraction). The sorted NK cells were then washed with CM by centrifuging, and the resulting pellet was resuspended with fresh CM. After that, NK cells were checked for purity and yield and used for consecutive experiments.

2.9 Cell sorting of NK cells

NK cells from metaclusters M6 and M8 were sorted at the Flow cytometry facility at the UCL Cancer Institute by the facility personnel using a BD FACS Aria Fusion housed in a class II biosafety cabinet.

Only markers with fluorescence intensity above 10,000 units were selected to facilitate the cell selection in the cell sorter. The markers selected to sort cells from metacluster M6 were (NK-M6) were $CD57^-$ $CD69^+$ $PDL1^+$; NK cells from metacluster 8 (NK-M8) were $CD57^+$ $CD69^+$ $PDL1^+$.

Cells were stained as indicated in section 2.5 under sterile conditions. The fluorochromes used were CD57-FITC (clone TB01; Invitrogen), CD69-APC (clone H1.2F3; Invitrogen), and PDL1-BV421 (clone MIH3, Biolegend). Cells were stained with the viability dye eFluor™780 (Thermo Fischer) as per manufacturer instruction and were kept in ice until acquisition time.

The purity achieved after the sort is shown in Figure 2.2.

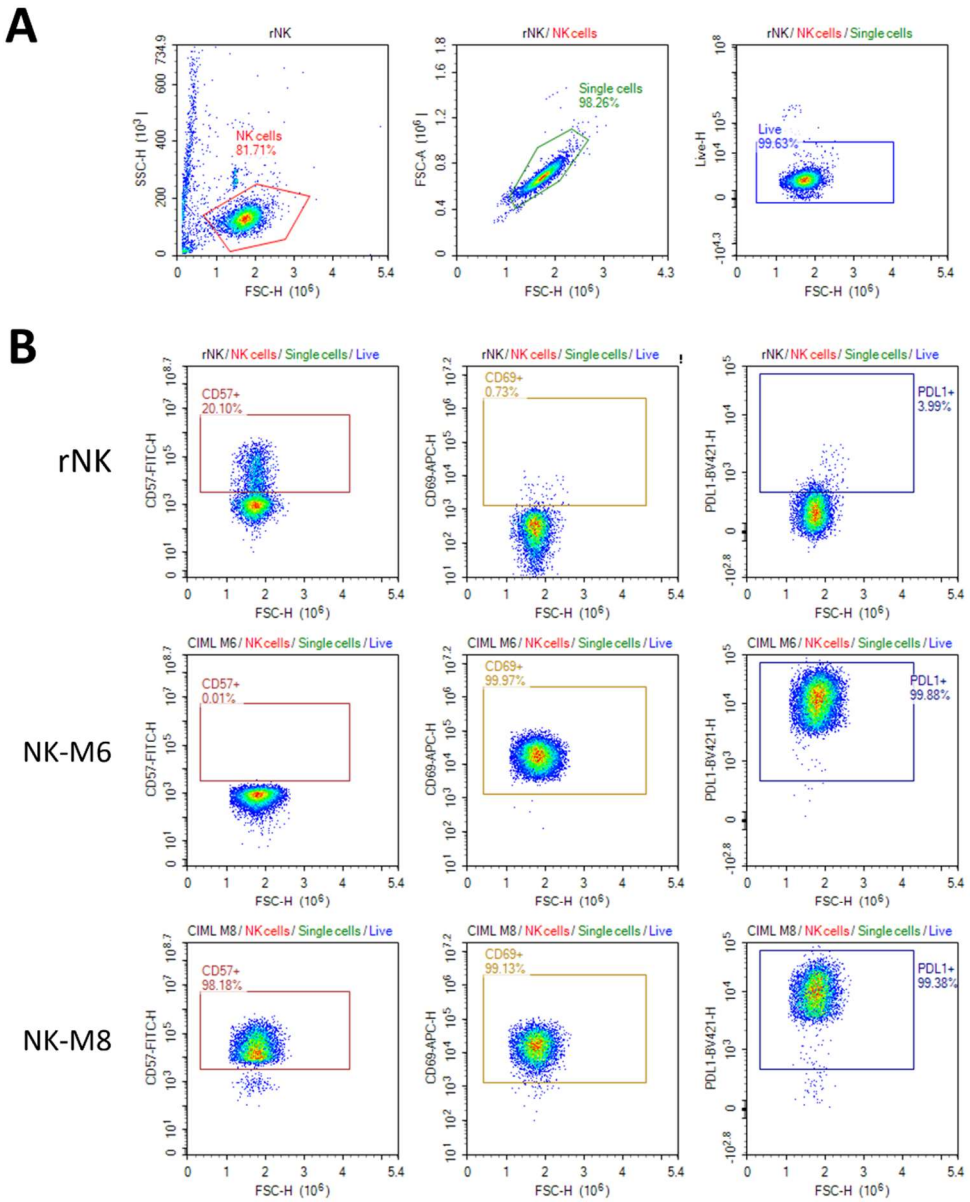

Figure 2.2 Purity of the selected NK cell populations after the cell sort

Flow cytometry plots show the purity of the sort. (A) General gating strategy for every condition. A FSC versus SSC plot was created around the cell population of interest (excluding debris). After that, the gate was projected onto a second dot plot of FSC-A versus FSC-H to select single cells. After that, single cells were projected onto a third plot showing the viability dye to select live cells. (B) Cells were then visualised for CD57, CD69 and PDL1 to visualise the purity of the sort for every condition.

2.10 Proliferation assay

Freshly isolated peripheral blood NK cells were stained with CellTrace Violet™ (Invitrogen) following the manufacturer instructions and set up on round-bottom tubes for a 5-day co-incubation with CM alone (rNK) and with INB16 at a 1:2 ratio (TpNK cells) at 37˚C, 5% v/v CO2. On day 0 and day 5, NK cells were harvested and stained with Zombie Yellow Fixable viability kit (Biolegend) to identify viable cells and with CD56-APC/Cy7 and CD3-BV650 to identify NK cells. Stained cells were acquired by flow cytometry, and NK cells were gated on the VioBlue channel to visualise cell proliferation (Figure 2.3).

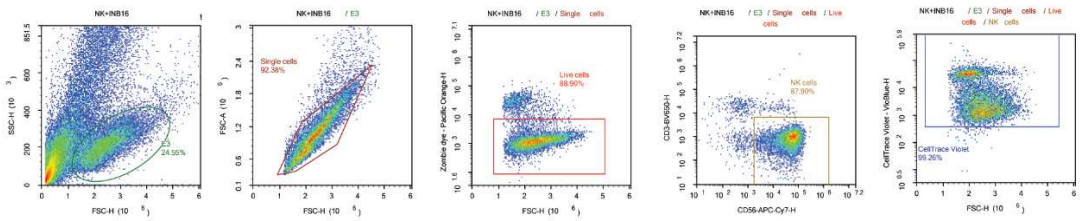

Figure 2.3 Gating strategy of the NK cell proliferation assay

Flow cytometry plots show the proliferation assay. A FSC versus SSC plot was created around the cell population of interest (excluding debris). After that, the gate was projected onto a second dot plot of FSC-A versus FSC-H to select single cells. After that, single cells were projected onto a third plot and live cells were selected, which were projected onto a fourth plot to identify NK cells as $CD56^{+}$ and $CD3^{-}$. NK cells were finally projected into a fifth plot showing the VioBlue channel to visualise the proliferation dye.

2.11 Cytotoxicity assays

2.11.1 Flow cytometry-based killing assay

Cytotoxicity assays were used to determine the capacity of NK cells to kill a given target. This was done by measuring the viability of target cells by flow cytometry after being co-incubated with effector cells.

NK cells or PBMCs were isolated and primed the day previous to the cytotoxicity assay as described before in section 2.6. An effector:target (E:T) ratio of 5:1 and a co-incubation of 4 hours were used as previously standardised in the laboratory. Effector cells were washed with HBSS by centrifugation and resuspended at a final concentration of $1.5x10^6$ cells/mL in CM. Target cells were harvested and labelled with PKH67 dye as described previously in section 2.7.1 and resuspended at a final concentration of $0.3x10^6$ cells/mL (5 times less than effector cells). Both effector and targets were co-incubated by adding 100µL of effectors (150,000 cells) and 100µL of targets (30,000) into a round-bottom 96-well plate, achieving the aforementioned 5:1 ratio. Two extra conditions were added to control for the spontaneous lysis of target cells, which included target cells at 0 hours and target cells at 4 hours. Once the plate was set up, it was incubated at 37ºC for 4 hours. At 0h and after 4h, the correspondent cell suspensions were resuspended in 10% TOPRO3 (20µL) and analysed by flow cytometry (Figure 2.4). At least 10,000 events were acquired after gating on PKH67 positive cells, and the number of TOPRO3 negative cells was determined. After, the percentage of NK cell specific lysis was calculated as the mean percentage of cell death minus the percentage of background cell death (Equation 2.1):

$$\%\ specific\ lysis = \frac{Live\ target\ cells\ at\ 0h - \quad target\ cells\ at\ 4h}{Live\ target\ cells\ at\ 0h} x100$$

Equation 2.1. Calculation of % specific lysis in a flow cytometry based cytotoxicity assay

In some experiments, the % delta lysis was calculated to visualise the change in % specific lysis in TpNK cells compared to rNK cells. The % delta lysis was calculated according to the following formula:

$$\%\ delta\ lysis = \frac{\%\ specific\ lysis\ TpNK - \%\ specific\ lysis\ rNK}{\%\ specific\ lysis\ rNK} x100$$

Equation 2.2. Calculation of % delta lysis in a flow cytometry-based cytotoxicity assay

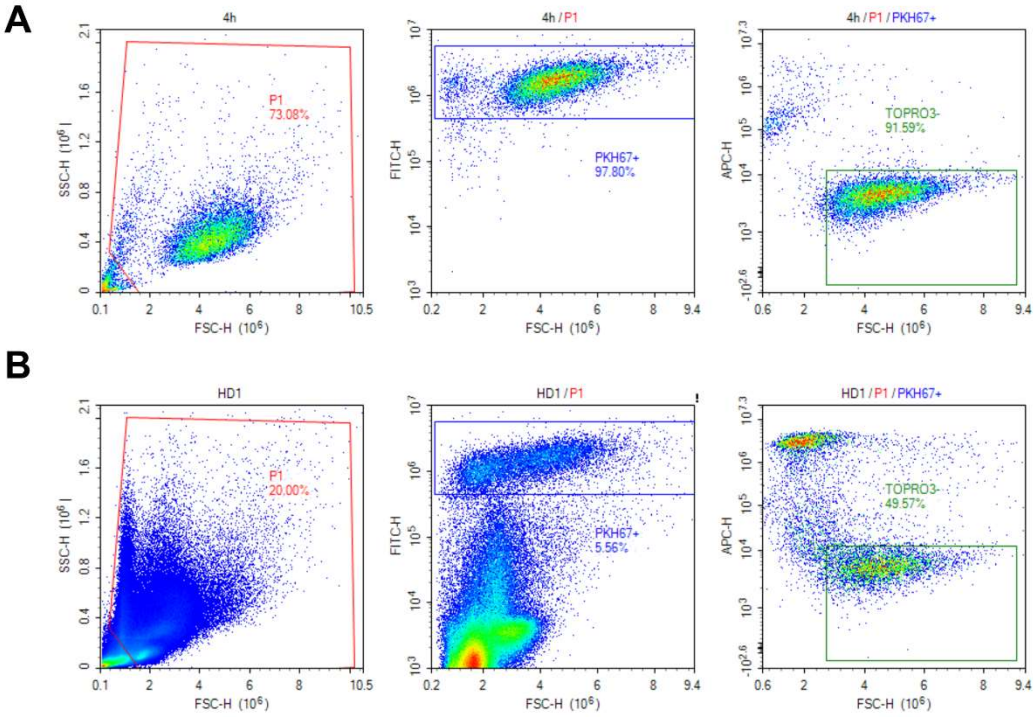

Figure 2.4. Gating strategy for a flow cytometry-based cytotoxicity assay.

Representative plots showing the gating strategy used for a cytotoxicity assay for K562 alone at 4h (A) and K562 with rNK cells at 4h (B). Target cells were labelled with PKH67 dye (FITC), and then the gate was projected into another dot plot to visualise TOPRO3 (APC). TOPRO3-negative cells were gated, and then cell concentration was obtained.

2.11.2 Real-time based killing assay (xCELLigence system)

In Chapter 4, the NK cell cytotoxic capacity of the adherent cell lines SKOV3 and DU145 was tested in the xCELLigence Real-Time Cell Analysis (RTCA) system (Agilent). The xCELLigence system utilises non-invasive electrical impedance to monitor the adherence of cells in a continuous and quantitative readout. A special microtiter e-plate is used where the bottom is fused with gold microelectrodes that allow the transmission of electrical impedance in supplemented CM, which will work as an electrically conductive solution. This technology works by measuring changes in the interaction of the electrodes/solution via the adhesion of adherent cells to the bottom of the plate. The impedance is then translated into a unitless parameter known as Cell Index, which is directly correlated with the number of viable cells (Ke et al., 2011).

From the cell index, it is possible to calculate the % cytolysis using the following formula:

$$\%\ cytolysis = \frac{(Cell\ index_{no\ effector} - Cell\ index_{effector})}{Cell\ index_{no\ effector}} x100$$

Equation 2.3 Calculation of % cytolysis in the xCELLigence system

From the % cytolysis, the area under the curve (AUC) can be calculated using the following formula:

$$AUC = \%cytolysis\ x\ hour$$

Equation 2.4 Calculation of AUC in the xCELLigence system

2.11.2.1 Basic cytotoxicity assay

The steps followed to perform a basic cytotoxicity assay on the xCELLigence system are represented in Figure 2.5. The adherent cell lines SKOV3 and DU145 were passaged the day before seeding on the xCELLigence system (day -1) so the cell density would not exceed 80% the next day. On the day of the experiment (day 0), the cell lines were harvested and resuspended at $0.1x10^6$ cells/mL, allowing for 5,000 cells in 50uL (previously optimised). To measure the background reading, 50µL of CM was added to each well of the

e-plate, after which the harvested target cells were seeded at 5,000 cells/well and let sediment for 30 minutes at room temperature before starting the reads. The adhesion and growth rate of the target cells were monitored overnight before adding the effector cells the next day (day 1).

On day 1, effector cells were harvested and set up to have an E;T ratio of 5:1. To do that, NK cells were put at the concentration of $0{,}25x10^6$ cells/mL, and 100uL of cell suspension (25,000 cells) was added to the corresponding wells on the e-plate. The e-plate was then put back into the xCELLigence system, and measurements were taken every 15 minutes for 100 hours.

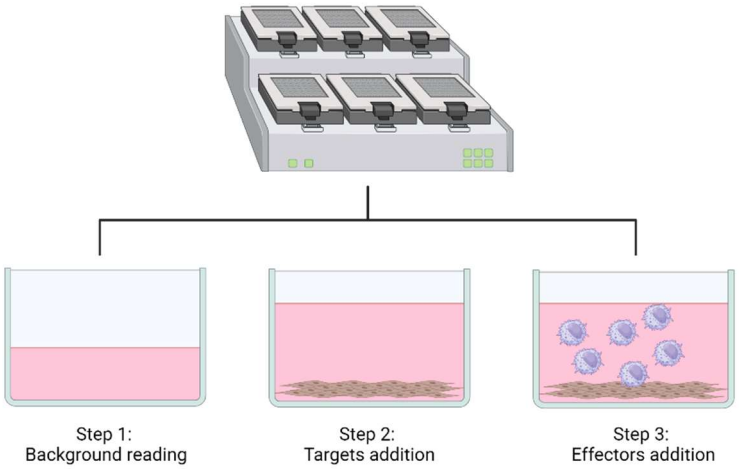

Figure 2.5 Basic cytotoxicity protocol using the xCELLigence system

Infographic showing the steps followed to perform a basic cytotoxicity assay using the xCELLigence system. Image created on Biorender.

2.11.2.2 Sequential cytotoxicity assay

The xCELLigence system (Agilent) was used to measure sequential killing. NK cells were put in the e-plate for 24 hours, and then the same NK cells were recovered and transferred into a new e-plate for another 24 hours, for a total of 3 times (Figure 2.6).

SKOV3 cells were seeded and harvested as explained in section 2.11.2.1 and seeded into an e-plate (plate 1) on day -1. On day 0, target cells were added as explained previously at an E:T ratio of 5:1 and were co-incubated for 24 hours. Also on day 0, a new e-plate (plate 2) was seeded with SKOV3 as done previously until the next day. On day 1, the NK cells on plate 1 were recovered by vigorously pipetting to detach them from target cells and seeded into plate 2, where they were co-incubated for a further 24 hours. Also on day 1, a new plate (plate 3) was seeded as previously and incubated for 24 hours. Finally, on day 2, the same procedure was repeated, where NK cells from plate 2 were recovered and transferred to plate 3 and tested for 24 hours.

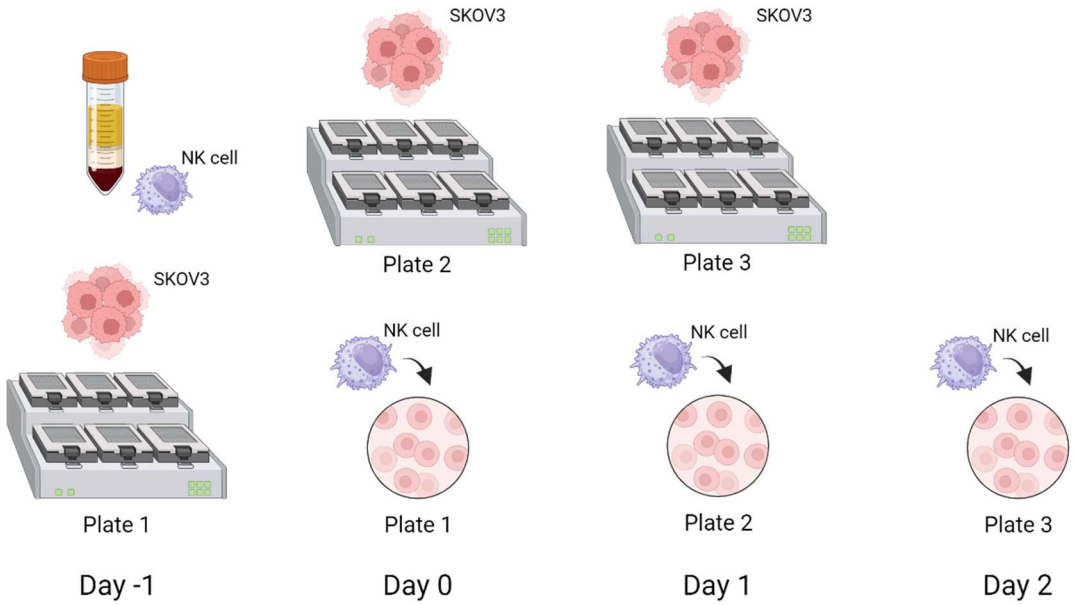

Figure 2.6 Cytotoxicity protocol to determine sequential killing using the xCELLigence system

Infographic showing the steps followed in the sequential killing cytotoxicity assay using the xCELLigence system. Image created on Biorender.

2.12 Cytokine 30-Plex Human Panel

Serum samples from the patients were acquired on the indicated days and frozen at -80^{o}C. On the day of the experiments, samples were thawed and analysed according to the manufacturer's instructions in a Cytokine 30-Plex Human Panel (catalogue number LHC6003M, Thermo Fisher), including cytokines, chemokines and growth factors. Plates were acquired with the Luminex™ platform (Thermo Fisher).

2.13 Immunophenotyping of NK cell markers

The expression of several surface and intracellular NK cell markers was analysed by utilising both conventional and spectral flow cytometry. Conventional flow cytometry detects emitted photons that will be collected into individual detectors, whereas spectral flow cytometry uses prisms to capture all the emitted light. Because all the light is collected, spectral flow cytometry provides more information for each fluorophore, allowing for increased resolution and sensitivity; fluorophores with similar emission profiles can still be differentiated, providing more possibilities in panel design.

2.13.1 Conventional flow cytometry

Four panels with different NK cell markers for activation, inhibition and maturation were created (Appendix Table 7.1). A minimum of 10^5 NK cells (pure or in PBMCs) were immunophenotyped in 4 test tubes for a total of 4 panels. Cells were washed in PBS by centrifuging, and the pellet was resuspended in 100μL of PBS. After that, cells were stained with 1μL of Zombie Yellow™ dye (BioLegend) for 15 minutes at 4^{o}C to allow for gating of viable cells. After incubation, cells were washed with staining buffer by centrifuging, and the pellet was resuspended in 100μL of staining buffer. A master mix solution was created with all the mAbs in the same panel with staining buffer to a final volume of 100μL; the solution was added, and cells were incubated for 15 minutes at 4^{o}C. Cells were then washed with staining buffer by centrifuging, and the pellet was resuspended in 100μL of staining buffer prior to acquisition. Stained cells were acquired in a Novocyte flow cytometer

(Agilent) for a minimum of 10,000 $CD56^+$ $CD3^-$ events after gating cells using FSC and SSC. Data was analysed using the NovoExpress software (Agilent).

2.13.2 Spectral flow cytometry

Spectral flow cytometry allowed for the generation of a large single panel that included 31 NK cell markers (Appendix

Table 7.2 Table 7.2); having everything in one panel presents multiple advantages like the use of less sample or also the possibility to analyse data utilising non-supervised clustering algorithms.

A minimum of $3x10^5$ purified NK cells were plated in round-bottom 96-well plates for staining. Cells were washed in PBS by centrifugation at 700xg for 3 minutes. After that, cells were resuspended in 50µL of PBS containing Live/dead Blue stain (Thermo Fischer) and incubated at room temperature in the dark for 15 minutes. When the incubation finished, cells were washed in PBS by centrifuging at 700xg for 3 minutes. A master mix solution containing all the surface antibodies with PBS was added in a final volume of 60 µL and in the presence of Brillant stain buffer (Biolegend) and Fc block (Invitrogen); cells were then incubated for 20 minutes at 4ºC. After incubation, cells were washed twice in PBS by centrifugation at 700xg for 3 minutes, and samples were fixed with Perm Fix (BD Biosciences) in the dark for 15 minutes at room temperature. Next, intracellular staining was performed by washing cells in Perm Wash Buffer (BD Biosciences) by centrifuging at 700xg for 3 minutes. The intracellular staining mix was made in Perm Wash Buffer (BD Biosciences), and cells were incubated at room temperature for 45 minutes in the dark. To finalise, cells were washed in PBS by centrifuging at 700xg for 3 minutes, and cell pellets were resuspended in 200uL of PBS. Cells were acquired using a spectral flow cytometer (Aurora, Cytek) and analysed using Flowjo (Tree Star).

2.13.2.1 Panel design

Multiple parameters were taken into consideration when designing the spectral flow cytometry panel:

Intensity of expression of the antigen and fluorochrome brightness: a literature search was performed beforehand to determine how dim or bright the marker of interest was expressed. For highly expressed markers, dimer fluorochromes were chosen as they cause less spillover; for rare markers, bright fluorochromes were chosen so that they would allow detection.

Similarity index: number that ranges from 0 to 1 that indicates how similar is the spectra of two fluorochromes; similarity indexes of >0.98 were not used together. If pairs of fluorochromes had very high similarity indexes, then markers that were not co-expressed together were chosen. To assess the similarity index, the Cytek Full Spectrum Viewer tool was used (https://spectrum.cytekbio.com) (Figure 2.7).

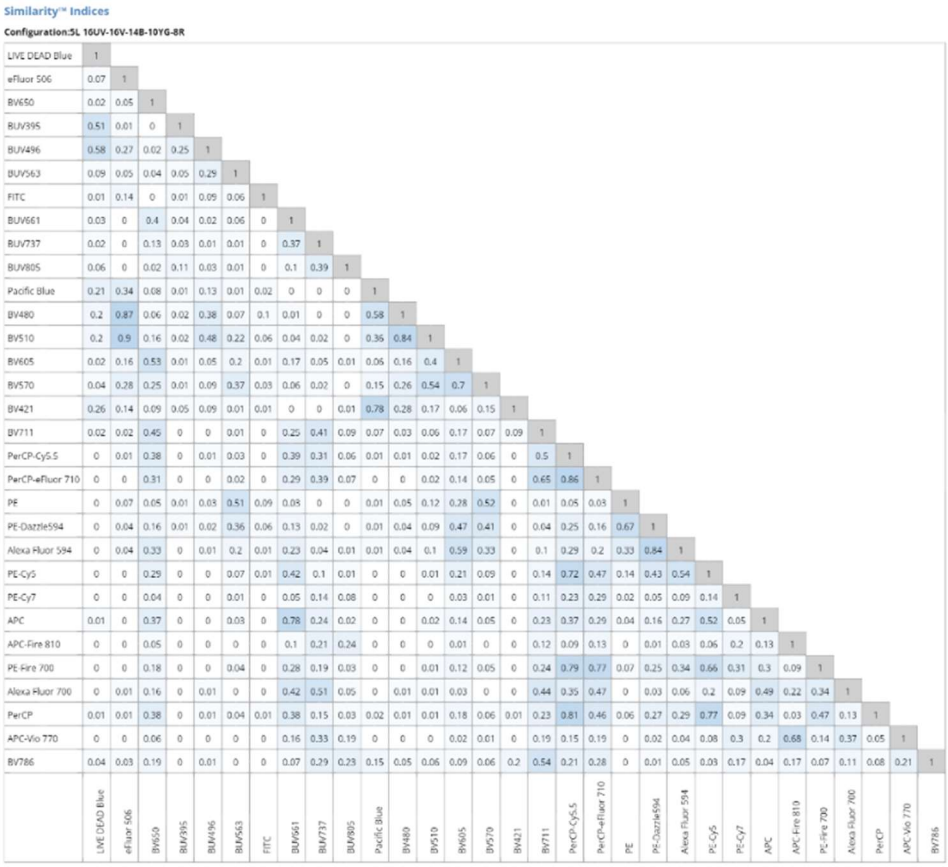

Figure 2.7. Similarity indexes among the flow cytometry panel fluorochromes

Similarity index was assessed using the Cytek Full Spectrum Viewer tool (https://spectrum.cytekbio.com).

Complexity index: overall measure of the uniqueness of all the dyes in the panel. A reference number has not been determined, but it is advisable to use lower indexes. The complexity index was assessed using the Cytek Full Spectrum Viewer tool (https://spectrum.cytekbio.com).

After designing the panel, the antibodies were titrated to determine the optimal staining intensity. The manufacturer's recommended staining volume was tested, followed by subsequent dilutions of the antibody, to a total of five. After that, the median fluorescence (MeFI) of each fluorochrome was obtained and plotted, and the optimal staining concentration was selected (Figure 2.8).

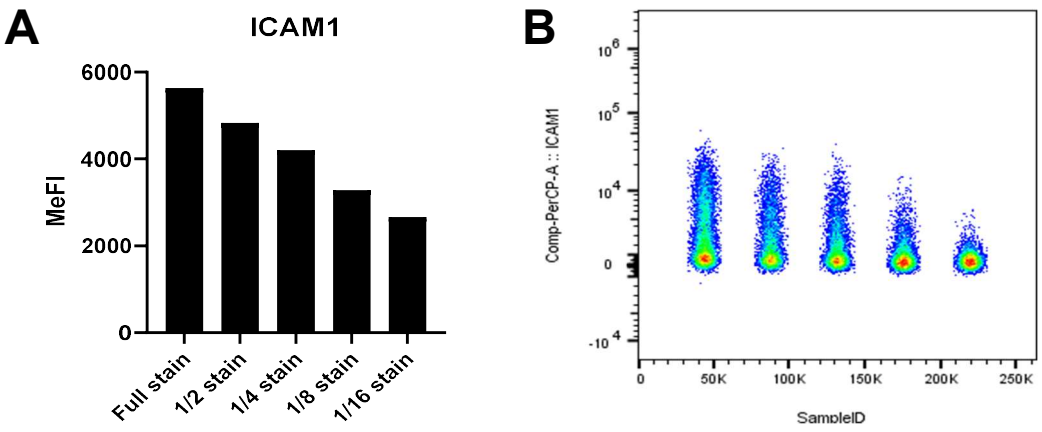

Figure 2.8. Representative example of the titration of ICAM1

A) MeFI of the different staining dilutions. B) Flow cytometry plots showing the different staining indexes.

Because of the complexity of the panel, single stained controls were performed to determine whether the individual fluorochromes mixed in the whole panel looked similar to single stained controls. Accordingly, different NK cell samples were stained for the whole panel and each individual marker. The obtained data was analysed using Flowjo (Tree Star) by overlaying histograms of the single stained control and the whole stained sample to look at the similarities of the spectra (Figure 2.9).

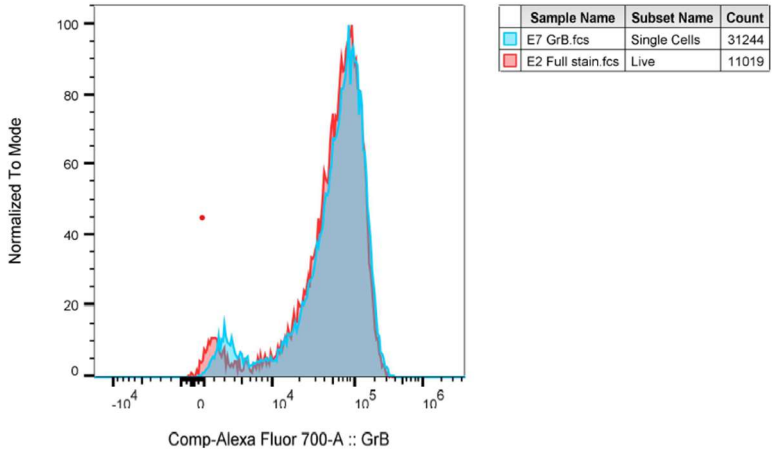

Figure 2.9. Representative histogram of full stained control overlayed with single stained control

Staining of the corresponding marker in the whole panel was overlaid with the staining of the same fluorochrome in a single stain control. Spectra was plotted in a histogram to look at the overlay of both markers using FlowJo (Tree Star).

2.13.2.2 Data analysis of multi-parameter flow cytometry

I used unsupervised multidimensional analysis to evaluate the co-expression of different NK cell markers with similar phenotypical characteristics using different algorithms in Cytobank (www.cytobank.org). The visual interactive Stochastic Neighbour Embedding (viSNE) algorithm allows the visualisation of high-dimensional single-cell data based on the t-Distributed Stochastic Neighbour Embedding (tSNE) algorithm; this generates 2-dimension plots where the positions of cells reflect their proximity in the high-dimensional space. The colour of the plot represents the density of expression. NK cells were manually gated for singlets, live cells and $CD56^{+}$ $CD3^{-}$ (Figure 2.10); after that, viSNE analysis was performed on 30 parameters on 3 concatenated donors and equal sampling. The settings used were 1,000 iterations and perplexity 30. I used the FlowSOM algorithm to identify clusters based on the viSNE results. The algorithm was run with equal event sampling; the Cytobank's default parameters were used, which include 10 metaclusters, 100 clusters, a cluster size of 100 and 10 iterations.

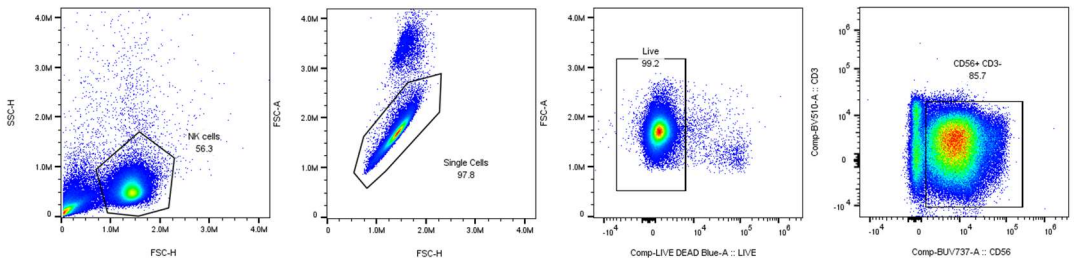

Figure 2.10. Spectral flow cytometry gating strategy

A FSC versus SSC plot was created around the cell population of interest. After that, the gate was projected onto a second plot of FSC-H versus FSC-A to identify single cells from doublets. From that, a third plot was projected showing FSC versus Live/Dead Blue staining where the negative population (live) was selected. To finalise, a fourth plot was projected of CD56 versus CD3 to identify NK cells as $CD56^{+}$ $CD3^{-}$.

2.14 Immunophenotyping of NK cell ligands in cancer cells

I determined the expression of NK cell ligands on the surface of cancer cells to investigate the differences in NK cell sensitivity. Three panels including ligands involved in activation and inhibition of NK cells were developed (Appendix Table 7.3). A minimum of 10^5 cancer cells were immunophenotyped for each panel. Cells were placed in polycarbonate tubes, washed with staining buffer by centrifuging, and pellet resuspended in 100µL of staining buffer. A master mix containing all the antibodies in every panel was created in a final volume of 100µL. The master mix was added, and the cells were incubated for 15 minutes at 4^{o}C. After that, cells were washed again to remove unbound antibodies by centrifuging with staining buffer. To finalise, cell pellets were resuspended in 100µL of staining buffer before acquisition. Stained cells were acquired in a Novocyte flow cytometer (Agilent) for a minimum of 10,000 using FSC and SSC. Data was analysed using the NovoExpress software (Agilent).

2.15 Proteomics analysis

I looked at the proteomics signature of NK cells treated with different conditions. Levels of mRNA do not always correspond to levels of protein; thus, proteomics may be a more powerful tool for measuring changes in cells

(Y. Liu et al., 2016). Cells were treated overnight with different stimuli and the next day were depleted from the overnight stimuli, as explained in section 1.8, by removing dead cells and positive sorting the NK cells (all conditions were treated equally to allow for comparison between them). After that, cells were checked for purity and yield and washed with ice-cold PBS twice by centrifuging. The pellet was then dried and transferred to -80^{o}C. Frozen cell pellets were shipped on dry ice for mass spectrometry proteomics analysis to Biognosys AG.

Data analysis of the proteomics data was carried out by Byognosis AG. For that, protein intensities for each protein were analysed for testing the differential protein abundance using a two-sample t-test. P-values were corrected for overall false discovery rate using the q value approach. The q value is a measure of significance in terms of false discovery rate rather than false positive rate, avoiding false positive results (Storey & Tibshirani, 2003). The distances in heatmaps were calculated using the “Manhattan” distance method, a mathematical formula-based model to measure the distance between data points. Gene Ontology (GO) enrichment analysis to identify biological processes, molecular functions and cellular components was performed in Spectronaut software (Biognosys AG) using a human gene associations file obtained from the European Bioinformatics Institute (2016-10-03). Only terms with a minimum of 2 members were considered.

2.16 Assessment of mitochondrial function

2.16.1 Extracellular flux assays

NK cells were seeded at 3x10^{5} cells per well in Seahorse cell plates pre-coated with CellTak (Corning). NK cells were incubated for 45 minutes in a CO_2-free incubator at 37°C before loading the plate in a Seahorse analyser (Agilent). The oxygen consumption rate (OCR) and extracellular acidification rate (ECAR) were measured in XF RPMI medium supplemented with 10mM glucose, 1mM pyruvate and 2mM glutamine in response to oligomycin (1µM), FCCP (1.5µM), rotenone/antimycin A (0.5µM) and 2-DG (50mM) (Agilent). Maximum respiration is the average OCR value post-FCCP injection. The spare respiratory capacity (SRC) was as the OCR values post-FCCP injection

minus basal OCR. Glycolysis was calculated as the basal ECAR values minus post-2-DG injection values. Glycolytic reserve was calculated as post-rotenone/antimycin A injection ECAR values minus basal ECAR values.

2.16.2 Mitochondrial depolarisation assay

Mitochondrial membrane potential was assessed by measuring tetramethylrhodamine methyl ester (TMRM) staining by flow cytometry. NK cells were stained with TMRM at 25nM (Sigma Aldrich) according to manufacturer's instructions. After a 30-minute incubation, cells were washed with PBS and subjected to surface staining as described in section 2.5. After that cells were stained with LIVE/Dead™ Fixable Aqua (Thermo Fischer) according to manufacturer's instructions. Samples were acquired on a BD Fortessa X20 flow cytometer and analysed using FlowJo (Tree Star).

2.17 Conjugate formation assay

The conjugate formation assay was used to determine the number of conjugates occurring between rNK cells and rNK or TpNK cells.

NK cells were freshly isolated and divided into two groups: the first one was cultured in CM to generate rNK; the second group was co-incubated with INB16 lysates at a ratio 1:2 stimulator:responder to generate TpNK cells. Cells were incubated overnight at 37^{o}C. The following day, TpNK cells were washed by centrifugation 3 times to remove lysates (rNK cells were treated equally for comparison). Cells were counted, and rNK cells were further divided into 2 groups, the first half was labelled with CellTrace™ Violet (CTV) dye and the second half with CellTrace™ CFSE (CFSE) dye. All TpNK cells were labelled with CellTrace™ Violet. After that, cells were set up at the concentration of $2.5x10^{6}$ cells/mL and 100uL of cell suspension were added at a 1:1 ratio into a round-bottom tube to have the following conditions: rNK(CFSE):rNK(CTV) and rNK(CFSE):TpNK(CTV). Cells were incubated at 37^{o}C for 0, 15, 30, 45 and 60 minutes, and when each timepoint was met, cells were gently vortexed and fixed with 0.5% paraformaldehyde. Forming conjugates were defined as $CFSE^{+}$ CTV^{+} double-positive on the flow cytometer. Samples were acquired in the flow cytometer (Novocyte, Agilent), and the stopping gate was set at

10,000 events in the double positive CFSE$^+$ CTV$^+$ gate (Figure 2.11). Data was analysed using the NovoExpress software (Agilent).

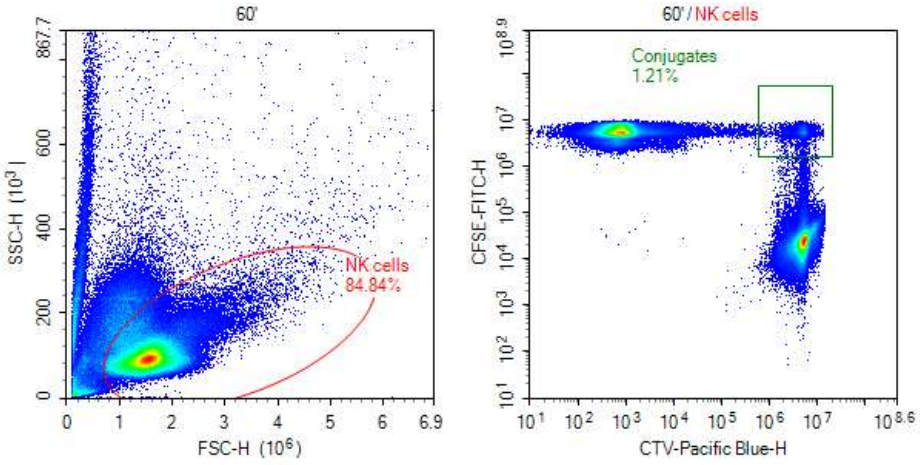

Figure 2.11. Gating strategy for the detection of conjugates with flow cytometry

NK cells were gated on the FSC/SSC and after that a plot was projected for CTV and CFSE axis. Conjugates were gated as CFSE$^+$ CTV$^+$ double-positive.

2.18 Calcium flux measurements

The Calcium Flux Assay Kit (Abcam) is a fluorescence-based assay for detecting intracellular calcium mobilisation using a flow cytometer. I used this method to determine if there would be changes in calcium flux in rNK cells when co-incubating them with TpNK cells.

NK cells from fresh blood were isolated as indicated and set up overnight with INB16 at a 1:2 ratio to generate TpNK cells; NK cells were also incubated with CM to have rNK cells.

The next day, part of the rNK cells were labelled with CellTrace Violet™ (Thermo Fisher) as previously indicated. After that, rNK cells were labelled with the 520AM dye as indicated by the manufacturer; rNK cells were prepared in 0.5mL in Assay Buffer (Abcam) at the cell density of 1x10^6 – 2x10^6 cells/mL. After that, the 520AM dye (Abcam) was prepared right before usage by adding 100µL of DMSO into the vial containing the dye; then, 1µl of 520AM dye was

added into the 0.5mL of cell suspension and incubated at 37º for 30 minutes. After that, rNK cells were centrifuged at 300G for 5 minutes to remove the dye and resuspended in 0.4mL of HBSS (with 20 mM HEPES).

Once the rNK cells were labelled with the 520AM dye, the leftover rNK cells and TpNK cells used as stimulatory agents were prepared. I added an additional positive control of 2µg/mL ionomycin, which is known to induce calcium mobilisation (Pinton et al., 2008). According to the protocol, the stimulatory agents are added 5x concentrated.

Resting NK cells was analysed first in the flow cytometer before the addition of the stimulatory agents. Resting NK cells were acquired for 30 seconds; after that, 100µL of rNK cells, TpNK cells or ionomycin were added to the tubes. The sample containing ionomycin was analysed immediately after addition for further 20 minutes. The samples containing rNK cells or TpNK cells as stimulatory agents were incubated for 50 minutes and then were acquired in the flow cytometer for a further 2 minutes. Samples were acquired in a Novocyte flow cytometer (Agilent) and analysed using NovoExpress (Agilent). The flow cytometry gating strategy is shown in Figure 2.12.

Calcium flux increase was calculated by obtaining the median fluorescence intensity of the dye before and after the addition of stimulation. After that, the delta increase was calculated with the following formula:

$$Delta\ increase = \frac{(Flux\ after\ stimuli - flux\ before\ stimuli)}{Flux\ before\ stimuli} x100$$

Equation 2.5 Calculation of the delta increase in calcium flux by NK cells

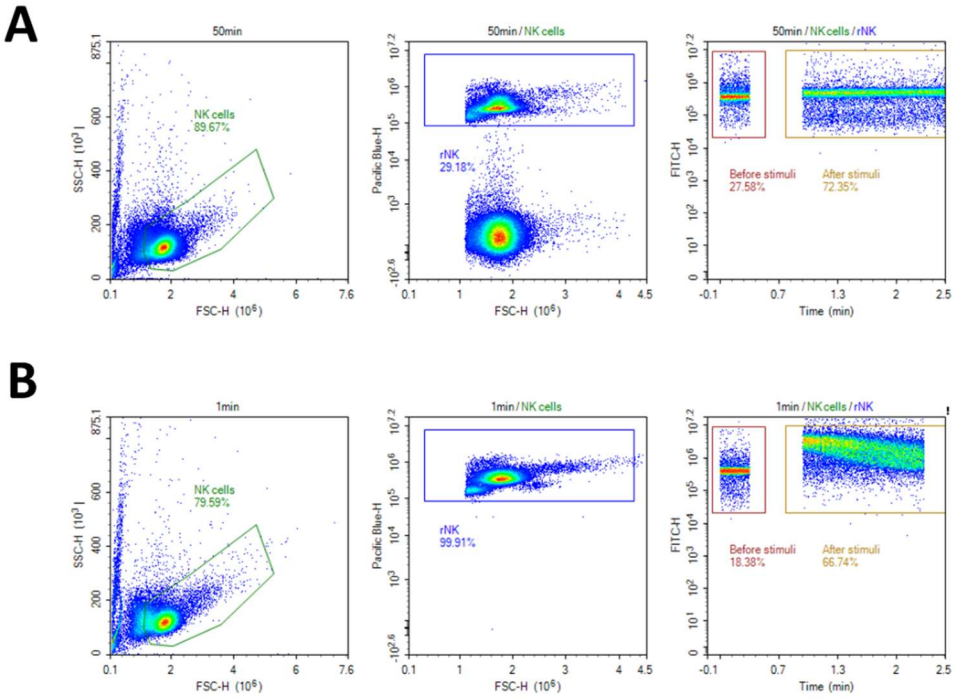

Figure 2.12. Gating strategy for calcium flux analysis in NK cells

The NK cell population was visualised in the FSC vs SSC plot, which was after projected into a FSC vs Pacific Blue plot to gate the rNK cells which were labelled with CellTrace Violet™; the rNK cell gate was then projected into a third plot showing time in the X axis and the FITC channel in the Y axis, to visualise calcium changes over time. Representative flow cytometry plots of (A) rNK incubated with other rNK cells and (B) rNK cells incubated with ionomycin (positive control).

2.19 NK cell imaging

NK cell homotypic interactions were visualised by both live cell imaging and confocal microscopy.

2.19.1 Live imaging: Nikon CT Biostation

The Nikon CT Biostation (Nikon) is a fluorescence microscope that is built on an incubator, therefore it allows to image cells live. The plates analysed were read at a 10x magnification, and images were taken every 15 minutes for a period of 16 hours. A ratio of 1:1 was used, and NK cell density was optimised

to 2,000 cells per condition (2,000 rNK to 2,000 rNK or 2,000 rNK to 2,000 TpNK) on a 96-well flat-bottom plate and run in duplicates.

NK cells were freshly isolated from PBMCs, and half of the obtained population was labelled with PKH26 dye (Sigma-Aldrich) as indicated in section 2.7.1. After that, NK cells were set up for overnight co-incubation to obtain the following conditions: rNK cells unlabelled, rNK cells labelled with PKH26, and TpNK cells primed with INB16 lysate labelled with PKH26. The following day, cells were washed three times with HBSS by centrifugation to remove the lysates (all conditions were treated equally to allow for comparison) and were counted and set up at the concentration of $0.02x10^6$ cells/mL. After that, NK cells were plated in a 96-well flat-bottom plate to a final number of 4,000 cells per condition by co-incubating at a 1:1 ratio, containing 2,000 rNK cells unlabelled with 2,000 rNK cells PKH26 labelled; the second condition set up contained 2,000 rNK cells unlabelled with 2,000 TpNK cells PKH26 labelled. Once cells were plated, the plate was placed inside the Nikon CT Biostation (Nikon) for a period of 16 hours. Images were taken every 15 minutes at an x10 magnification and the resulting images were analysed in ImageJ. For analysis, cell contacts were enumerated when 2 cells were coming together and their membranes were touching (Figure 2.13); if cells were separating and coming together again this was counted as a separate contact.

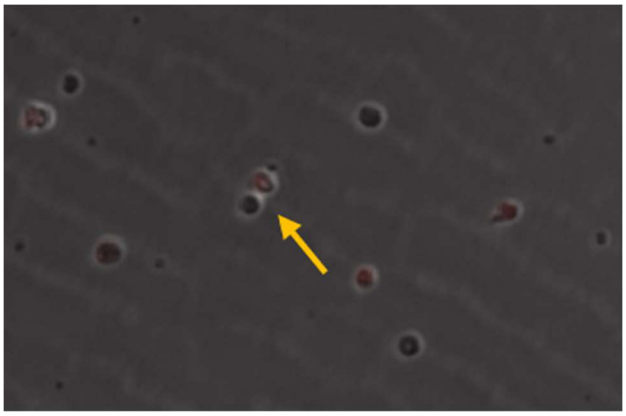

Figure 2.13. Representative image of a cell-cell interaction in a Nikon CT Biostation

Image shows two NK cells in contact. One cell is labelled with PKH26 dye (red colour), and the other cell is unlabelled.

2.19.2 Confocal imaging

Confocal imaging was used to visualise NK-NK interactions since it allows for higher-resolution images compared to other types of microscopy.

2.19.2.1 General preparation of slides

The protocol for general preparation of slides was designed by combining different protocols for confocal imaging (Campbell, 2010; Orange et al., 2003).

Fresh or frozen NK cells were used for confocal imaging and set at a concentration of $5x10^6$ cells/mL. For co-incubation experiments, stained rNK cells or TpNK cells (cells were stained as indicated in sections 2.19.2.2 and 2.19.2.3) were mixed in a 96-well round-bottom plate at a 1:1 ratio (times will vary depending on the experiment, between 15 minutes and 1 hour).

After, 50µL of cell suspension was added to a poly-L-lysine-coated glass slides (Sigma-Aldrich) at 37°C and incubated until CM was dry. Once the slide was dry, it was dipped 3 times into a 50mL Falcon tube containing PBS to remove cells that did not adhere. After that, 100µL of 4% paraformaldehyde was added to the slide to fix cells for 15 minutes at room temperature in the dark. The slide was again dipped 3 times into a 50mL Falcon tube containing PBS and gently blotted into a tissue. After that, 1 drop of mounting media (ProLong Gold antifade reagent (Invitrogen)) was added to the staining region using a Pasteur pipette and a coverslip was added on top, making sure no bubbles were forming. Slides were then left to dry overnight in the dark and stored at 4ºC before visualisation.

2.19.2.2 Staining of cells with CellTracker™

For visualisation, NK cells were labelled with different dyes depending on the experimental set up.

CellTracker™ Green CMFDA (Invitrogen) is a fluorescent dye that diffuses through the cell membrane into the cell with green excitation/emission spectra. NK cells were set up at the concentration of 10^6 cells/mL in serum-free CM. The dye concentration was optimised to 5µM (Figure 2.14) and incubated for 20 minutes at 37ºC.

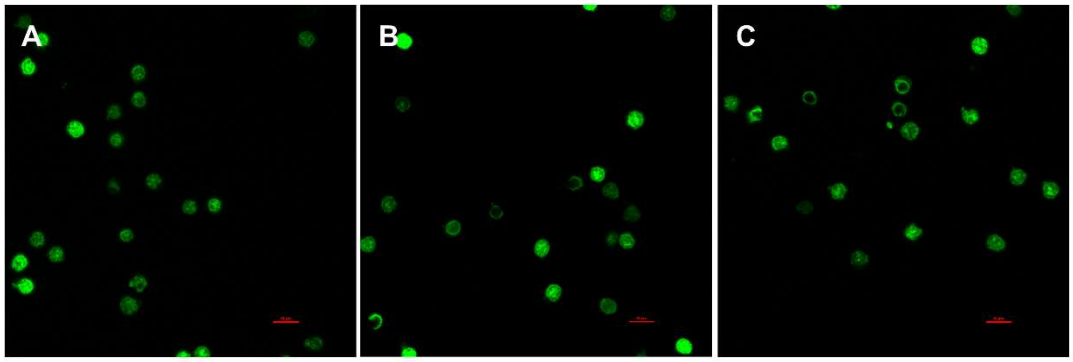

Figure 2.14. Optimisation of CellTracker™ Green CMFDA (Invitrogen) concentration.

Concentrations of (A) 0.5μM, (B) 2μM and (C) 5μM were tested.

CellTracker™ Orange CMRA (Invitrogen) is a fluorescent dye that diffuses through the cell membrane into the cell with an orange excitation/emission spectra. NK cells were set up at the concentration of 10^6 cells/mL in serum-free CM. The dye concentration was optimised to 7.5μM (Figure 2.15) and incubated for 20 minutes at 37°C.

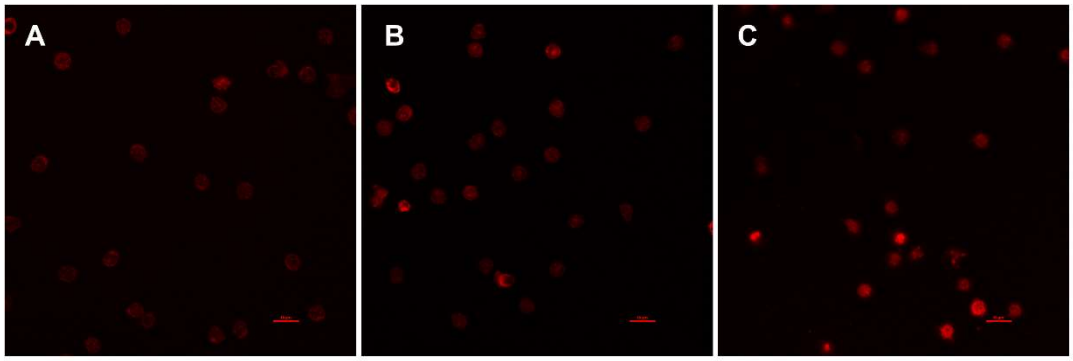

Figure 2.15. Optimisation of CellTracker™ Orange CMRA (Invitrogen) concentration.

Concentrations of (A) 2μM, (B) 5μM and (C) 7.5μM were tested.

2.19.2.3 Actin and nuclear staining

For the visualisation of actin I used the Alexa Fluor 568 phalloidin kit (Invitrogen) and the NucBlue™ Fixed Cell Stain ReadyProbes™ reagent (Invitrogen) for nuclear staining. Cells were prepared following the general method for slide preparation (section 12.2.1) with the difference that after fixing the cells with 4% paraformaldehyde, cells were washed x3 in PBS and permeabilised in 0.1% Triton™ X-100 detergent (Thermo Fischer) for 15 minutes at room temperature. After that, cells were washed again x3 with PBS and x3 concentrated actin solution was prepared (previously optimised (Figure 2.16)) in PBS+1%BSA, adding 200µL of solution to the slides and incubating for 30 minutes at RT. Slides were washed x3 with PBS, and 2 drops of NucBlue™ Fixed Cell Stain ReadyProbes™ reagent (Invitrogen) were added to stain the nucleus for 5 minutes at room temperature in the dark. To finalise, slides were washed x3 with PBS, blotted carefully on a tissue, and one drop of mounting media and a coverslide were mounted on top. Slides were stored in the dark at 4^{o}C until they were imaged, after which they were stored long-term at -20^{o}C.

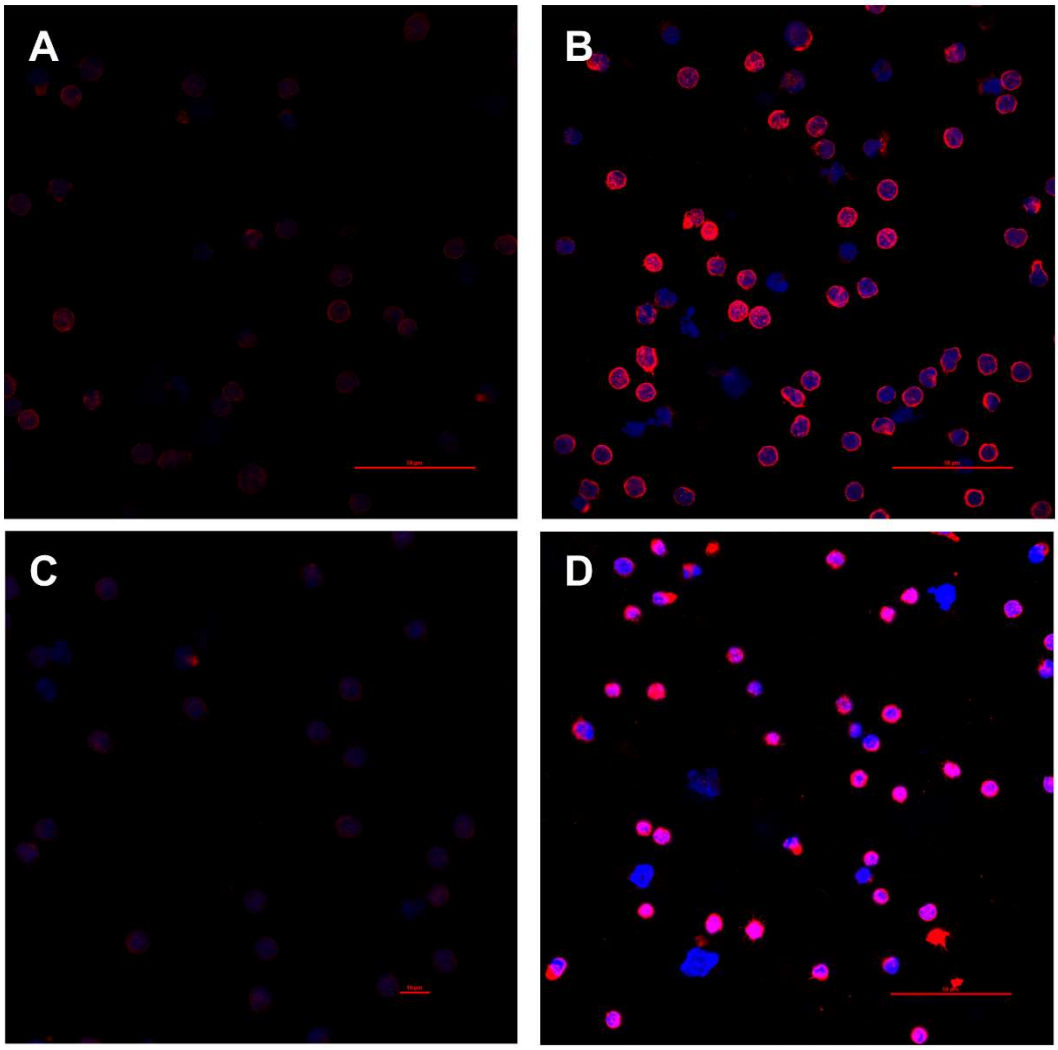

Figure 2.16. Optimisation of actin and nuclear staining

NK cells were stained for actin with Alexa Fluor 568 phalloidin kit (Invitrogen) in colour red and for the nucleus with NucBlue™ Fixed Cell Stain ReadyProbes™ reagent (Invitrogen) in blue. Dyes were tested at different times and concentrations; A) 30 minutes x1 concentrated; B) 30 minutes x3 concentrated; C) 60 minutes x1 concentrated; D) 60 minutes x3 concentrated.

2.19.2.4 Optical configuration of the microscope

The microscope used for this project was a Nikon Ti Eclipse C2 laser scanning confocal microscope driven by NIS Elements software (Nikon). This microscope can image 4 colours per experiment with excitation lasers being DAPI (405nm), GFP (488nm), RFP (561nm) and Far Red (637nm); the

emission filters being DAPI/Cy5 dual, GFP (525/50nm) and RFP (595/40nm). The objectives available were 10X Plan Fluor DLL air, 20X Plan Apo λ air, 40X S Plan Fluor air, 40X Plan Apo λ air and 60X Apo λS oil. The size of NK cells is 6-7μm therefore, the 40X and 60X objectives were mostly used in to visualise NK cells.

NK cells were visualised at around 3,300μm in the Z axis, where fine tuning was performed to ensure defined images. The following optical configurations were saved as default and were finely adjusted for every individual experiment: laser intensity was set up at 2%, HV at 100 and offset (contrast) between -3 and -10. Live scanning was kept at the minimum possible to avoid photobleaching. Images were analysed using NIS Elements software (Nikon).

2.20 Statistical analysis

All statistical analysis was carried out in Graph Pad Prism 10. Different tests were performed depending on the nature of the data obtained (Figure 2.17). Normality of the data was checked prior to statistical analysis. For comparisons of two independent groups, the paired t-test was used to compare parametric data; for non-parametric data, the Mann-Whitney test was used to compare unpaired data and the Wilcoxon test was used to compare paired data. For comparisons between more than 2 groups, a 1-way ANOVA was used for parametric data; for non-parametric data, the Kruskal-Wallis 1-way ANOVA was used to compare unpaired data, and the Friedman 1-way ANOVA was used to compare paired data. Differences were considered significant at $P < 0.05$, and P values denoted with asterisks as follows: $*P < 0.05$, $**P < 0.01$, and $***P < 0.001$.

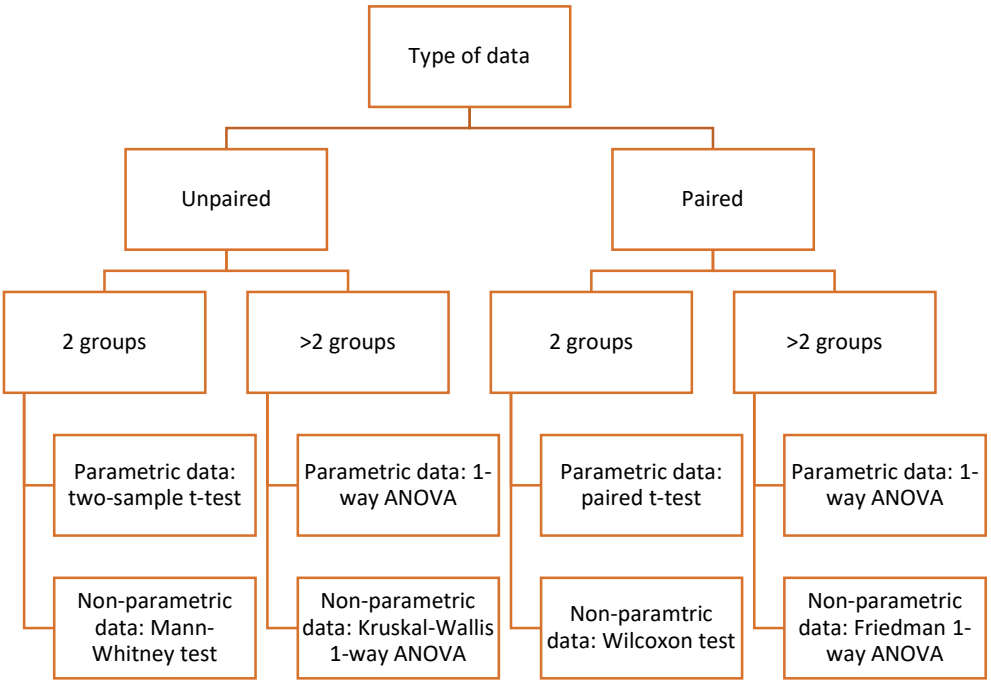

Figure 2.17. Decision tree for statistical analysis of continuous data

Chapter 3 In-depth characterisation of the phenotype and proteome profile of tumour-primed NK cells

3.1 Introduction

Since the discovery that NK cells could acquire memory-like characteristics in a mouse model of CMV infection (J. C. Sun et al., 2009), many other types of memory NK cells have been identified (Pal et al., 2017; Romee et al., 2012). Although adaptive and CIML-NK cells have been thoroughly investigated, memory NK cells developed in the context of tumour-priming remain far less studied.

Phenotypically, adaptive NK cells have been characterised by being NKG2C^{+}, CD57^{hi}, CD25^{hi}, NKG2A^{-} and FCεRγ^{-} (Béziat et al., 2013; Foley et al., 2012; Lopez-Vergès et al., 2011b; J. C. Sun et al., 2009). CIML-NK cells have been described as CD25^{hi} CD94^{hi} NKG2A^{hi} CD69^{hi} NKp46^{hi} (Cooper et al., 2009; Romee et al., 2012, 2016). This is in keeping with the phenotype of highly activated and differentiated cells.

The generation of tumour-primed NK cells has been defined by the Lowdell group and others (Dufva et al., 2023; North et al., 2007; Pal et al., 2017), suggesting that tumour-priming can induce the formation of memory-like NK cells (Pal et al., 2017). As previously reported by the Lowdell lab, NK cells that are primed overnight by exposure to the ALL cancer cell line CTV-1, or its cloned daughter cell line INB16, are phenotypically CD69^{high}, CD25^{high}, CD16^{low}, NKG2D^{low}, and DNAM1^{low} (Sabry et al., 2019). Pal and colleagues reported the generation of tumour-memory NK cells by tumour-priming with ALL and AML cell lines; these NK cells were tumour-primed overnight and then rested for one week in the presence of low-dose cytokines in order to allow for the generation of memory features. These tumour-memory NK cells were characterised by their expression of CD56^{bright}, CD94^{hi}, CD16^{hi}, CD57^{int}, KLRG1^{int} and iKIR^{int} (Pal et al., 2017). Recently, Dufva and colleagues reported the effects of exposing NK cells to various haematological cancer cell lines to identify determinants of NK cell resistance and susceptibility (Dufva et

al., 2023). They identified a shift in the transcriptomic signature of NK cells from a resting to an activated state with different changes in the receptor expression depending on the target cell utilised. It is apparent that when NK cells come into contact with a cancer cell, NK cells are differentially “imprinted” generating a distinct signature depending on the cancer target cells used for priming.

Despite these recent advances, memory-NK cells arising from the interaction with cancer cells remains ill defined. Here, I studied the initial events leading to the generation of memory in both TpNK and CIML-NK cells by studying their phenotype and proteomic profile to identify commonalities and differences that could be used to better define NK cell memory.

3.2 Experimental aims

In order to study the initial events leading to NK cell memory, different types of stimulated NK cells were generated. TpNK cells were generated by exposing NK cells to the cancer cell line INB16 (1:2 ratio) overnight; CIML-NK cells were generated by exposing NK cells to the cytokine cocktail IL-12/15/18 overnight. For comparison purposes, NK cells were also exposed to low-dose IL15 overnight. The specific aims of this chapter were:

1. Characterise the phenotype of tumour-primed NK cells compared to IL15-activated NK cells and CIML-NK cells, utilising a multi-parameter flow cytometry panel including markers of activation, maturation, inhibitory and adhesion molecules

2. Identify receptor co-expression patterns amongst differentially primed NK cells to identify shared subpopulations/clusters with memory characteristics

3. Characterise the proteomic profile of tumour-primed NK compared to IL15-activated NK cells and CIML-NK cells to identify signature proteins that might further define NK cell memory

3.3 Results

3.3.1 Study of NK cell receptor expression

A well-curated 30-colour phenotypic panel was used to investigate the expression of different surface molecules in TpNK cells, CIML-NK cells, and IL15-activated NK cells compared to rNK of purified NK cells from 3 different healthy donors. This includes NK cell markers for activation (CD16, CD25, CD69, NKG2D, TRAIL), maturation/differentiation (CD57), inhibitory molecules/checkpoint inhibitors (PD-L1, LAG3, TIM3) and adhesion molecules (CD62L, ICAM1). Manual flow cytometry gating was done to identify the % expression and median fluorescence intensity (MeFI) of the positive population of every marker. Furthermore, I also used an unbiased method using optimised t-distributed stochastic neighbour embedding (viSNE) dimensionality reduction (Van der Maaten & Hinton, 2008). This high granularity analysis allowed the identification of unique or shared subpopulations depending on each priming condition relative to resting NK cells.

3.3.1.1 Activating receptors

3.3.1.1.1 CD16

CD16 is an NK cell marker of activation and is required to mediate ADCC. Its downregulation marks NK cell activation (Grzywacz et al., 2007; Romee et al., 2013) and is also needed to induce NK cell serial killing (Srpan et al., 2018). In the viSNE plots (Figure 3.1 A), CD16 is highly expressed on rNK, IL15-activated NK cells and TpNK, but significantly reduced in CIML-NK which cluster differently to the other conditions. These changes are also reflected in percentage expression shown in Figure 3.1 B; rNK, IL15-activated NK, and TpNK cells show high expression of CD16 (~90%), and CIML-NK cell expression is downregulated (~55%). MeFI is shown in Figure 3.1 C, where there is a slight reduction in TpNK cells and a more prominent reduction in CIML-NK cells compared to rNK cells.

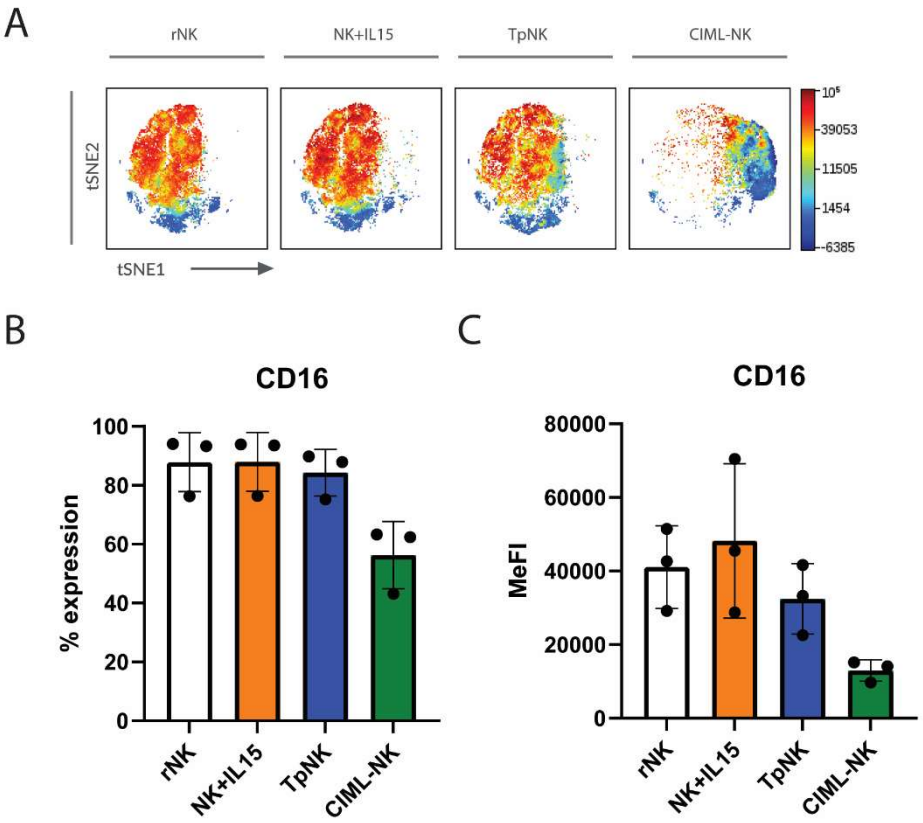

Figure 3.1. CD16 expression by resting and memory-like NK cells

(A) viSNE plots show the expression of CD16 across the indicated types of NK cells. Each point on the viSNE map represents a single cell, and colour depicts the intensity of protein expression. (B, C) The bar chart shows the analysis of (B) % expression and (C) MeFI of the positive population. Bars represent the means ±SD of 3 different donors indicated by the dots. Comparisons were made between rNK and the different stimulatory conditions using the Kruskal-Wallis 1-way ANOVA with Dunn's multiple-comparison test for non-parametric distributions. Statistical significance is indicated as: *P <0.05: **P <0.01: ***P <0.001. The absence of an asterisk indicates non-significance.

3.3.1.1.2 CD25

The IL2 receptor (IL2-R) in humans is composed of the IL2/15Rβ-chain (CD122) and the common γ-chain (CD132), which can respond to high concentrations of IL2. The formation of the high-affinity IL2 receptor demands the formation of a trimer, with the addition of the IL2-Rα chain or CD25. This

increases the affinity for IL2, which drives proliferation and enhanced cytotoxicity (Caligiuri et al., 1990, 1993; S.-H. Lee et al., 2012; Minami et al., 1993).

In the viSNE analysis (Figure 3.2 A), both rNK cells and IL15-activated NK cells show very low levels of expression of CD25; the increase in CD25 expression on TpNK cells is confined to the appearance of a new population/cluster (Figure 1.2A); by contrast, CIML-NK cells show high expression of CD25. An upregulation in % expression of CD25 in both TpNK cells (~35%) and CIML-NK cells (~100%) is noted (Figure 3.2 B), and similar changes are observed in the expression of the MeFI (Figure 3.2 B). These data are in keeping with previous observations in TpNK cells (Sabry et al., 2019) and CIML-NK cells (Romee et al., 2016).

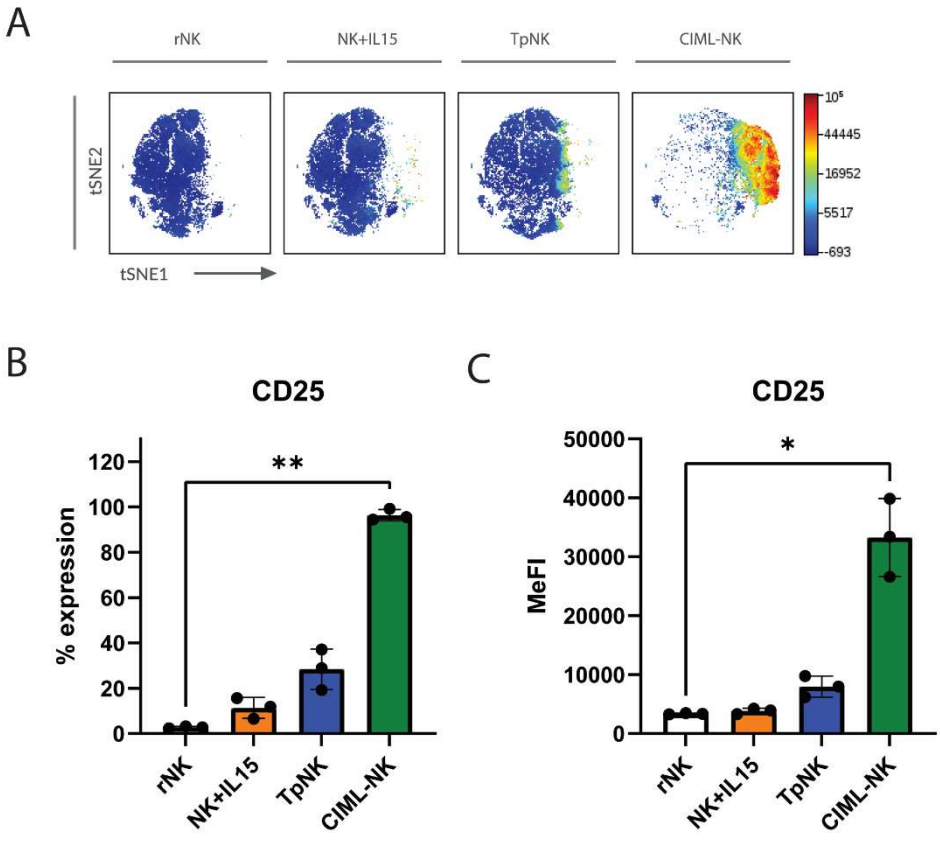

Figure 3.2. CD25 expression by resting and memory-like NK cells

(A) viSNE plots show the expression of CD25 across the indicated types of NK cells. Each point on the viSNE map represents a single cell, and colour depicts the intensity of protein expression. (B, C) The bar chart shows the analysis of (B) % expression

and (C) MeFI of the positive population. Bars represent the means ±SD of 3 different donors indicated by the dots. Comparisons were made between rNK and the different stimulatory conditions using the Kruskal-Wallis 1-way ANOVA with Dunn's multiple-comparison test for non-parametric distributions. Statistical significance is indicated as: *P <0.05: **P <0.01: ***P <0.001. The absence of an asterisk indicates non-significance.

3.3.1.1.3 CD69

CD69 is another NK cell activation marker (Borrego et al., 1999), and its upregulation is a hallmark of tumour priming and has been previously reported in other studies from our group (North et al., 2007; Sabry et al., 2019). The expression of CD69 is represented in Figure 3.3 and shows a very similar trend to CD25 expression, presented in the viSNE analysis (Figure 3.3 A). The % expression of CD69 is shown in Figure 3.3 B; rNK cells show low levels of CD69 expression (~5%), and this is increased in IL15-activated NK cells (~40%), TpNK cells (~60%) and CIML-NK cells (~100%). MeFI (Figure 3.3 C) shows a significant upregulation on CIML-NK cells compared to rNK cells; the rest of the conditions show similar expression levels to rNK cells.

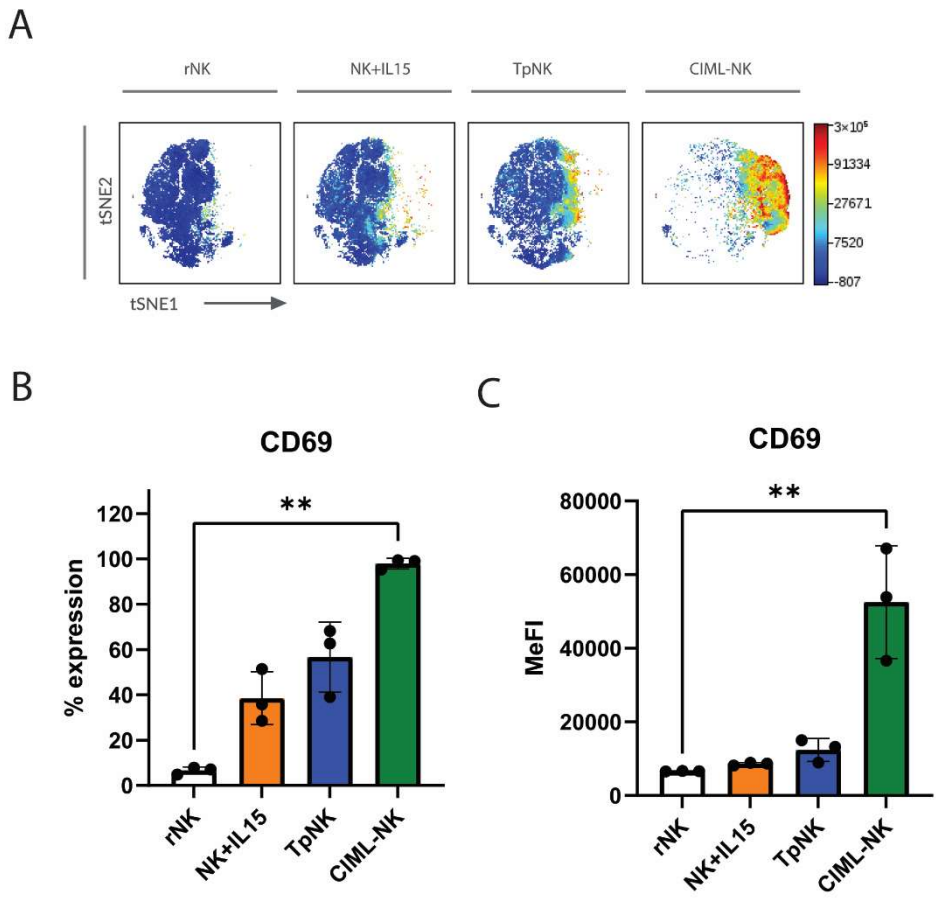

Figure 3.3. CD69 expression by resting and memory-like NK cells.

(A) viSNE plots show the expression of CD69 across the indicated types of NK cells. Each point on the viSNE map represents a single cell, and colour depicts the intensity of protein expression. (B, C) The bar chart shows the analysis of (B) % expression and (C) MeFI of the positive population. Bars represent the means ±SD of 3 different donors indicated by the dots. Comparisons were made between rNK and the different stimulatory conditions using the Kruskal-Wallis 1-way ANOVA with Dunn's multiple-comparison test for non-parametric distributions. Statistical significance is indicated as: *P <0.05: **P <0.01: ***P <0.001. The absence of an asterisk indicates non-significance.

3.3.1.1.4 NKG2D

NKG2D is an activating cell surface receptor expressed constitutively on NK cells and is the ligand for ULBP1-6 and MICA/B (Bauer et al., 1999). The expression of NKG2D is shown in Figure 3.4. The viSNE plots (Figure 3.4 A)

show medium/low NKG2D expression intensity in rNK, IL15-activated NK cells and CIML-NK cells across all clusters, with a lower expression in TpNK cells. The % NKG2D expression (Figure 3.4 B) in rNK, IL15-activated NK and CIML-NK cells indicates high levels of expression for all three conditions (~80-90%) and a downregulation in TpNK cells (~65%). The MeFI expression (Figure 3.4 C) shows a non-significant downregulation in TpNK cells compared to rNK. These findings on TpNK cells confirm previous observations (North et al., 2007; Sabry et al., 2019).

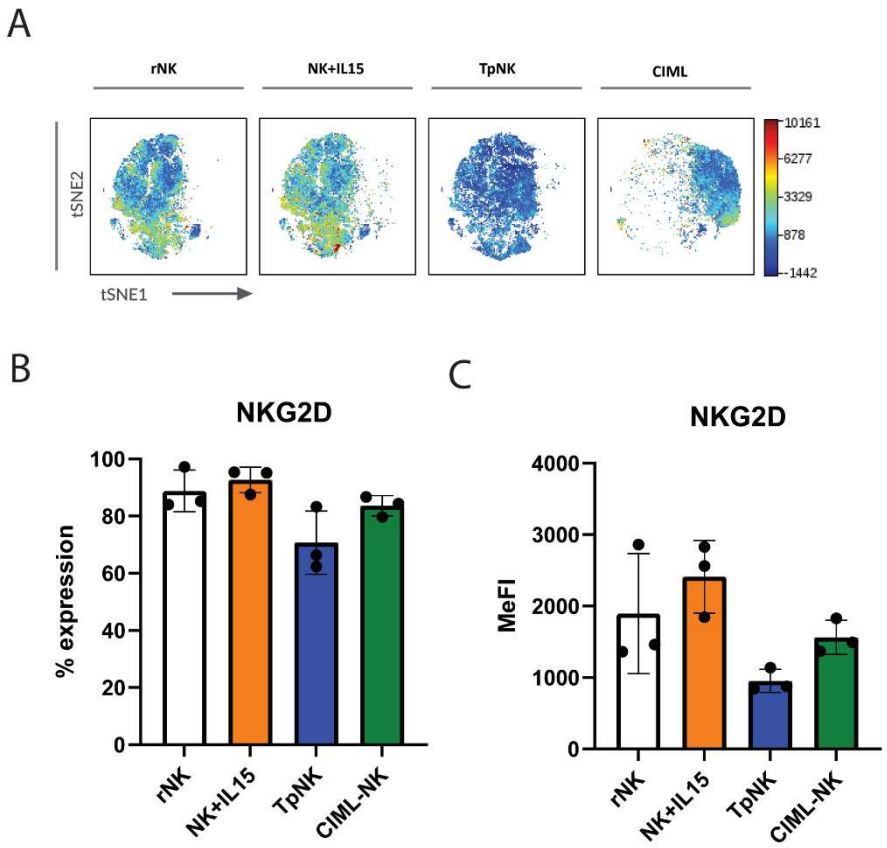

Figure 3.4. NKG2D expression by resting and memory-like NK cells.

(A) viSNE plots show the expression of NKG2D across the indicated types of NK cells. Each point on the viSNE map represents a single cell, and colour depicts the intensity of protein expression. (B, C) The bar chart shows the analysis of (B) % expression and (C) MeFI of the positive population. Bars represent the means ±SD of 3 different donors indicated by the dots. Comparisons were made between rNK and the different stimulatory conditions using the Kruskal-Wallis 1-way ANOVA with Dunn's multiple-comparison test for non-parametric distributions. Statistical

significance is indicated as: *P <0.05: **P <0.01: ***P <0.001. The absence of an asterisk indicates non-significance.

3.3.1.1.5 TRAIL

NK cells also exert cytotoxicity via the engagement of death receptors that belong to the TNF family of cytokines, like the tumour necrosis factor-related apoptosis-inducing ligand (TRAIL/Apo2L), that induces caspase-mediated apoptosis in the target cell (Falschlehner et al., 2009; Wiley et al., 1995).

The expression of TRAIL is shown in Figure 3.5. The viSNE analysis (Figure 3.5 A) indicates low to no intensity of expression of TRAIL in rNK, IL-15 primed NK cells and TpNK cells, and high expression in CIML-NK cells. The % expression (Figure 3.5 B) reveals very low levels of expression on rNK, IL15-primed NK and TpNK cells (~5%) and a significant upregulation in CIML-NK cells (~40%). The MeFI analysis (Figure 3.5 C) shows a moderate increase of TRAIL in IL15-primed NK and a significant increase in CIML-NK cells, possibly driven by the presence of IL15 in these cultures. The upregulation of both TRAIL % expression and MeFI in CIML-NK cells has been reported previously (Romee et al., 2016).

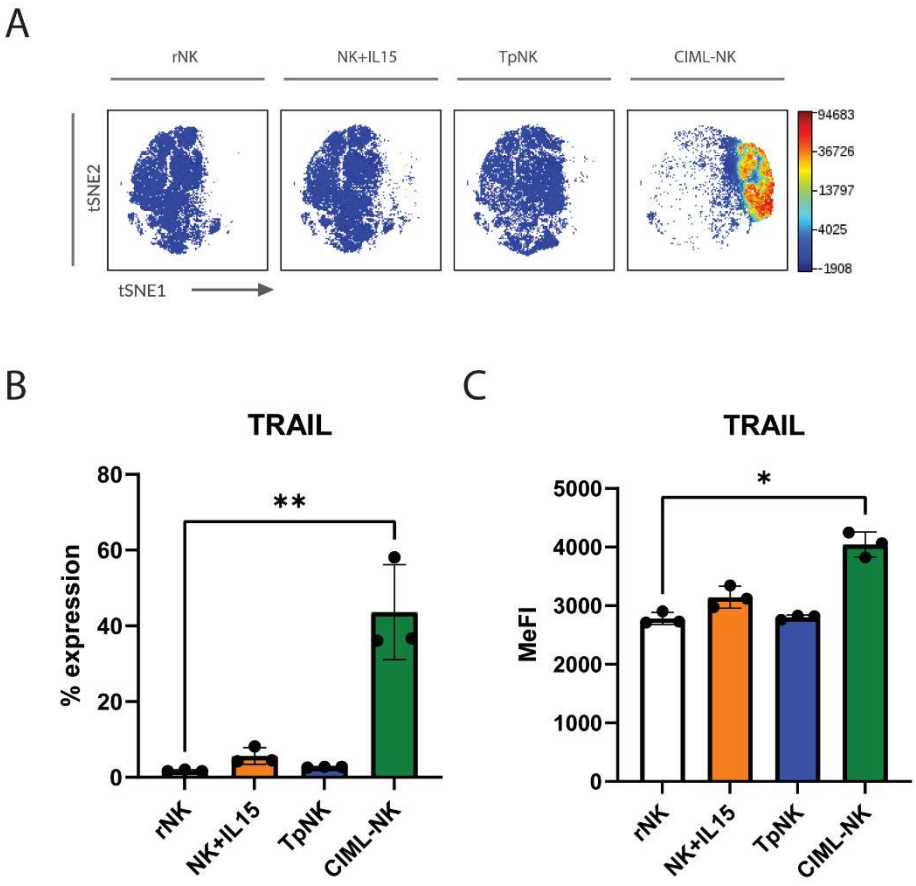

Figure 3.5. TRAIL expression by resting and memory-like NK cells

(A) viSNE plots show the expression of TRAIL across the indicated types of NK cells. Each point on the viSNE map represents a single cell, and colour depicts the intensity of protein expression. (B, C) The bar chart shows the analysis of (B) % expression and (C) MeFI of the positive population. Bars represent the means ±SD of 3 different donors indicated by the dots. Comparisons were made between rNK and the different stimulatory conditions using the Kruskal-Wallis 1-way ANOVA with Dunn's multiple-comparison test for non-parametric distributions. Statistical significance is indicated as: *P <0.05: **P <0.01: ***P <0.001. The absence of an asterisk indicates non-significance.

3.3.1.2 Maturation/differentiation markers

3.3.1.2.1 CD57

The increase in CD57 in NK cells has been reported as a marker of highly mature NK cells (Björkström et al., 2010; Lopez-Vergès et al., 2010; Nielsen

et al., 2013). In the viSNE plots (Figure 3.6 A), we observed CD57 expression in specific clusters for all NK cell conditions. The % expression of CD57 (Figure 3.6 B) is similar in rNK, IL-15 primed NK cells and CIML-NK cells (~40%) but is upregulated in TpNK cells (~75%). The MeFI (Figure 3.6 C) shows a similar expression of CD57 on rNK, IL-15 primed NK cells and CIML-NK cells, and it is downregulated in TpNK cells.

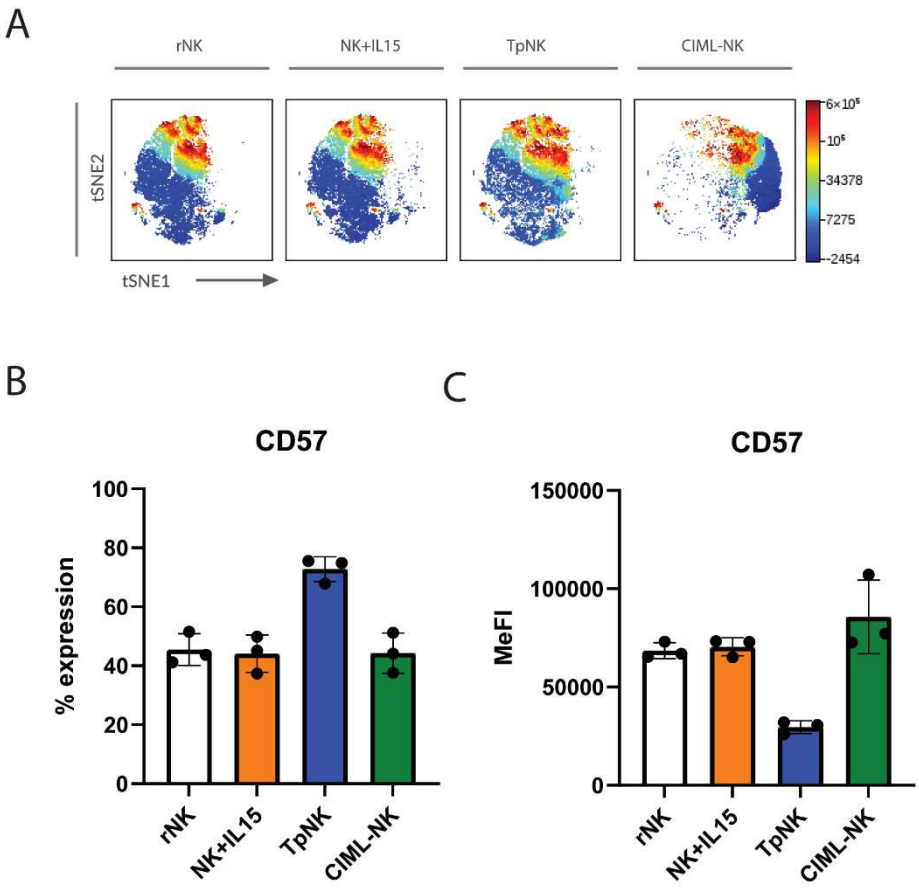

Figure 3.6. CD57 expression by resting and memory-like NK cells

(A) viSNE plots show the expression of CD57 across the indicated types of NK cells. Each point on the viSNE map represents a single cell, and colour depicts the intensity of protein expression. (B, C) The bar chart shows the analysis of (B) % expression and (C) MeFI of the positive population. Bars represent the means ±SD of 3 different donors indicated by the dots. Comparisons were made between rNK and the different stimulatory conditions using the Kruskal-Wallis 1-way ANOVA with Dunn's multiple-comparison test for non-parametric distributions. Statistical significance is indicated as: *P <0.05: **P <0.01: ***P <0.001. The absence of an asterisk indicates non-significance.

3.3.1.3 Adhesion molecules

3.3.1.3.1 CD62L

CD62L is an L-selectin from the family of adhesion molecules involved in the trafficking of lymphocytes in and out of blood circulation by mediating rolling and adhesion to the blood vessel wall (Bevilacqua, 1993). It has been suggested that $CD56^{dim}$ $CD62L^{+}$ NK cells represent an intermediate step in the maturation of NK cells from $CD56^{bright}$ to the mature $CD56^{dim}$ $CD62L^{-}$. These subsets are cytokine producers but also can exert direct cytotoxicity through ligand engagement (Juelke et al., 2010).

In the viSNE analysis (Figure 3.7 A), CD62L is expressed across different clusters in rNK, IL15-primed NK cells and TpNK, but its expression is reduced in CIML-NK. The % expression (Figure 3.7 B) is similar in rNK and IL-15 primed NK cells (~70%); a non-significant reduction is observed in TpNK cells (~50%) and CIML-NK cells (~40%) compared to rNK cells. The MeFI expression (Figure 3.7 C) shows a non-significant reduction in IL15-primed NK and TpNK cells compared to rNK cells and a significant decrease in CIML-NK cells.

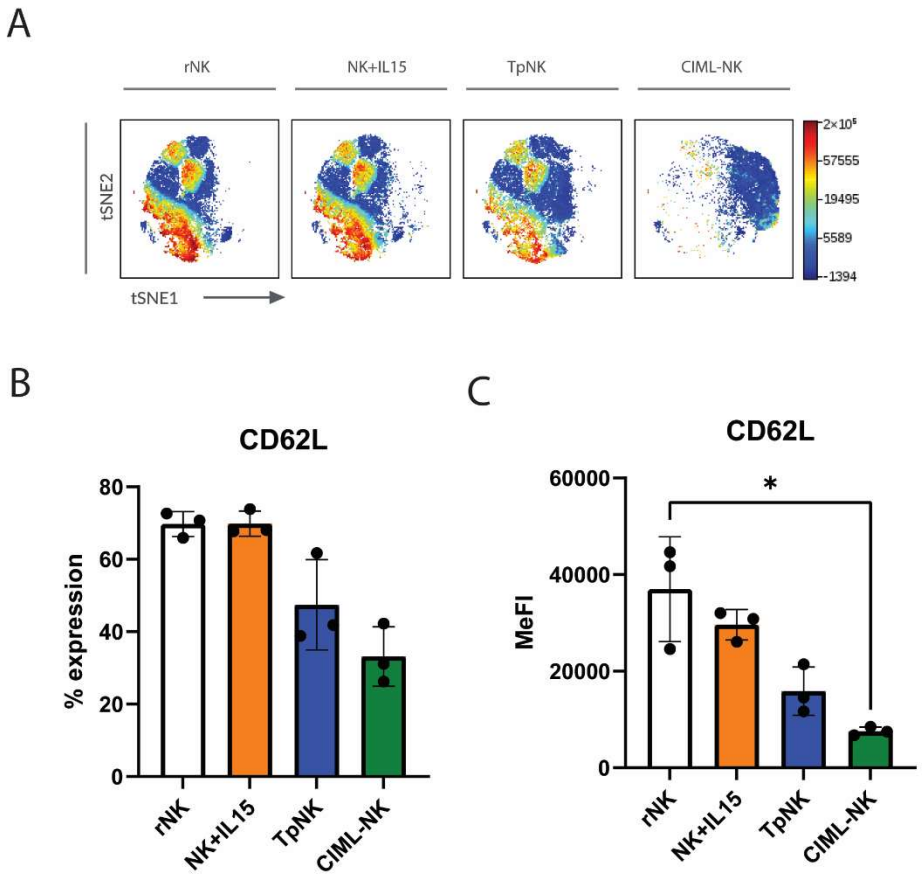

Figure 3.7. CD62L expression by resting and memory-like NK cells

(A) viSNE plots show the expression of CD62L across the indicated types of NK cells. Each point on the viSNE map represents a single cell, and colour depicts the intensity of protein expression. (B, C) The bar chart shows the analysis of (B) % expression and (C) MeFI of the positive population. Bars represent the means ±SD of 3 different donors indicated by the dots. Comparisons were made between rNK and the different stimulatory conditions using the Kruskal-Wallis 1-way ANOVA with Dunn's multiple-comparison test for non-parametric distributions. Statistical significance is indicated as: *P <0.05: **P <0.01: ***P <0.001. The absence of an asterisk indicates non-significance.

3.3.1.3.2 ICAM1

ICAM1 is another adhesion molecule that mediates leukocyte migration and can also signal to activate NK cells by binding to LFA1 (Barber et al., 2004; Chong et al., 1994; Wee et al., 2009). The expression of ICAM1 is shown in

Figure 3.8. The viSNE analysis (Figure 3.8 A) shows a general low expression in rNK cells and IL15-primed NK cells. TpNK cells also show overall low expression with the exception of higher expression in a small subcluster. CIML-NK cells are characterised by a higher expression of ICAM1, as shown in the viSNE plots (Figure 3.8 A). The % expression of ICAM1 (Figure 3.8 B) is very low on rNK cells (~5%) and trends towards higher expression in IL15-primed NK cells (~15%) and TpNK cells (20%). CIML-NK cells show a significant enhancement up to ~80%. MeFI expression (Figure 3.8 C) shows similar levels of expression on rNK and IL15-primed NK, a non-significant increase in fluorescence in TpNK and a significant increase in CIML-NK cells.

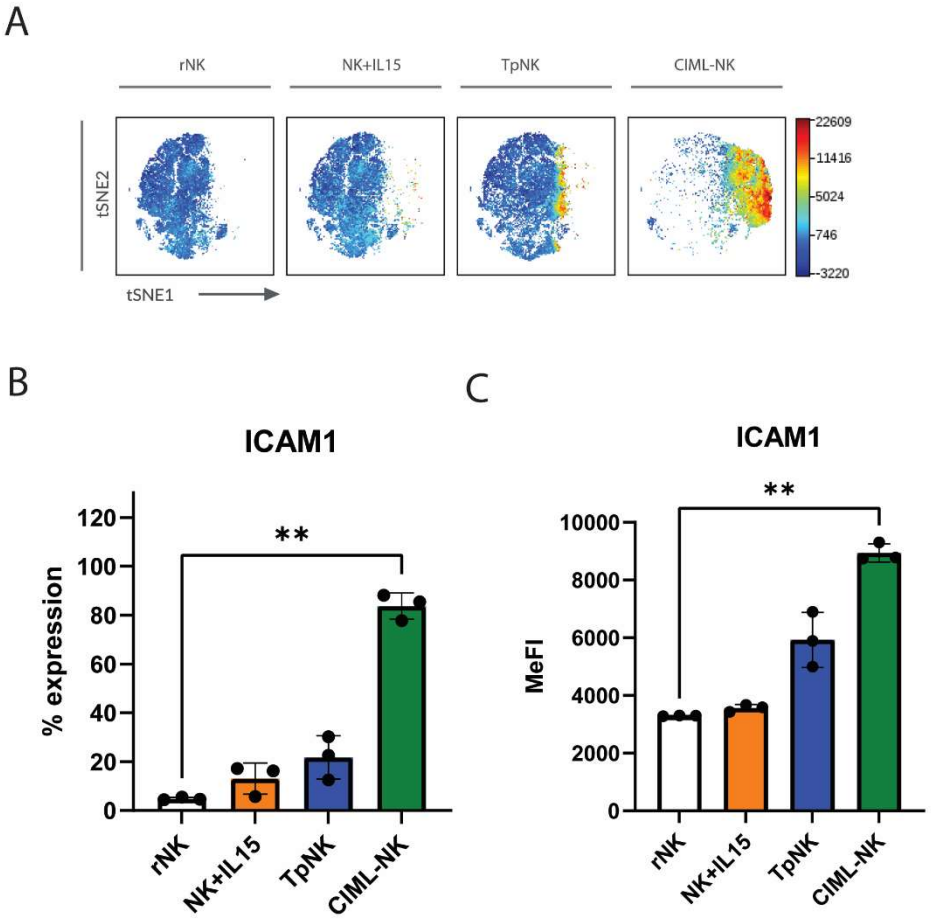

Figure 3.8. ICAM1 expression by resting and memory-like NK cells

(A) viSNE plots show the expression of ICAM1 across the indicated types of NK cells. Each point on the viSNE map represents a single cell, and colour depicts the intensity of protein expression. (B, C) The bar chart shows the analysis of (B) % expression and (C) MeFI of the positive population. Bars represent the means ±SD of 3 different

donors indicated by the dots. Comparisons were made between rNK and the different stimulatory conditions using the Kruskal-Wallis 1-way ANOVA with Dunn's multiple-comparison test for non-parametric distributions. Statistical significance is indicated as: *P <0.05: **P <0.01: ***P <0.001. The absence of an asterisk indicates non-significance.

3.3.1.4 Inhibitory receptors/checkpoint inhibitors

We next wanted to assess whether these NK cells were activated and functional without showing signs of exhaustion. Hence, a number of different receptors that have been associated with NK cell exhaustion were examined. LAG3 and TIM3 are checkpoint inhibitors that have been associated with both T cell (Wherry, 2011) and NK cell exhaustion (Judge et al., 2020; A. M. Merino et al., 2020; Roe, 2022), although their actual role on NK cells is still controversial. PD-L1 is one of the ligands of the immune checkpoint inhibitor PD1, and its expression in NK cells is associated with the hampering of T cell responses in the TME (Diniz et al., 2022; J. Zhou et al., 2019).

The expression of PD-L1 is shown in Figure 3.9. The viSNE analysis (Figure 3.9 A) shows that rNK cells, IL15-primed NK cells and TpNK cells do not express PD-L1, but it is considerably induced in CIML-NK cells. This was also confirmed by manual gating, looking at % expression and MeFI with a significant upregulation only observed in CIML-NK cells compared to the other priming conditions (Figure 3.9 B and Figure 3.9 C).

The expression of LAG3 is shown in Figure 3.10. The viSNE analysis (Figure 3.10 A) shows an overall low expression of LAG3 in rNK, IL15-primed NK cells and TpNK cells and an increased expression in CIML-NK cells. The % expression (Figure 3.10 B) shows ~1% expression in rNK, IL15-primed NK cells and TpNK cells, with a significant increase in CIML-NK cells (~15%). The study of the MeFI (Figure 3.10 C) shows similar results, with low levels of expression in rNK, IL15-primed NK and TpNK cells and a moderate increase in CIML-NK cells.

The expression of TIM3 is shown in Figure 3.11. Unsupervised viSNE analysis (Figure 3.11 A) shows overall low levels of expression of TIM3 in rNK, IL15-primed NK and TpNK cells, with the exception of a small subcluster in CIML-NK cells showing high levels of expression (Figure 3.11 A). The % expression (Figure 3.11 B) is similar to PD-L1 and LAG3, with negligent expression levels in rNK, IL15-primed NK cells and TpNK cells, and a significant upregulation in CIML-NK cells. MeFI levels (Figure 3.11 C) were comparable across all rNK, IL15-primed NK and TpNK cells, and a moderate significant increase in CIML-NK cells.

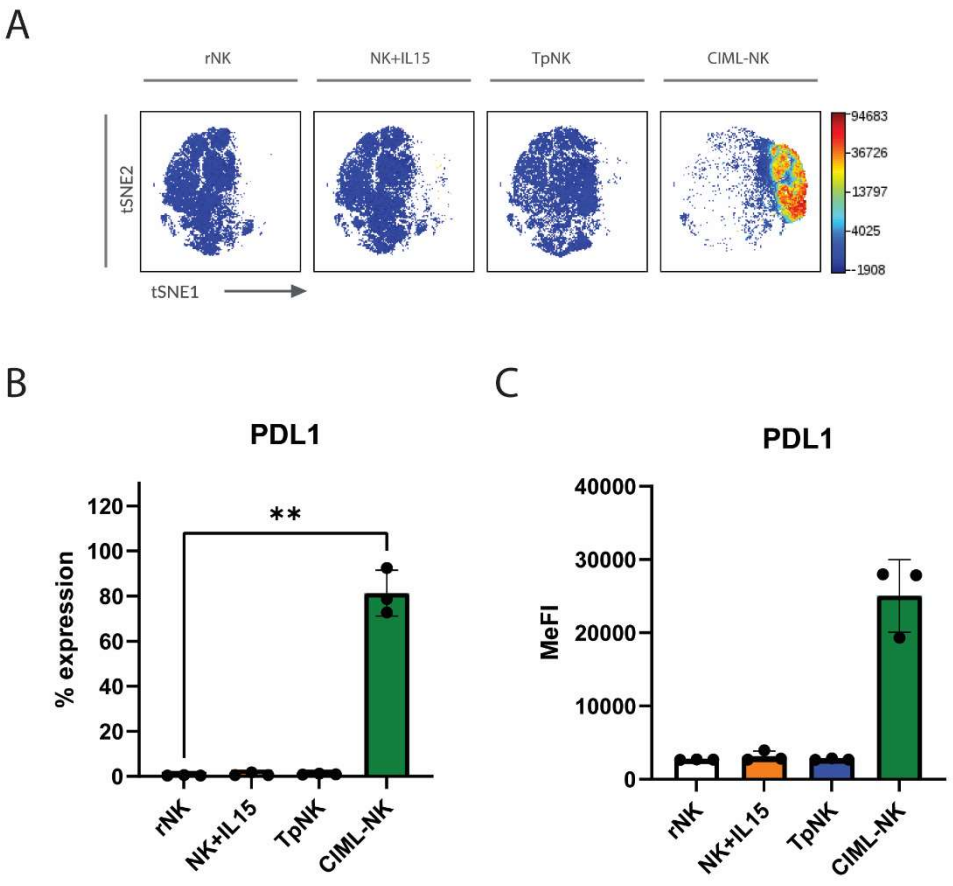

Figure 3.9. PDL1 expression by resting and memory-like NK cells

(A) viSNE plots show the expression of PDL1 across the indicated types of NK cells. Each point on the viSNE map represents a single cell, and colour depicts the intensity of protein expression. (B, C) The bar chart shows the analysis of (B) % expression and (C) MeFI of the positive population. Bars represent the means ±SD of 3 different donors indicated by the dots. Comparisons were made between rNK and the different stimulatory conditions using the Kruskal-Wallis 1-way ANOVA with Dunn's multiple-

comparison test for non-parametric distributions. Statistical significance is indicated as: *P <0.05: **P <0.01: ***P <0.001. The absence of an asterisk indicates non-significance.

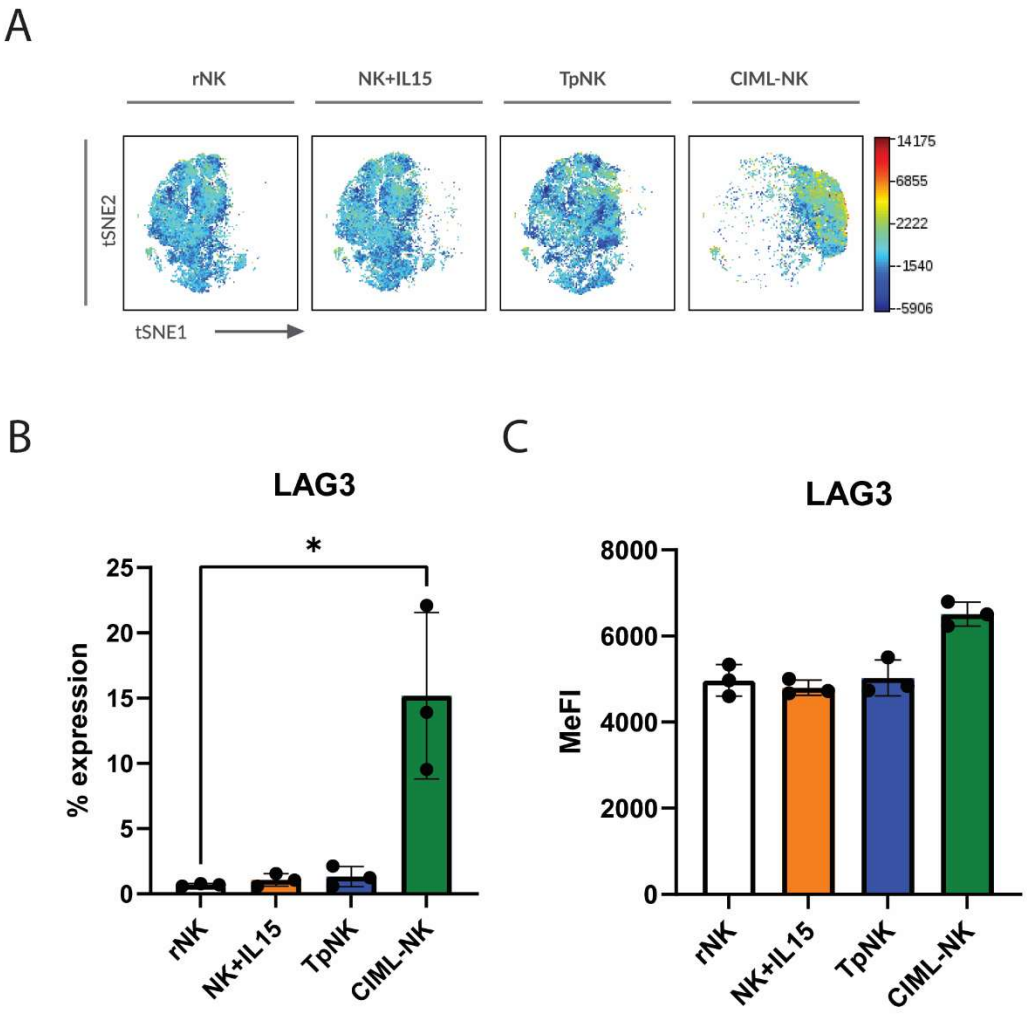

Figure 3.10. LAG3 expression by resting and memory-like NK cells

(A) viSNE plots show the expression of LAG3 across the indicated types of NK cells. Each point on the viSNE map represents a single cell, and colour depicts the intensity of protein expression. (B, C) The bar chart shows the analysis of (B) % expression and (C) MeFI of the positive population. Bars represent the means ±SD of 3 different donors indicated by the dots. Comparisons were made between rNK and the different stimulatory conditions using the Kruskal-Wallis 1-way ANOVA with Dunn's multiple-comparison test for non-parametric distributions. Statistical significance is indicated

as: *P <0.05: **P <0.01: ***P <0.001. The absence of an asterisk indicates non-significance.

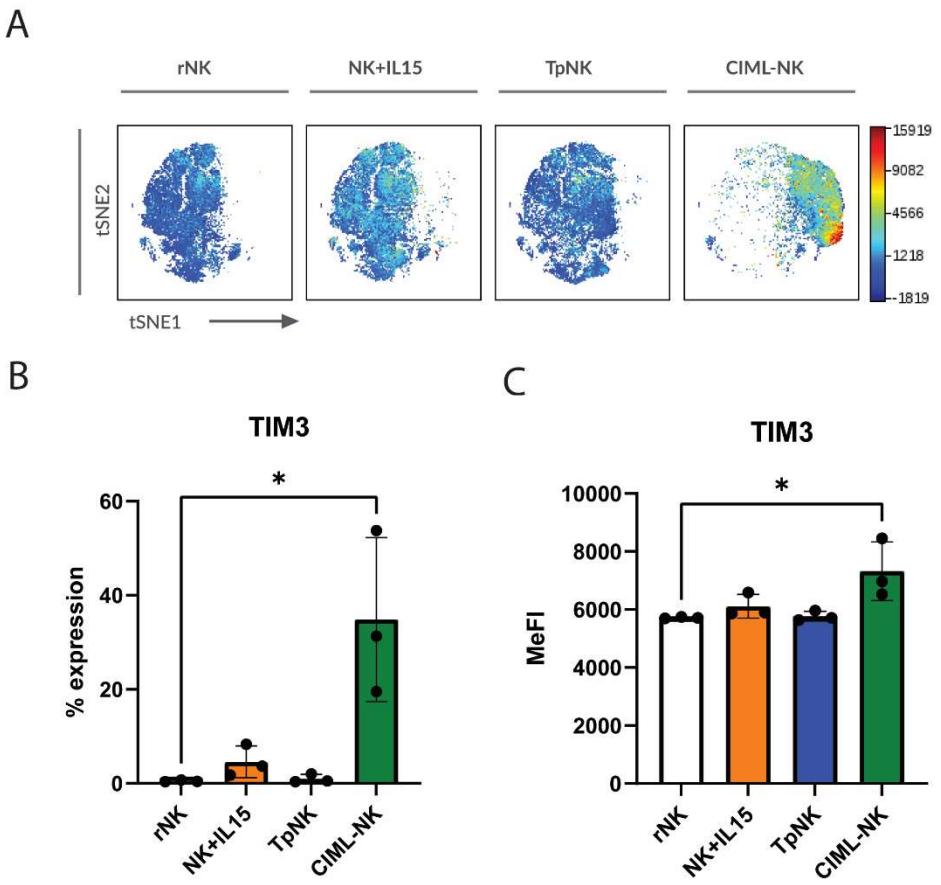

Figure 3.11. TIM3 expression by resting and memory-like NK cells

(A) viSNE plots show the expression of TIM3 across the indicated types of NK cells. Each point on the viSNE map represents a single cell, and colour depicts the intensity of protein expression. (B, C) The bar chart shows the analysis of (B) % expression and (C) MeFI of the positive population. Bars represent the means ±SD of 3 different donors indicated by the dots. Comparisons were made between rNK and the different stimulatory conditions using the Kruskal-Wallis 1-way ANOVA with Dunn's multiple-comparison test for non-parametric distributions. Statistical significance is indicated as: *P <0.05: **P <0.01: ***P <0.001. The absence of an asterisk indicates non-significance.

3.3.1.5 Metacluster analysis of NK cell subpopulations

Next, I performed FlowSOM analysis on the viSNE results obtained from the phenotypical characterisation of NK cells at rest and following stimulation with different priming conditions. FlowSOM is an unsupervised clustering algorithm that helps identify metaclusters based on their phenotype. This allowed me to discover the co-expression patterns of receptors amongst different subpopulations of NK cells, which could be either unique or shared across different conditions.

Ten metaclusters were identified (Figure 3.12 A), with the changes in abundance of each metacluster shown in Figure 3.12 B. Resting NK cells and IL15-activated NK cells are characterised by the presence of metaclusters 1, 2 and 7, accounting for 23.62%, 36.53% and 32.28% in rNK cells and 23.93%, 36.72% and 30.36% in IL15-activated NK cells respectively (Figure 3.12 B). TpNK cells have a more prominent metacluster 3 (increasing from 0.53% in rNK to 13.74% in TpNK cells) and a more prominent metacluster 8 (11.5% relative to 0.63% in rNK). In contrast, CIML-NK cells show a distinct phenotype enriched for metacluster 8 (33.8%) and a new metacluster 6, which was not observed in any other conditions but represented 52.4% of the cells.

Next, I analysed the receptor expression of the individual metaclusters that represented more than 10% of the populations by determining the MeFI of the whole population (Figure 3.12 C). Emphasis was placed on the marker expression of metacluster 3, which was more prominent in TpNK cells; metacluster 6, as it was unique to CIML-NK cells; and metacluster 8, which was expanded in both TpNK and CIML-NK cells.

Metacluster 1 consists of the $CD56^{bright}$ NK cell subset as it shows high expression of CD56 (data not shown) as well as low expression of CD16 (J. Yu et al., 2013). Thus, these cells are more immature and predominantly secrete cytokines.

The NK cells present in metacluster 2 represent an immature subset characterised by low expression of CD57 but have high expression of CD16 and CD38. The high expression of CD16 suggests that these cells have high

ADCC cytotoxic capacity. Besides being an activation marker, CD38 has been shown to play a role on NK cell fratricide (Gurney et al., 2022); which could act as a potential mechanism to limit responses in NK cells with high cytotoxic potential.

Metacluster 3 is characterised by high expression of NKG2A, CD69, CD57, CD45RA and CD2. The high expression of CD2 in this cluster is particularly intriguing as the Lowdell group has previously shown that the interaction of CD2 on the NK cell with its ligand CD15 on INB16 during tumour-priming is crucial to achieve the primed state (Sabry et al., 2011).

The uniquely expressed metacluster 6 in CIML-NK cells is characterised by high expression of CD69, Granzyme B, CD38, CD25 and PD-L1. The high expression of several NK cell activation markers suggests that the cells in this metacluster are activated with high cytotoxic potential. The high expression of the inhibitory marker NKG2A suggests a potential mechanism for these cells to increase their threshold for activation and thus limit NK cell responses.

The NK cells from metacluster 7 are characterised by having high expression of CD57 and CD16, suggesting these are terminally differentiated NK cells (Björkström et al., 2010; J. Yu et al., 2013). Metacluster 7 is one of the most abundant in rNK cells, which shows that these mature NK cell populations are present in high numbers in the peripheral blood of healthy individuals.

Metacluster 8 is restricted to TpNK and CIML-NK and defined by high expression of Granzyme B, CD45RA, CD69, CD38, and low expression of NKG2A. The high expression of CD57, together with low NKG2A expression in this cluster, suggests that these cells are highly mature and differentiated (Björkström et al., 2010; Lopez-Vergès et al., 2010).

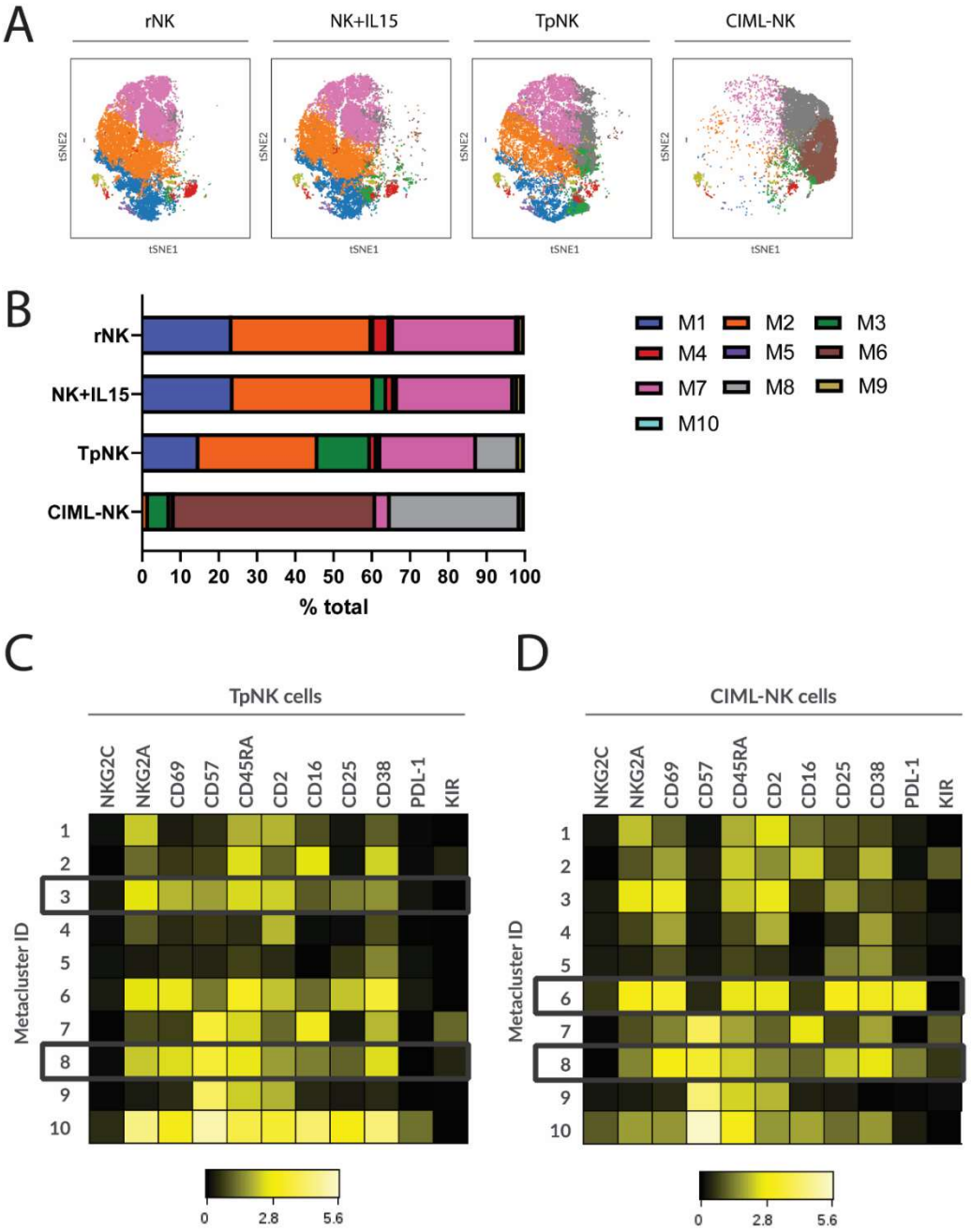

Figure 3.12. TpNK and CIML-NK cells share a unique phenotypical metacluster containing mature NK cells

Freshly isolated peripheral blood NK cells were incubated overnight at 37˚C as indicated. The next day, cells were washed, and the expression of 30 different NK cell markers was analysed using spectral flow cytometry. After that, viSNE and FlowSOM analysis clustered on 30 NK cell phenotypic markers was performed (A) viSNE plots of the different metaclusters across all conditions. (B) Stacked bars show changes in the % cell numbers of each metacluster for every condition. (C)(D) Heatmaps show the fluorescence intensity of the total of cells on the indicated markers of metaclusters

1 to 10, with metaclusters of interest highlighted in (C) TpNK and (D) CIML-NK. Plots show the data from 3 concatenated donors.

3.3.2 Proteomics analysis

In order to further characterise the initial events leading to the generation of NK cell memory, I explored the proteomic profile of rNK cells compared to TpNK, CIML-NK and NK cells activated with IL15. Levels of mRNA do not always correspond to protein levels; thus, proteomics may be a more powerful tool for measuring cell changes (Y. Liu et al., 2016). In total, 9,253 proteins represented by 204,407 peptide ion variants were quantified across all samples. Hierarchical clustering analysis using the Manhattan distance measure using all protein z-score values across all samples was carried out, and the clustered data (Figure 3.13 A) show a strong separation according to the priming condition. The volcano plot shows the 9,253 proteins quantified with the red dots showing protein candidates significantly changed after exposure to INB16 (Figure 3.13 B). Amongst the most upregulated proteins KPNA2, GCAT, MTHFD1L, MST1, FAR2, CDCA7L, PRC1 and NKD2 were identified.

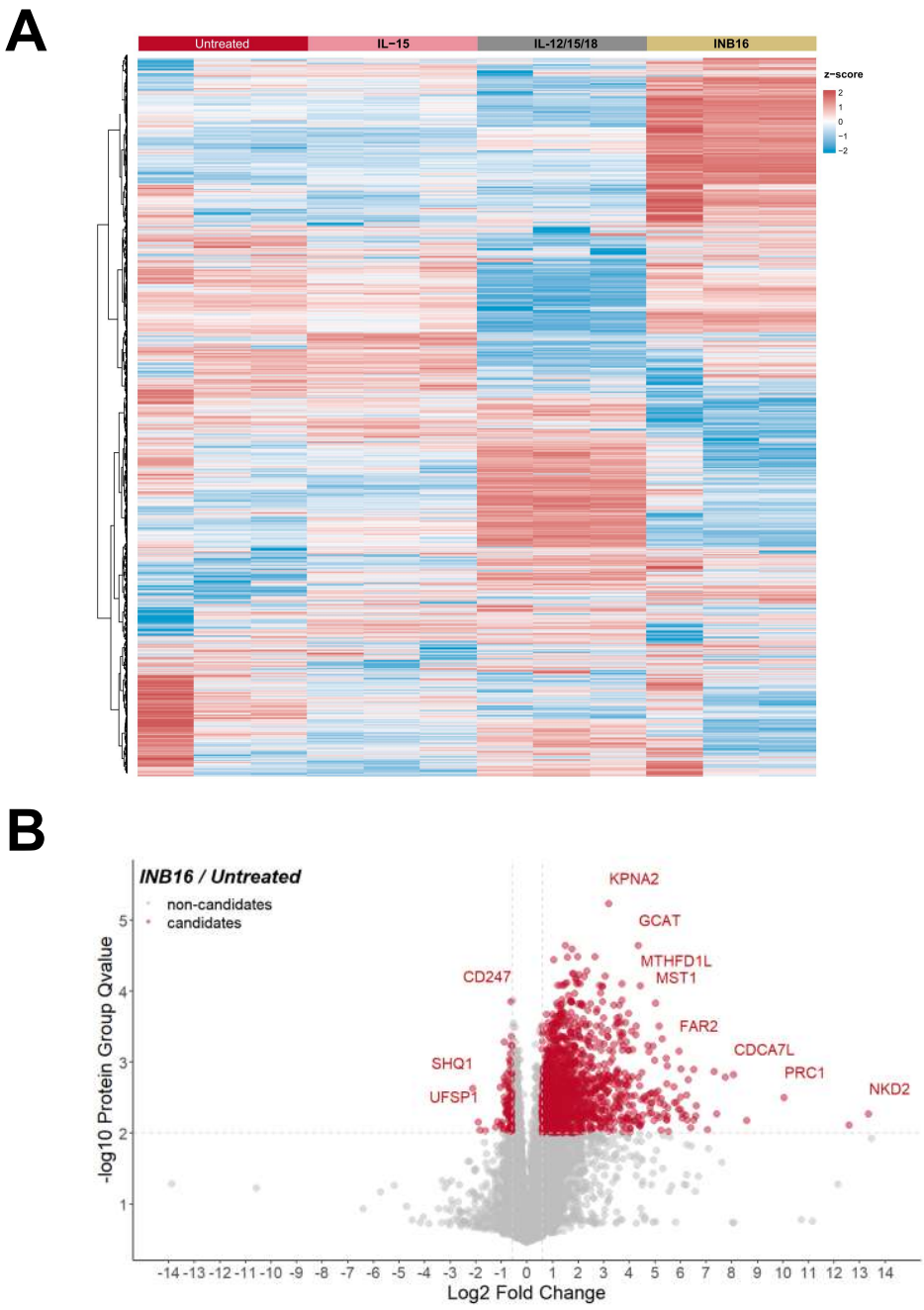

Figure 3.13. Proteome-wide protein profile of different types of stimulated NK cells

(A) Hierarchical clustering analysis using the Manhattan distance measure using all protein z-score values across all samples. (B) Volcano plot shows the 9,253 proteins quantified with the red dots showing protein candidates significantly changed after exposure to INB16 (TpNK cells) compared to rNK cells.

This next led to the identification of proteins which were statistically significantly upregulated ($p < 0.001$) and with an absolute average log ratio of >4 log, and looked at the overlap amongst the three different conditions (Figure 3.14). Of the 249 proteins identified in TpNK cells, 41 are shared with CIML-NK (Table 3.1), 20 with IL15-activated NK cells and 18 with all three conditions. CIML-NK upregulated 179 proteins, of which 23 are shared with IL15-activated NK cells. Sixty-three proteins are only upregulated by IL15 activation. Notable proteins within the 41 are ADAM28, APOC2, FERM2, INF-G, LOXL3, P3H3, RM14, RM21 and SL9A9, each of which may contribute to memory-like function.

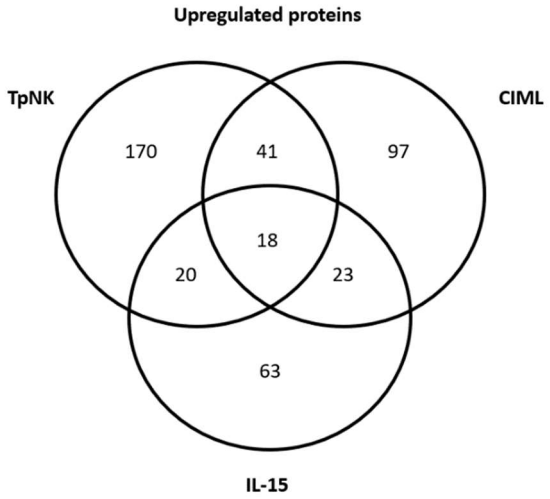

Figure 3.14. Venn diagram showing the intersection of upregulated proteins across the three different NK cell conditions

Venn diagram generated by the intersection list of the proteins significantly ($p<0.001$) upregulated by more than 4 log compared to NK cells incubated in medium alone.

Protein	Function
ADAM28	Leukocyte transmigration through integrin binding
APC11	Control of cellular progression through mitosis
APOC2	Increases hydrolysis of triglycerides
C1TM	Folic acid metabolic process
C4BPA	Positive regulation of protein catabolic process
CBX2	Chromatin remodelling and histone modification
CF298	Cilia and flagella associated protein – unknown function
CTIP	DNA endonuclease. Controls cell cycle
EPOP	Modulation of active gene transcription
FERM2	Regulator of integrin activation
FOXM1	Required for entry to mitosis
IFNG	Gamma interferon
KBL	Metabolic processes
KBTB3	Unknown function
LOXL3	Disrupts STAT3 dimerization
MCM5	G1/S transition of mitotic cell cycle. DNA replication
MCM6	G1/S transition of mitotic cell cycle. DNA replication
MOFA1	Unknown function
NEIL3	Removal of DNA lesions arising from oxidative stress
NFYA	Nuclear transcription factor
NT5D3	Cellular hydrolase
P3H3	Catalyses hydroxylation of lysine residues in collagen alpha chains.
PABP4	Unknown function
PLAL1	Unknown function
POMP	Mediates ER binding, recruits the remaining β-subunits into the nascent complex and supports final proteasome maturation
PSB5	Unknown function
RL8	RNA binding and cytoplasmic translation
RL27	Ribosomal protein probably associated with resistance to oxidative stress
RL36	Anti-oxidant activity
RL39	Structural constituent of ribosome – involved in translation
RM14	Involved in mitochondrial translation and metabolism

RM21	Involved in protein synthesis within mitochondria
RS30	Ribosomal protein – unknown function
SLC9A9	Regulates endosome maturation. Promotes recycling of transferrin receptors
STXB4	Positive regulation of cell cycle G1/S phase transition
TET5A	One of a family of TET proteins involved in control of cell growth
TRIB3	Regulation of glucose transport
TULP3	Regulation of transcription
TYSY	Maintains dTMP pool which is critical for DNA repair and replication
WDR47	Unknown function
WDR62	Localises katanin at spindle poles to ensure synchronous chromosomal segregation

Table 3.1. Proteins induced in both TpNK and CIML-NK cells

List of proteins upregulated by >4 logs and p<0.01 on TpNK cells and CIML-NK.

Gene Ontology (GO) enrichment analysis identified 444 biological processes, 137 cellular components and 263 molecular functions significantly enriched in TpNK cells relative to untreated controls. Figure 3.15 A shows the top 20 enriched biological processes enriched in TpNK cells. The main changes relate to mitochondrial function, as well as changes in cell metabolism and DNA replication.

In CIML-NK cells, GO enrichment analysis identified 284 biological processes, 64 cellular components, and 163 molecular functions that are significantly enriched compared to untreated controls. Figure 3.15 B shows the top 20 enriched biological processes enriched in CIML-NK cells; the main changes relate to processes involved in the cytotoxic activity of NK cells.

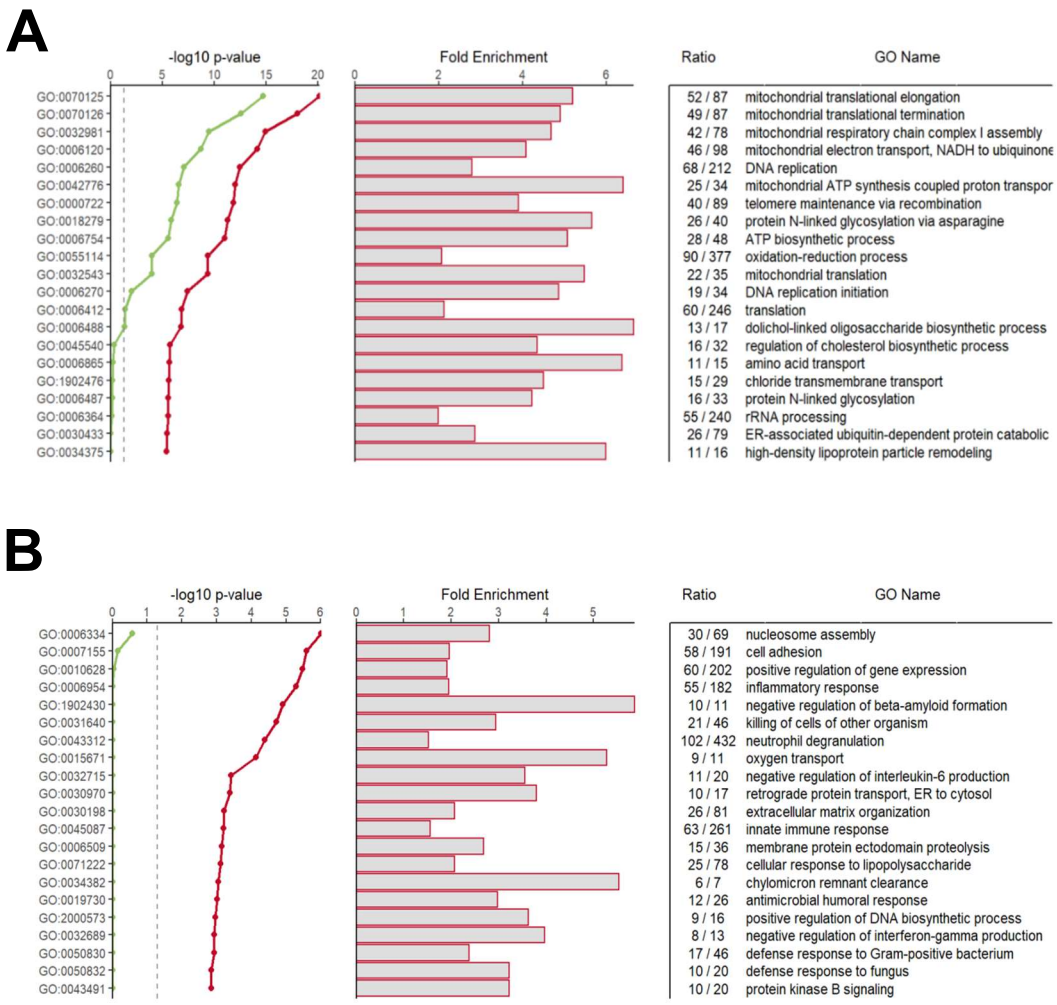

Figure 3.15. Top 20 enriched biological processes in TpNK and CIML-NK cells

GO enrichment analysis carried out with the proteins significantly changed between samples from NK cells treated with (A) INB16 and untreated controls and (B) NK cells treated with IL12/15/18 and untreated controls, showing the top 20 enriched biological processes enriched in each condition. Red line represents enrichment p-value; green line represents enrichment p-value Benjamini-Hochberg corrected.

The analysis identified that both TpNK cells and CIML-NK cells upregulated proteins related to lytic function (Figure 3.16 A). In contrast, NK cells co-incubated with INB16 led to the upregulation of 60 proteins associated with mitochondrial survival and fitness compared to 36 proteins upregulated in CIML-NK and 24 proteins upregulated by IL15-activated NK cells (Figure 3.16

B). This finding was intriguing and was investigated in functional assays measuring metabolic function in Chapter 4.

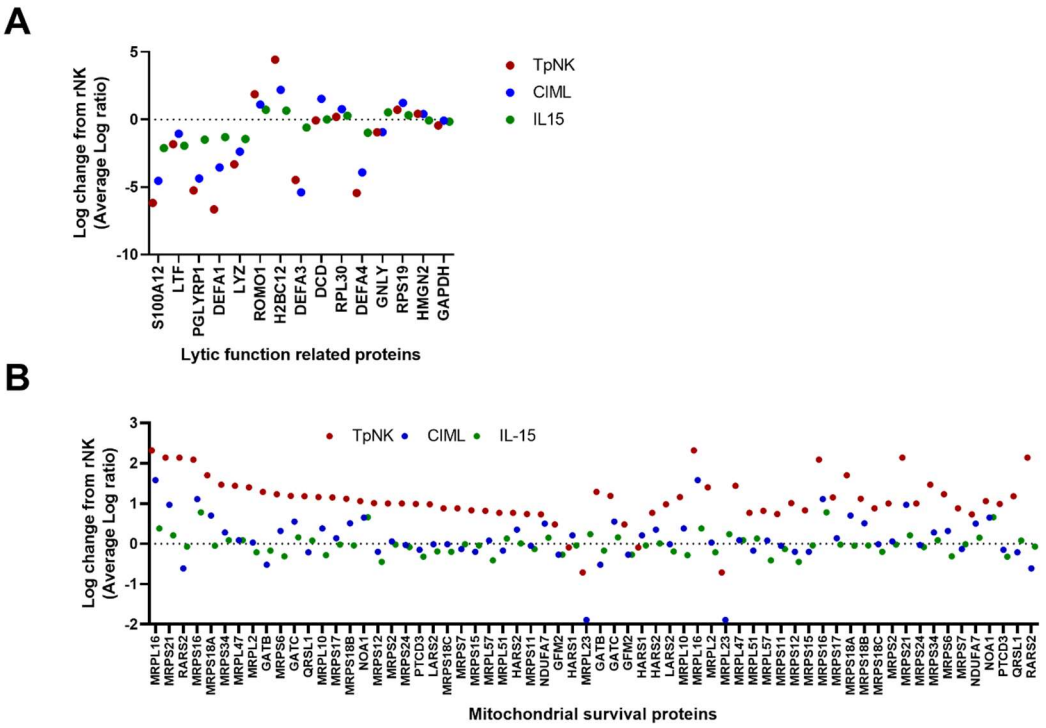

Figure 3.16. Upregulated proteins corresponding to lysis and mitochondrial survival across different NK cell conditions

Graphs show the average Log ratio from rNK in TpNK, CIML-NK and IL15-treated NK cells corresponding to (A) lytic function-related proteins and (B) mitochondrial survival proteins.

3.4 Discussion

Memory-like NK cells have been studied extensively in the context of CMV and CIML-NK cells, but the idea that memory-NK cells can arise from tumour-priming remains far less studied. The Lowdell group has previously reported the generation of TpNK cells and their ability to enhance the lysis of NK-resistant cancer cell lines (North et al., 2007), which generates tumour-memory NK cells (Pal et al., 2017). The effects on tumour-priming of NK cells have also been described by others, Dufva and colleagues recently reported that the exposure of NK cells to various haematological cancer cell lines imprints the NK cells at the transcriptomic level inducing different sensitivity to target cells (Dufva et al., 2023). In this chapter, we examined the characteristics occurring at the initial phase of the formation of cytokine- and tumour-memory NK cells by high-parameter flow cytometry and proteomics.

While memory-NK cells have been previously studied, a consistent phenotype has yet to be identified across the various types. Adaptive NK cells have been described as being NKG2C^{+} CD57^{hi} CD25^{hi} NKG2A^{-} and FCεRγ^{-} (Béziat et al., 2013; Foley et al., 2012; Lopez-Vergès et al., 2011b; J. C. Sun et al., 2009); and CIML-NK cells have been characterised as being CD25^{hi} CD94^{hi} NKG2A^{hi} CD69^{hi} NKp46^{hi} (Cooper et al., 2009; Romee et al., 2012, 2016). Tumour-memory NK cells generated by Pal and colleagues were described as being CD56^{br}, CD94^{hi}, CD16^{hi}, CD57^{int}, KLRG1^{int} and iKIR^{int} (Pal et al., 2017), although it seems that the acquisition of the phenotype in tumour-memory NK cells depends on the priming agent utilised (Dufva et al., 2023).

Several phenotypic attributes previously described to define memory-like NK cells were used to investigate memory NK cells in response to tumour priming. In this work, TpNK cells showed downregulation of CD16, upregulation of CD25, and upregulation of CD69, suggesting that these cells are activated despite the absence of cytokines in the priming stage (North et al., 2007; Sabry et al., 2019). This was similar to the phenotype of CIML-NK cells, which was also characterised by having downregulation of CD16 and upregulation of both CD25 and CD69, in keeping with previous observations (Romee et al., 2016).

The downregulation of NKG2D on TpNK cells is consistent with previous findings (North et al., 2007; Sabry et al., 2019). Typically, the downregulation of NK cell activation markers like NKG2D has been regarded as a sign of NK cell dysfunction. However, this might be a sign of a tumour-specific NK cell response; a tumour-primed NK cell that is waiting for more stimulation in order to trigger cytotoxicity might have downregulated specific receptors that are involved in the priming stage (Sabry & Lowdell, 2013). This is in keeping with the observations by our group and others that NK cells with downregulated activation markers like NKG2D or NKp46 display better killing of target cells (Gati et al., 2004; Penack et al., 2005).

The changes observed in CD57 expression, a marker for terminally differentiated NK cells (Björkström et al., 2010; Lopez-Vergès et al., 2010), are of interest. Notably, the increase in the percentage of NK cells expressing CD57 together with a reduction in intensity suggests that tumour-priming may initiate the maturation of CD57-ve NK cells, leading to a gradual increase in CD57 expression to levels associated with fully mature NK cells. It is possible that increasing the time of exposure of TpNK cells to the priming agent would drive a MeFI increase in the CD57+ population. It is likely that when an NK cell comes into contact with INB16, this drives its maturation and, hence, its ability to exert cytotoxicity. This was not observed in the CIML-NK cells generated here, nor has it been described in the literature (Romee et al., 2016). The observed downregulation in CD62L also supports the idea of maturation of TpNK cells as it is known that the loss of CD62L represents an intermediate state in NK cell maturation, going from $CD56^{dim}$ $CD62L^{+}$ NK cells to $CD56^{dim}$ $CD62L^{-}$ $CD57^{+}$, where this population exerts high cytotoxicity against cancer cells as well as decreased proliferative capacity (Juelke et al., 2010; Lopez-Vergès et al., 2010).

Another interesting observation is that CIML-NK cells were marked by the upregulation of PD-L1, TIM3 and LAG3, which were not observed in any of the other conditions. The upregulation of TIM3 and LAG-3, well-characterised markers of exhaustion in T cells (Wherry, 2011), represents a state of overstimulation that results in reduced proliferation and effector function. Whether NK cells share similar pathways of exhaustion with T cells requires

further definition. Inhibitory receptors that have been related to NK cell exhaustion include PD-1, LAG-3, TIM-3, TIGIT and CD98, but there seems to be controversies on what their actual role is (Judge et al., 2020; A. M. Merino et al., 2020; Roe, 2022). PD-L1 expression on NK cells has also been shown to limit T cell responses in the TME (Diniz et al., 2022; J. Zhou et al., 2019). CIML-NK cells display a phenotype of highly activated NK cells, but it could be that these cells are challenged or could impair other immune responses in the context of the TME.

I next wanted to elucidate whether tumour- and cytokine-primed NK cells shared phenotypic hallmarks of memory NK cells. A new metacluster 8 shared between TpNK cells and CIML-NK cells suggests that NK cell priming, despite variations in the activation mechanism employed, can lead to comparable phenotypes. The main characteristic of this cluster was the high expression of CD57 and the absence of NKG2A, which are characteristics of mature and terminally differentiated NK cells (Björkström et al., 2010; Lopez-Vergès et al., 2010). It could be that the presence of metacluster 8 is related to the acquisition of memory functions in TpNK and CIML-NK cells.

One of the most notable finding was the overrepresentation of metacluster 3 in TpNK cells, which is characterised by having high expression of CD2. CD2 is a co-stimulatory molecule that is important in the context of tumour-priming with INB16; research from the Lowdell group has shown that the CD2-CD15 interaction is crucial in order to prime an NK cell (Sabry et al., 2011). Thus, the higher abundance of metacluster 3 that expresses high levels of CD2 further confirms that finding. It is tempting to speculate that the expansion of a metacluster that expresses high levels of CD2 could be related to NK cells interacting with the priming agent via CD15-CD2 interaction.

Proteomic analysis was used to determine whether there is a proteomic “fingerprint” of NK cell memory by comparing TpNK and CIML-NK. For that, analysis was performed in proteins upregulated by more than 4 log in the two memory populations and identified 41 proteins shared by CIML-NK and TpNK, some of which are discussed next.

One of the proteins upregulated was APOC2, which mediates triglyceride hydrolysis. This will increase the amount of fatty acids that NK cells can use as nutrients, which are used as substrates for oxidation and energy production, membrane synthesis, energy storage and production of signalling molecules and, therefore, are essential for cell survival and proliferation both under normoxia and hypoxia (Mylonis et al., 2019). This may provide the NK cells with an advantage to navigate the hypoxic TME.

FERM2 is another protein that was upregulated in memory-NK cells. FERM2 is a regulator of integrin activation, which are crucial in cell trafficking (Grégoire et al., 2007; Shannon & Mace, 2021) and also in the formation of the immunological synapse (Evans et al., 2009), the most critical event for NK cell cytotoxicity. All these would provide memory-NK cells with enhanced function.

LOXL3 expression in TpNK and CIML-NK cells may also be part of the memory fingerprint since the disruption of STAT3 dimerisation by LOXL3 will likely enhance NK cell lysis and DNAM-1 expression. In line with this, STAT3-KO mice show increased DNAM-1 expression and increased NK-mediated tumour-cell lysis (Gotthardt et al., 2014).

Several upregulated proteins shared by both memory-NK cell types are associated with DNA repair arising from oxidative stress (NEIL3, RL27, RL36, TYSY) which may be involved in resistance to intratumoural hypoxia. Others, such as RM14 and RM21, are involved in mitochondrial metabolism.

SLC9A9 is another upregulated protein that could be involved in the generation of memory. Besides contributing to endosome maturation, it also promotes the recycling of transferrin receptors. High expression of transferrin receptors has been associated with the sequestering of the inhibitory NK cell receptor KLRG1, impairing binding to cadherins on tumour cells (Schweier et al., 2014). The recycling of transferrin receptors by SLC9A9 appears unique to memory-NK cells since it was not induced by IL15 in this study nor by IL2 in our previous work (Sabry et al., 2019). The continuous expression of transferrin receptors on memory-NK would remove a major inhibitory signal and lower the threshold for activation by natural cytotoxicity receptors, enhancing NK cell cytotoxicity against cancer cells.

There are also several upregulated proteins by both memory-NK cells that are related to mitosis and cell cycle: APC11, CTIP, EPOP, FOXM1, MCM5, MCM6, STXB4, TET5A, TULP3 and WDR62; suggesting enhanced proliferative capacity by both TpNK and CIML-NK cells.

Pal and colleagues performed a similar study to ours where they generated TIML-NK cells by exposing the NK cells to NALM16, a B-ALL cell line, and looked at the transcriptomic signatures of TIML- and CIML-NK cells. One of their most interesting findings was that only TIML-NK cells upregulated genes involved in metabolic processes, including *CYP1B1, ALDOC, TKTL1, AGMAD* and *VDR* (Pal et al., 2017). This aligns with our observations of high upregulation of mitochondrial proteins with strong upregulation of CYP1B1. These data suggest that when NK cells come into contact with a cancer cell, changes in their mitochondria probably result from increased metabolic demand to exert cytotoxicity towards the cancer cell. Upregulation of mitochondrial survival proteins may indicate enhanced mitochondrial fitness and may provide an opportunity for NK cell activation without mitochondrial damage. This suggests that TpNK cells may have a survival advantage, especially within the hostile TME (Chang et al., 2015; Kouidhi et al., 2016).

Although the concept of “NK cell memory” is well established, it is plausible that NK cells with memory function can be derived through more than one mechanism. Memory-like NK cells have been studied extensively in the context of CMV and CIML-NK cells, but the idea that memory-NK cells can arise from tumour-priming remains far less studied. Here, we observe how TpNK and CIML-NK cells share some subpopulations with similar phenotypic/proteomic characteristics despite being generated by different stimuli, and speculate that the memory properties arise from those groups of cells.

Chapter 4 In-depth characterisation of the function of tumour-primed NK cells

4.1 Introduction

One of the hallmarks of NK cell memory is the enhanced functional response upon a second encounter with a target cell. Adaptive NK cells display enhanced capacity for ADCC and IFNγ secretion as described in the context of human CMV infection but also chronic viral infections with HIV-1 and HCV (Foley et al., 2012; Oh et al., 2016; Peppa et al., 2018; J. Zhou et al., 2015). CIML-NK cells are also characterised by enhanced IFNγ secretion and anti-tumour cytotoxicity. After an initial co-incubation with the triple-cytokine cocktail and a period of 7-day rest, these NK cells are then capable of exerting superior cytotoxicity against a variety of cancer cells (Cooper et al., 2009; Romee et al., 2012, 2016). Work from the Lowdell group and others have described that tumour-priming of NK cells results in NK cells with memory-like properties characterised by enhanced cytotoxicity upon exposure to a second target cell (North et al., 2007; Pal et al., 2017; Sabry et al., 2019). The proliferation in response to an antigen or the priming agent has also been regarded as a hallmark of memory NK cells and has been defined in adaptive NK cells (J. C. Sun et al., 2009), CIML-NK cells (Romee et al., 2012), and TIML-NK cells (Pal et al., 2017).

In Chapter 3, I identified an expanded NK cell metacluster 8 in tumour-primed and CIML-NK cells. This metacluster was delineated by higher expression of CD57 and lower expression of NKG2A in keeping with a mature or terminally differentiated population (Björkström et al., 2010; Lopez-Vergès et al., 2010). Furthermore, CIML-NK cells expanded a new metacluster 6, which was not present in any other conditions, characterised by Granzyme B^{high}, $CD25^{high}$, $CD69^{high}$, $CD38^{high}$ and $CD2^{int}$ expressions. The expansions of these two distinct metaclusters prompted me to interrogate if these NK cell subpopulations had different functional capacities.

Another interesting finding from Chapter 3 was the upregulation by CIML-NK cells of LAG3 and TIM3, markers linked to NK cell exhaustion (Judge et al.,

2020; A. M. Merino et al., 2020; Roe, 2022). Some populations of NK cells are found to be exhausted; in serial killing assays, it has been shown that an NK cell eventually loses its ability to exert cytotoxicity even if it is conjugating with the target cell, likely due in part to depletion of cytolytic granules (Vanherberghen et al., 2013). Thus, serial cytotoxicity assays were performed to elucidate whether different populations of CIML-NK cells were perhaps highly cytotoxic but became exhausted after some time.

Another crucial aspect of cellular memory is the changes that occur at the metabolic level. For instance, it is well described that a hallmark of the transition from a naïve T cell to a memory T cell induces changes in their metabolism, including increases in mitochondrial spare respiratory capacity (SRC) and oxidative phosphorylation (OXPHOS) (van der Windt et al., 2012, 2013). Fatty acid oxidation is also required by memory T cells to support mitochondrial metabolism, cell survival, and function (J. Lee et al., 2014; O'Sullivan et al., 2014). Similarly, NK cells have been shown to undergo changes in their metabolism when activated, and more recently, there have been reports on the metabolic features of adaptive NK cells and CIML-NK cells (Cichocki et al., 2018; Frank et al., 2015; Terrén et al., 2021). Glycolysis and OXPHOS are two of the main sources of energy for NK cells, and it is known that NK cells switch to using both sources when activated (Donnelly et al., 2014; Keating et al., 2016; Wang et al., 2020). Reports have shown that adaptive NK cells contain increased oxidative mitochondrial respiration, mitochondrial membrane potential, and spare respiratory capacity, indicating superior metabolic fitness, which might relate to enhanced NK cell performance (Cichocki et al., 2018). CIML-NK cells also have increased glycolytic capacity and OXPHOS (Terrén et al., 2021), but some evidence points at an increment in mitochondrial superoxide levels, which might render them unfit (Terrén et al., 2022). NK cells induce fatty acid oxidation during exposure to viral-infected and cancer cells, suggesting that that fatty acid oxidation promotes NK cell metabolic resilience (Schimmer et al., 2023; Sheppard et al., 2024). Currently, no data on the metabolic requirements of tumour-memory NK cells are available. The importance of mitochondrial health in determining the functional capacity of NK cells, together with the

observations made in Chapter 3 showing an increase in mitochondrial survival proteins in TpNK cells, provided the rationale for interrogating the metabolic profile of TpNK cells.

Despite the different conditions used to generate memory-like NK cells, it is plausible that these populations share functional capacities and metabolic profiles. In this chapter, I therefore determined the cytotoxic potential and metabolic features of tumour-primed NK cells in relation to CIML-NK cells.

4.2 Experimental aims

The experimental aims of this chapter were to characterise the cytotoxic capacity and metabolic function of tumour-memory NK cells to better define NK cell memory. TpNK cells were compared to CIML-NK cells. The specific aims were:

1. Characterise the proliferation capacity of TpNK cells

2. Evaluate the cytotoxic capacity of TpNK cells against a variety of solid and haematologic cancer cell lines in a flow cytometry assay

3. Compare the cytotoxic capacity of TpNK and CIML-NK cells against solid cancer cell lines using a real-time cytotoxicity assay

4. Compare the cytotoxic capacity of different NK cell subpopulations identified in Chapter 3 against solid cancer cell lines using a real-time cytotoxicity assay to investigate both conventional and serial killing capacity

5. Investigate the metabolic profile of both TpNK and CIML-NK cells by assessing glycolysis, mitochondrial respiration and mitochondrial depolarization

4.3 Results

4.3.1 Proliferation of TpNK cells

The ability to proliferate has been defined in different subsets of memory-NK cells. Adaptive NK cells proliferate after exposure to CMV (J. C. Sun et al., 2009). CIML-NK cells proliferate after a short exposure to IL12/15/18 (Romee et al., 2012) and TIML-NK cells after exposure to target cells (Pal et al., 2017). In order to further define tumour-memory NK, I studied the ability of TpNK cells to proliferate after coming in contact with INB16. A proliferation assay was set up over 5 days comparing rNK with TpNK cells in the absence of cytokines (Figure 4.1). NK cells were labelled with the cellular dye CellTrace Violet™ (Thermo Fisher), which allows for the visualisation of cell proliferation as with every division, which can be quantified by flow cytometry (Methods section 2.7.2). Figure A shows the gating strategy utilised for the experiment, and Figures B and C show histograms and bar plots, respectively, quantifying NK cell proliferation. After 5 days, the ability of TpNK cells to proliferate is significantly enhanced compared to rNK cells (Figure 4.1 C), which also correlates with an increase in the absolute cell number in TpNK cells (Figure 4.1 D). These results indicate that TpNK cells have proliferative capacity similarly to adaptive, CIML-NK and other tumour-memory NK cells.

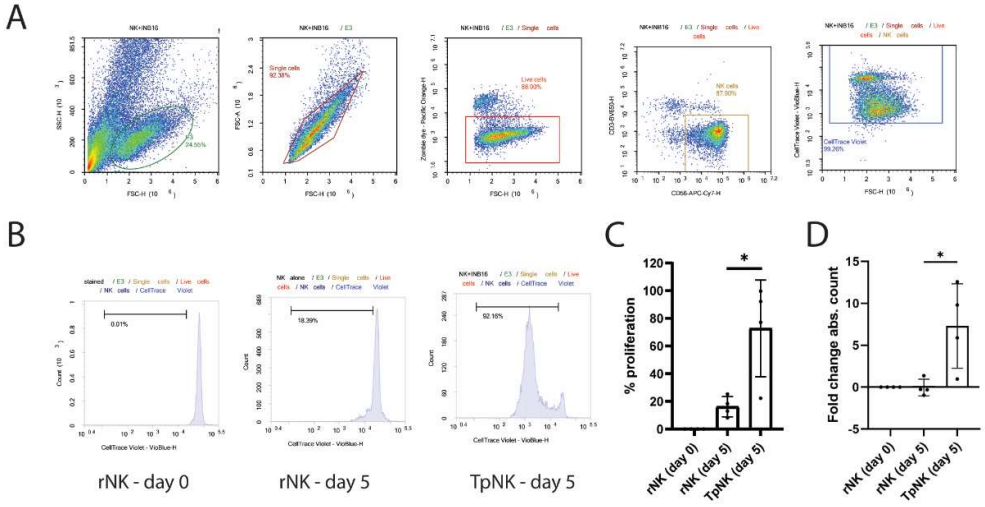

Figure 4.1. Proliferation of TpNK cells

Freshly isolated peripheral blood NK cells were stained with CellTrace Violet™ (Invitrogen) and set up for a 5-day co-incubation with CM alone (rNK) and with INB16

at a 1:2 ratio (TpNK cells). The fluorescence of the dye was measured by flow cytometry on day 0 and then on day 5. (A) Gating strategy of the assay. NK cells were gated as $CD56^{+}$ $CD3^{-}$ after debris, doublets and death cell exclusion. Thereafter, cell proliferation was measured based on the fluorescence intensity of the CellTrace Violet dye on the VioBlue channel. (B) Histogram plots show NK cell proliferation measured by the brightness of the dye. (C) The bar chart represents the % proliferation of the indicated conditions. (D) Fold change of the absolute cell count of the indicated conditions. Bars represent the means ± SD of 4 different donors as indicated by the dots. Data was tested for normality, and comparisons were made between rNK on day 5 and TpNK cells on day 5 using the paired t-test. Statistical significance is indicated as: *P <0.05: **P <0.01: ***P <0.001.

4.3.2 NK cell cytotoxicity

4.3.2.1 Evaluation of the cytotoxic capacity of TpNK cells against a variety of solid and haematologic cancer cell lines

In order to expand on existing data, the cytotoxic capacity of TpNK cells against a variety of cell lines from solid and haematological cancers was evaluated. Flow cytometry-based cytotoxicity assays were set up against tumour cell lines of hematologic cancers (Raji, U266, MDS-L, K562), renal cell carcinoma (786O and ACHN), and ovarian cancer (SKOV3, OVCAR) (Figure 4.2). Figure 4.2 A shows the gating strategy used to assess the killing of the correspondent target cells. Target cells were labelled with the membrane dye PKH67, and the viability dye TOPRO3 was used to identify live cells, from which cell death was then calculated (Methods section 2.11.1). In line with previously published data (Katodritou et al., 2011; North et al., 2007; Sabry et al., 2011, 2019), TpNK cells generated from healthy donors (HD) show significantly enhanced lysis *in vitro* of the NK-resistant cancer cell lines Raji, 786O, ACHN, SKOV3, U266, and MDS-L. TpNK did not show enhanced killing of NK-sensitive cell lines like K562 and OVCAR (Figure 4.2 B). The ability of NK cells to degranulate (measured by CD107a surface expression) and the secretion of cytokines (IFNγ and TNFα) was also assessed in Figure 4.2 C,

showing increased expression of CD107a and TNFα and IFNγ compared to rNK cells.

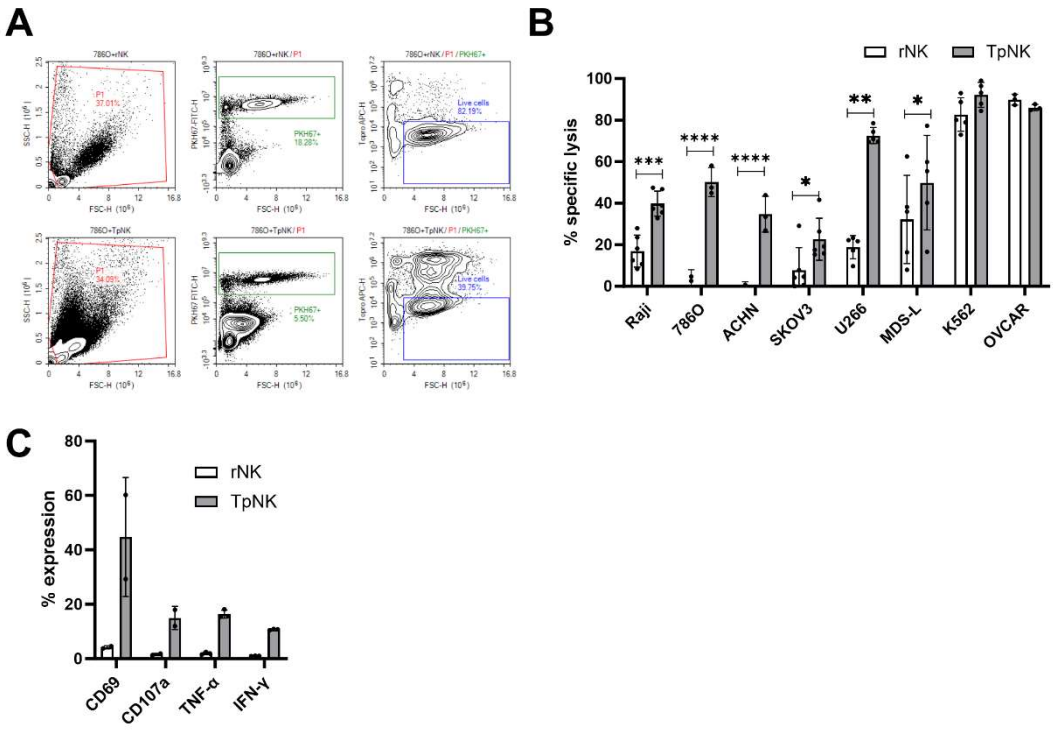

Figure 4.2. Cytotoxicity of TpNK cells against various targets

(A) Gating strategy of the assay. Target cells are gated as PKH67+ in the FITC channel. Thereafter, live cells are gated as TOPRO3 -ve in the APC channel. (B) Freshly isolated peripheral blood NK cells from HD were incubated as indicated overnight at 37˚C. The next day, cells were set up for a 4h-cytotoxicity assay against haematological cancer cell lines (Raji, U266, MDS-L and K562), renal cell carcinoma (786-O and ACHN) and ovarian cancer (SKOV3 and OVCAR) at E:T ratio 5:1. Bars represent the means ± SD of 3-6 different donors as indicated by the dots. Data was tested for normality, and comparisons were made between rNK and the different stimulatory conditions using the paired t-test. Statistical significance is indicated as: *P <0.05: **P <0.01: ***P <0.001. The absence of an asterisk indicates non-significance. (C) Freshly isolated peripheral blood NK cells were incubated as indicated overnight at 37˚C. Surface and intracellular expression of different markers were analysed in NK cells the next day by flow cytometer. Bars represent the means ± SD of 2 different donors as indicated by the dots.

4.3.2.2 Comparison of the cytotoxic capacity of TpNK and CIML-NK cells against solid cancer cell lines

Next, I compared the cytotoxic capacity of TpNK and CIML-NK cells to determine if both types of memory NK cells show a similar cytotoxic potential. Resting NK, TpNK and CIML-NK cells were tested against two NK-insensitive cancer cell lines, the epithelial ovarian cancer cell line SKOV3 (Figure 4.3) and the epithelial prostate cancer cell line DU145 (Figure 4.4) in the xCELLigence system, which allows for continuous monitoring of target cell death after addition of effector cells.

The cytotoxic capacity of NK cells against SKOV3 is represented in Figure 4.3; Figure 4.3 A shows a representative graph of the normalised cell index, and Figure 4.3 B shows a representative graph of the % cytolysis. The % cytolysis (Figure 4.3 B) shows that rNK cells can kill around 10% of SKOV3 target cells after 10 hours of co-incubation, which does not increase over a prolonged 100-hour period. TpNK cells show enhanced cytotoxicity compared to rNK cells and can kill around 40% of target cells at 40 hours, which then reduces slightly to around 30% over 100 hours. CIML-NK cells exhibit high cytotoxicity (~60% cytolysis addition), which increases over time, reaching around 95% cytolysis after 100 hours of co-incubation. Figure 4.3 C shows the area under the curve (AUC), measured as % cytolysis x hour and thus correlates with the amount of cytotoxicity induced throughout the experiment. TpNK and CIML-NK cells show a significant increase in cytotoxicity compared to rNK cells. CIML-NK cells show enhanced cytotoxicity compared to TpNK cells, albeit not significant.

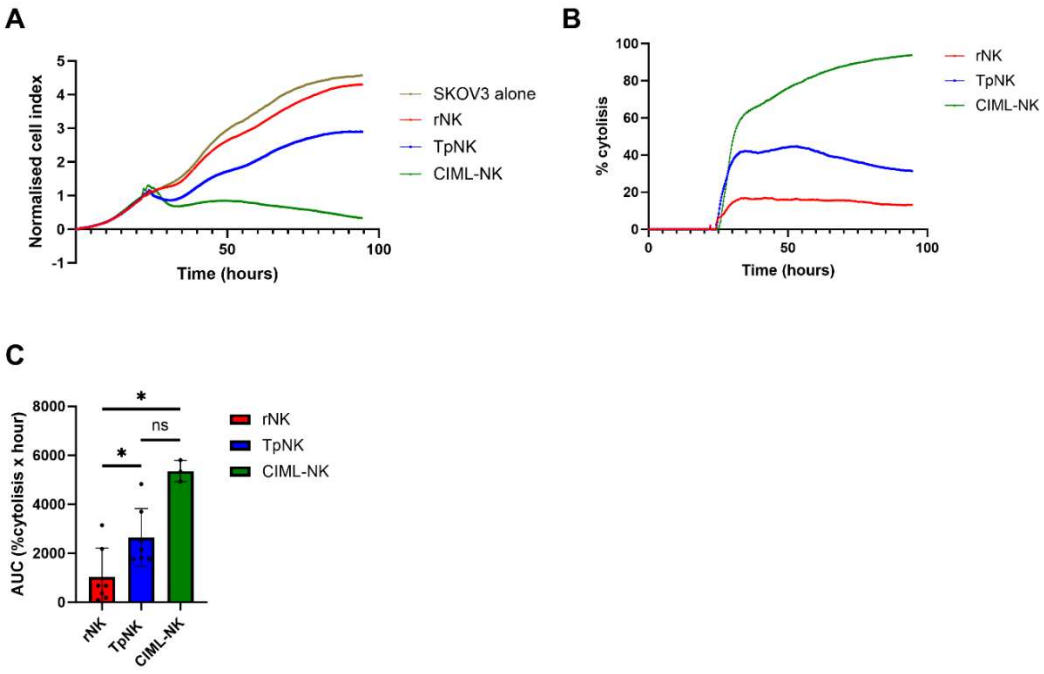

Figure 4.3. Cytotoxicity of TpNK and CIML-NK against SKOV3

(A)(B)(C) NK cells were isolated from PBMCs on day -1 and incubated overnight as indicated. On day -1, SKOV3 was seeded on the xCELLigence plate at the right concentration. On day 0, NK cells were added at a 5:1 E:T ratio to the corresponding wells on the xCELLigence plate and tested for cytotoxicity. (A) Representative graph of normalised cell index of SKOV3 growth for 100 hours with the indicated target cells. (B) Representative graph of % cytolysis of SKOV3 with the indicated target cells for 100 hours. (C) AUC was calculated as % cytolysis x hour for the indicated target cell against SKOV3. Bars represent the means ±SD of 3-7 different donors, indicated by the individual dots. Data was tested for normality, and comparisons were made between rNK and the different stimulatory conditions using a one-way ANOVA with Tukey multiple comparisons test for parametric data. Statistical significance is indicated as: *P <0.05: **P <0.01: ***P <0.001.

Another target used was the epithelial prostate cancer cell line DU145 (Figure 4.4), which is known to be resistant to NK cell killing (Hood et al., 2019; Sabry et al., 2011). Figure 4.4 A shows a representative graph of the normalised cell index. Cytotoxic capacity, as indicated by % cytolysis (Figure 4.4 B), indicates that rNK cells can kill a maximum of 30% of DU145 cells at 50 hours. Beyond this point, rNK cells cannot induce DU145 lysis, exhibiting a behaviour that

suggests NK cell exhaustion. TpNK cells show enhanced cytotoxicity compared to rNK cells and achieve a maximum of 45% cytotoxicity at 50 hours. Compared to rNK cells, TpNK cells display increased killing capacity beyond that point and for the whole experiment duration. CIML-NK cells exhibit heightened cytotoxicity upon initial contact, effectively eliminating 60% of DU145 cells within the first 5 hours. Subsequently, they sustain cytotoxic activity throughout the experiment, achieving a peak of approximately 95% cytolysis by the end of the experiment. Figure 4.4 C shows the AUC, which indicates an increase in cytotoxicity by TpNK and CIML-NK cells compared to rNK cells. Similar to SKOV3, CIML-NK cells show enhanced cytotoxic capacity against DU145 compared to TpNK cells.

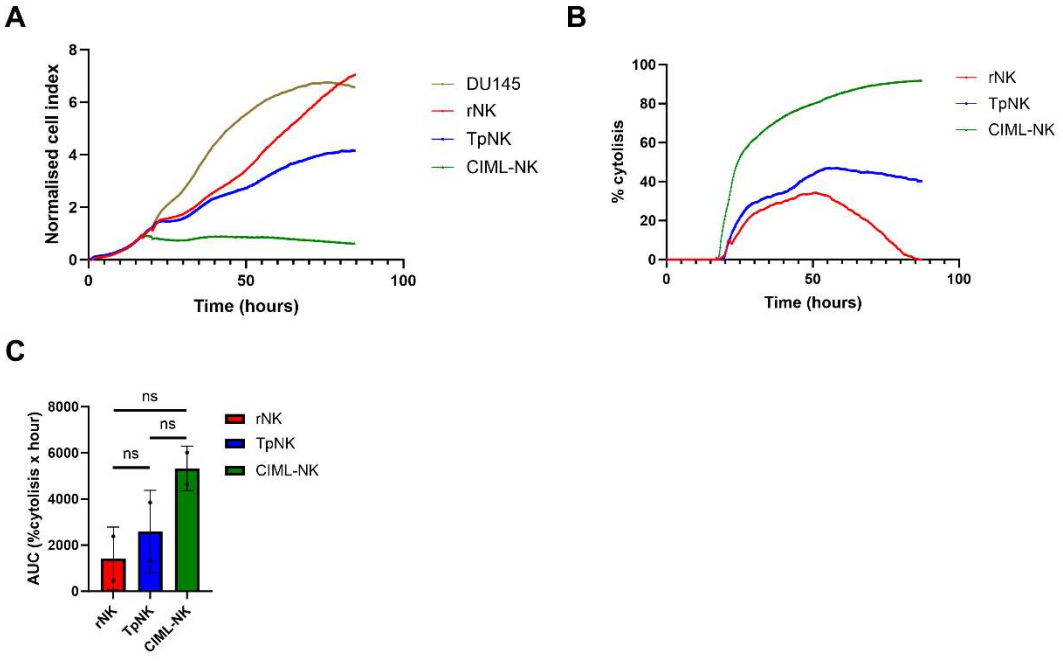

Figure 4.4. Cytotoxicity of TpNK and CIML-NK against DU145

(A)(B)(C) NK cells were isolated from PBMCs on day -1 and incubated overnight as indicated. On day -1, DU145 was seeded on the xCELLigence plate at the right concentration. On day 0, NK cells were added at a 5:1 E:T ratio to the corresponding wells on the xCELLigence plate and tested for cytotoxicity. (A) Representative graph of normalised cell index of DU145 growth for 100 hours with the indicated target cells. (B) Representative graph of % cytolysis of DU145 with the indicated target cells for 100 hours. (C) AUC was calculated as % cytolysis x hour for the indicated target cell against DU145. Bars represent the means ±SD of 2 different donors, indicated by the

individual dots. Comparisons were made using the Kruskal-Wallis one-way ANOVA with Dunn's multiple-comparisons test for non-parametric data. Statistical significance is indicated as: *P <0.05: **P <0.01: ***P <0.001.

4.3.2.2.1 Expression of NK cell ligands in cancer cell lines

NK cell recognition of targets depends on receptor-ligand interactions with the molecules on the target cell's surface. In order to investigate the differences between rNK, TpNK and CIML-NK cell cytotoxicity, we examined the expression of 17 cognate ligands on SKOV3 and DU145. These ligands can be divided into various categories based on which NK cell receptor they interact with. There are (1) the HLA-I classical molecules, including pan-HLA and HLA-C, which will mainly interact with NK cell inhibitory receptors like iKIRs. (2) The HLA-I non-classical molecule HLA-E interacts with the stimulating receptor NKG2C and the inhibitory receptor NKG2A. (3) The TRAIL receptors, TRAIL-R1/R2/R3, interact with TRAIL molecules on the NK cell to exert TRAIL-mediated apoptosis. (4) The ligands that interact with NKG2D include MICA/B and the ULBP family ligands. We included (5) CD15 and LFA3 ligands for the CD2 receptor expressed on NK cells. Also, (6) the NKp30 ligand, B7-H6; (7) the CD155 and CD112 ligands, which can be both activating if they interact with DNAM1 or inhibitory if they interact with TIGIT. Lastly, given the findings in Chapter 3 regarding the elevated PD-L1 levels in CIML-NK cells, the expression of its receptor PD1 was also assessed (8).

Figure 4.5 illustrates the ligand expression of SKOV3, whereas Figure 4.6 depicts the ligand expression of DU145. SKOV3 (Figure 4.5) exhibits high levels of HLA-I molecules, several NKG2D ligands such as ULBP3 and ULBP 2/5/6, and CD155, TRAIL-R1/2, and LFA3. Conversely, DU145 (Figure 4.6) demonstrates elevated levels of classical HLA-I ligands, pan-HLA, and HLA-C, with no expression of ULBP molecules. Similar to SKOV3, DU145 expresses CD155, TRAIL-R2/3, and LFA3.

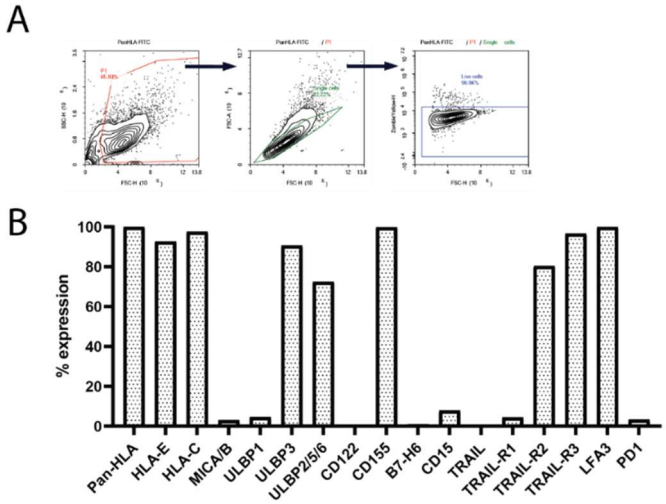

Figure 4.5. Phenotypical screening of NK cell ligands in SKOV3

SKOV3 was screened for 17 NK cell receptor ligands using flow cytometry. (A) Gating strategy used to assess phenotype. Target cells were gated after debris, doublets and death cell exclusion. Thereafter, the expression of each individual marker was determined in the corresponding channel. (B) The bar graphs show the % expression of the indicated receptors for SKOV3. Bars represent the mean of 3 replicates.

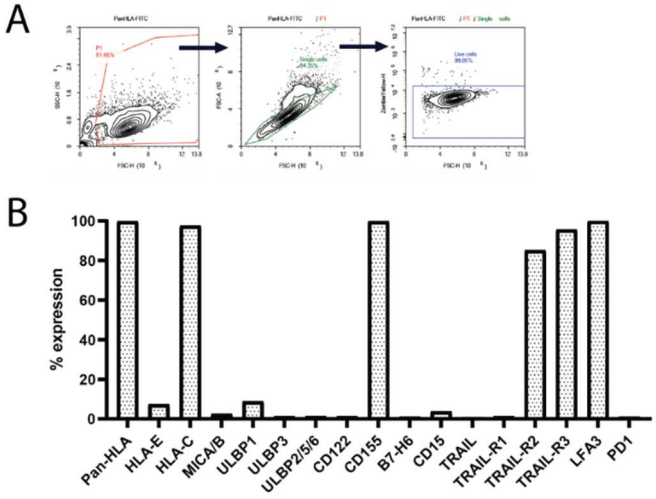

Figure 4.6. Phenotypical screening of NK cell ligands in DU145

DU145 was screened for 17 NK cell receptor ligands using flow cytometry. (A) Gating strategy used to assess phenotype. Target cells were gated after debris, doublets and death cell exclusion. Thereafter, the expression of each individual marker was determined in the corresponding channel. (B) The bar graphs show the % expression of the indicated receptors for DU145. Bars represent the mean of 3 replicates.

4.3.2.3 Comparison of the cytotoxic capacity of different metaclusters in memory-NK cells

The finding in Chapter 3 of metaclusters M6 and M8 expanding in TpNK and CIML-NK cells prompted me to investigate whether those metaclusters exhibited different cytotoxic profiles indicative of distinct functions. Metacluster 8 was characterised by having high expression of CD57 and low NKG2A, as well as being $CD69^{high}$ and $CD38^{high}$, suggestive of mature NK cells (Björkström et al., 2010; Lopez-Vergès et al., 2010). Metacluster 6 was restricted to CIML-NK, and these cells were characterised by having a very cytotoxic profile, with an expression of Granzyme B^{high}, $CD25^{high}$, $CD69^{high}$ and $CD38^{high}$. The observed differences in phenotype suggest potential distinctions in their cytotoxic capacity. To assess this, I initiated memory-NK cells by co-incubating NK cells with the triple cytokine cocktail IL12/15/18 and sorted the populations corresponding to metaclusters M6 and M8 utilising a cell sorter (Methods section 2.9). The xCELLigence device was used to measure cytotoxicity in real-time and to increase our understanding of their cytotoxicity profiles. The target cell chosen was the ovarian cancer cell line SKOV3, a well-known adherent NK-cell resistant cancer cell line.

4.3.2.3.1 Conventional killing

First, the cytotoxic capacity of the NK cells from both metaclusters was tested by performing a conventional cytotoxicity assay against SKOV3 (Figure 4.7). Figure 4.7 A shows a representative example of the normalised cell index, and Figure 4.7 B shows the % cytolysis. The measurement of the % cytolysis (Figure 4.7 B) shows that rNK cells are capable of exerting very low killing of SKOV3, where % cytolysis reaches a maximum of 10% at around 35 hours and then remains at 5% for the whole duration of the experiment. NK cells from metacluster M8 display higher cytotoxicity compared to rNK cells, reaching 50% cytolysis at 40 hours, which is then reduced over time. NK cells from metacluster M6 also display enhanced cytolysis, reaching a maximum of 65% cytolysis after 40 hours, which is then reduced over time. Figure 4.7 C shows a significant difference in the cytotoxic capacity of NK cells from metacluster M8 compared to metacluster M6. These findings align with the

observations from Chapter 3 regarding the phenotypic profile of NK cells in metacluster 6, exhibiting elevated levels of Granzyme B, CD25, CD69, and CD38, typical of highly cytotoxic and activated NK cells.

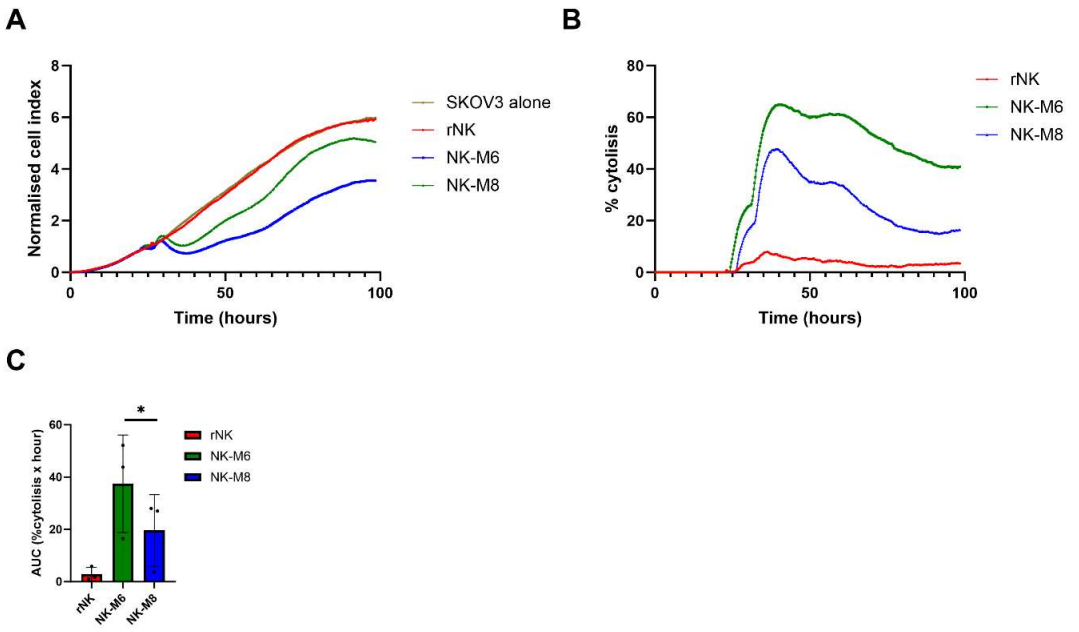

Figure 4.7. Cytotoxicity of NK cells from metaclusters M6 and M8 against SKOV3

(A)(B)(C) NK cells were isolated from PBMCs on day -1 and incubated overnight as indicated. On day -1, SKOV3 was seeded on the xCELLigence plate at the right concentration. On day 0, NK cells were sorted to obtain NK cells from M6 and M8 using a BD FACS Aria Fusion. Cells were then added to the corresponding wells on the xCELLigence plate and tested for cytotoxicity. (A) Representative graph of normalised cell index of SKOV3 growth for 100 hours with the indicated target cells. (B) Representative graph of % cytolysis of SKOV3 with the indicated target cells for 100 hours. (C) AUC was calculated as % cytolysis x hour for the indicated target cell against SKOV3. Bars represent the means ±SD of 3 different donors. Data was tested for normality, and comparisons were made between NK-M6 and NK-M8 using the paired t-test. Statistical significance is indicated as: *P <0.05: **P <0.01: ***P <0.001.

4.3.2.3.2 Serial killing

The observation in Chapter 3 that CIML-NK cells exhibited a phenotype reminiscent of immune exhaustion prompted further investigation into whether cells from metaclusters M6 and M8 were capable of sequential killing. While NK cell exhaustion remains incompletely characterised, and there is conflicting data regarding the existence of an "exhausted NK cell" phenotype (Judge et al., 2020; A. M. Merino et al., 2020; Roe, 2022), studies have explored the ability of NK cells to engage in serial killing, suggesting that some NK cells may perform multiple kills before becoming functionally exhausted (Vanherberghen et al., 2013). As a result, cytotoxicity assays focusing on serial killing were conducted to determine whether NK cells from these metaclusters could exhibit both high cytotoxicity and exhaustion.

NK cells from metacluster M6 and M8 were set up in a cytotoxicity assay (Methods section 2.11.2.2) where the NK cells were allowed to interact with SKOV3 targets for 24 hours and then were transferred to new SKOV3 for 24 hours, for a total of 3 times (Figure 4.8 A). Figure B shows normalised cell index, and Figure C shows % cytolysis across the 3 days.

On day 1, the % cytolysis of rNK shows little cytotoxicity against SKOV3; on the contrary, NK cells from metacluster M8 rapidly lyse around 75% of the target cells on the first 10 hours after being added, and then cytotoxicity plateaus for the rest of the assay (Figure 4.8 C). NK cells from metacluster M6 exhibit a similar pattern, rapidly lysing SKOV3 cells to around 85%, followed by a plateau for the remaining duration of the experiment. On day 2, the killing capacity of rNK cells remains low, similar to on day 1. However, the cytotoxic capacity of NK cells from metacluster M8 and M6 is reduced to 30 and 40%, respectively, at its maximum point and decreases rapidly after 10 hours of addition. When NK cells are moved into the third plate on day 3, rNK cells show low cytotoxicity. NK cells from metacluster M6 and M8 show further reduced activity compared to the previous day, reaching 10 and 20%, respectively, at their maximum point. AUC shows no significant differences between the cytotoxic capacity of NK cells from metacluster M6 and M8, but there is a trend towards NK cells from metacluster M6 exerting better

cytotoxicity (Figure 4.8 D). Another intriguing finding is that the cytotoxic capacity of NK cells from both metaclusters is reduced after each day, suggesting that these cells cannot exert sequential killing.

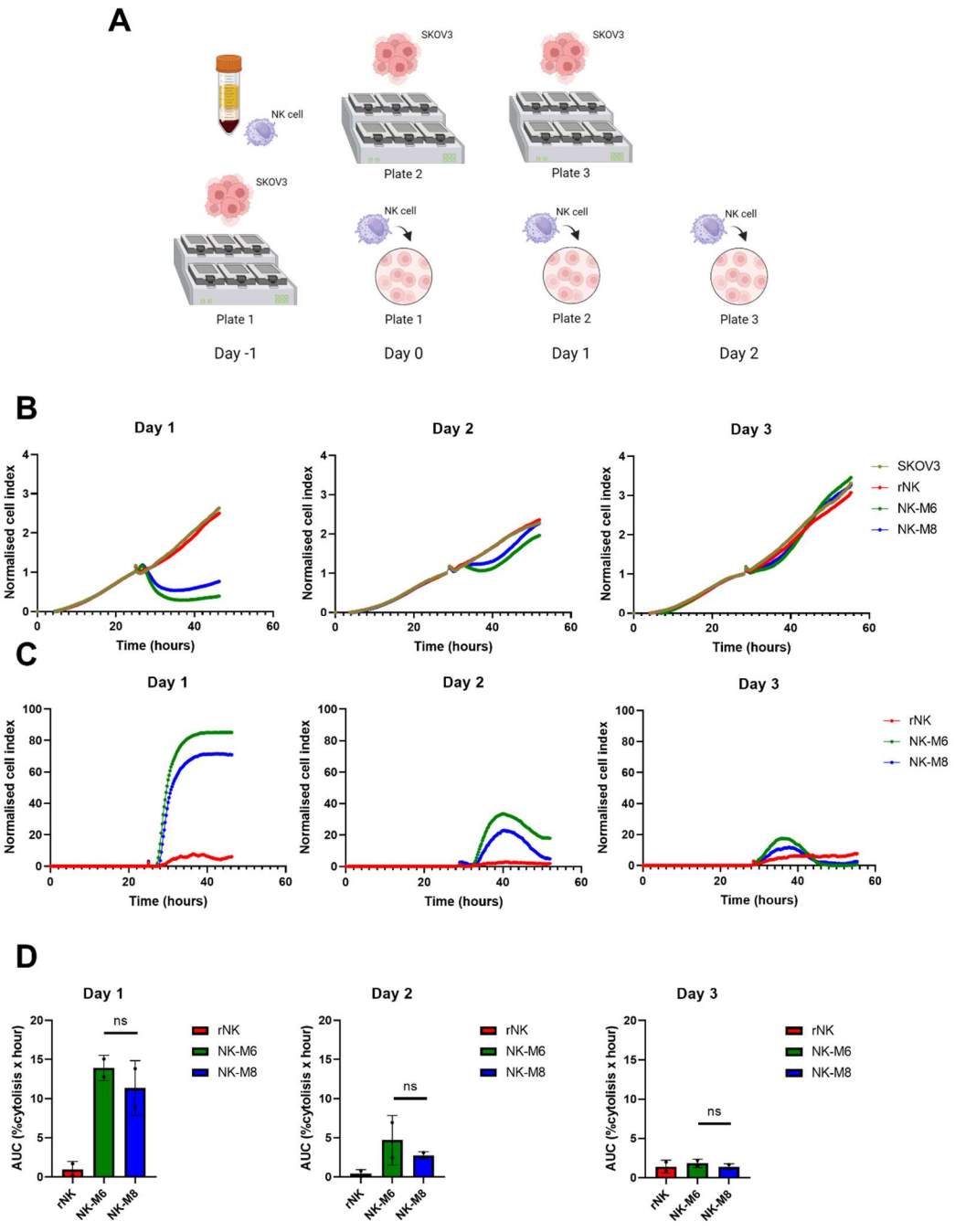

Figure 4.8. Serial cytotoxicity capacity of NK cells from metaclusters M6 and M8 against SKOV3

(A) Infographic describing the experimental approach to the serial cytotoxicity assay. NK cells were isolated from PBMCs on day -1 and incubated overnight as indicated.

On day -1, SKOV3 was seeded on the xCELLigence plate at the right concentration (plate 1). On day 0, NK cells were sorted to obtain NK cells from M6 and M8 using a BD FACS Aria Fusion. Cells were added to the corresponding wells on the xCELLigence plate and tested for 24 hours. Also, on day 0, a second plate of SKOV3 (plate 2) was seeded on the xCELLigence. On day 1, the NK cells in plate 1 were transferred to plate 2 and tested for the second time for 24 hours. Also, on day 1, a third plate of SKOV3 (plate 3) was seeded on the xCELLigence. On day 2, the NK cells in plate 2 were transferred to plate 3 and tested for the third time for 24 hours. (B) Representative graph of normalised cell index of SKOV3 growth across 3 consecutive killings for the indicated target NK cells. (C) Representative graph of % cytolysis of SKOV3 growth across 3 consecutive killings for the indicated target NK cells. (D) AUC was calculated as % cytolysis x hour across 3 consecutive killings for the indicated target NK cells. Bars represent the means ±SD of 3 different donors. Comparisons were made between NK-M6 and NK-M8 using the paired t-test. Statistical significance is indicated as: *P <0.05: **P <0.01: ***P <0.001.

4.3.3 Metabolic function of NK cells

Following the observed increase in mitochondrial survival proteins in TpNK cells in Chapter 3, I subsequently investigated whether these changes resulted in enhanced metabolic fitness through a series of metabolic assays. A Seahorse assay was used to evaluate the real-time metabolism of NK cells by measuring their glycolysis and mitochondrial respiration after tumour-priming, compared to CIML-NK cells. Cells use two primary energy-producing pathways: glycolysis and OXPHOS. While rNK cells mostly rely on OXPHOS to meet their energy needs, they strongly upregulate both glycolysis and OXPHOS pathways when activated (Donnelly et al., 2014; Keating et al., 2016; Wang et al., 2020). This allows the NK cells to increase their energy production in parallel with the synthesis of molecules required for effector functions (Donnelly et al., 2014; Keating et al., 2016; Keppel et al., 2015). To further confirm the changes observed in our proteomics assay, mitochondrial depolarisation, an indicator of mitochondrial health, was also measured (Surace et al., 2021; Terrén et al., 2021).

4.3.3.1 Glycolysis

First, the extracellular acidification rate (ECAR) was analysed, which is a measure of lactate production and glycolysis at the basal state and after the addition of rotenone (Rot) and antimycin A (AA). Rotetone interferes with complex I and antimycin A disrupts complex III of the electron transport chain. Separately, 2-deoxy-glucose (2-DG) was added, a competitive inhibitor of glycolysis (Figure 4.9 A). TpNK and CIML-NK cells exhibit elevated basal glycolysis in comparison to rNK cells, with CIML-NK cells demonstrating higher levels than TpNK cells (Figure 4.9 B). Additionally, the measurement of maximal glycolytic rate reflects a similar pattern, with TpNK cells displaying higher mean rates than rNK cells, and CIML-NK cells exhibiting the highest rate (Figure 4.9 C).The glycolytic reserve is measured as the difference between the maximum glycolytic capacity and the basal glycolytic rate, and it indicates a cell's capability to respond to an energetic demand. In this assay, no significant differences in glycolytic reserve were observed by any of the different NK cell conditions (Figure 4.9 D). The increase in glycolysis by both TpNK and CIML-NK cells is an indicator of activation, as it will allow the NK cells to meet their energy needs.

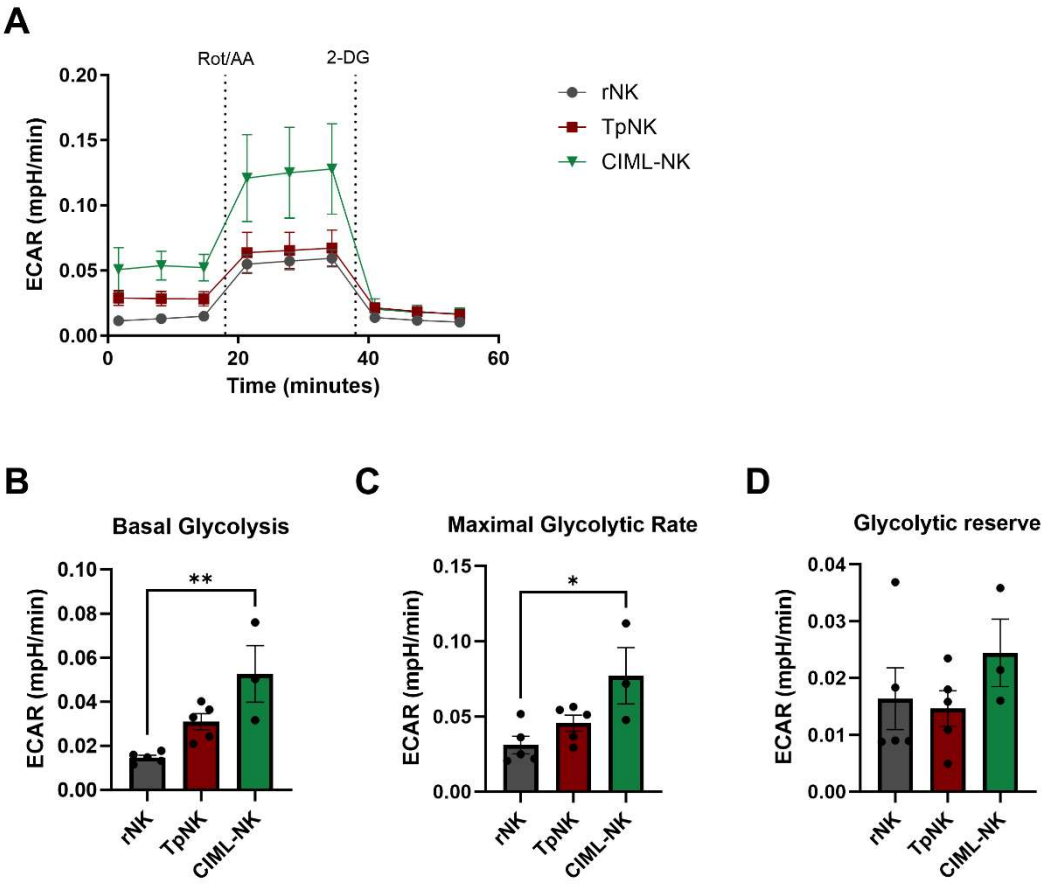

Figure 4.9. Glycolytic rates of TpNK and CIML-NK cells

Freshly isolated NK cells were incubated overnight at 37°C as indicated. The next day, cells were prepared by removing dead cells and positively selecting NK cells to remove stimulatory agents. After that, (A)(B)(C)(D) glycolytic function was measured according to manufacturer's protocol in Seahorse XF platform (Agilent). Data were normalised to cell count and cell viability per well using normalisation function. Bars represent the means ±SD of 5 different donors. Data was tested for normality, and comparisons were made between all conditions using a one-way ANOVA with Tukey multiple comparisons test for parametric data. Statistical significance is indicated as: *P <0.05: **P <0.01: ***P <0.001. The absence of an asterisk indicates non-significance.

4.3.3.2 Oxidative phosphorylation

Next, mitochondrial respiration was assessed by measuring oxygen consumption rate (OCR), a measure of OXPHOS, at basal levels and following the addition of a stressor mix made with rotetone, antimycin A, oligomycin and carbonyl cyanide-4 (trifluoromethoxy) phenylhydrazone (FCCP) (Figure 4.10 A). Oligomycin is an ATP synthase inhibitor, which will impact electron flow through the electron transport chain (ETC) and thus is linked to cellular ATP production. FCCP is an uncoupling agent that collapses the proton gradient and disrupts the mitochondrial membrane potential. As a result, electron flow through the ETC is uninhibited, and oxygen consumption reaches the maximum, which will allow for the calculation of spare respiratory capacity, a measure of the ability of the cell to respond to increased energy demands or stress. Finally, a mixture of rotetone and antimycin A shuts down mitochondrial respiration and therefore allows for the calculation of non-mitochondrial respiration. The results show that both TpNK cells and CIML-NK cells exhibit enhanced basal mitochondrial respiration relative to rNK cells, with CIML-NK cells displaying the highest OCR (Figure 4.10 B). When assessing maximal mitochondrial respiration (Figure 4.10 C), TpNK cells demonstrate the highest increase, although not statistically significant, while CIML-NK cells exhibit a trend towards reduced levels compared to rNK cells. Furthermore, there is a significant difference between TpNK and CIML-NK cells. These findings suggest that CIML-NK cells are operating at maximum capacity and may not respond to further stimulation. In assessing spare respiratory capacity (Figure 4.10 D), TpNK cells exhibit a trend towards the highest OCR among the three conditions. Additionally, CIML-NK cells display a significantly reduced spare respiratory capacity compared to TpNK cells, indicating that while CIML-NK cells are highly cytotoxic, they have a diminished capacity to respond to cellular stress relative to TpNK cells.

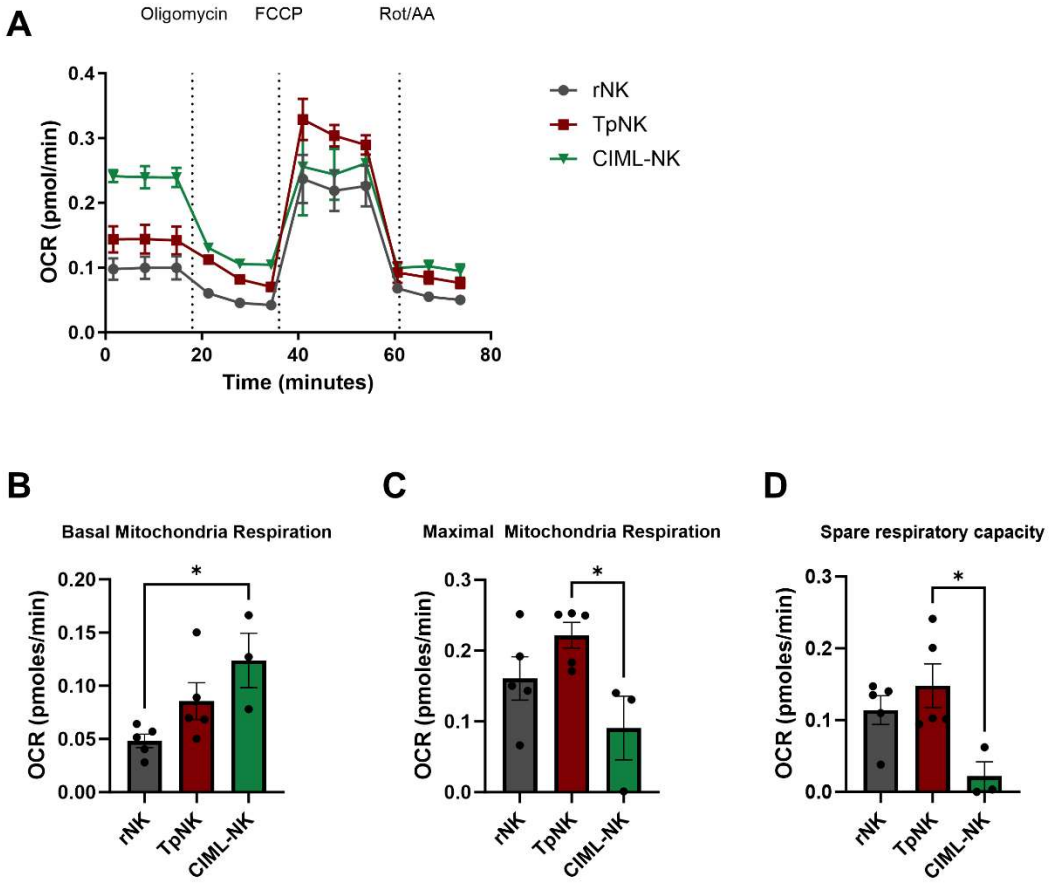

Figure 4.10. Oxidative phosphorylation rates of TpNK and CIML-NK cells

Freshly isolated NK cells were incubated overnight at 37°C as indicated. The next day, cells were prepared by removing dead cells and positively selecting NK cells to remove stimulatory agents. After that, (A)(B)(C)(D) mitochondrial respiration was measured according to the manufacturer's protocol in the Seahorse XF platform (Agilent). Data were normalised to cell count and cell viability per well using normalisation function. Bars represent the means ±SD of 5 different donors. Data was tested for normality, and comparisons were made between all conditions using a one-way ANOVA with Tukey multiple comparisons test for parametric data. Statistical significance is indicated as: *P <0.05: **P <0.01: ***P <0.001. The absence of an asterisk indicates non-significance.

4.3.3.3 Mitochondrial depolarization

Lastly, mitochondrial membrane potential of the different types of stimulated NK cells was assessed by measuring tetramethylrhodamine methyl ester (TMRM) staining. TMRM is a cell-permeant dye accumulating in active mitochondria with intact membrane potentials. Mitochondrial membrane potential is used as an indicator of mitochondrial energy status (Surace et al., 2021; Terrén et al., 2021). TMRM expression was measured by flow cytometry across the different types of NK cells (Figure 4.11). Figure A and B show representative flow cytometry contour plots (Figure 4.11 A) and histogram plots (Figure 4.11 B); rNK cells, IL15-activated NK cells, and CIML-NK show no expression of TMRM, suggesting low membrane potential; on the other hand, TpNK cells have 100% expression of TMRM suggestive high membrane potential (Figure 4.11 C).

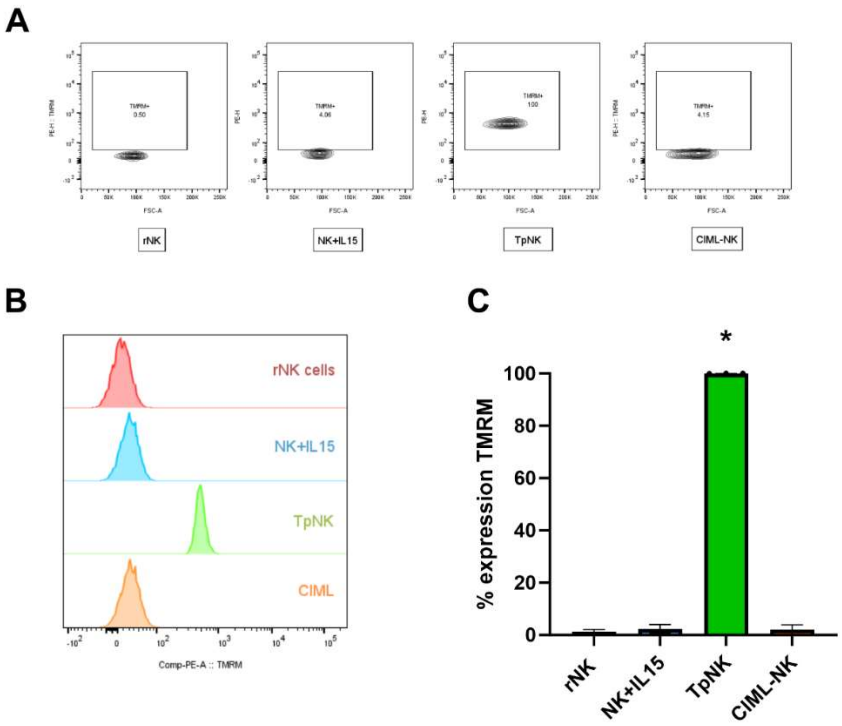

Figure 4.11. Mitochondrial membrane potential of TpNK and CIML-NK cells

Freshly isolated NK cells were incubated overnight at 37°C as indicated. The next day, cells were stained for CD56+, CD3-, Live/Dead Acqua and TMRM on a BD

Fortessa X20. (A) Contour plots and (B) histograms show TMRM staining across the different NK cell conditions. (C) Percentage expression of TMRM across the different NK cell conditions. Bars represent the means ±SD of 3 different donors. Data was tested for normality and comparisons across all conditions were made using the Kruskal-Wallis one-way ANOVA with Dunn's multiple-comparisons test for non-parametric data. Statistical significance is indicated as: *P <0.05: **P <0.01: ***P <0.001. The absence of an asterisk indicates non-significance.

4.4 Discussion

The Lowdell group previously characterised tumour-primed NK cells, highlighting their enhanced cytotoxicity upon secondary exposure to target cells, resembling features of NK cell memory, regardless of the priming agent (North et al., 2007; Sabry et al., 2011, 2019). This chapter expands on those findings by examining tumour-primed NK cells against a larger variety of cancer cell lines, both adherent and suspension. Interestingly, enhanced cytotoxicity was observed against cancer cell lines inherently resistant to resting NK cells, such as Raji, 786O, ACHN, SKOV3, and U266. However, NK cells did not exhibit lysis of cancer cell lines already susceptible to resting NK cells, such as K562 and OVCAR.

An unresolved question is whether there are differences in the cytotoxic profiles of TpNK cells and CIML-NK cells. Chapter 3 revealed characteristics of cytotoxicity in both TpNK and CIML-NK cells, along with significant differences in phenotypic and proteomic profiles between the two. Utilising the xCELLigence system, I investigated the cytotoxic profiles of both TpNK and CIML-NK cells in real-time. Both cell types demonstrated enhanced cytotoxicity against NK-resistant targets SKOV3 and DU145, with CIML-NK cells exhibiting higher cytotoxicity compared to TpNK cells.

The enhanced cytotoxicity observed in CIML-NK cells compared to TpNK cells may be attributed to several mechanisms postulated by Pahl and colleagues in their review article (Pahl et al., 2018). These mechanisms include a reduced threshold of activating receptor signalling (Bryceson et al., 2006; Horng et al., 2007; Jensen et al., 2017), increased expression of activating receptors, and a decreased response to HLA-I ligands (Draghi et al., 2005; Ewen et al., 2018).

Previous research conducted by our group demonstrated that tumour-primed NK cells undergo a process where CD16 is shed, leading to the release of CD3ζ. Subsequently, CD3ζ binds to the intracellular domain of CD2 in the NK cells, forming a complex with CD15 in INB16. This interaction results in the phosphorylation of CD3ζ, LAT, and STAT5, ultimately reducing the threshold signalling required for NK cells to exert cytotoxicity (Sabry et al., 2011). These

findings suggest that TpNK cells exhibit a similar reduction in the threshold of activating receptor signalling as observed in cytokine-activated NK cells.

In Chapter 3 of this thesis, phenotypic assessment of both tumour- and cytokine-activated NK cells demonstrated increased expression of activating receptors (CD69, CD25). In addition, FlowSOM analysis showed that CIML-NK cells are composed of mainly 2 metaclusters (M6 and M8), both of which display a cytotoxic profile. In contrast, TpNK cells are made of 5 big metaclusters (M1, M2, M3, M7 and M8), not all of which demonstrate highly cytotoxic profiles. This suggests that CIML-NK cells have a higher percentage of NK cells that are ready-to-kill compared to TpNK cells, which could explain differences in the cytotoxicity observed.

The finding that cytokine-stimulated NK cells have a lower response to HLA-I ligands is intriguing. In a study, authors reported that NK cells stimulated with IL12/15/18 for 2 days showed decreased expression of the inhibitory KIR2DL2/L3, KIR2DL1 and KIR3DL1 (Ewen et al., 2018). Authors reported that this downregulation of expression resulted in less inhibition of cancer cells expressing HLA-I molecules, reducing the NK cell sensitivity to HLA-I inhibition. The metacluster study in Chapter 3 showed that CIML-NK cells undergo a considerable reduction of metacluster M7 (from ~37% to ~4%), which is high in iKIR expression. Interestingly, TpNK cells did not show a considerable reduction in metacluster M7 expression (from ~37% to ~25%); thus, they have a higher expression of iKIRs compared to CIML-NK cells. This reduction in iKIRs in specific populations of CIML-NK cells could likely cause enhanced cytotoxicity compared to TpNK cells.

Another possible explanation for the observed differences in cytotoxicity between TpNK and CIML-NK cells may be related to the expression of TRAIL receptors by both SKOV3 and DU145. In Chapter 3, we noted the upregulation of TRAIL in CIML-NK cells, whereas this was not observed in TpNK cells. It is conceivable that CIML-NK cells possess the ability to engage target cells through the TRAIL pathway and induce apoptosis. While the primary mechanism of NK cell cytotoxicity is through the release of cytotoxic granules, it has been reported that NK cells may switch to cytotoxicity via death-cell

receptors in the later stages of serial killing (Prager et al., 2019). Therefore, CIML-NK cells may demonstrate superior cytotoxicity against SKOV3 and DU145 due to their possession of additional cytotoxic mechanisms. Further investigations should include cytotoxicity assays against target cell lines devoid of TRAIL ligands.

Another noteworthy finding was the identification of novel metaclusters within the memory-NK cell populations, specifically metacluster M6 and M8 (Chapter 3). This prompted an investigation into potential differences among various cytotoxic subsets of NK cells. To this end, NK cells from metaclusters 6 and 8 were sorted, and cytotoxicity assays were conducted against SKOV3. Both NK cells from M6 and M8 demonstrated heightened cytotoxicity compared to rNK cells, with NK cells from metacluster M6 exhibiting the highest cytotoxic capacity. These findings are consistent with our observations in Chapter 3, where NK cells from metacluster M6 cells exhibited a phenotype indicative of enhanced cytotoxicity, characterised by elevated expression of CD69, Granzyme B, CD38, and CD25.

Studies have observed instances of serial killing in NK cells, wherein a single NK cell has demonstrated the capacity to perform up to 10 sequential kills (Bhat & Watzl, 2007; Choi & Mitchison, 2013; Srpan et al., 2018; Vanherberghen et al., 2013). However, specific populations of NK cells can become exhausted over time after performing serial killing (Vanherberghen et al., 2013). An important observation from the studies mentioned is that the NK cell populations that can induce sequential killing have a critical role, as most cytotoxicity against a target is performed in a serial fashion (Choi & Mitchison, 2013). The findings in this chapter do not support the notion that cells from metaclusters M6 or M8 exhibit serial killing behaviour. Instead, they displayed a cytotoxicity pattern similar to that observed in conventional killing assays on the first day of contact with target cells. Beyond this initial interaction, NK cells progressively lost their killing ability on subsequent days, indicating that serial killing did not occur. One limitation of this assay is the need to transfer NK cells from one well to another for each sequential kill, potentially resulting in cell loss during the process. During the assay, it was observed that NK cells remained tightly attached to target cells in the well. It is possible that the NK

cells that remained firmly attached, likely representing the most cytotoxic subset, were not transferred to the next well. Research has shown that a significant portion of NK cells do not exert cytotoxicity, with a minority responsible for most kills (Vanherberghen et al., 2013). Therefore, the reduced serial killing may be attributed to adding fewer cells to the next well or omitting cells with the highest cytotoxic capacity.

In this chapter, I wanted to elucidate whether the differences in mitochondrial survival protein expression in TpNK and CIML-NK cells observed in the proteomics study (Chapter 3) correlated with metabolic function. Both TpNK and CIML-NK cells showed higher glycolysis capacity than rNK cells, with CIML-NK cells displaying the greatest increase, as seen by others (Terrén et al., 2021). This increase in glycolysis is in keeping with the enhanced cytotoxic capacity in both TpNK and CIML-NK cells seen in this chapter, CIML-NK being the more cytotoxic of the two. An increase in glycolysis is required for NK cells in order to exert enhanced cytotoxicity (Donnelly et al., 2014; Keating et al., 2016; Wang et al., 2020).

The evaluation of OXPHOS showed that both TpNK and CIML-NK cells have enhanced basal mitochondrial respiration. However, whilst TpNK cells also show an increase in maximal mitochondrial respiration, CIML-NK cells have reduced capacity compared to rNK cells, demonstrating that CIML-NK cells are operating at their maximum capacity and, therefore may not be receptive to further stimulation. A study found that the enhanced OXPHOS on CIML-NK cells is lost over time, indicating that increased mitochondrial activity is not sustained for extended periods (Terrén et al., 2021).

Spare respiratory capacity, an indicator of a cell's ability to respond to increased energy demand or stress, was also assessed in this study. TpNK cells exhibited enhanced spare respiratory capacity, whereas CIML-NK cells displayed reduced capacity compared to rNK cells, which aligns with previous research (Surace et al., 2021; Terrén et al., 2021).

Due to the distinctive metabolic profile of TpNK cells, I conducted further investigations into their characteristics by examining mitochondrial membrane potential using TMRM staining. Mitochondrial membrane potential relates to

the mitochondrial capacity of ATP generation, and thus it is an indicator of mitochondrial function and overall capacity of the cell to produce energy, corresponding to improved cellular fitness and cytotoxic activity (Surace et al., 2021). Previous studies have demonstrated that adaptive NK cells exhibit heightened mitochondrial potential (Cichocki et al., 2018). In contrast, CIML-NK cells display reduced mitochondrial polarisation (Surace et al., 2021), consistent with the findings presented in this thesis. In this thesis I show that, like adaptive NK cells, TpNK cells exhibit increased mitochondrial membrane potential. This suggests that when an NK cell comes into contact with a viral- or tumour-transformed cell, specific metabolic changes occur in order to respond to the increase in energy demand.

These findings, combined with the proteomics study results from Chapter 3, suggest that the alterations observed in mitochondrial survival proteins could translate into superior metabolic fitness of TpNK characterised by enhanced mitochondrial respiration, spare respiratory capacity, and mitochondrial potential, making them more similar to adaptive NK cells (Cichocki et al., 2018).These attributes/metabolic traits could enhance their resilience to cellular stress over CIML-NK cells. The mechanisms driving the changes in memory-NK cell metabolism are largely unknown; however, in adaptive NK cells the activation of the signalling pathway mTORC1 has been identified as a mechanism to sustain oxidative metabolism and thus respond to increased energy demands (Frank et al., 2015), whether this is also the case in other types of memory-NK cells requires further study.

The results in this chapter support the notion that TpNK cells arising in response to tumour interactions have defined characteristics of immunological memory. Hallmarks of T cell memory include increases in OXPHOS and spare respiratory capacity, which are also evident in TpNK cells (van der Windt et al., 2012, 2013).

Chapter 5 NK cell homotypic interactions as a mechanism for NK cell activation and memory

5.1 Introduction

NK cells are a heterogeneous population which includes different subsets with distinct functions (C. Yang et al., 2019), which translates into different functional capabilities of NK cells. Previous observations indicate that, in some instances, very few NK cells are responsible for most of the cytotoxicity exerted against different targets (Vanherberghen et al., 2013). Given the heterogeneity of NK cells and their varying reactivity to different targets, it is reasonable to assume that these cells have developed distinct mechanisms for activation.

Despite limited research, evidence suggests that NK cells can activate other NK cells in a homotypic manner. Kim and colleagues elegantly demonstrated *in vitro* that the density of NK cells seeded in a well controls their degree of activation and proliferation (T.-J. Kim et al., 2014). This was demonstrated by generating a microwell system that allowed the authors to control the number of NK cells in each well. NK cells were grown in 'lonesome microwells', in which single-occupancy 'orphan' cells experienced no cell-cell contact; and 'social microwells', in which cells were allowed to contact each other freely. Authors reported that NK cells in 'social' microwells had enhanced responsiveness to exogenous IL2 and IL15, evidenced by increased CD25 expression and Stat3 phosphorylation. This process depended on 2B4/CD48 interaction. They observed that whilst 2B4 was present in the synapse with other NK cells, other receptors like NKG2D were distributed randomly. Experiments using blocking antibodies showed that blocking 2B4 abolished the proliferation and activation of NK cells in the 'social' microwells down to levels observed in the 'lonesome' microwells (T.-J. Kim et al., 2014).

In a follow-up paper from the same group, the authors employed the same microwell system to investigate this phenomenon further. They found that IL2 captured by the IL2-receptor on one NK cell could trigger IL2-receptor signalling in surrounding NK cells through intercellular contact and through

polarising CD25, MTOC, and lytic granules towards neighbouring NK cells. This was supported by a further study from the same group, in which NK cells from wild-type (WT) mice and NK cells from a CD25-knockout (KO) mouse were mixed at a 1:1 ratio. The authors observed proliferation of the KO NK cells mixed with the WT NK cells but not when the KO NK cells were alone, suggesting that the WT NK cells were trans-presenting IL2 to the neighbouring KO NK cells (M. Kim et al., 2017).

Similar findings were observed by the Lowdell group in two clinical trials in AML patients who received tumour-primed NK cells from haploidentical donors. In the first trial, patients did not have activated NK cells before the start of the treatment, which was marked by the expression of low levels of CD69 on NK cells. They observed that 6 out of 7 patients showed enhanced activation of autologous NK cells weeks after treatment with a single infusion of allogeneic, tumour-primed NK cells (Kottaridis et al., 2015). Similarly, in a second clinical trial, increases in % expression of CD69 were observed in NK cells of 4/8 patients weeks after the NK cell infusion (Fehniger et al., 2018). Because few (if any) donor NK cells were detected after 7 days in the patient's blood, this suggested that the infused NK cells might have activated endogenous NK cells in a homotypical manner.

To date, NK cell homotypic interactions have received little attention. However, evidence suggests it might be a biologically relevant effect that should be further explored to increase our understanding of NK cell biology as well as the development of NK cell-based therapies.

5.2 Experimental aims

In this chapter, I sought to investigate homotypic interactions between NK cells and, specifically, whether TpNK cells can activate rNK cells in a homotypical manner. The specific aims of the chapter were to:

1. Identify phenotypic changes in rNK cells co-incubated with TpNK cells

2. Assess differences in calcium flux dynamics in rNK cells co-incubated with TpNK cells

3. Assess conjugate formation dynamics in rNK cells co-incubated with TpNK cells using both flow cytometry and live imaging

4. Identify changes in F-actin formation in NK cells utilising confocal microscopy

5.3 Results

5.3.1 Phenotypical changes in rNK cells interacting with TpNK cells

First, I investigated if TpNK cells induce changes in the receptor expression of rNK cells (Figure 5.1). The surface expression of CD16 was chosen as the downregulation of CD16 marks NK cell activation (Grzywacz et al., 2007; Harrison et al., 1991; Romee et al., 2013). The experimental set-up of the assay is shown in Figure 5.1 A. Briefly, TpNK and rNK cells were co-incubated with labelled rNK cells overnight. The next day, the expression of CD16 was assessed by flow cytometry. Figure 5.1 B shows the gating strategy utilised for this experiment. As observed in Figure 5.1 C and D, in 3 out of 4 donors, CD16 was downregulated when rNK cells were co-incubated with TpNK cells both in % expression (Figure 5.1 C) and MeFI (Figure 5.1 D). This suggests that TpNK can activate rNK cells, leading to downregulation of CD16.

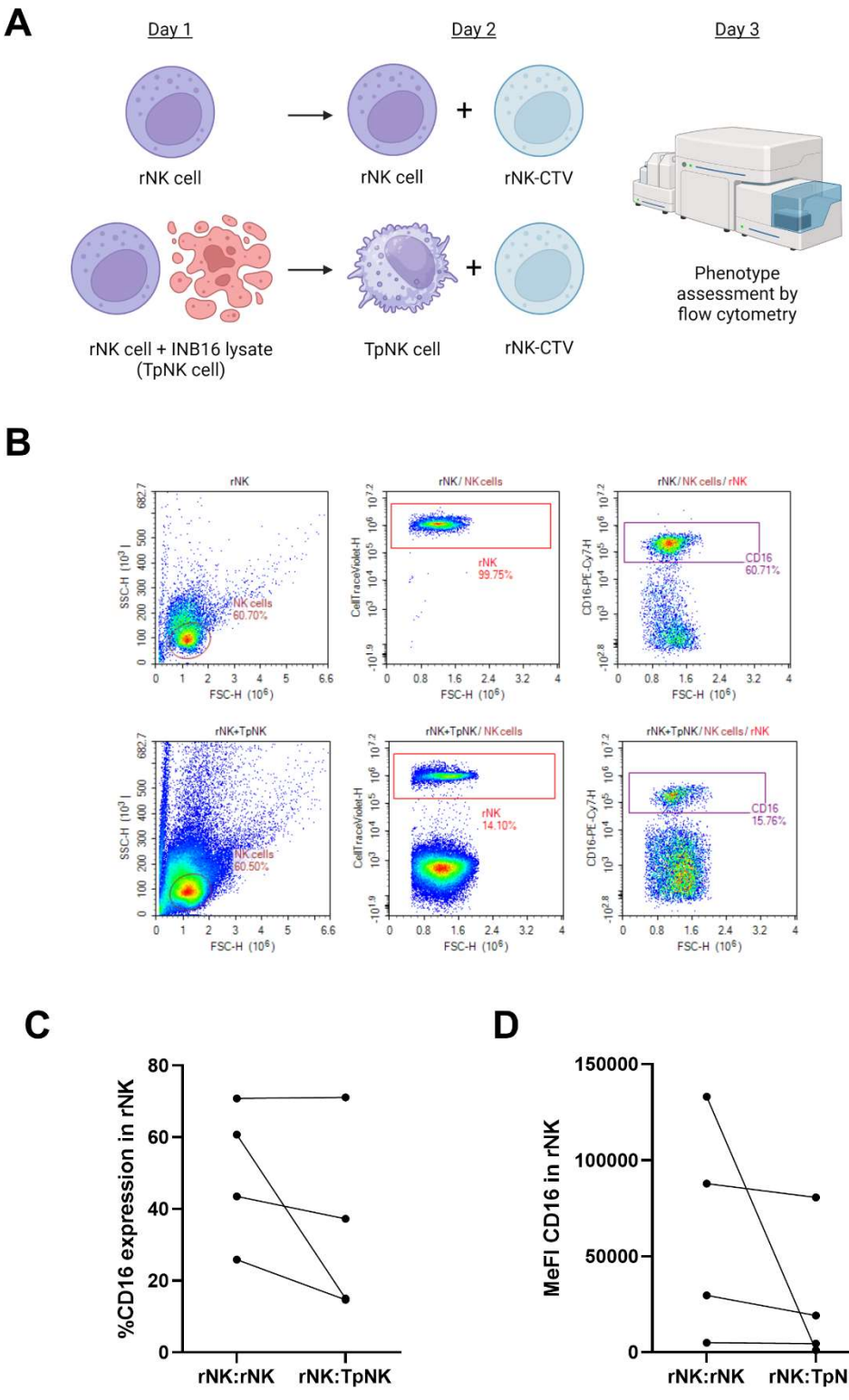

Figure 5.1. NK cells downregulate CD16 upon TpNK cell interaction

(A) Infographic shows the experimental protocol utilised. Freshly isolated NK cells were primed overnight with INB16 lysates (TpNK cells) or with CM (rNK). The next day, TpNK cells were washed in order to remove lysate. Half of the rNK cells were

labelled with CellTrace Violet™ dye and co-incubated overnight with autologous non-labelled rNK and non-labelled TpNK cells at a 1:1 ratio in order to have 2 conditions of rNK:rNK and rNK:TpNK. On day 3, cells were stained with CD16 mAb and acquired in a Novocyte flow cytometer. (B) Gating strategy of the experiment. NK cells were identified in the FSC vs SSC plot; the gate was projected onto an FSC vs Vioblue channel plot in order to identify rNK cells labelled with CellTrace Violet™ dye; the rNK cell gate was then projected into a third plot showing FSC vs PE/Cy7 channel in order to visualise CD16 staining. (C)(D) Individual data points represent the (C) % of CD16 expression and (D) MeFI of CD16 for the indicated conditions. Connecting lines represent the data from paired donors in each condition of 4 different donors.

5.3.2 Calcium flux measurements

To investigate the potential of TpNK cells to directly interact with rNK leading to their activation, I performed calcium flux measurements. It is known that rapid mobilisation of calcium in NK cells is induced in different settings, including receptor engagement on the NK cell (Bryceson et al., 2006), NK cell interaction with target cells (Wülfing et al., 2003), and upon synapse formation in the immunological synapse (Verron et al., 2021)

To evaluate whether TpNK cells would induce changes in calcium influx on rNK cells upon interaction (Figure 5.2), rNK cells were labelled with the 520AM dye (Abcam). Cells expressing calcium channels were preloaded with the dye, and fluorescence enhanced upon calcium binding was detected utilising flow cytometry. Labelled rNK cells were co-incubated with unlabelled rNK cells or TpNK cells, and calcium flux was assessed after 50 minutes. The addition of ionomycin was used as a positive control for the experiment, as ionomycin is a calcium ionophore that facilitates the transport of Ca^{2+}, which induces a surge in intracellular calcium mobilisation (Methods section 2.18). Figure 5.2 A shows the gating strategy utilised for this experiment. No significant difference in calcium mobilisation is observed when rNK cells are co-incubated with other rNK (rNK-rNK) compared to when rNK cells are co-incubated with TpNK cells (rNK-TpNK) (Figure 5.2 B). A substantial increase in calcium mobilisation is observed upon adding ionomycin to rNK cells. This indicates

that the lack of any discernible differences in the other conditions is not due to experimental errors or variations (Figure 5.2 B).

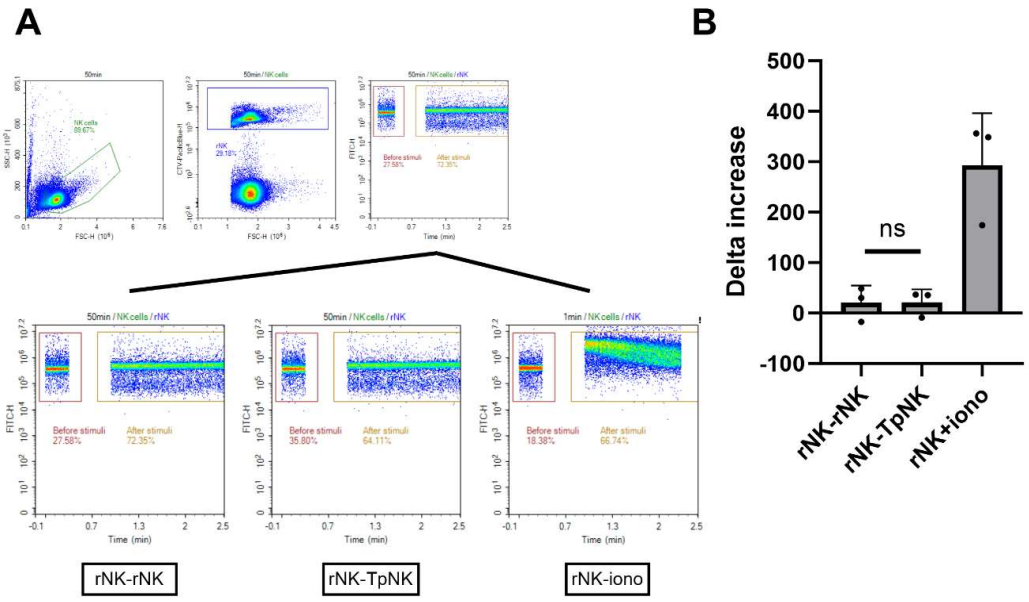

Figure 5.2. Calcium flux dynamics of rNK and TpNK cells

Freshly isolated NK cells were primed overnight with INB16 (TpNK) or with CM (rNK). The next day, overnight stimulation was removed by removing death cells with the Death Cell Removal Kit (Miltenyi) and by sorting NK cells with CD56+ microbeads (this was done in both TpNK cells and rNK cells to allow for comparison). After that, part of the rNK cells were labelled with CellTrace Violet™ and with 520AM dye following protocol for the Calcium Flux Assay kit (Abcam). The rest of the rNK and TpNK cells were prepared and added to the labelled rNK cells for 50 minutes. A positive control of ionomycin (iono) was prepared and added to the labelled rNK cells for 1 minute. Cells were acquired in the Novocyte flow cytometer before and after adding the stimulatory agents. (A) Gating strategy and representative plots for each condition. A first plot with FSC vs SSC was used to identify NK cells. The gate was then projected onto a second plot showing FSC vs CellTrace Violet™- Pacific Blue to identify the rNK cell population. After that, the gate was projected onto a third plot showing time vs 520AM – FITC. The plots below are representative examples of the calcium flux profile of the individual conditions. (B) Bar charts represent the delta increase MeFI of calcium flux of the indicated conditions. Bars represent the means ± SD of 3 different donors, indicated by the individual dots. Comparisons were made between rNK-rNK and rNK-TpNK cells using the paired t-test. Statistical significance is indicated as: *P <0.05: **P <0.01: ***P <0.001.

5.3.3 Live imaging of NK cell homotypic interactions

NK cell activation through homotypic interactions requires cell-to-cell contact (M. Kim et al., 2017; T.-J. Kim et al., 2014). Therefore, I examined next if TpNK cells require direct cell contact to activate autologous rNK cells.

The dynamics of NK cells were assessed utilising live imaging by evaluating the number of cell-to-cell contacts in cells containing only rNK cells compared to wells containing a mix of rNK and TpNK cells (Methods section 2.19.1). NK cells were visualised live for 16 hours in a Nikon CT Biostation, a device containing a fluorescence microscope with a built-in incubator (Figure 5.3 A). Images were taken every 15 minutes, and the number of contacts between two NK cells were visually counted in every timeframe. A contact was defined as the moment where the cell membranes of two different NK cells touched, and are indicated in Figure 5.3 B with yellow arrows. The % of contacts for every condition are shown in Figure 5.3 C and indicate that in the wells containing a mix of rNK cells and TpNK cells, the number of contacts between NK cells is significantly higher compared to wells where only rNK cells are present (Figure 5.3 C). This suggests that TpNK cells may have a more motile phenotype and greater capacity to screen their environment by establishing more contacts with other NK cells.

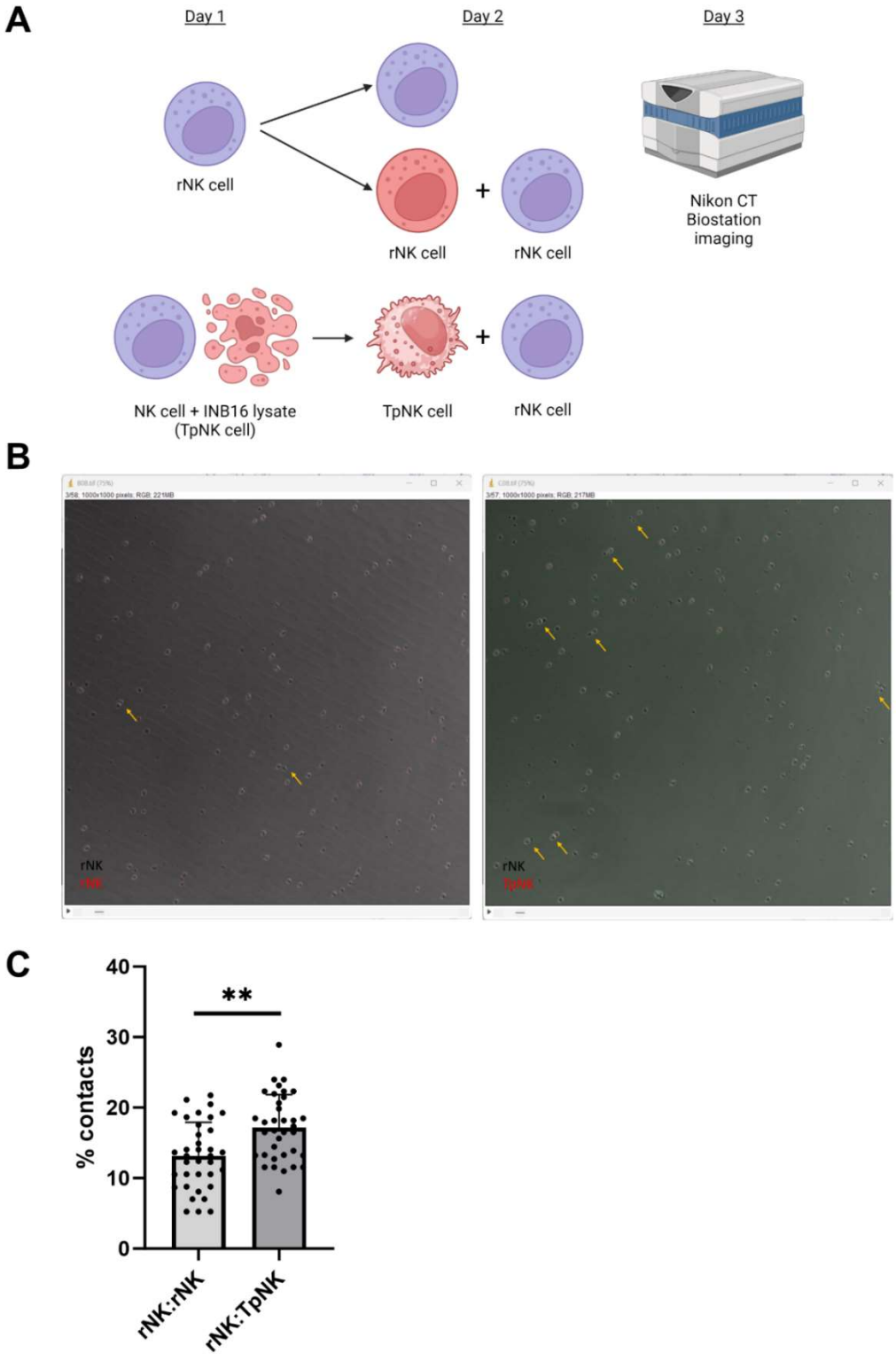

Figure 5.3. Live dynamics of rNK cells and TpNK cells.

(A) Freshly isolated NK cells were primed overnight with INB16 lysate (TpNK) or with CM (rNK). The next day, TpNK cells were washed in order to remove lysate. Half of the rNK and TpNK cells were labelled with PKH26 dye. After that, NK cells were then

plated in a 96-well flat-bottom plate at a 1:1 ratio in order to have rNK unlabelled: rNK-PKH26 (rNK:rNK) and rNK unlabelled:TpNK-PKH26 (rNK:TpNK). The plate was then placed inside the Nikon CT Biostation (Nikon) for 16 hours, and images were taken every 15 minutes at an x10 magnification; the resulting images were analysed in ImageJ. For analysis, cell contacts were enumerated when 2 cells were coming together and their membranes were touching; if cells were separating and coming together again, this was counted as a separate contact. The % contacts were calculated by considering the total number of cells in the image. (B) Timeframe image of the Nikon CT Biostation for both conditions; yellow arrows show contacts between cells. (C) The bar chart represents the % total number of cells in contact with the indicated conditions. Bars represent the means ± SD of 1 donor; dots represent internal replicates of the different frame shots. Comparisons were made between rNK:rNK and rNK:TpNK cells using the paired t-test. Statistical significance is indicated as: *P <0.05: **P <0.01: ***P <0.001.

5.3.4 Conjugate formation

To confirm previous findings further, I assessed the conjugate formation capacity of wells containing only rNK cells compared to wells containing a mix of rNK and TpNK cells. This was evaluated by flow cytometry by looking at the conjugate formation of NK cells labelled with different dyes at various time points (Figure 5.4 A and methods section 2.17). Conjugates were visualised in the flow cytometer as doublets and then projected into another plot gated in the double-positive population (Figure 5.4 B). Despite the variability of the results, a trend is observed towards an increased number of conjugates in wells containing a mix of rNK and TpNK cells compared to wells containing just rNK cells (Figure 5.4 C). This is in keeping with the enhanced contact formation induced by TpNK cells described previously (Figure 5.3) and indicates that TpNK cells have superior motility and capability of establishing conjugates and contacts with other NK cells.

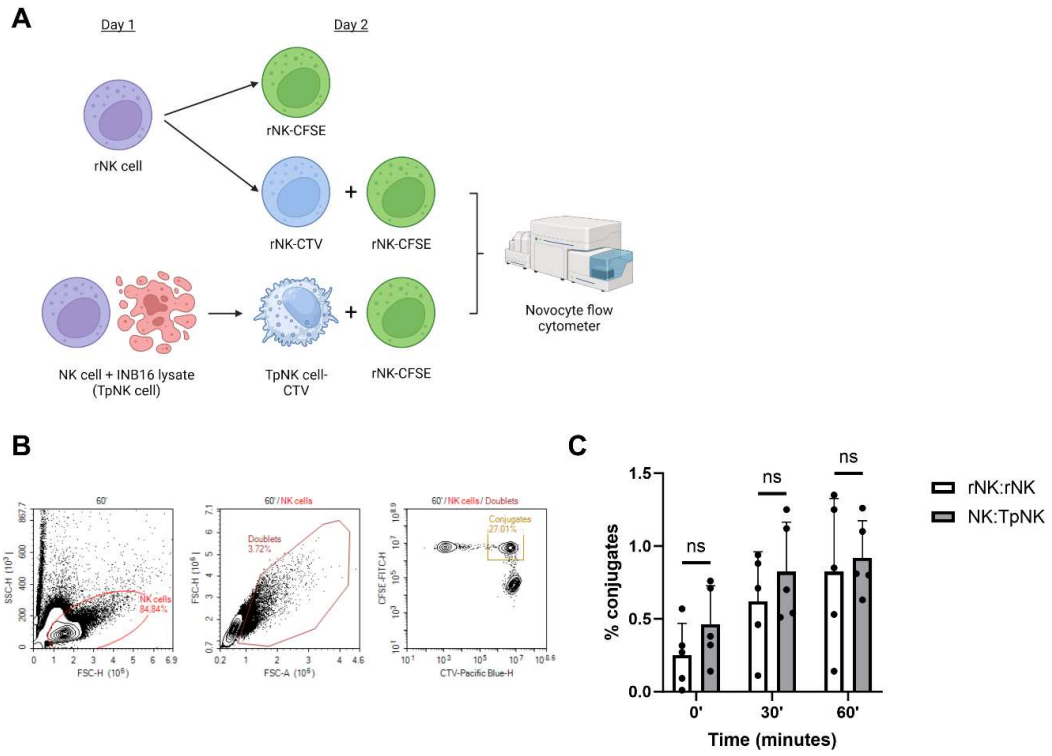

Figure 5.4. Conjugate formation dynamics of TpNK and rNK cells

(A) Freshly isolated NK cells were primed overnight with INB16 lysate (TpNK) or with CM (rNK). The next day, TpNK cells were washed in order to remove lysate. The rNK cells were separated into 2 groups; half of them were labelled with CellTrace CFSE™ (CFSE) and the other half with CellTrace Violet™ (CTV); TpNK cells were also labelled with CellTrace Violet™ (CTV). NK cells were then co-incubated at various time points at a 1:1 ratio as follows: rNK-CFSE with rNK-CTV (rNK:rNK) and rNK-CFSE with TpNK-CTV (rNK:TpNK). After each timepoint was met, cells were fixed with 0.5 paraformaldehyde and acquired in the Novocyte flow cytometer. (B) Flow cytometry plots show the experiment's gating strategy. A first plot with FSC vs SSC was used to identify NK cells. The gate was then projected onto a second plot showing FSC-A vs FSC-H to identify doublets. Doublets were then projected into a third plot of CTV-PacificBlue vs CFSE-FITC to identify conjugates at the double-positive gate. (C) Bar chart representing the % of conjugates of the indicated conditions at various time points, and show the means ± SD of 5 different donors as indicated by the dots. Comparisons were made between rNK and TpNK cells using the paired t-test. Statistical significance is indicated as: *P <0.05: **P <0.01: ***P <0.001.

5.3.5 Confocal imaging

In order for NK cells to recognise a target cell, the formation of the immunological synapse is a crucial step, which involves cytoskeleton reorganisation, including the polymerisation of F-actin towards the area of contact with the target cell (Mace et al., 2009, 2010, 2014). Another critical element for NK cell recognition is the formation of nanotubes, which are membranous structures that physically link cells over long distances (Chauveau et al., 2010). Nanotube structures have been observed to be formed between NK cells and between NK cells and cancer cells (Chauveau et al., 2010; Mace et al., 2014). After preliminary evidence of NK cell homotypic interactions shown in this chapter, I used confocal microscopy to investigate F-actin organisation in NK cells (Figure 5.5).

Images show NK cells visualised as single cells, as evidenced by blue nuclear staining, where F-actin (in red colour) is visualised as a ring shape around the NK cells and forming patches inside the cells (Figure 5.5). NK cell conjugates were also visualised and are shown in the magnified squares in Figure 5.5. In the conjugate, F-actin polymerises towards the immune synapse (seen by an increase in the intensity of the red dye), indicating NK-to-NK cell interactions. Nanotube formations were also visualised between two NK cells, as evidenced by the formation of little tubular structures emerging from the NK cell body (Figure 5.6). The formation of nanotubes, together with the polymerisation of actin towards the immune synapse in NK cell doublets, suggests that NK cells interact with each other in a homotypical manner.

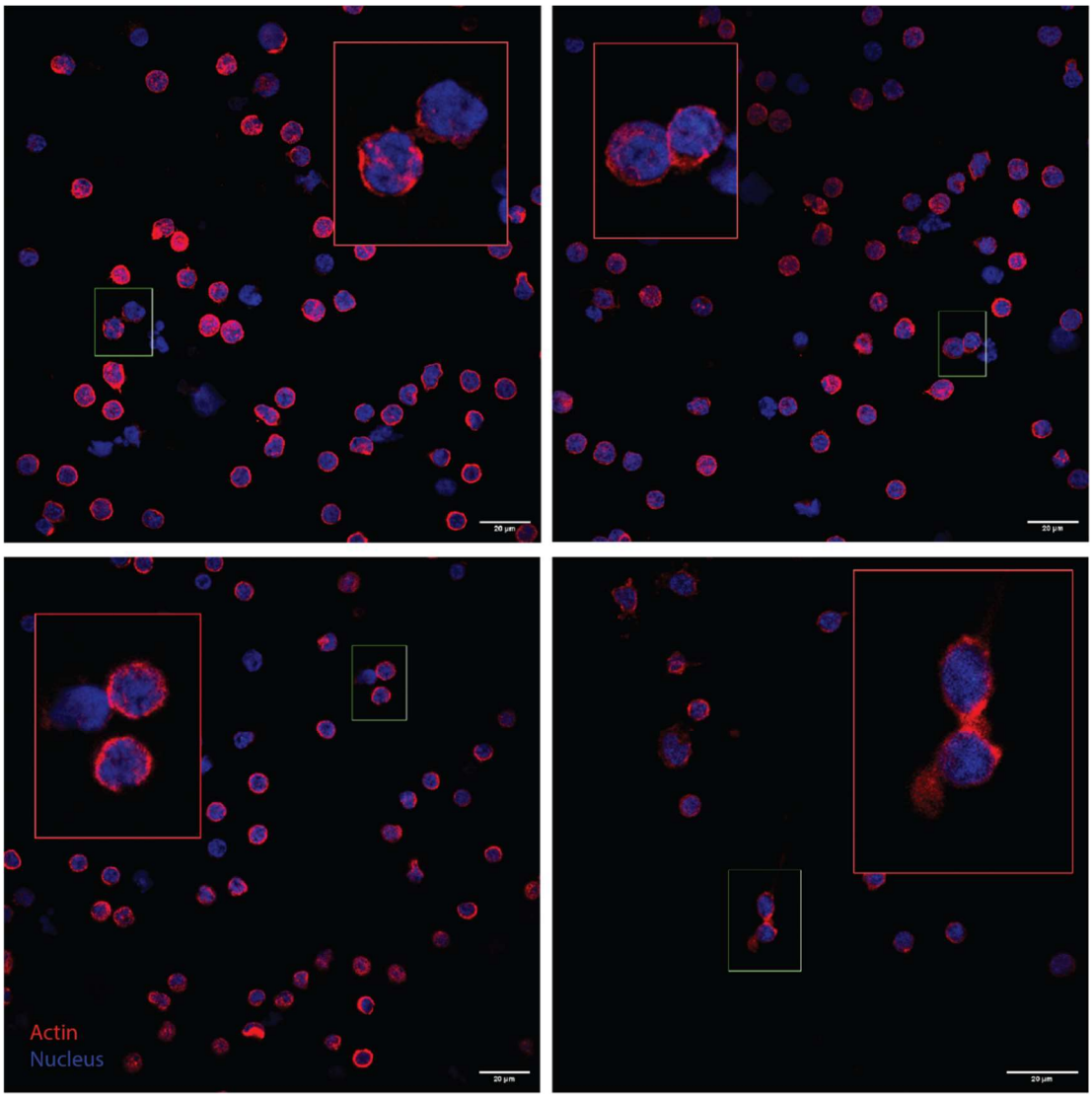

Figure 5.5. Actin polymerisation in NK cell homotypic interactions

Freshly isolated NK cells were prepared for confocal acquisition as previously described and stained for actin with Alexa Fluor 568 phalloidin kit (Invitrogen) in colour red and for the nucleus with NucBlue™ Fixed Cell Stain ReadyProbes™ reagent (Invitrogen) in blue as indicated by the manufacturer. Once prepared, the slides were visualised in a Nikon Ti Eclipse C2 laser scanning confocal microscope driven by NIS Elements software (Nikon). Images were analysed and processed using ImageJ. Screenshots in the red box represent the magnification of a structure of interest in the green box.

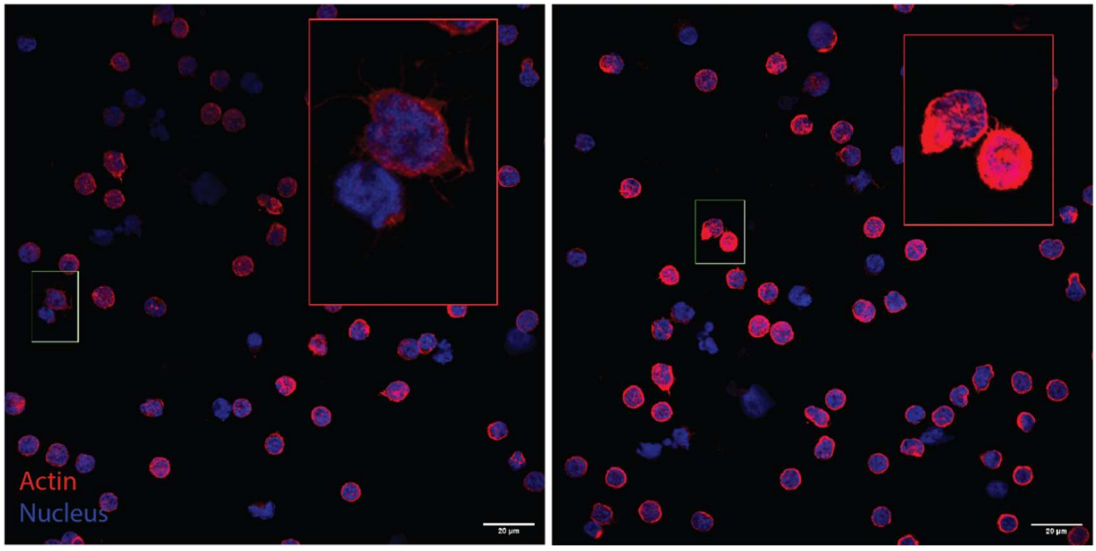

Figure 5.6. Nanotubes formation in NK cell homotypic interactions

Freshly isolated NK cells were prepared for confocal acquisition as previously described and stained for actin with Alexa Fluor 568 phalloidin kit (Invitrogen) in colour red and for the nucleus with NucBlue™ Fixed Cell Stain ReadyProbes™ reagent (Invitrogen) in blue as indicated by the manufacturer. Once prepared, the slides were visualised in a Nikon Ti Eclipse C2 laser scanning confocal microscope driven by NIS Elements software (Nikon). Images were analysed and processed using ImageJ. Screenshots in the red box represent the magnification of a structure of interest in the green box.

After establishing that NK cells modified F-actin when they were in a conjugate, I investigated the differences in F-actin polymerisation between wells containing a mix of rNK and TpNK cells and wells containing rNK cells alone (Figure 5.7 and Figure 5.8). Unlabelled autologous rNK cells were co-incubated with rNK or TpNK cells that had been pre-labelled with CellTracker™ green (in green colour) and stained for F-actin (in red colour) (experimental details can be found in the Methods section 2.19.2).

Figure 5.7 shows rNK cells (unlabelled) co-incubated with autologous rNK cells (green colour). NK-to-NK cell interactions are evidenced by the polymerisation of actin towards other rNK cells, forming a conjugate, shown in the magnified squares (top left and right, and bottom right images in Figure

5.7). The formation of nanotubes between two rNK cells was also observed (Figure 5.5, bottom right image).

Figure 5.8 shows rNK cells (unlabelled) co-incubated with autologous TpNK cells (green colour). Similarly, rNK-TpNK interactions are also observed, evidenced by increased F-actin polymerisation towards the union site between cells (Figure 5.8). Nanotube structures are also observed between interacting cells (Figure 5.8, top right image). In some instances, TpNK cells exhibited elongated morphologies and nanotubular structures connected to other NK cells, presenting polymerised F-actin towards the synapse (Figure 5.8, bottom left image).

Overall, differences in F-actin polymerisation or nanotube formation were not observed between co-cultures containing just rNK cells or between co-cultures containing a mix of rNK and TpNK cells. Because both rNK cells and TpNK cells can induce conjugates and contacts to a certain degree, it is not surprising to observe changes in F-actin in both groups. This suggests that both rNK cells and TpNK cells can interact in a homotypical manner with autologous NK cells but that this interaction does not determine the ability of an NK cell to activate another NK cell.

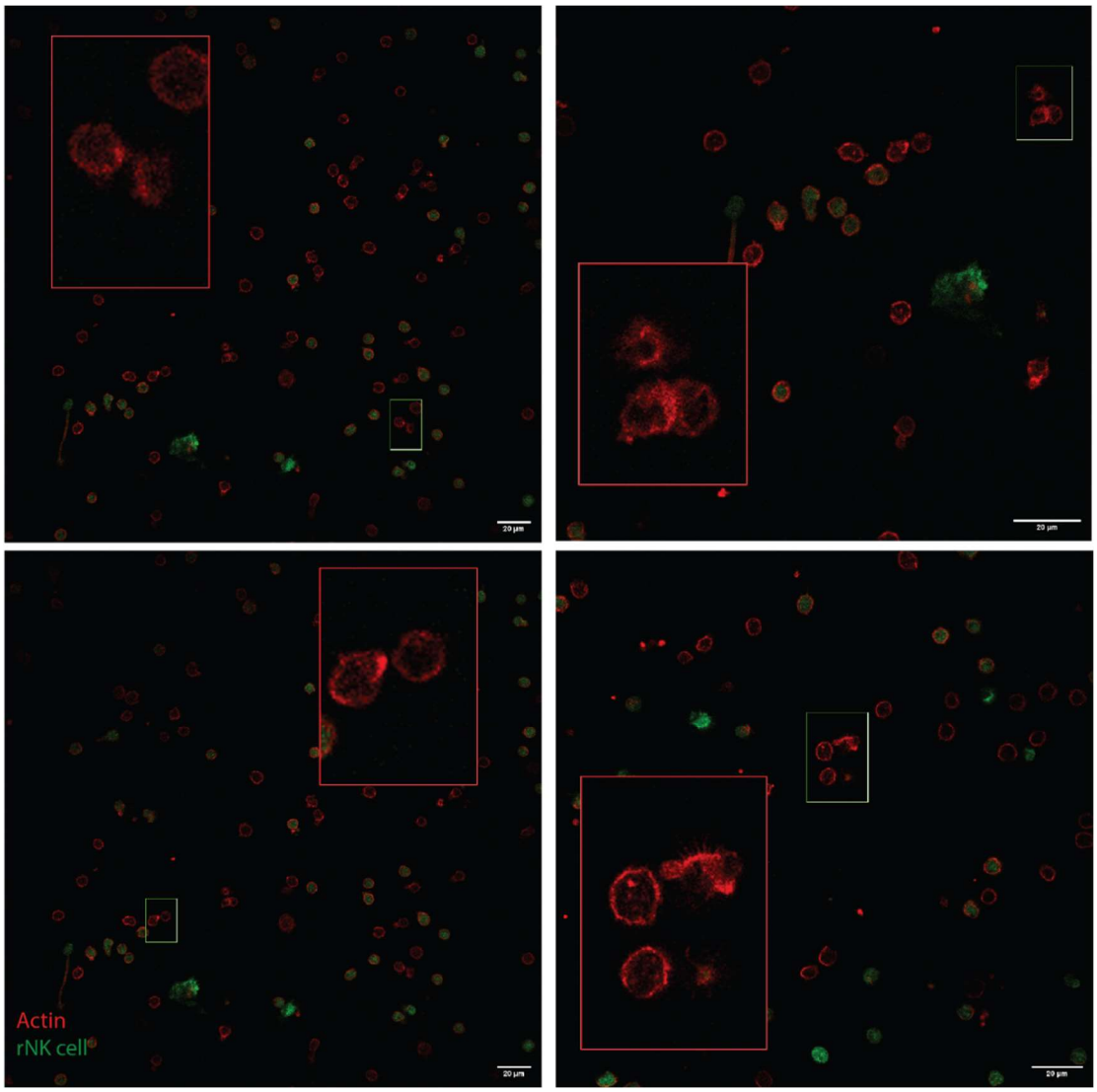

Figure 5.7. NK cell homotypic interactions with autologous rNK cells

Freshly isolated NK cells were isolated; half of the rNK cells were stained with CellTracker™ Green CMFDA (Invitrogen) in green colour and co-incubated overnight with CM. The next day, labelled rNK cells were co-incubated with unlabelled rNK cells at a 1:1 ratio for 1 hour and then prepared for confocal acquisition as previously described. Actin was stained with Alexa Fluor 568 phalloidin kit (Invitrogen) in red colour as indicated by the manufacturer. Once prepared, slides were visualised in a Nikon Ti Eclipse C2 laser scanning confocal microscope driven by NIS Elements software (Nikon). Images were analysed and processed using ImageJ. Screenshots in the red box represent the magnification of a structure of interest in the smaller green box.

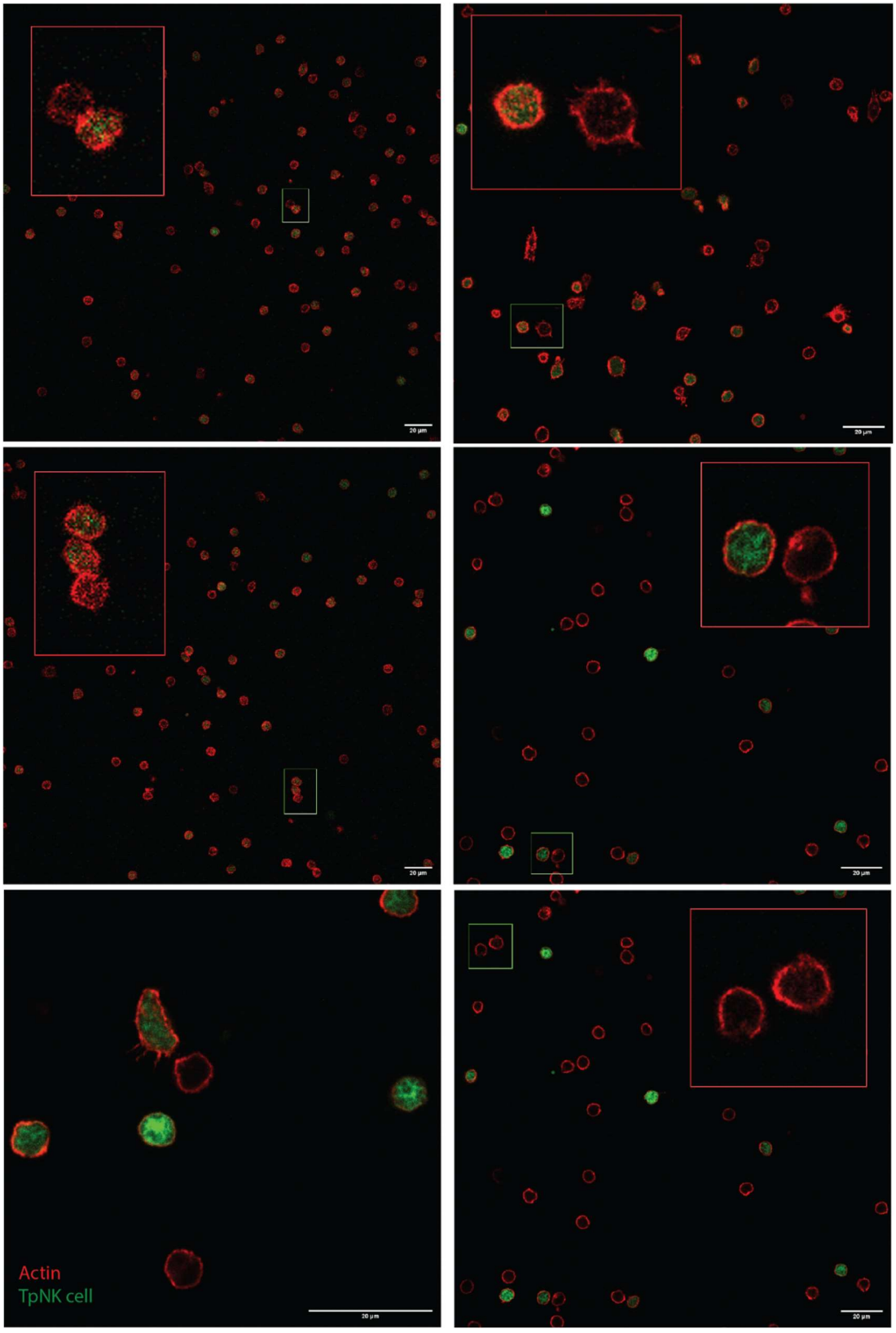

Figure 5.8. NK cell homotypic interactions with autologous TpNK cells

Freshly isolated NK cells were isolated; half were stained with CellTracker™ Green CMFDA (Invitrogen) in green colour and co-incubated overnight with INB16 lysate to

generate TpNK cells. The next day, TpNK cells were washed to remove lysate and were co-incubated with unlabelled rNK cells at a 1:1 ratio for 1 hour and then prepared for confocal acquisition as previously described. Actin was stained with Alexa Fluor 568 phalloidin kit (Invitrogen) in colour red as indicated by the manufacturer. Once prepared, slides were visualised in a Nikon Ti Eclipse C2 laser scanning confocal microscope driven by NIS Elements software (Nikon). Images were analysed and processed using ImageJ. Screenshots in the red box represent the magnification of a structure of interest in the smaller green box.

5.4 Discussion

NK cells are activated through various direct and indirect mechanisms, which play a critical role in immune responses. These mechanisms include the recognition of tumour- and virus-transformed cells via NK cell receptors and exposure to exogenous cytokines like IL2 or IL15. Additionally, interactions with other immune cells, such as NK-DC crosstalk, are essential for optimal NK cell responses (Lucas et al., 2007; O'Connor et al., 2006). Less explored ways by which NK cells become activated include NK-NK homotypic interactions (M. Kim et al., 2017; T.-J. Kim et al., 2014). In this chapter I focused on investigating homotypic interactions between NK cells in the context of tumour priming.

The findings support that TpNK cells can activate other autologous rNK cells, as marked by the downregulation of CD16 in the rNK cell population, which could be potentially mediated via homotypic interactions. In a previous study, Kim and colleagues examined changes in CD25 expression to determine NK cell activation (M. Kim et al., 2017; T.-J. Kim et al., 2014). CD25 would be a less relevant marker in our experimental setup as cytokines were not used to activate NK cells. Despite that, it would be relevant to screen other NK cell receptors to assess this phenomenon further.

Given that NK cells undergo an increase in intracellular calcium upon interaction with other cells (Bryceson et al., 2006; Verron et al., 2021; Wülfing et al., 2003), calcium flux was assessed on rNK cells that were mixed with TpNK cells to support our hypothesis. However, differences in calcium mobilisation were not observed in this experimental setup. It is possible that the low number of NK-to-NK cell contacts occurring would make changes in calcium flux challenging to quantify in a flow cytometry assay. The use of microscopy could represent an alternative and more sensitive method to visualise calcium changes at the individual cell level.

As part of target recognition, NK cells display brief, exploratory interactions with their environment before they make contact with a potential candidate target cell. CD62L and PSGL1 are thought to be involved in tethering movements, and more robust contacts are made by CD2, DNAM1, NKG2D

and LFA1 (Mace et al., 2014). In this chapter, we observed that TpNK cells increased conjugate formation and contacts, in keeping with a more motile phenotype with tethering exploratory behaviour. Olofsson and colleagues (Olofsson et al., 2014) compared the migration dynamics of non-activated vs IL2 activated NK cells and found multiple differences between the two. Activated NK cells had a more motile and migratory phenotype, characterised by increased contacts and duration of the conjugates against target cells. The findings in this chapter are consistent with previous research, even though here the NK cells were stimulated with cancer cells. The TpNK cells' dynamic phenotype would increase their chances of activating other rNK cells through increased interactions. Future work should include imaging experiments to visualise the receptors mentioned above in the membrane of TpNK cells.

Interestingly, the formation of nanotubes was observed in both rNK cells and TpNK cells. During the initial steps of NK cell interaction with a target cell, nanotubes seem to serve as intercellular tethers formed after the initial contact to guide the NK cell towards the target cell (Mace et al., 2014). The frequencies of nanotubes increase when there are more receptor/ligands available for interaction (Chauveau et al., 2010), and when NK cells are treated with cytokines, the frequency of nanotube formation doubles (Chauveau et al., 2010). Although the authors' primary focus in this study was the formation of nanotubes between NK cells and target cells, they also observed the presence of nanotubes between two NK cells (Chauveau et al., 2010). The data presented in this chapter are consistent with these observations, which demonstrate the formation of nanotubes in rNK cells and TpNK cells when interacting with other NK cells. These findings imply that NK cells may recognise other NK cells through a mechanism involving nanotube formation.

When a target cell is recognised by an NK cell, this is followed by the formation of the immunological synapse, which involves the polymerisation of F-actin towards the contact area between the cells (Mace et al., 2009, 2010, 2014). Kim and colleagues found that intact F-actin and nanotubes were required during NK cell activation via homotypic interactions with other NK cells (T.-J. Kim et al., 2014). In keeping with these findings, I observed that both rNK cells

and TpNK cells induce F-actin polymerisation towards the immune synapse when they come in contact with another NK cell, albeit to a different extent.

The results provided in this chapter provide some preliminary evidence of rNK-TpNK interactions, but the exact mechanisms require further definition.

One possibility is that this activation is based on receptor-ligand interactions in both NK cells. It is known that NK cells express some ligands that will interact with their own receptors. In a mouse model, NK cells expressing the ligand CD48, which interacts with the NK cell receptors CD2 and 2B4, were needed for NK cell homotypic interactions (K. M. Lee et al., 2006). Indeed, in human NK cells, 2B4 and CD48 interact in a *cis* manner to modulate NK cell responses (Claus et al., 2016). It is possible that 2B4/CD48 interactions could be involved in NK-to-NK cell activation.

Another possibility is trogocytosis, the intercellular transfer of plasma membrane patches. In the context of NK-cancer cell interactions, tumour cells use trogocytosis to “dress” NK cells with NKG2D ligands to induce NK cell fratricide and achieve immune escape (Nakamura et al., 2013). A similar phenomenon was observed in NK cells acquiring the NKG2D ligand MICA from target cells upon cell contact, which was then transferred to neighbouring NK cells in a homotypical manner, triggering NK cell degranulation (McCann et al., 2007). INB16 expresses several NK cell ligands, such as MICA/B (Sabry et al., 2019), which could be transferred to tumour-primed NK cells via trogocytosis. Possible functional consequences of this observation would be that MICA-positive NK cells would stimulate neighbouring NK cells via NKG2D interaction.

Regarding why NK cells require homotypic interactions to activate each other, Kim and colleagues speculated that IL2 trans-presentation occurring within multi-cellular clusters of NK cells ensures the availability of IL2, which can be a limited resource during the early stages of immune responses (M. Kim et al., 2017). Tregs are reliant on IL2, for which they have a high affinity (Gasteiger et al., 2013). In this scenario, NK cells that also require IL2 for their survival would need to compete with Tregs, and these homotypical interactions would provide a reliable source of IL2 in a hostile environment. However, this

hypothesis does not fit our particular model since cytokines were not used to activate NK cells. It is well known that NK cells are a heterogeneous population where NK cells with multiple roles exist (C. Yang et al., 2019). Furthermore, it has been shown that a minority of NK cells are responsible for the majority of the kills (Vanherberghen et al., 2013). Thus, from a cancer point of view, it is conceivable that NK cells that achieve activation after recognising a tumour cell would, in turn, activate another NK cell in order to amplify the activation response.

Finally, the results in this chapter need to be interpreted with caution given the small numbers/preliminary nature and lack of a confocal microscope with high magnification at our institute to visualise NK cells. Microwell technology and/or live imaging confocal microscopy can be used in future experiments. Despite these limitations, our data provide preliminary evidence that tumour-primed NK cells can activate rNK through potential homotypic interactions.

Chapter 6 Generation of tumour-memory NK cells in patients with myeloid haematological malignancies

6.1 Introduction

One of the most important functions of NK cells in cancer is immunosurveillance, by which NK cells patrol the body to eliminate arising cancer cells. It has been shown that patients with primary NK cell deficiencies have an increased risk for malignancies (Lorenzi et al., 2013; Orange, 2013; Spinner et al., 2014). Imai and colleagues performed a prospective study of more than 3,500 healthy people, showing that participants with less potent cytotoxic NK cells had a statistically significantly increased risk of cancer over the 11-year follow-up period (K. Imai et al., 2000). Furthermore, the degree of NK cell infiltration in tumour tissues is a prognostic factor in many solid tumours, where reduced NK cell function is associated with worse outcomes (Coca et al., 1997; Ishigami et al., 2000; Mandal et al., 2016; Villegas et al., 2002).

It is widely understood that cancer patients have an impaired immune system, including NK cells (Kiessling et al., 1999). Frequently reported dysfunctions include reduced cell numbers, dysregulation of antigen expression, and a display of weaker functional abilities such as cytokine secretion and cytotoxicity. In MDS, reports show that patients exhibit lower numbers of NK cells compared to healthy controls (Gleason et al., 2014; Hejazi et al., 2015; Montes et al., 2019). The investigation of antigen expression has revealed an impaired phenotype, with a reported loss of NKG2D, NKp30, NKp46, CD16 and CD161 expression (Epling-Burnette et al., 2007; Gleason et al., 2014; Hejazi et al., 2015; Montes et al., 2019). Recent studies suggest that NK cell dysfunction in MDS may be attributed to the presence of NK cells with immature phenotypes characterized by an increase in the proportion of $CD56^{bright}$ NK cells, higher ‘early’ KIR expression (KIR2DL2/3), and lower ‘late’ KIR expression (KIR2DL1 and KIR3DL) in MDS patients (Hejazi et al., 2015; Montes et al., 2019; Schönberg et al., 2011). The function of MDS-NK cells is also compromised, with reports showing impaired cytokine secretion (Hejazi

et al., 2015; Kiladjian et al., 2006), lower degranulation upon exposure to leukemic targets (Carlsten et al., 2010), a substantial reduction in perforin and granzyme B loading of the granules (Hejazi et al., 2015), and an impaired lysis of both cancer cells and CD34+ blasts (Carlsten et al., 2010; Epling-Burnette et al., 2007; Hejazi et al., 2015; Kiladjian et al., 2006). These studies demonstrate an NK cell phenotype characterized by a lack of maturation markers and the downregulation of NK cell activation receptors in MDS patients associated with NK cell functional impairment.

Tumours evade NK cells by using a variety of mechanisms. This includes the reduction of ligands for NK cells, which will impair NK cell recognition (Classen et al., 2003; Raulet et al., 2013); the presence of soluble factors, contributing to a suppressive TME (Frumento et al., 2002; Viel et al., 2016; Young et al., 2018); and hypoxia and low-level nutrient availability, that will suppress NK cell metabolisms and antitumour activity (O'Brien & Finlay, 2019).

AML and MDS are a group of heterogeneous clonal hematopoietic stem cell disorders characterised by cytopaenias leading to ineffective haematopoiesis and increased blast production, resulting in bone marrow failure (Corey et al., 2007; Döhner et al., 2015). MDS is a milder version of the disease, where patients with <20% myeloblasts in the bone marrow or peripheral blood are generally classified as MDS and patients with ≥20% are regarded as AML (Estey et al., 2022). On average, 30% of MDS patients progress into secondary AML, which tends to be fatal (Breccia et al., 2010; Germing et al., 2006; Greenberg et al., 1997). The heterogeneous nature of the disease requires a complex and personalised variety of therapeutic approaches. Among the choices for AML/MDS treatment, allogeneic HSCT is the only therapy with curative potential. Allogeneic HSCT is associated with a high risk of serious complications such as infections and GVHD; since these diseases are often presented in an elderly cohort, this option is unavailable to many patients (Döhner et al., 2015; Nachtkamp et al., 2009). The Food and Drug Administration (FDA) has only approved five drugs for the treatment of MDS: the immunomodulatory agent lenalidomide, the hypomethylating agents azacitidine and decitabine, and more recently, the hypomethylating agent cedazuridine, and the erythroid maturation agent Luspatercept-aamt (Xu &

Hansen, 2021). No drug has been approved for second-line treatments like immunotherapy, occasioning a large unmet need for patients who do not respond to licensed treatments (Chandhok et al., 2019).

NK cell immunotherapy has shown positive results in solid and haematological cancers (Sabry & Lowdell, 2020) and thus could be a suitable option for non-responders. Different immunotherapeutic strategies for NK cell modulation have been developed for MDS treatment both pre-clinically as well as in clinical trials. Clinical trials in MDS can be mainly classified into two types: the first one involves adoptive immunotherapy using allogeneic donor NK; the second approach has been to potentiate the patients' own NK cells *in vivo* (Table 6.1) (Arellano-Ballestero et al., 2023).

Pre-clinical studies have reported enhanced MDS patient-derived NK cell proliferation, granule secretion and cytotoxicity after exposure to IL2, showing that NK cell dysfunction can be overcome (Epling-Burnette et al., 2007; Hejazi et al., 2015). Some trials using IL2-activated adoptive NK cell therapy have shown good results in patients with relapsed or refractory AML, with complete remissions in up to 50% of the patients (Bachanova et al., 2014). At the moment, there is an ongoing trial utilising IL2-activated umbilical cord-derived NK (NCT04347616).

IL15 is another cytokine that has been used in the clinical setting, but as opposed to IL2, IL15 holds some advantages, such as its superior role in the stimulation of NK cells and T cells and also the fact that it does not stimulate Treg proliferation (Tian & Wei, 2017; Y. Yang & Lundqvist, 2020). IL15 infusions have been given to patients in some trials (NCT01385423, NCT02395822, NCT02890758); however, it has been related to cytokine release syndrome in some patients (Cooley et al., 2019).

CIML-NK cells have also been explored in patients with AML; the infused NK cells expanded *in vivo* were associated with some clinical responses in over half of the patients treated, including complete remissions (Berrien-Elliott et al., 2022; Romee et al., 2016). Currently, two ongoing clinical trials use CIML-NK cells in haematologic malignancies (NCT04024761, NCT06138587).

The use of feeder-cell *ex vivo* is another alternative for the expansion and activation of NK cells. This method has been extensively tested *in vitro*, showing large NK cell expansions using both K562-mbIL15-41BBL (Fujisaki, Kakuda, Imai, et al., 2009; C. Imai et al., 2005) and K562-mbIL21 (Ciurea et al., 2017; Denman et al., 2012; Vasu et al., 2020), which is currently being trialled (NCT04220684).

Allogeneic CAR-NK cells have been used for treating MDS/AML patients; nonetheless, one of the main challenges to developing CAR therapies for MDS/AML remains the lack of specific ligands which are usually expressed in normal myeloid cells (Gurney et al., 2021; Haubner et al., 2019). CAR-NK cells targeting CD33 have been utilised in AML, where no significant adverse effects were reported however, no clinical effort was seen (Tang et al., 2018). Ongoing trials on MDS include allogeneic CAR-NK cells targeting NKG2D ligands (NCT04623944) and CAR.70/IL15-transduced NK cells derived from cord blood (NCT05092451).

The *in vivo* potentiation of the patient's own NK cells is another alternative that has been considered, including the infusion of BiKE and TriKEs. Enhanced NK cell responses are reported in vitro utilising BiKEs engaging CD16 and CD33 (Gleason et al., 2014); and TriKEs engaging CD16, CD33 and a modified IL15 linker to induce NK cell proliferation (Felices et al., 2016; Sarhan et al., 2018). A trial testing TriKE GTB-3550 in haematological malignancies (NCT03214666) terminated, but no results have been posted.

Tumour-primed allogeneic NK cells have been previously utilised in two phase I/II, open-label trials of adoptive immunotherapy in patients with AML in partial remission (PR) or in CR but with a high risk of relapse (Fehniger et al., 2018; Kottaridis et al., 2015). Allogeneic NK cells from haploidentical donors were incubated with an INB16 lysate that was removed. After that, NK cells were cryopreserved, shipped and infused into the patients one day after completion of lymphoreductive chemotherapy. These were the first trials of an adoptive NK cell therapy that did not require cytokine support. A total of 19 patients were treated in the two trials, with one patient with chemo-resistant AML achieving CR, which was sustained for over 11 months, 3 patients achieving CR, and 2

patients remaining relapse-free for 32.6 to 47.6+ months. Having shown previously that NK cell function in patients with AML (Lowdell et al., 2002) and MDS (Tsirogianni et al., 2019) is predictive of duration of remission, the Lowdell group postulated that activating endogenous NK cells in patients with AML/MDS, in whom NK cell function is defective, could boost their activity and improve overall survival. Tumour-priming of endogenous NK cells *in vivo* is currently being trialled in patients with advanced MDS or multiply relapsed AML (NCT05933070). Patients receive three weekly infusions of a replication-incompetent preparation of the INB16 cell line (INKmune™). These patients receive no lymphoreductive conditioning chemotherapy and no cytokine support, resulting in a treatment that is well tolerated and compatible with an elderly patient cohort. This chapter presents the data of one patient with advanced, tri-lineage MDS and two patients with treatment-refractory AML who completed treatment.

APPROACH/TREATMENT	TRIAL PHASE	STATUS	PATIENT NUMBER	TRIAL IDENTIFIER	REFERENCES
ADOPTIVE NK CELL IMMUNOTHERAPY					
+ CYTOKINE STIMULATION WITH IL-2/-15/CIML	Phase I	Completed	26	NCT01385423	(Cooley et al., 2019)
		Ongoing	91	NCT05400122, NCT02890758, NCT04024761, NCT06138587	(Alvarez et al., 2014, 2020)
	Phase II	Completed	17	NCT02395822	(Cooley et al., 2019)
	Phase I/II	Completed	89	NCT01898793	(Berrien-Elliott et al., 2022)
		Ongoing	23	NCT04347616	(de Jonge et al., 2023)
+ EXPANDED K562-MBIL21	Phase I	Ongoing	30	NCT04220684	(Ciurea et al., 2017; Denman et al., 2012; Fujisaki, Kakuda, Imai, et al., 2009; Fujisaki, Kakuda, Shimasaki, et al., 2009b; C. Imai et al., 2005; Vasu et al., 2020)
+ CAR NK CELLS	Phase I	Ongoing	90	NCT04623944	(Dong et al., 2020; Sinha et al., 2017; Tang et al., 2018)
	Phase I/II	Ongoing	188	NCT05092451, NCT05092451	
***IN VIVO* NK CELL ACTIVATION**					
BIKE/TRIKE	Phase I/II	Completed	12	NCT03214666	(Felices et al., 2016; Gleason et al., 2014; Sarhan et al., 2018)
INB16 PRIMING	Phase I	Ongoing	12	NCT05933070	(Fehniger et al., 2018; Kottaridis et al., 2015)

Table 6.1. Summary of NK cell-based clinical trials for MDS

Abbreviations: IL, interleukin; CIML, cytokine-induced memory-like; mbIL21. membrane-bound IL-21; CAR, chimeric antigen receptor; BiKE/TriKE, bi/trispecific killer cell engagers.

6.2 Experimental aims

The experimental aims of this chapter were to characterise NK cells from MDS patients at the functional and phenotypical level. After that, I evaluated whether NK cells from the same MDS patients can be tumour-primed and if tumour-memory NK cells could be generated. Finally, I analysed the data from our clinical trial (NCT05933070) and compassionate use cases in MDS and AML patients treated with INKmune™ in a longitudinal study of the changes in function and phenotype of these patients. The specific aims of the chapter were:

1. Evaluate the % of NK cells in MDS patients compared to healthy donors

2. Evaluate the cytotoxic capacity of NK cells from MDS patients compared to healthy donors

3. Evaluate the phenotypic profile of NK cells from MDS patients compared to healthy donors

4. Study whether the generation of TpNK cells from MDS patients induces a phenotype that is similar to the one reported in healthy donors

5. Assess the phenotype of the NK cells from one MDS and two AML patients treated with INKmune™ in a clinical trial

6. Assess the *ex vivo* cytotoxic capacity of the NK cells from one MDS and two AML patients treated with INKmune™ in a clinical trial

7. Evaluate the cytokine and chemokine profile of longitudinal serum samples from patient MDS#01

6.3 Results

6.3.1 Patient characteristics

Peripheral blood samples from patients at UCL Hospital (London, UK) with MDS and similar haematologic malignancies were acquired for subsequent experiments. The characteristics of the patients are found in Table 6.2. From the 21 patients analysed, 15 were diagnosed with MDS, 4 were diagnosed with myelodysplastic/myeloproliferative neoplasms (MDS/MPN), and 2 were diagnosed with therapy-related MDS; the only information available from patients MDS003 and MDS005 was their disease diagnose. MDS/MPNs are clonal myeloid disorders with both dysplastic and proliferative features but are not properly classified as either MDS or chronic myeloproliferative disorders (Arber et al., 2016), but because of the similarities with MDS, these patients were included in the cohort. Therapy-related MDS includes a series of complications in patients receiving cytotoxic therapy for cancer or non-malignant disorders; exposure to these agents can lead to the development of MDS (Bhatia & Deeg, 2011). The patients represent a cohort of 14 males and 5 females, with a 72.5-year-old average; at the time of obtaining the samples, 5/21 patients were receiving chemotherapy (1 patient lenalidomide and 4 patients azacitidine).

The International Prognostic Scoring System (IPSS) score was applied in patients with MDS to assess the prognosis of primary untreated adult patients. It considers the following parameters: percentage of leukemic blast cells in the marrow; type of chromosomal changes in the marrow cells (cytogenetics); presence of one or more low blood cell counts (cytopaenias). The revised IPSS (IPSS-R) covers the same disease factors as the IPSS, but the factors are identified in a more detailed way. The molecular IPSS (IPSS-M) takes mutations in 31 genes into account, as well as cytogenetics, bone marrow blasts, haemoglobin and platelet count (Arber et al., 2016; Elsa et al., 2022). This score will be used as a prognostic indicator to predict the course of the patient's disease; low-risk MDS will progress in a slower fashion, whereas high-risk MDS is likely to progress more quickly and progress into AML.

STUDY ID	AGE	GENDER	DIAGNOSIS	DISEASE STAGE	IPSS-R	IPSS-M	TYPE OF CHEMO	DURATION OF CHEMO
MDS001	87	M	MDS	Excess blasts 1	High	High	None	
MDS002	76	M	MDS	5q-	Intermediate		Lenalidomide	24 months
MDS003			MDS					
MDS004	80	F	MDS		Low		None	
MDS005			MDS					
MDS006	64	M	MDS/MPN				Azacitidine	6 years
MDS007	61	M	MDS/MPN				Azacitidine	1 week
MDS008	73	M	MDS, therapy related		Low		None	
MDS009	76	M	MDS		Low		None	
MDS010	58	M	MDS	Relapsed post sibling bone marrow transplant			Azacitidine	10 months
MDS011	92	F	MDS	5q-			None	
MDS012	80	F	MDS				None	
MDS013	81	F	MDS				None	
MDS014	67	M	MDS		Low		None	
MDS015	59	M	MDS		Low		None	
MDS016	70	M	MDS		Intermediate	Moderate/low	None	
MDS017	69	M	MDS				None	
MDS018	72	M	MDS/MPN				None	
MDS019	81	M	MDS/MPN				Azacitidine	6 weeks
MDS020	80	F	MDS		Low		None	
MDS021	52	M	MDS, therapy-related				None	

Table 6.2 Patient characteristics

Chemo, chemotherapy; IPSS-R, Revised International Prognostic Scoring System; IPSS-M, Molecular International Prognostic Scoring System; MDS, myelodysplastic syndrome; MDS/MPN, myelodysplastic/myeloproliferative neoplasms.

6.3.2 NK cell numbers in MDS patients

First, I evaluated NK cell frequencies out of total lymphocytes, given that the proportions of NK cells may be reduced in patients with MDS. It is well known that MDS patients display fewer NK cells (Gleason et al., 2014; Hejazi et al., 2015; Montes et al., 2019), contributing to the overall immune dysfunction observed in cancer.

I identified the percentage of NK cells in the peripheral blood of HD and MDS patients and observed significant differences between the 2 groups (Figure 6.1). The mean percentage of NK cells in HD was 8.65±5.55; on the other hand, MDS patients had a mean percentage of 2.93±2.25 (p value<0.001) (Figure 6.1 B). These results correlate with the observation that MDS patients have reduced NK cell numbers (Gleason et al., 2014; Hejazi et al., 2015; Montes et al., 2019).

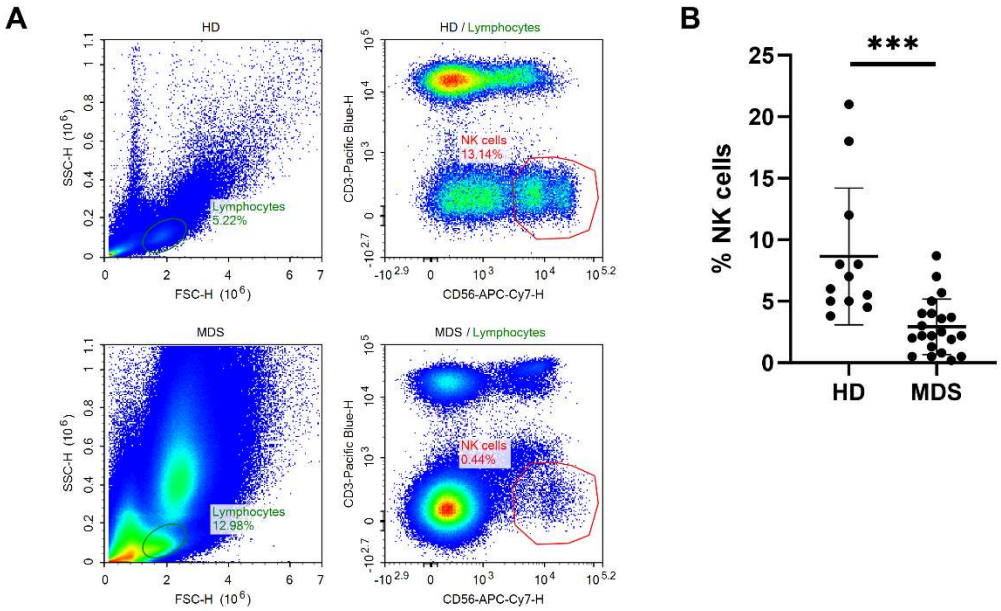

Figure 6.1. Percentage expression of NK cells in HD and patients with MDS

Freshly isolated PBMCs from HD and MDS patients were immunophenotyped for CD3 and CD56 to identify the % NK cells. (A) Representative flow cytometry plots showing the gating strategy to identify the % of NK cells in HD (top) and MDS patients (bottom) (B) Graph shows the % of NK cells in HD and MDS patients. Bars represent the means ±SD of the different donors, which are indicated by the individual dots.

Data were tested for normality, and comparisons were made between the indicated groups using the unpaired t-test. Statistical significance is indicated as: *P <0.05: **P <0.01: ***P <0.001.

6.3.3 Cytotoxic capacity of the NK cells from MDS patients

PBMCs from HD and MDS patients were isolated and set up in a 4-hour cytotoxicity assay against the MDS-derived cell line, MDS-L (Figure 6.2 A). Both NK cells from HD and MDS patients exhibited a wide range from 5% to 95% cytotoxicity, with no significant differences between rNK cells from HD and MDS patients. The NK cell cytotoxic capacity of the MDS patients clustered into two distinct groups, which I classified as high-killing capacity (>50% specific lysis) or low-killing capacity (<50% specific lysis).

Resting NK cells from the MDS patients were incubated overnight with INB16 to generate TpNK cells, which were then set up in a 4-hour killing assay against MDS-L (Figure 1.2 B). The % change was calculated by comparing TpNK cell samples with untreated controls, as explained in the methods (Methods section 2.11.1).

When the samples were grouped according to high or low degree of cytotoxicity, patients who initially had lower ability to lyse MDS-L showed increased killing capacity after tumour-priming, whereas patients who initially had high killing capacity showed no significant changes (Figure 6.2 B).

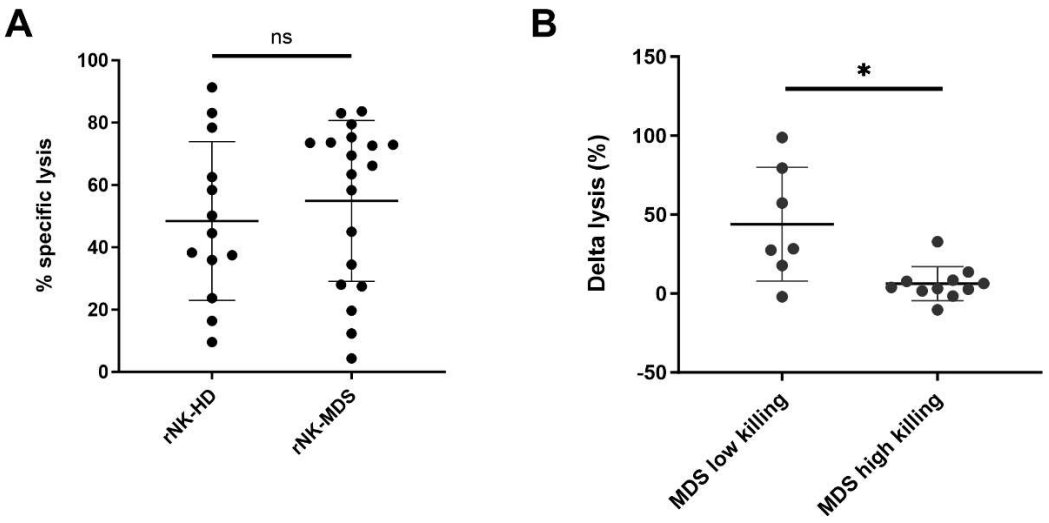

Figure 6.2. Cytotoxic profile of MDS patients and HD against MDS-L

Freshly isolated PBMCs from HD and MDS patients were isolated and co-incubated overnight at 37˚C with medium alone (rNK) and with INB16 (TpNK) at a 1:2 ratio, which was set up according to % NK identified as $CD56^{+}$ $CD3^{-}$. The next day, rNK and TpNK were set up for a 4h-cytotoxicity assay against MDS-L at an E:T ratio of 5:1. Percentage of specific lysis was calculated by subtracting the number of target cells undergoing spontaneous lysis. (A) Graphs show % specific lysis ±SD of rNK cells from HD and MDS patients against MDS-L (B) Graph shows the % delta lysis ±SD against tumour primed NK cells from MDS patients against MDS-L and segregated according to their degree of killing. Bars represent the means of the different donors, indicated by the individual dots. Data were tested for normality, and comparisons were made between the indicated groups using the unpaired t-test. Statistical significance is indicated as: *P <0.05: **P <0.01: ***P <0.001.

6.3.3.1 Cytotoxic capacity of the NK cells from MDS patients considering the patient's clinical parameters

Next, we stratified NK cell responses according to the clinical parameters of our cohort. (Figure 6.3).

In Figure 6.3 A, patients were stratified according to their sex. Although not statistically significant, there is a trend towards female patients having higher

specific lysis (mean ~66%), compared to males who showed a broad range (~5% to ~85%).

Figure 6.3 B shows patients stratified according to their age (above or below 65 years old). The mean for the > 65-year-old group is ~53% specific lysis, whereas the mean for the < 65-year-old group is ~58%, where the difference is not statistically significant. Thus, in our study, age does not appear to be a determinant for NK cell-specific lysis.

In Figure 6.3 C, patients were plotted according to their IPSS-R score. Patients with intermediate/high IPSS-R scores show a lower mean % specific lysis of ~22%, whereas patients with low IPSS-R scores show a mean of ~59%, where the difference is statistically different. Thus, patients with a more advanced disease stage have NK cells with a higher degree of impairment.

Finally, in Figure 6.3 D, patients were stratified according to whether they had had chemotherapy or not at the time of taking the samples. Although not statistically significant, patients receiving chemotherapy trend towards lower mean NK cell-specific lysis (~43%) compared to patients who did not receive chemotherapy, with a mean NK cell-specific lysis of ~61%.

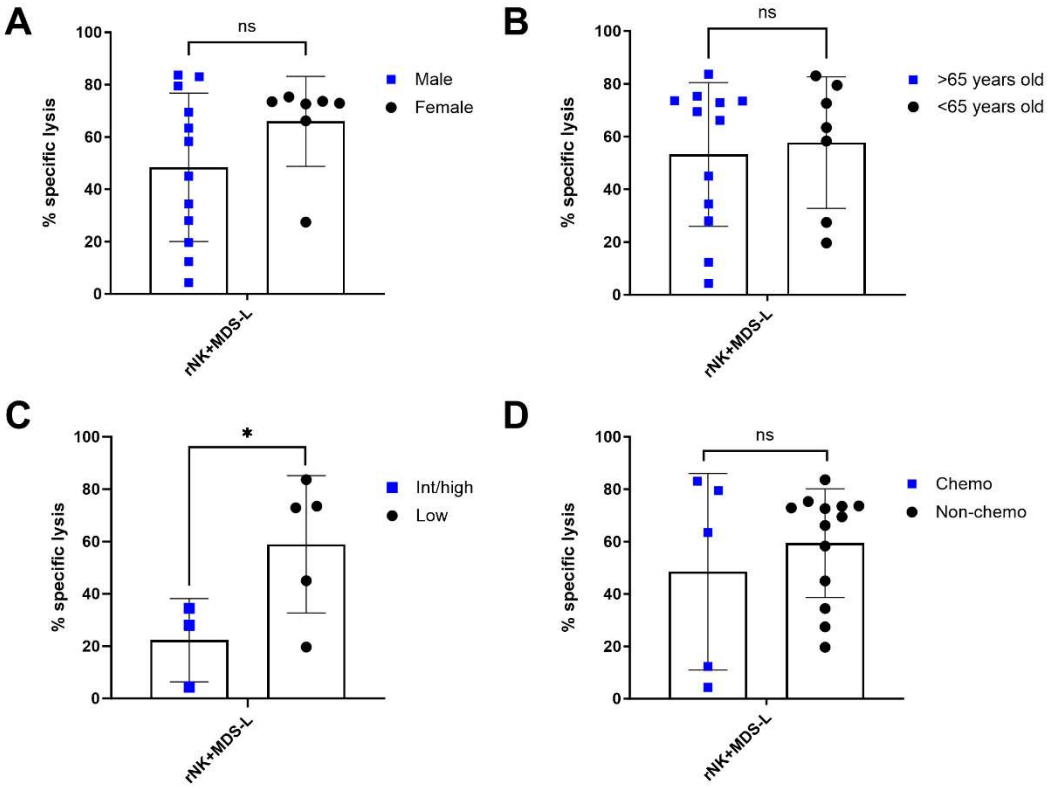

Figure 6.3 Cytotoxic profile of the NK cells from MDS patients considering their clinical parameters

Freshly isolated PBMCs from HD and MDS patients were isolated and co-incubated overnight at 37˚C with medium alone (rNK) and with INB16 (TpNK) at a 1:2 ratio, which was set-up according to % NK identified as $CD56^{+}$ $CD3^{-}$. The next day, rNK were harvested and set up for a 4h-cytotoxicity assay against MDS-L at an E:T ratio of 5:1. Percentage of specific lysis was calculated by subtracting the number of target cells undergoing spontaneous lysis. Graphs show % specific lysis of rNK cells from MDS patients against MDS-L. Patients were stratified according to (A) gender, (B) age, (C) IPSS, and (D) chemotherapy administration. Bars represent the means of the different donors, indicated by the individual dots. Data were tested for normality, and comparisons were made between the indicated groups using the unpaired t-test. Statistical significance is indicated as: *P <0.05: **P <0.01: ***P <0.001.

6.3.4 Phenotypic profile of the NK cells from MDS patients

6.3.4.1 *Ex vivo* NK cells from MDS patients

Next, the phenotype of MDS-NK cells was explored to try and provide some insights into the observed functional differences. I used a well-curated flow cytometry panel to look into various markers including activation, inhibition and differentiation markers, as well as co-stimulatory molecules.

The phenotypical profile of *ex vivo* cells from HD was compared to those from MDS patients. Figure 6.4 shows the % expression and MeFI of the positive population of the indicated markers classified by function. Activation NK cell markers show downregulation of CD16 in MDS samples compared to HD both in % expression and MeFI (P value 0.083 and 0.049, respectively). CD25 is also upregulated in the MDS-NK cells, both in % expression and MeFI (p value 0.087). CD69 is significantly upregulated in % expression in MDS samples (p value 0.04) and shows a trend towards being upregulated in MeFI. The NCRs NKp30 and NKp80 are both downregulated in MDS samples; the % expression and MeFI of NKp30 has a p value of 0.001 and a p value of 0.030 respectively, and NKp80 shows a MeFI of 0.030. The % expression of KIR2DS4 shows a trend towards being downregulated in MDS samples, and MeFI is significantly downregulated (p value 0.023).

I next examined NK cell co-stimulatory molecules. DNAM1 % expression is downregulated in MDS patients (p value 0.056), and no changes are seen in MeFI. The % expression of ICAM1 is significantly upregulated in MDS samples (p value 0.046), whereas MeFI shows no significant changes.

When looking at % expression, the maturation marker CD57 shows a trend towards being downregulated in MDS patients, whereas no differences is observed in MeFI.

Finally, I looked at NK cell inhibitory markers; no differences in the % expression or MeFI of CD94 are observed. TIGIT is significantly upregulated in MDS patients, both in % expression and MeFI (p value 0.005 and 0.024, respectively). No changes are observed in the levels of expression of TIM3.

Overall, circulating NK cells from patients with MDS were characterised by lower expression of the activating markers CD16, NKp30, NKp80 and KIR2DS4; lower expression of the maturation marker CD57; and increased expression of the inhibitory marker TIGIT.

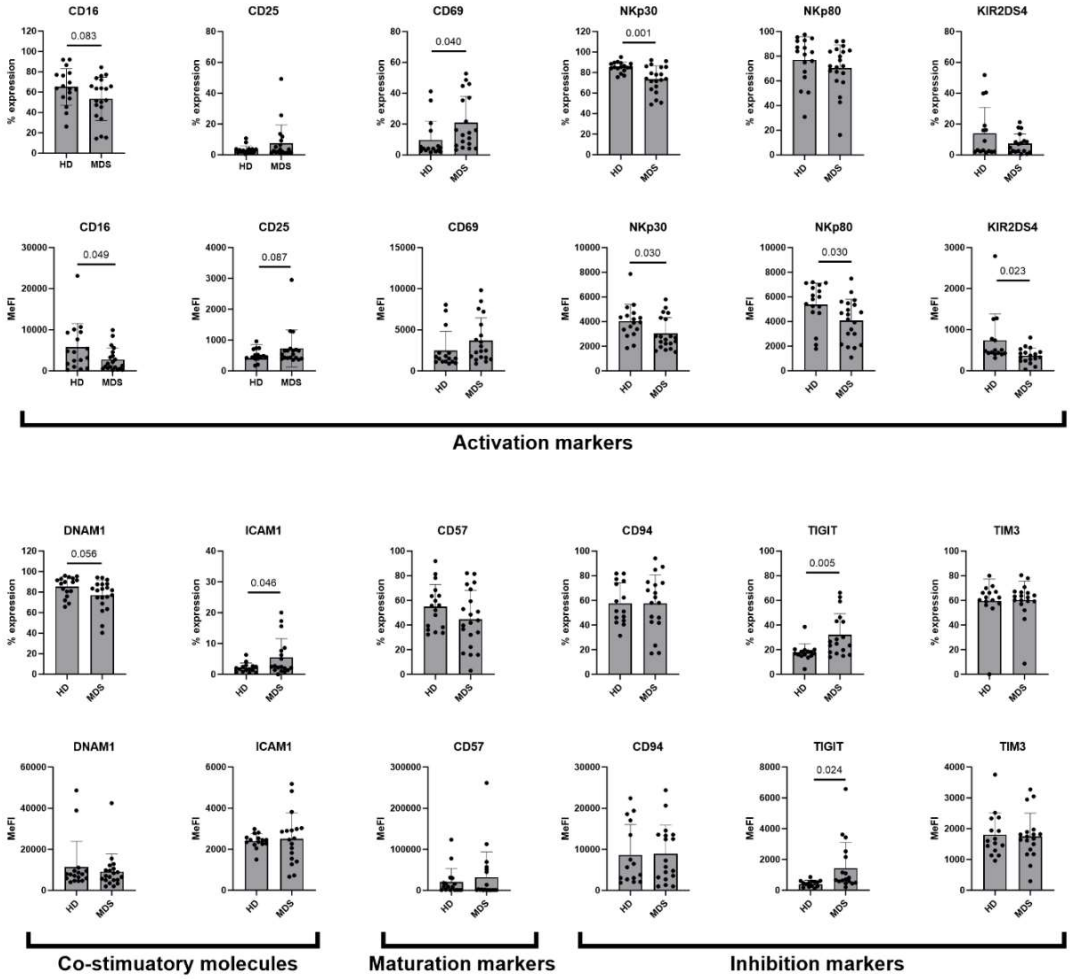

Figure 6.4. Phenotypic profile of NK cells from MDS patients and HD

Freshly isolated PBMCs from HD and MDS patients were immunophenotyped for the indicated markers in a Novocyte flow cytometer (Agilent), data were analysed using the NovoExpress software (Agilent). Graphs show the % expression and MeFI of the positive population of HD and MDS patients for individual NK cell markers as indicated. Bars represent the means ±SD of the individual donors indicated by the dots. Data were tested for normality, and comparisons were made between the indicated groups using the unpaired t-test. Statistical significance is indicated with the p value number; when not indicated, p value is >0.1.

6.3.4.2 Tumour-priming of the NK cells from MDS patients

6.3.4.2.1 Study of NK cell receptor expression

I next looked at the phenotype of MDS-NK cells before and after tumour-priming to see if there would be changes in the receptor expression similar to the ones observed in TpNK cells in Chapter 3. Unsupervised multidimensional analysis was performed using the viSNE algorithm to evaluate the co-expression of the markers at the single-cell level. Figure 6.5 shows the viSNE plots before and after tumour-priming of the distinct markers together with % expression and MeFI of the positive population with TpNK cells compared to rNK cells.

The activating markers CD25, CD16 and CD2 showed no significant differences when comparing rNK cells with TpNK cells. CD69 is upregulated in TpNK cells, both in % expression (p value 0.014) and MeFI (p value >0.1). I also observe a slight downregulation of NKG2D both in % expression (p value 0.022) and MeFI (p value >0.1). The maturation marker CD57 is upregulated in TpNK cells both in % expression (p value 0.095) and MeFI (p value 0.029). The co-stimulatory molecule CD62-L shows a downregulation in % expression (p value 0.082) and upregulation in MeFI (p value 0.062). The other co-stimulatory molecule ICAM1 show a very slight upregulation in TpNK cells in % expression (p value 0.095) and an upregulation in MeFI (p value >0.1).

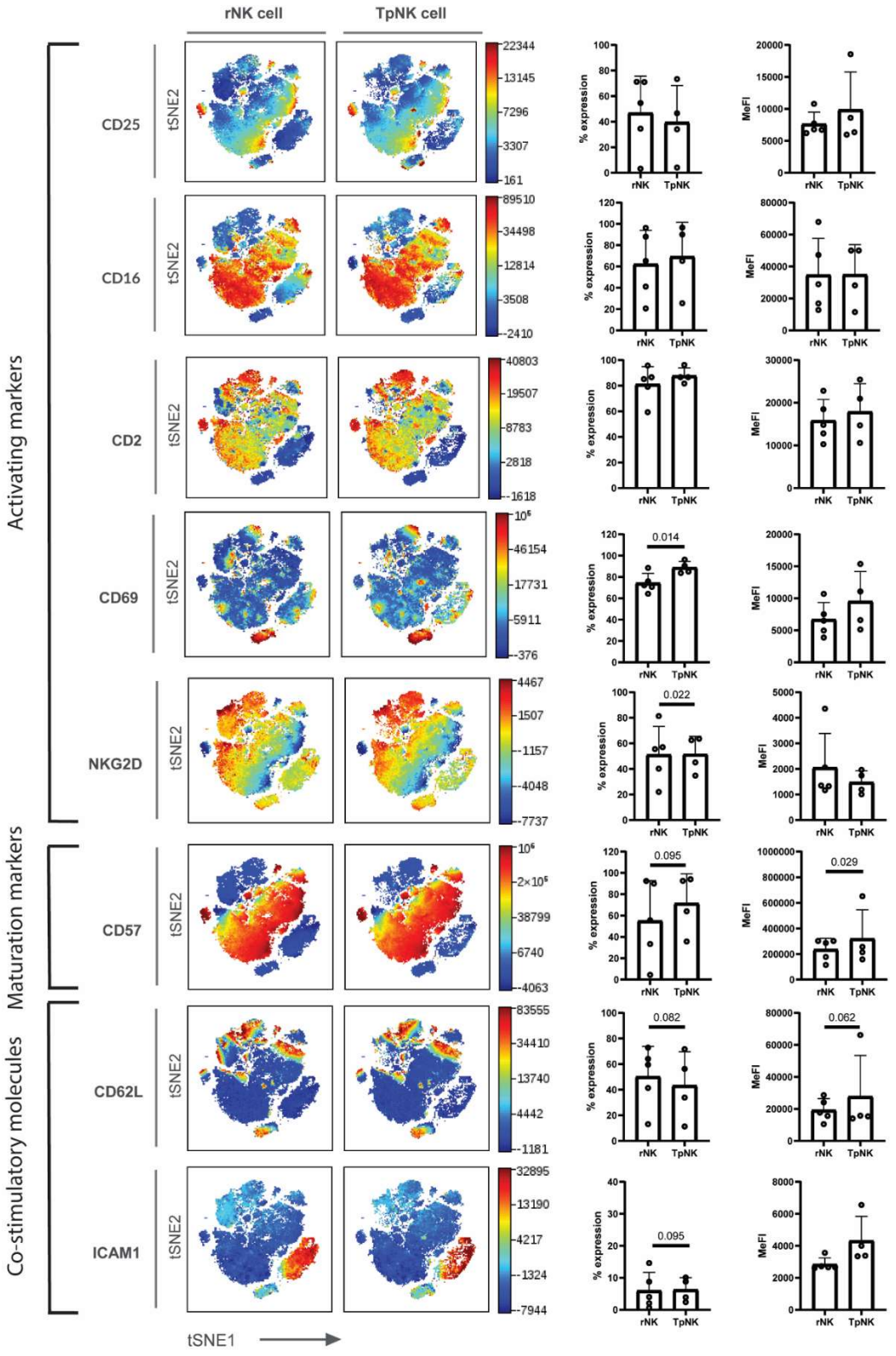

Figure 6.5. Phenotypic profile of rNK and TpNK cells from MDS patients

Freshly isolated PBMCs from HD and MDS patients were isolated and co-incubated overnight at 37˚C with medium alone (rNK) and with INB16 (TpNK) at a 1:2 ratio, which was set-up according to % NK identified as $CD56^{+}$ $CD3^{-}$. The next day, rNK

and TpNK were phenotyped for the indicated markers in an Aurora flow cytometer (Cytek), and data were analysed using FlowJo (TreeStar) and Cytobank (Beckman Coulter) software. viSNE plots of NK cells from MDS patients before and after tumour-priming of the indicated markers. Bar plots show % expression and MeFI of the positive population of the indicated markers; every dot represents an individual donor (n=4-5). Data were tested for normality, and comparisons were made between rNK and TpNK cells using the unpaired t-test. Statistical significance is indicated with the p value number; when not indicated, p value is >0.1.

6.3.4.2.2 Metacluster analysis of NK cell subpopulations

Unsupervised high-dimensional analysis was followed by FlowSOM clustering in order to identify metaclusters based on the NK cell receptors selected previously and reveal related phenotypic clusters to compare rNK cells from TpNK cells from MDS patients (Figure 6.6).

In Figure 6.6 A, the distribution and abundance of the different metaclusters is shown, and Figure 6.6 B shows the changes in % cell numbers of each metaclusters. The more abundant metaclusters identified are metacluster 1, 3, 7 and 8. Metacluster 1 has an abundance of ~18% in rNK cells and is reduced to ~6% in TpNK cells; metacluster 3 has an abundance of ~25% in rNK cells and increases up to ~38% in TpNK cells; metacluster 7 has an abundance of ~28% in rNK cells and is increased to ~34% in TpNK cells; metacluster 8 has an abundance of ~20% in rNK cells and is reduced to 12% in TpNK cells. I next wanted to visualise the intensity of expression of selected NK cell markers for each metacluster (Figure 6.6 C). Metacluster 1, which is reduced in TpNK cells, is characterised by ICAM1^{high}, CD57^{low}, CD16^{low} and LAG3^{high}. Metacluster 3, which is increased in TpNK cells, is characterised by Granzyme B^{high}, CD57^{high}, CD2^{high} and CD16^{high}. Metacluster 7 is increased in TpNK cells and is characterised by KIR^{high}, Granzyme B^{high}, CD57^{high}, CD2^{high} and CD16^{high}. Metacluster 8, which is reduced in TpNK cells, is characterised by Granzyme B^{low}, CD57^{low}, CD2^{high}, CD16^{low} and CD62L^{high}. Overall, the increases of metaclusters M3 and M7, which have a high expression of CD57, KIR, CD16, and CD2 and the decrease of metaclusters M1 and M8, which

have a low expression of Granzyme B, CD57 and CD16, suggest that TpNK cells are acquiring the phenotype of mature NK cells (Björkström et al., 2010; Lopez-Vergès et al., 2010); similarly to our observations on TpNK cells from HD described in Chapter 3. Overall, these results indicate that NK cells from MDS patients can be tumour-primed and exhibit the phenotype of mature NK cells.

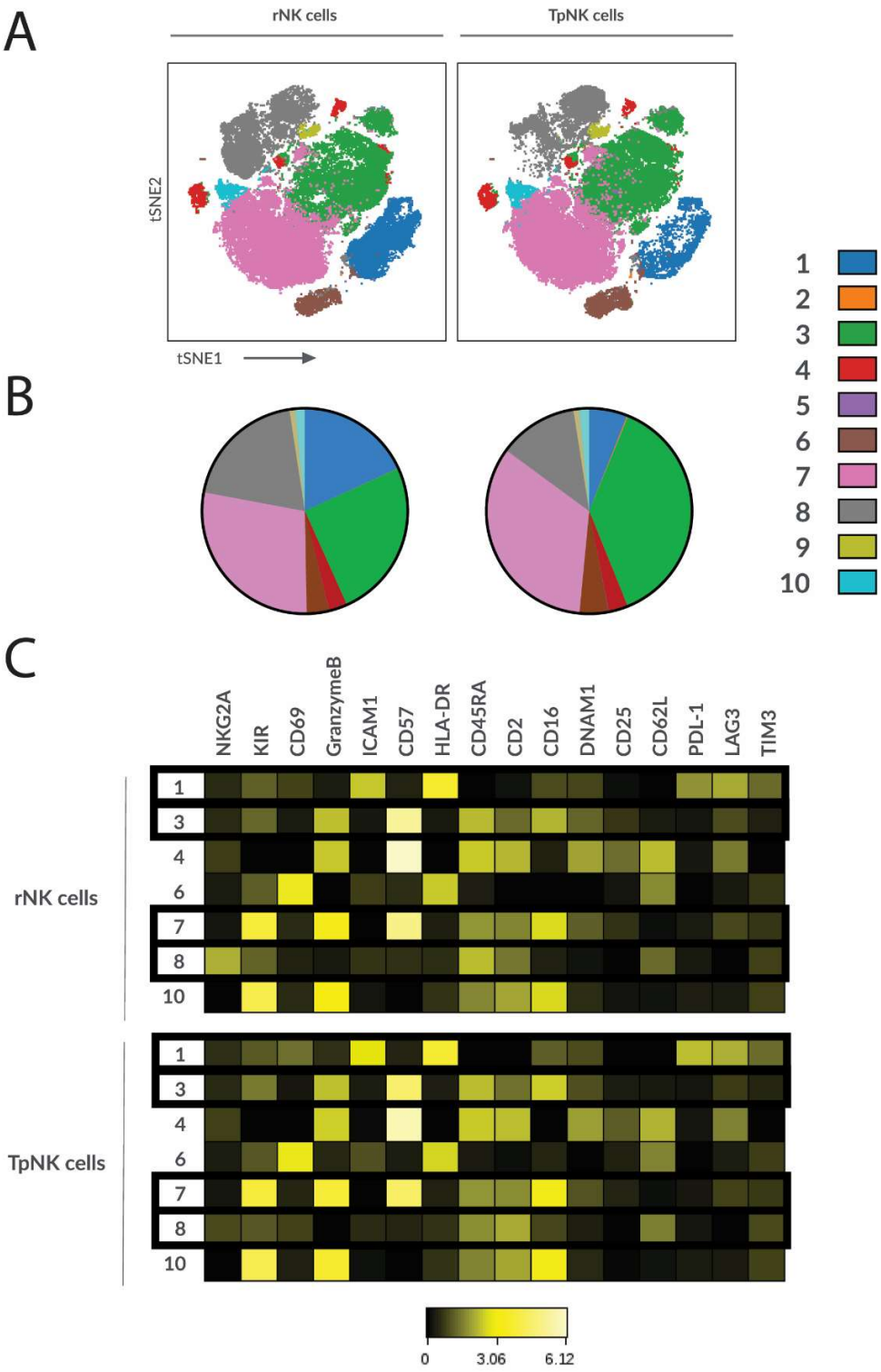

Figure 6.6. Metacluster phenotype of rNK and TpNK cells from MDS patients

Freshly isolated PBMCs from HD and MDS patients were isolated and co-incubated overnight at 37˚C with medium alone (rNK) and with INB16 (TpNK) at a 1:2 ratio, which was set-up according to % NK identified as $CD56^{+}$ $CD3^{-}$. The next day, rNK

and TpNK were harvested and phenotyped for the indicated markers in an Aurora flow cytometer (Cytek), data were analysed using Cytobank (Beckman Coulter) software. Unsupervised clustering analysis clustered on 30 NK cell phenotypic markers was performed using the FlowSOM algorithm (n=4-5). (A) viSNE plots of the different metaclusters across all conditions. (B) Pie charts show changes in % cell numbers of each metacluster for every condition. (C) Heatmap show intensity of expression of the indicated markers.

6.3.5 Monitoring of MDS/AML patients treated with INKmune™ in a clinical trial

The data from one patient with advanced, tri-lineage MDS and two patients with treatment-refractory AML who have completed treatment and follow-up for four months is presented here (Table 6.3). In this clinical trial (NCT05933070), tumour-priming of endogenous NK cells *in vivo* is being tested. All patients received three doses of $1x10^8$ INKmune™ on days 1, 8 and 15, and a longitudinal assessment was performed of NK cell activation (marked by CD69 upregulation) and lytic function throughout treatment (Figure 6.7 A). The frequencies of activated NK cells increased in all patients until day 29 (Figure 6.7 B), when monitoring of the compassionate cases ended. The MDS trial patient was followed according to protocol and show an increased percentage of activated NK until the end of monitoring on Day +119, over one hundred days after the last INKmune™ treatment.

An increase in NK cell activation coincided with enhanced lytic activity in all 3 patients after treatment, which is maintained on day 73 in patient MDS#01 and in bone marrow at day 140 in patient AML#01 (Figure 6.7 C).

Following NK cells phenotypic assessment, patient MDS#01 (Figure 6.7 D) and AML#01 (Figure 6.7 E) show increased intensity of expression of CD57 and CD2. This mirrored the effect that we previously observed *in vitro* (Chapter 3), where TpNK cells had a greater abundance of metacluser M8, which was $CD57^{high}$, and metacluster M3, which was $CD2^{high}$. Furthermore, both patients show NK cells with low granzyme B levels, which increas throughout the course of the treatment, in fluorescence intensity in MDS#01 and in %

expression in AML#01. It is known that patients with MDS have NK cells that are deficient in their killing machinery (Hejazi et al., 2015); the data here shows that this dysfunction can be reversed by INKmune™ treatment.

The cytokine and chemokine profile (Cytokine 30-Plex Human Panel, Thermo Fisher) was examined in longitudinal serum samples from patient MDS#01. Levels of IL-15, TNFα, MIP-1β, and MIP-1α increase until day 29 and then drop on day 43. Similarly, IL8 secretion increases with each INKmune™ infusion and falls to the pre-treatment level by day 43 (Figure 6.8), suggesting a systemic *in vivo* effect by tumour-priming.

These results suggest that treatment with INKmune™ is safe and well-tolerated. Furthermore, INKmune™ can not only reach the NK cells of the patient *in vivo* but also generates TpNK cells, akin to our observations *in vitro*. To our knowledge, this is the first time that NK cells that bear the features of memory-like NK cells have been generated *in vivo* with a cell product without the need for cytokine support.

SUBJECT	CODE	AGE	DIAGNOSIS	STAGE AT TREATMENT	OUTCOME POST TREATMENT
MDS#01	L003	Patient in their 70s	MDS-EB2 Tri-lineage dysplasia	Tri-lineage dysplastic. Failed 16 cycles of Azacytidine. 19% BM blasts, *RAD21* VAF 40%. Weekly red cell and platelet transfusions ECOG 2.	Improvement from ECOG2 – ECOG 0. Discharged from hospital with reduced platelet and RBC transfusion dependence. Alive >2 years.
AML#01	C01	Patient in their 20s	AML	Congenital GATA2 mutation. Relapsed post 3x allogeneic-HSCT. 8 months as in-patient with cytopaenias, blood product dependent and infections.	Stabilized counts at 2 months, reduced bone pain, neutrophil recovery and discharged home 3 weeks post completion of treatment. Disease recurrence at 6 months and died.
AML#02	C02	Patient in their 20s	AML-M6	Relapsed post 2x haploidentical m/m HSCT – 5% blasts.	Counts stabilized for 4 months allowing discharge to home. Bridged to third allogeneic HSCT.

Table 6.3. Summary of clinical characteristics of the three patients treated with INKmune™

AML, acute myeloid leukaemia; BM, bone marrow; EB, excess blasts; ECOG, Eastern Cooperative Oncology Group; HSCT, hematopoietic stem cell transplant; MDS, myelodysplastic syndrome; RBC, red blood cells; VAF, variant allele frequencies.

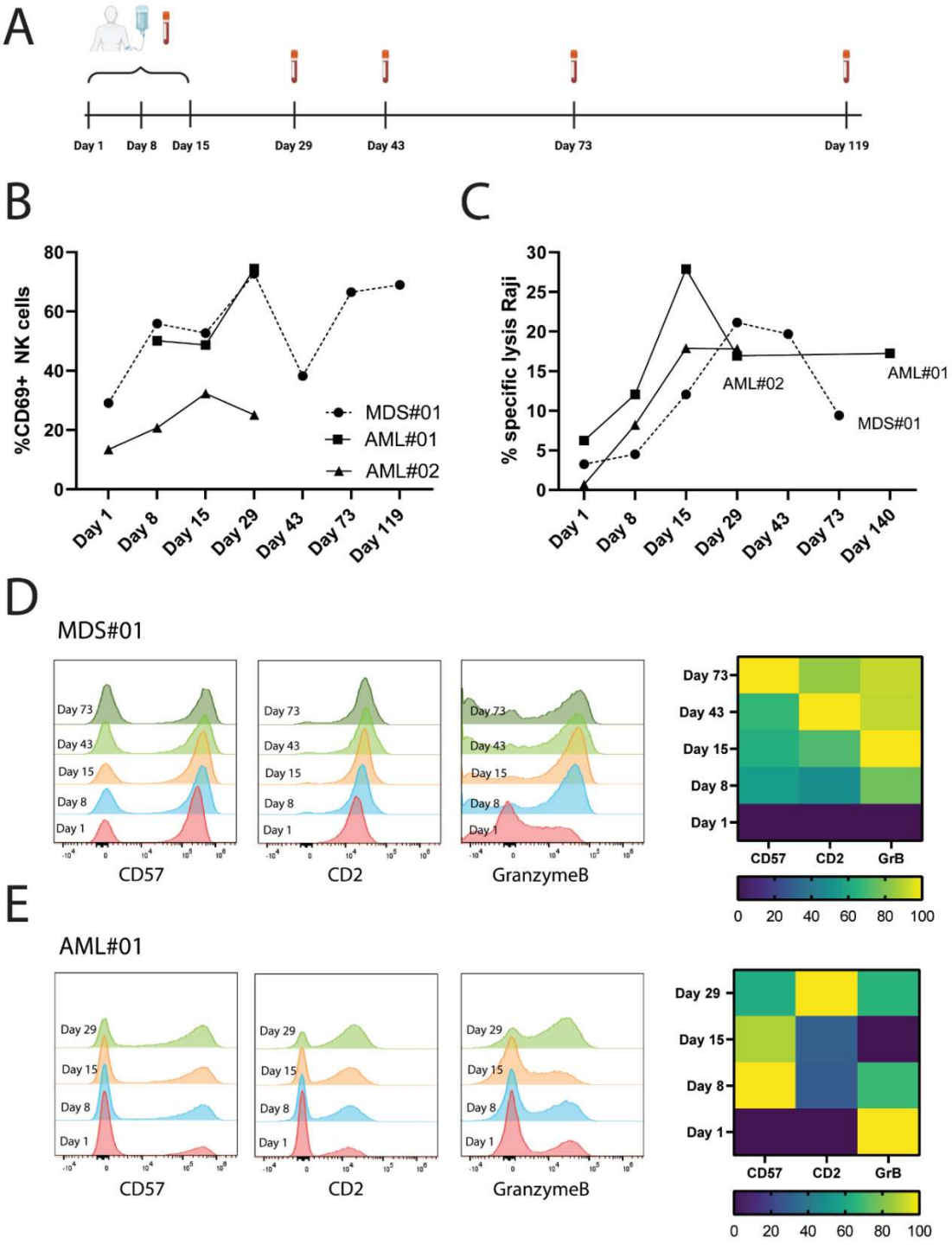

Figure 6.7. INKmune™ generates memory-like NK cells *in vivo* in patients with MDS and AML

(A) Infographic represents the treatment course. Patients receive 3 infusions of INKmune™ on days 1, 8 and 15. Blood samples are taken on days 1, 8, 15, 29, 43, 73 and 119. (B) PBMCs from MDS and AML patients were isolated on the indicated days and immunophenotyped for CD69 using a Novocyte flow cytometer (Agilent),

data were analysed using the NovoExpress software (Agilent). Scatter plot represents the percentage of CD69+ NK cells in each patient (Y axis) on the indicated dates (X axis). (C) PBMCs from MDS and AML patients were isolated on the indicated days and immunophenotyped for CD3 and CD56 in order to identify the % NK cells. PBMCs were set-up for a 4h-cytotoxicity assay against Raji at an E:T ratio of 5:1. Percentage of specific lysis was calculated by subtracting the number of target cells undergoing spontaneous lysis. Scatter plot represents the percentage of specific lysis of Raji mediated by the patient's NK cells (Y axis) on the indicated days (X axis). (D)(E) PBMCs from MDS and AML patients were isolated on the indicated days and immunophenotyped for the indicated markers using an Aurora flow cytometer (Cytek); data were analysed using the FlowJo software (TreeStar). Histograms show the expression of CD57, CD2 and granzyme B on the indicated days and heatmap representing MeFI of the positive population normalised to the lowest value of each column for patient (D) MDS#01 and (E) AML#01.

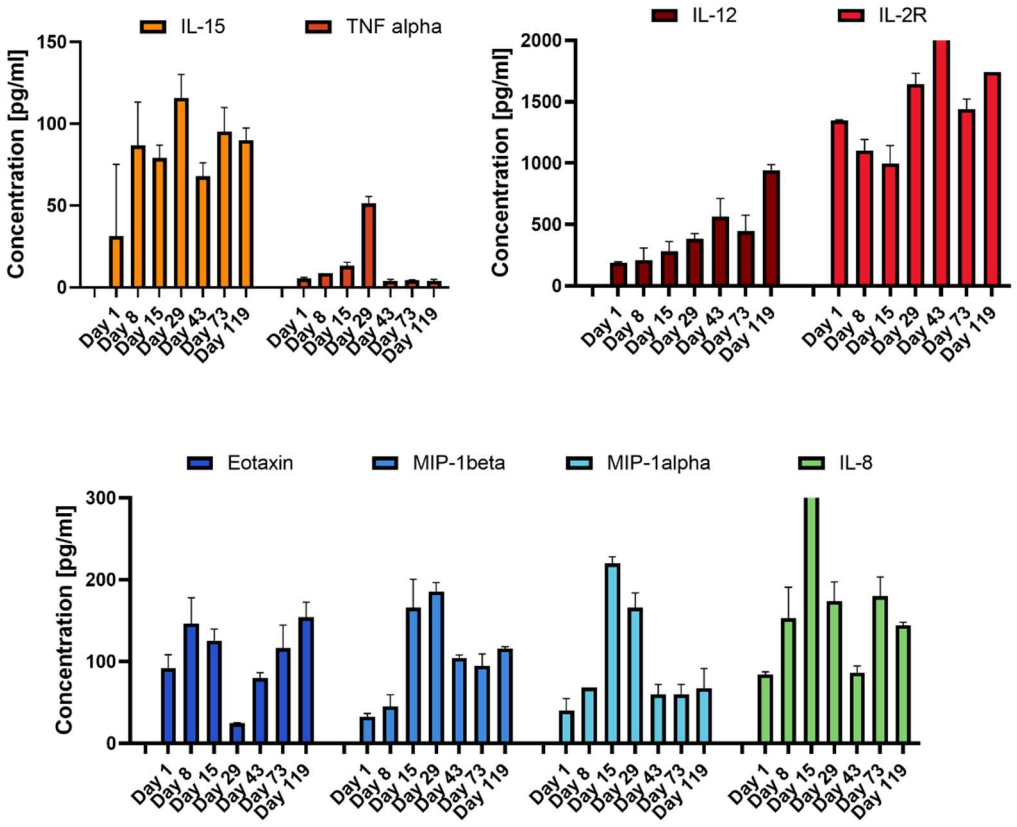

Figure 6.8. Patient MDS#01 exhibits a cytokine profile that suggests systemic changes after INKmune™ treatment

Serum samples from patient MDS#01 were collected on the indicated days and frozen down at -80°C. On the day of the experiment, samples were thawed and analysed using a Cytokine 30-Plex Human Panel (Thermo Fisher) according to manufacturer's instructions and acquired with Luminex™ platform (Thermo Fisher). Bars represent the means ± SD of 3 replicates of the indicated cytokines across different days.

6.4 Discussion

The dysregulation of NK cells in cancer patients has been widely reported, including NK cells in MDS patients. Different studies have shown lower levels of degranulation and cytotoxicity of MDS-derived NK cells compared to healthy controls of both the NK-sensitive cell line K562 as well as CD34+ blasts (Carlsten et al., 2010; Epling-Burnette et al., 2007; Hejazi et al., 2015; Kiladjian et al., 2006). The ability of MDS-NK cells to secrete cytokines like TNFα and IFNγ has also been shown to be reduced (Hejazi et al., 2015; Kiladjian et al., 2006). A very interesting observation came from the Hejazi study, where they showed no difference in the mobilization of CD107a when MDS-NK cells were exposed to K562. However, they showed a significant decrease in MDS-NK cell killing activity without any associated changes in CD107a expression compared to healthy donors. This observation prompted them to investigate whether degranulating MDS-NK cells were properly armed with cytotoxic molecules. They observed a substantial reduction in perforin and granzyme B loading of granules in MDS-NK cells, which explained why MDS-NK cells were still able to mobilize CD107a to the cell surface without effective killing of target cells (Hejazi et al., 2015).

Here, I report that patients with MDS display a very wide range of cytotoxicity against the MDS cell line MDS-L, ranging from 5% to 95% cytotoxicity. The most interesting finding of this study is that patients can be clustered into “low killing capacity” and “high killing capacity” according to their ability to lyse MDS-L. When patients are stratified according to these criteria, patients whose NK cells have high killing capacity do not benefit from tumour-priming of their NK cells, as the specific lysis remains similar. On the other hand, patients classified as “low killing capacity” display a significant enhancement in their ability to lyse target cells after tumour-priming. This observation is interesting as it suggests that tumour-priming is particularly beneficial in patients whose NK cells are most dysfunctional.

Similarly, Tsirogianni and colleagues performed a longitudinal study on patients with MDS that had been treated with azacytidine. They studied the capacity of MDS-derived NK cells to lyse K562 and found that patients whose

NK cell lysis capacity was above a critical threshold could be predictive for survival beyond 2 years. Patients below that critical threshold showed a median overall survival of 18 months compared to those falling above the threshold with a median survival of 52 months, suggesting that NK cell anti-tumour functions may be critical in the response to MDS (Tsirogianni et al., 2019). What this suggests is that if the NK cell cytotoxicity of MDS patients can be increased above this critical threshold, their overall survival would increase. Hence, tumour-priming of NK cells arises as a powerful tool for patients who have less cytotoxic NK cells, as the significant increase in their cytotoxic capacity described here could push them above the aforementioned critical threshold and thus increase their overall survival.

Another interesting finding in this thesis was that patients exhibited distinct degrees of NK cell cytotoxicity when grouped according to different clinical parameters. MDS-NK cells from females showed an enhanced cytotoxic activity; this finding correlates with a study that found that women over the age of 70 years old had enhanced NK cell cytotoxic activity compared to men (Al-Attar et al., 2016). Another finding of this thesis was that patients with low IPSS-R scores displayed enhanced NK cell cytotoxicity, which has been thoroughly documented in the literature (Aggarwal et al., 2011; Epling-Burnette et al., 2007). The administration of chemotherapy also affected the patients' NK cells, with increased NK cell cytotoxic capacity in patients who were not undergoing treatment; it has been well described in the literature that chemotherapeutic agents are known to have a negative effect on the state of NK cells (Dauguet et al., 2011; Markasz et al., 2007; Najima et al., 2018). This is of particular concern as chemotherapy could be acting as a double-edged sword, on the one hand, by eliminating the patients' cancer cells but at the same time impairing the patient's immune system, and thus hampering its capacity to help clear the disease.

Additional to dysfunctional NK cell cytotoxicity, the receptor expression of MDS-NK cells has also been reported to be impaired by some. In our studies, NK cell activation markers were downregulated compared to healthy controls, with significant reductions in CD16, NKp30, NKp80, KIR2DS4 and DNAM1. Carlsten et al. found that the downregulation of NKG2D and DNAM-1

expression in bone marrow-derived NK cells from MDS patients was reportedly associated with elevated blast counts and high-risk disease (Carlsten et al., 2010). Other studies investigating peripheral blood NK cells from MDS patients have reported loss of NKG2D, NKp30, NKp46, CD16 and CD161 expression (Epling-Burnette et al., 2007; Gleason et al., 2014; Hejazi et al., 2015; Montes et al., 2019). Recent studies suggest that NK cell dysfunction in MDS may be attributed to the presence of NK cells with immature phenotypes characterized by an increase in the proportion of $CD56^{bright}$ NK cells, higher 'early' KIR expression (KIR2DL2/3), and lower 'late' KIR expression (KIR2DL1 and KIR3DL) (Hejazi et al., 2015; Montes et al., 2019; Schönberg et al., 2011). Even though I did not observe significant changes in the KIR repertoire (data not shown), CD57 expression showed a trend towards being decreased on MDS-NK cells, suggesting a phenotype of immature NK cells (Björkström et al., 2010; Lopez-Vergès et al., 2010). Aside from the studies mentioned above, some other reports have shown conflicting data regarding the phenotype of MDS-NK cells. Early studies found no changes in the receptor repertoire of MDS-derived NK cells (Kiladjian et al., 2006); others have found changes in bone-marrow-derived NK cells but not in NK cells from PBMCs in MDS patients (Carlsten et al., 2010). These differences observed amongst different studies might be attributed to the heterogeneous nature of this disease, the NK cell source, or the timing of samples, especially as it relates to the administration of chemotherapeutic agents, which are known to affect the state of NK cells (Dauguet et al., 2011; Markasz et al., 2007; Najima et al., 2018). The study in this thesis suggests that MDS-derived NK cells are characterised by a lack of maturation markers and the downregulation of NK cell activation receptors in MDS patients, which correlates with what others have previously reported.

I next wanted to investigate if tumour-primed MDS-NK cells displayed a similar phenotype to the one observed in Chapter 3 could be generated, where I used NK cells from HD. In Chapter 3, I generated TpNK cells that were characterised by displaying the phenotype of activated NK cells, marked by downregulations in CD16, and upregulation in CD25, CD69 and ICAM1; as well as the phenotype of mature NK cells, characterised by downregulation of

CD62L and upregulation of CD57. The TpNK cells generated in this chapter using NK cells from MDS patients show a similar phenotype, characterised by the upregulation of CD69, ICAM1, and CD57 and the downregulation of NKG2D and CD62L.

When studying the phenotype of the MDS-NK cells at the metacluster level, metaclusters with high levels of expression of CD57, CD2, CD16 and Granzyme B are expanded. This correlates with the data shown in Chapter 3, where tumour-primed NK cells expanded populations characterised by high expression of CD57 and CD2. High expression of CD57 and CD16 are indicators of terminally differentiated NK cells (Björkström et al., 2010; Lopez-Vergès et al., 2010), denoting that tumour-priming of NK cells induces NK cell maturation not only in HD but also in patients with myeloid leukaemia. The increase of populations expressing high levels of Granzyme B also indicates NK cell maturation (Fehniger et al., 2007). Overall, these results indicate that TpNK cells with memory features can be generated from MDS-NK cells in a similar manner as shown in this thesis with healthy donors (Chapter 3).

There have been many clinical trials utilising NK cells in both solid and haematological cancers (Sabry & Lowdell, 2020). In the context of MDS/AML, several clinical trials have used allogeneic NK cells, which show a good safety profile and complete remissions in some patients (Arellano-Ballestero et al., 2023; Bachanova et al., 2014; Curti et al., 2011; Vela et al., 2018). Despite many advances in the field of NK cell immunotherapy, the infusion of cytokines in order to sustain NK cells *in vivo* continues to be common practice but adds clinical complexity and needs careful monitoring for adverse effects.

The Lowdell group has previously reported in two clinical trials in patients with AML that infusions of haploidentical NK cells that had been primed with the cell line INB16 could lead to sustained *in vivo* function without the need of cytokine support, offering an alternative to the use of IL2, IL15 or IL15RA (Fehniger et al., 2018; Kottaridis et al., 2015). In this thesis, I present the results of three patients treated with intravenous infusions of a replication-incompetent preparation of the INB16 cell line (INKmune™), with no conditioning and no cytokine support (NCT05933070). Doses were well

tolerated and clinical improvement was seen in all three patients. A remarkable finding was that the patients' NK cell phenotype mirrored the one observed in tumour-primed NK cells *in vitro* in HD (Chapter 3), as well as the phenotype of tumour-primed MDS-NK cells in this chapter, characterized by NK cells upregulating CD57 and CD2. Together with the enhancement in NK cell function for more than 70 days in patient MDS#01 and more than 100 days in patient AML#01, the presented results indicate that NK cells with features resembling immunological memory were generated *in vivo* in these patients.

The study of the cytokine and chemokine profile in patient MDS#001 indicated changes in IL15, TNFα, IL12, eotaxin, MIP-1α, MIP-1β and IL8; which increased after each dose on days 1, 8 and 15; this suggests a systemic effect of INKmune™. The changes in cytokines and chemokines observed in the patient's serum will have a general impact on the different immune populations. The IL-15Rα is expressed by T cells, NK cells, natural killer T cells, B cells, DCs, monocytes, and macrophages (Fujii et al., 2018; Mortier et al., 2009); IL15 binding to IL-15Rα enhances the survival and maturation of these populations, which contributes to the elimination of cancer cells. DCs and macrophages mainly secrete IL12; the IL12-high affinity receptor is expressed on activated T cells, NK cells and DCs, and by IL12 binding activates JAK2 and STAT pathways (L. Sun et al., 2015). The soluble IL2-Rα chain (commonly referred to as IL2R) interacts with IL2, enabling the trans-presentation of IL2 to immune cells that are expressing the intermediate affinity IL2-R to generate the high-affinity receptor on T cells, NK cells (Damoiseaux, 2020). The increase of the chemokines MIP-1α and MIP-1β will have important effects on lymphocyte trafficking (Schall et al., 1993).

In this chapter I show that tumour-memory NK cells can be generated from patients with MDS *in vitro* and in patients with MDS/AML *in vivo* in a clinical trial, in a similar manner as observed *in vitro* in NK cells from HD. NK cell dysfunction is often reported in cancer but it is also well known that this dysfunction can be restored, suggesting that these cells do not have inherent defects *per se*. Perhaps the lack of NK cell functionality in cancer patients is just the result of being in a suppressive tumour-microenvironment, together

with the lack of adequate stimulation, which can be overcome by tumour-priming (Sabry & Lowdell, 2013).

Chapter 7 Conclusion and future directions

7.1 Main findings of the thesis

The main objective of this thesis was to define how tumour-priming induces characteristics of immunological memory in NK cells. For that, I performed in-depth multi-parametric flow cytometry, proteomics analysis, and functional assays, including cytotoxicity and metabolic assays. Furthermore, I examined whether the effects of tumour-priming can be acquired by resting NK cells as a mechanism of NK cell activation. Finally, I set out to investigate whether tumour-memory NK cells can be generated from patients with MDS/AML both *in vitro* and *in vivo* as part of a clinical trial.

The main findings of this thesis are:

- Tumour-priming induces a specific phenotype on NK cells characterised by an overall enhancement in the expression of activation markers like CD69 and CD25. Furthermore, it induces NK cell maturation characterised by high CD57 expression. I identified subpopulations enriched in tumour-primed NK cells expressing high levels of CD57 and CD2 and low levels of NKG2A. All in keeping with the phenotype of an activated and terminally differentiated NK cell (Chapter 3).
- Tumour-priming enhances NK cell function by inducing proliferation, cytokine secretion and cytotoxicity enhancement against a variety of cancer cell lines from both solid and haematological malignancies, all in keeping with the characteristics of immunological memory (Chapter 4). This correlates with our proteomics study, where proteins related to increased cytotoxic capacity were identified in TpNK cells (Chapter 3).
- Tumour-priming of NK cells induces the expression of mitochondrial survival proteins (Chapter 3), which correlates with a functional enhancement of the NK cell metabolism, including an increase in glycolysis, mitochondrial respiration, spare respiratory capacity, and mitochondrial depolarisation. This supports the notion that TpNK cells have characteristics of immunological memory (Chapter 4).

- Preliminary evidence indicates that tumour-priming induces distinct motility dynamics on NK cells, characterised by an enhancement in the NK cell's ability to screen the environment by forming more conjugates and contacts with other NK cells. Furthermore, TpNK cells can activate other autologous rNK cells, as marked by the downregulation of CD16 in the rNK cell population in rNK-TpNK co-cultures, which could potentially be mediated via homotypic interactions (Chapter 5).
- Tumour-priming of NK cells from patients with MDS generates NK cells with memory characteristics *in vitro*. These cells express elevated levels of CD57 and CD2, closely resembling the phenotype previously characterized in TpNK cells obtained from healthy individuals (Chapter 3). Furthermore, these NK cells demonstrate improved cytotoxicity against various cancer cell lines. The same effects are observed in longitudinal samples obtained in patients with MDS/AML treated with INKmune™ as part of a clinical trial. These NK cells show enhanced cytotoxicity over a prolonged period of time, as well as a phenotype characterised by high expression of CD69, CD57 and CD2, suggesting the generation of tumour-memory NK cells *in vivo* (Chapter 6).

7.2 Role of CD2

As seen throughout this thesis, the CD2 receptor is a pivotal element in the context of tumour-priming of NK cells. Early work from the Lowdell group uncovered this for the first time (Sabry et al., 2011). In the context of tumour-priming, CD2 on the NK cells interacts with CD15 on the target cell, inducing CD16 shedding and releasing CD3ζ from the intracellular domain of CD16 to bind to the intracellular domain of CD2. Notably, CD2 on T cells has constitutive CD3ζ and, when ligated, leads to downstream phosphorylation of ZAP-70. In contrast, ligation of CD2 on NK cells by CD15 leads to the phosphorylation of CD3ζ, then phosphorylation of LAT and finally of STAT5, with subsequent IFNγ secretion. Further evidence came when the NK-resistant cancer cell line Raji was transfected to express CD15, which then became sensitive to rNK killing, and this could be blocked by anti-CD15 or anti-CD2 antibodies (Sabry et al., 2011). This was in line with the much earlier

report of the blockade of NK lysis of K562 by either anti-CD2 or anti-CD15 (Warren et al., 1996).

In Chapter 3, I identified the enrichment of a metacluster expressing high levels of CD2 in response to tumour-priming. It could be speculated that the expansion of a metacluster that expresses high levels of CD2 could be related to NK cells interacting with the priming agent via CD15-CD2 interaction (Sabry et al., 2011). However, more research needs to be done to prove this hypothesis. In Chapter 6, the expression of CD2 was also increased in tumour-primed NK cells generated from patients with MDS *in vitro*, and enhanced CD2 expression was observed on the NK cells of MDS/AML patients treated with INKmune™ over the course of several weeks. This indicates that CD2 may have a critical role in the generation of tumour-primed and tumour-memory NK cells.

In adaptive NK cells, Liu and colleagues described a synergy between CD2 and CD16, which was unique to hCMV seropositive individuals; this interaction triggered IFNγ and TNFα secretion and increased signalling through CD16, resulting in enhanced ADCC and contributing to the characteristics of memory in adaptive NK cells (L. L. Liu et al., 2016). CD2 has also been found to be highly expressed in memory T cells, as opposed to naïve T cells (Lo et al., 2011); and it is upregulated on activated T cells compared to resting T cells (Lo et al., 2011; D.-M. Zhu et al., 2006).

It appears that CD2 engagement could have a crucial role in the formation of NK cell memory, both in the context of tumour cell memory as well as during CMV infection. This observation has also been made by others (Sheppard & Sun, 2021).

In addition to its role as a co-stimulatory molecule, CD2 is also crucial in cytokine receptor rearrangement and the formation of the immunological synapse on NK cells (Orange et al., 2003). CD2 expression increases the frequency of NK cell nanotubes to targets, where CD2 is located at the tip of the nanotube (Comerci et al., 2012). It is possible that the increased CD2 expression in TpNK cells results in enhanced formation of nanotubes. This

could facilitate not just NK:target cell interaction but also NK-NK recognition and the subsequent priming of resting NK cells in a homotypical manner.

7.3 Role of CD57

Another NK cell marker shown to be important in this thesis is CD57. Similar to CD2, I have observed increased CD57 expression on tumour-primed NK cells as well as the enrichment of populations expressing high levels of CD57. These observations were also made when generating tumour-memory NK cells from MDS/AML patients both *in vitro* and *in vivo*. This data suggests a crucial role of CD57 in the context of tumour-priming and tumour-memory NK cells.

CD57 was first identified on NK cells (Abo & Balch, 1981) and subsequently also identified on CD8+ T cells, where most of the research has been done. On T cells, CD57 has been regarded as a marker of terminally differentiated cells, as well as, perhaps wrongly, a marker of senescent T cells (Sze et al., 2001). $CD57^+$ T cells exhibit short telomeres and telomerase activity, low proliferative capacity and increased apoptosis, but still, they are capable of secreting cytokines and have high cytotoxic potential (Brenchley et al., 2003; Chattopadhyay et al., 2009; Focosi et al., 2010; Le Priol et al., 2006).

Similar to its role in T cells, at the beginning, it was also thought that in NK cells, CD57 could be a marker of poor proliferative capacity and immune-senescence (Brenchley et al., 2003; Focosi et al., 2010). Later studies showed that $CD57^+$ NK cells comprise a subset of NK cells that suggest a high degree of maturity, characterised by $NKG2A^-$, KIR^+ and $CD16^+$. Similar to the observations on T cells, these $CD57^+$ NK cells show decreased proliferative function, enhanced IFNγ secretion and enhanced cytotoxicity (Björkström et al., 2010; Lopez-Vergès et al., 2010). Observations in patients undergoing HSCT have been made where months after the transplant, a population of $CD56^{dim}$ NK cells differentiates to be $CD57^+$ KIR^+ (Björkström et al., 2010), suggesting that these NK cells have reached a terminal differentiated state. In NK cell memory, CMV-derived adaptive NK cells have been characterised by being $CD57^{high}$ (Kared et al., 2018; Lopez-Vergès et al., 2010), and TIML-NK cells have been defined as $CD57^{int}$ (Pal et al., 2017).

It appears that CD57 is a marker of highly differentiated NK cells and an important marker in memory NK cell populations. The observations made in this thesis on the acquisition of CD57 in TpNK cells, together with its importance in adaptive and CIML-NK cells, provide evidence that perhaps high expression of CD57 is common in all subtypes of memory NK cells, in keeping with a phenotype of maturation and terminally differentiation.

7.4 Characteristics of NK cell memory

While CMV-derived adaptive NK cells and CIML-NK cells have been thoroughly characterised, tumour-memory NK cells still remain a mystery.

Similar to memory T cells, several characteristics that resemble immunological memory have been described in NK cells. These traits include increased persistence over extended periods, enhanced cytotoxicity upon re-exposure, a mature and fully developed phenotype, the ability to proliferate in response to antigens, epigenetic imprinting, and clonal expansion.

All of these characteristics have been described in adaptive NK cells. Adaptive NK cells persist for extended periods of time (J. C. Sun et al., 2009); display enhanced IFNγ and ADCC against CMV-infected cells upon a second re-exposure (Béziat et al., 2013; Foley et al., 2012; Lopez-Vergès et al., 2011a); and display a phenotype of terminally differentiated NK cell, characterised by being NKG2C^{+}, CD57^{+}, CD25^{+} and NKG2A^{-} (Béziat et al., 2013; Foley et al., 2012; Lopez-Vergès et al., 2011a; J. C. Sun et al., 2009). The idea that NK cells can recognise antigens has been proposed recently, and it suggests that adaptive NK cells can recognise the hCMV UL-40-derived peptide through HLA-E stabilisation in the surface of the infected cell (Hammer et al., 2018). Furthermore, adaptive NK cells are known to be epigenetically imprinted (J. Lee et al., 2015; Luetke-Eversloh et al., 2014; Schlums et al., 2015) and have a clonal origin (Rückert et al., 2022).

CIML-NK cells also possess characteristics that resemble immunological memory, including persistence over long periods of time (Romee et al., 2012), enhanced IFNγ secretion, and enhanced cytotoxicity upon a secondary

challenge (Romee et al., 2012). They are also known to be epigenetically imprinted (Luetke-Eversloh et al., 2014; Ni et al., 2016).

Initially termed tumour-primed NK cells by the Lowdell group (North et al., 2007; Sabry et al., 2011), it has become evident that these cells possess characteristics of immunological memory (Pal et al., 2017). Tumour-primed NK cells display enhanced cytotoxicity upon a second exposure to a cancer cell, which has been thoroughly described in this thesis and other studies from our group (North et al., 2007; Sabry et al., 2019). In this thesis, I have shown that tumour-primed NK cells have a mature phenotype, where tumour exposure drives CD57 expression in the NK cells. Furthermore, tumour priming drives the enrichment of populations that express high levels of CD2, which is known to be crucial as it interacts with CD15 in the priming cell (Sabry et al., 2011); perhaps the interaction with CD15 in the cancer cell drives the expression of CD2 in the NK cell. Another finding in this thesis is that tumour-memory NK cells can be generated in patients with haematological malignancies and that these cells persist in the patients for an extended period of time, as shown in adaptive and CIML-NK cells (Lopez-Vergès et al., 2011a; Shapiro et al., 2022).

Perhaps one of the most crucial questions remaining unanswered regarding tumour-memory NK cells is whether they are epigenetically imprinted. As of today, no studies have been done to answer this question. The Lowdell group and others have described that NK cell exposure to tumour cells induces changes in its proteome and genome (Dufva et al., 2023; Sabry et al., 2019), but no epigenetic studies have been conducted yet.

The concept of “NK cell memory” is well established, but it is apparent that NK cells with memory function can be derived through more than one mechanism. This may be due to the memory characteristics arising in different NK cell subsets or through different molecular pathways depending upon the way in which memory is induced. Memory-like NK cells have been studied extensively in the context of CMV and CIML-NK cells, but the idea that memory-NK cells can arise from tumour-priming remains far less studied. Irrespective of the mechanism of generation of memory-NK, the subsequent enhanced ability to kill tumour cells is a common factor. Our data identify some important

differences but also shared features between memory-NK cell types. More efforts should be made into better defining tumour-memory NK cells as this population arises as a powerful tool for immunotherapy.

7.5 NK cells and cancer immunotherapy: is it time for a new strategy?

Since the first NK cell trials dating back to the beginning of the 1970s (reviewed in (Ortaldo et al., 2014)), NK cells for cancer therapy have come a long way. Despite that, NK cell therapies face many challenges, such as low cell numbers and low persistence *in vivo*.

Developing better strategies for NK cell expansion and persistence post-infusion remains a central tenet of research, including the transduction of mbIL-15 constructs into the NK product (E. Liu et al., 2018). The use of feeder cells to increase the expansion of mature NK, or iPSC, as a reliable source of proliferative NK cells, promises to reduce the cost of manufacture of allogeneic NK cells for adoptive immunotherapy. This allows the use of multiple NK infusions and is a move away from the concept of “NK engraftment and cure” towards one of “NK injection and control”, where NK cell administrations become an ongoing treatment. The success of this strategy is predicated on the assumption that repeated infusions of allogeneic NK cells will not require lymphodepleting chemotherapy before each injection, which is currently being tested in trials. The need for adoptive NK immunotherapy may be avoided by enhancing endogenous NK function, and BiKEs/TriKEs and *in vivo* generation of memory NK cells are exciting off-the-shelf products that have shown interesting results that could benefit many patients as they are relatively inexpensive, are not personalized, and appear to be well tolerated, which might result in a surge of NK cell therapies in the upcoming years.

7.6 Sample size and statistical power

Power is the likelihood that a specific effect will be identified in a study if there is genuinely an effect. To estimate sample size, several considerations must be made in advance. Firstly, the biologically relevant effect size must be determined scientifically. This is determined before the experiment through a literature review or a pilot study. Secondly, it is important to understand the

variability of the data. The type of statistical analysis, study power, and significance levels are also essential for calculating sample size (Parker & Berman, 2003).

In the presented thesis, one of the major constraints was sample size. Working with primary NK cells presents challenges, particularly in obtaining sufficient cell numbers for experiments. Additionally, as the primary objective was to measure the effects of tumour-priming, cytokines were not added to isolated NK cells to maintain their viability, as this could have influenced the effects under study, adding complexity to the research.

In small-scale studies like in this thesis, it is important not to overstate conclusions and to be transparent about limitations. Therefore, the results in this thesis should be approached with caution. It is important to recognize that they offer only preliminary evidence and that the main findings require further study.

7.7 Future directions and remaining questions

The finding of NK cell subsets with properties resembling immune memory has been perhaps the most important discovery of the last 15 years in the NK cell field, challenging the concept that the innate immune response has no memory features. It is clear that NK cell memory can be derived through more than one program, and different types of NK cell memory have been identified. The generation of memory NK cells through the interaction with tumour cells remains far less studied, but it continues to be crucial to understand this phenomenon, as it could have significant implications in the field of NK cell immunotherapy.

The Lowdell group and others have identified cancer cell lines capable of generating memory NK cells. Which cancer cell lines are capable of inducing the memory program and why? What are the requirements that an NK cell needs to develop into a memory NK cell? After examining various cancer cell lines, the Lowdell group discovered that not all of them could induce tumour-priming on NK cells (North et al., 2007). Some receptor-ligand combinations have been identified to generate tumour-primed NK cells (Sabry et al., 2011),

but future experiments should further explore the ligand combinations necessary in the priming agent to achieve the primed state. Furthermore, assessing the transcriptome of NK cells after interacting with the priming agent in a time-course manner would help decipher what drives memory formation.

The identification of high expression of CD57 on tumour-memory NK cells (Chapters 3 and 6) is important and suggests that when NK cells come into contact with certain cancer cell lines, this induces their maturation, which was also seen in another study (Pal et al., 2017). Dufva and colleagues studied NK cell interactions with a wide range of cancer cell lines but did not look at the expression of CD57 or its gene B3GAT1. It would be interesting to study what cancer cells have the ability to induce NK cell maturation and perform time-course experiments to understand the expression dynamics of this marker and what potential role it plays in the context of NK-cancer cell interaction.

One of this study's biggest limitations is the lack of epigenetic data on tumour-memory NK cells. CMV-derived adaptive NK cells and CIML-NK cells have been characterised by being epigenetically imprinted, which is an important feature of memory NK cells and explains how these memory NK cells can pass their memory characteristics into the progeny, contributing to a population of long-lived NK cells (Lau et al., 2022). Thus, future work should aim to characterise the epigenetic landscape of tumour-memory NK cells.

Another outstanding question I tried to address in this thesis is whether NK cells can activate each other in a homotypical manner, as seen by others (M. Kim et al., 2017; T.-J. Kim et al., 2014; K. M. Lee et al., 2006). The evidence for this effect is very limited, but these preliminary data suggest that certain populations of NK cells might have more of an immunoregulatory role towards other NK cells. It has been suggested that this could benefit NK cells in a challenging TME (T.-J. Kim et al., 2014), but the exact function of this mechanism remains unknown. The preliminary data generated in this thesis should be expanded by looking at NK cell interactions using real-time imaging with high-resolution confocal microscopy and to identify what receptors might be involved in this process.

So many questions still remain around the topic of memory-NK cells. Did NK cell memory evolve to provide long-term immunity in organisms prior to the development of adaptive immunity? Perhaps acquired immunity may be defined by “antigen-specific memory”, whilst innate immunity may have memory-like function based upon prolonged primed state and thus a lower threshold for triggering function. Should we use the term “innate memory” instead of “memory-like”?

Overall, in this thesis, I have looked at the mechanisms driving tumour-NK cell memory induced by tumour priming of NK cells but I remain unable to define what NK memory is as a phenomenon. Future side-to-side comparisons of all the types of memory NK cells, including adaptive-, cytokine-, and tumour-memory NK cells, to identify similarities and differences might help define immunological memory in the innate immune system. NK cells were discovered in 1975, but we have only known about memory features in NK cells for 15 years. There are still so many questions around them, which makes this a very exciting time to be in the NK cell field.

Approximate word count: 50,000

References

Abel, A. M., Yang, C., Thakar, M. S., & Malarkannan, S. (2018). Natural killer cells: Development, maturation, and clinical utilization. *Frontiers in Immunology*, *9*(AUG), 1–23. https://doi.org/10.3389/fimmu.2018.01869

Abo, T., & Balch, C. M. (1981). A differentiation antigen of human NK and K cells defined by a monoclonal antibody (HNK-1). *The Journal of Immunology*, *127*, 1024–1029.

Abo, T., Miller, C. A., & Balch, C. M. (1984). Characterization of human granular lymphocyte subpopulations expressing HNK-1 (Leu-7) and Leu-11 antigens in the blood and lymphoid tissues from fetuses, neonates and adults. *European Journal of Immunology*, *14*(7), 616–623. https://doi.org/10.1002/eji.1830140707

Aggarwal, S., van de Loosdrecht, A. A., Alhan, C., Ossenkoppele, G. J., Westers, T. M., & Bontkes, H. J. (2011). Role of immune responses in the pathogenesis of low-risk MDS and high-risk MDS: implications for immunotherapy. *British Journal of Haematology*, *153*(5), 568–581. https://doi.org/10.1111/j.1365-2141.2011.08683.x

Al-Attar, A., Presnell, S. R., Peterson, C. A., Thomas, D. T., & Lutz, C. T. (2016). The effect of sex on immune cells in healthy aging: Elderly women have more robust natural killer lymphocytes than do elderly men. *Mechanisms of Ageing and Development*, *156*, 25–33.

Alvarez, M., Bouchlaka, M. N., Sckisel, G. D., Sungur, C. M., Chen, M., & Murphy, W. J. (2014). Increased Antitumor Effects Using IL-2 with Anti–TGF-β Reveals Competition between Mouse NK and CD8 T Cells. *The Journal of Immunology*, *193*(4), 1709 LP – 1716. https://doi.org/10.4049/jimmunol.1400034

Alvarez, M., Dunai, C., Khuat, L. T., Aguilar, E. G., Barao, I., & Murphy, W. J. (2020). IL-2 and anti-TGF-β promote NK cell reconstitution and anti-tumor effects after syngeneic hematopoietic stem cell transplantation. *Cancers*, *12*(11), 1–17. https://doi.org/10.3390/cancers12113189

Antoon, R., Wang, X.-H., Saleh, A. H., Warrington, J., Hedley, D. W., & Keating, A. (2022). Pancreatic cancer growth promoted by bone marrow mesenchymal stromal cell-derived IL-6 is reversed predominantly by IL-6 blockade. *Cytotherapy*, *24*(7), 699–710. https://doi.org/10.1016/j.jcyt.2021.12.005

Arber, D. A., Orazi, A., Hasserjian, R., Thiele, J., Borowitz, M. J., Le Beau, M. M., Bloomfield, C. D., Cazzola, M., & Vardiman, J. W. (2016). The 2016 revision to the World Health Organization classification of

myeloid neoplasms and acute leukemia. *Blood*, *127*(20), 2391–2405. https://doi.org/10.1182/blood-2016-03-643544

Arellano-Ballestero, H., Sabry, M., & Lowdell, M. W. (2023). A Killer Disarmed: Natural Killer Cell Impairment in Myelodysplastic Syndrome. *Cells*, *12*(4), 633. https://doi.org/10.3390/cells12040633

Ashkenazi, A., & Dixit, V. M. (1998). Death receptors: signaling and modulation. *Science (New York, N.Y.)*, *281*(5381), 1305–1308. https://doi.org/10.1126/science.281.5381.1305

Aurelius, J., Hallner, A., Werlenius, O., Riise, R., Moüllgård, L., Brune, M., Hansson, M., Martner, A., Thorén, F. B., & Hellstrand, K. (2017). NOX2-dependent immunosuppression in chronic myelomonocytic leukemia. *Journal of Leukocyte Biology*, *102*(2), 459–466. https://doi.org/10.1189/jlb.5VMA1116-454R

Aurelius, J., Martner, A., Riise, R. E., Romero, A. I., Palmqvist, L., Brune, M., Hellstrand, K., & Thorén, F. B. (2013). Chronic myeloid leukemic cells trigger poly (ADP-ribose) polymerase-dependent inactivation and cell death in lymphocytes. *Journal of Leukocyte Biology*, *93*(1), 155–160. https://doi.org/10.1189/jlb.0512257

Bachanova, V., Cooley, S., Defor, T. E., Verneris, M. R., Zhang, B., Mckenna, D. H., Curtsinger, J., Panoskaltsis-mortari, A., Lewis, D., Hippen, K., Mcglave, P., Weisdorf, D. J., Blazar, B. R., & Miller, J. S. (2014). *Clearance of acute myeloid leukemia by haploidentical natural killer cells is improved using IL-2 diphtheria toxin fusion protein*. *123*(25), 3855–3863. https://doi.org/10.1182/blood-2013-10-532531.V.B.

Bachier, C., Borthakur, G., Hosing, C., Blum, W., Rotta, M., Ojeras, P., Barnett, B., Rajangam, K., Majhail, N. S., & Nikiforow, S. (2020). A phase 1 study of NKX101, an allogeneic CAR natural killer (NK) cell therapy, in subjects with relapsed/refractory (R/R) acute myeloid leukemia (AML) or higher-risk myelodysplastic syndrome (MDS). *Blood*, *136*, 42–43.

Barber, D. F., Faure, M., & Long, E. O. (2004). LFA-1 contributes an early signal for NK cell cytotoxicity. *The Journal of Immunology*, *173*(6), 3653–3659.

Bauer, S., Groh, V., Wu, J., Steinle, A., Phillips, J. H., Lanier, L. L., & Spies, T. (1999). Activation of NK cells and T cells by NKG2D, a receptor for stress-inducible MICA. *Science (New York, N.Y.)*, *285*(5428), 727–729. https://doi.org/10.1126/science.285.5428.727

Bednarski, J. J., Zimmerman, C., Berrien-Elliott, M. M., Foltz, J. A., Becker-Hapak, M., Neal, C. C., Foster, M., Schappe, T., McClain, E., Pence, P. P., Desai, S., Kersting-Schadek, S., Wong, P., Russler-Germain, D. A., Fisk,

B., Lie, W.-R., Eisele, J., Hyde, S., Bhatt, S. T., … Fehniger, T. A. (2022). Donor memory-like NK cells persist and induce remissions in pediatric patients with relapsed AML after transplant. *Blood*, *139*(11), 1670–1683. https://doi.org/https://doi.org/10.1182/blood.2021013972

Benson, D. M. J., Cohen, A. D., Jagannath, S., Munshi, N. C., Spitzer, G., Hofmeister, C. C., Efebera, Y. A., Andre, P., Zerbib, R., & Caligiuri, M. A. (2015). A Phase I Trial of the Anti-KIR Antibody IPH2101 and Lenalidomide in Patients with Relapsed/Refractory Multiple Myeloma. *Clinical Cancer Research : An Official Journal of the American Association for Cancer Research*, *21*(18), 4055–4061. https://doi.org/10.1158/1078-0432.CCR-15-0304

Berrien-Elliott, M. M., Becker-Hapak, M., Cashen, A. F., Jacobs, M., Wong, P., Foster, M., McClain, E., Desai, S., Pence, P., Cooley, S., Brunstein, C., Gao, F., Abboud, C. N., Uy, G. L., Westervelt, P., Jacoby, M. A., Pusic, I., Stockerl-Goldstein, K. E., Schroeder, M. A., … Fehniger, T. A. (2022). Systemic IL-15 promotes allogeneic cell rejection in patients treated with natural killer cell adoptive therapy. *Blood*, *139*(8), 1177–1183. https://doi.org/10.1182/blood.2021011532

Berrien-Elliott, M. M., Cashen, A. F., Cubitt, C. C., Neal, C. C., Wong, P., Wagner, J. A., Foster, M., Schappe, T., Desai, S., McClain, E., Becker-Hapak, M., Foltz, J. A., Cooper, M. L., Jaeger, N., Srivatsan, S. N., Gao, F., Romee, R., Abboud, C. N., Uy, G. L., … Fehniger, T. A. (2020). Multidimensional Analyses of Donor Memory-Like NK Cells Reveal New Associations with Response after Adoptive Immunotherapy for Leukemia. *Cancer Discovery*, *10*(12), 1854–1871. https://doi.org/10.1158/2159-8290.CD-20-0312

Berrien-Elliott, M. M., Jacobs, M. T., & Fehniger, T. A. (2023). Allogeneic natural killer cell therapy. *Blood*, *141*(8), 856–868. https://doi.org/10.1182/blood.2022016200

Bevilacqua, M. P. (1993). Endothelial-leukocyte adhesion molecules. *Annual Review of Immunology*, *11*, 767–804. https://doi.org/10.1146/annurev.iy.11.040193.004003

Béziat, V., Liu, L. L., Malmberg, J. A., Ivarsson, M. A., Sohlberg, E., Björklund, A. T., Retière, C., Sverremark-Ekström, E., Traherne, J., Ljungman, P., Schaffer, M., Price, D. A., Trowsdale, J., Michaëlsson, J., Ljunggren, H. G., & Malmberg, K. J. (2013). NK cell responses to cytomegalovirus infection lead to stable imprints in the human KIR repertoire and involve activating KIRs. *Blood*, *121*(14), 2678–2688. https://doi.org/10.1182/blood-2012-10-459545

Bhat, R., & Watzl, C. (2007). Serial killing of tumor cells by human natural killer cells - Enhancement by therapeutic antibodies. *PLoS ONE*, *2*(3). https://doi.org/10.1371/journal.pone.0000326

Bhatia, R., & Deeg, H. J. (2011). Treatment-related myelodysplastic syndrome: molecular characteristics and therapy. *Current Opinion in Hematology*, *18*(2), 77–82. https://doi.org/10.1097/MOH.0b013e328343997a

Biron, C. A., Byron, K. S., & Sullivan, J. L. (1989). Severe herpesvirus infections in an adolescent without natural killer cells. *The New England Journal of Medicine*, *320*(26), 1731–1735. https://doi.org/10.1056/NEJM198906293202605

Björkström, N. K., Riese, P., Heuts, F., Andersson, S., Fauriat, C., Ivarsson, M. A., Björklund, A. T., Flodström-Tullberg, M., Michaëlsson, J., Rottenberg, M. E., Guzmán, C. A., Ljunggren, H. G., & Malmberg, K. J. (2010). Expression patterns of NKG2A, KIR, and CD57 define a process of CD56 dim NK-cell differentiation uncoupled from NK-cell education. *Blood*, *116*(19), 3853–3864. https://doi.org/10.1182/blood-2010-04-281675

Blake, S. J., Stannard, K., Liu, J., Allen, S., Yong, M. C. R., Mittal, D., Aguilera, A. R., Miles, J. J., Lutzky, V. P., de Andrade, L. F., Martinet, L., Colonna, M., Takeda, K., Kühnel, F., Gurlevik, E., Bernhardt, G., Teng, M. W. L., & Smyth, M. J. (2016). Suppression of Metastases Using a New Lymphocyte Checkpoint Target for Cancer Immunotherapy. *Cancer Discovery*, *6*(4), 446–459. https://doi.org/10.1158/2159-8290.CD-15-0944

Borrego, F., Robertson, M. J., Ritz, J., Peña, J., & Solana, R. (1999). CD69 is a stimulatory receptor for natural killer cell and its cytotoxic effect is blocked by CD94 inhibitory receptor. *Immunology*, *97*(1), 159–165. https://doi.org/10.1046/j.1365-2567.1999.00738.x

Bossi, G., & Griffiths, G. M. (1999). Degranulation plays an essential part in regulating cell surface expression of Fas ligand in T cells and natural killer cells. *Nature Medicine*, *5*(1), 90–96. https://doi.org/10.1038/4779

Boudreau, J. E., & Hsu, K. C. (2018). Natural killer cell education in human health and disease. *Current Opinion in Immunology*, *50*, 102–111. https://doi.org/10.1016/j.coi.2017.11.003

Brandt, C. S., Baratin, M., Yi, E. C., Kennedy, J., Gao, Z., Fox, B., Haldeman, B., Ostrander, C. D., Kaifu, T., Chabannon, C., Moretta, A., West, R., Xu, W., Vivier, E., & Levin, S. D. (2009). The B7 family member B7-H6 is a tumor cell ligand for the activating natural killer cell receptor NKp30 in humans. *The Journal of Experimental Medicine*, *206*(7), 1495–1503. https://doi.org/10.1084/jem.20090681

Braud, V. M., Allan, D. S., O'Callaghan, C. A., Söderström, K., D'Andrea, A., Ogg, G. S., Lazetic, S., Young, N. T., Bell, J. I., Phillips, J. H., Lanier, L. L., & McMichael, A. J. (1998). HLA-E binds to natural killer cell receptors CD94/NKG2A, B and C. *Nature*, *391*(6669), 795–799. https://doi.org/10.1038/35869

Breccia, M., Latagliata, R., Cannella, L., Carmosino, I., Santopietro, M., Loglisci, G., Federico, V., & Alimena, G. (2010). Refractory cytopenia with unilineage dysplasia: analysis of prognostic factors and survival in 126 patients. *Leukemia & Lymphoma*, *51*(5), 783–788. https://doi.org/10.3109/10428191003682759

Brenchley, J. M., Karandikar, N. J., Betts, M. R., Ambrozak, D. R., Hill, B. J., Crotty, L. E., Casazza, J. P., Kuruppu, J., Migueles, S. A., Connors, M., Roederer, M., Douek, D. C., & Koup, R. A. (2003). Expression of CD57 defines replicative senescence and antigen-induced apoptotic death of CD8+ T cells. *Blood*, *101*(7), 2711–2720. https://doi.org/10.1182/blood-2002-07-2103

Briercheck, E. L., Freud, A. G., & Caligiuri, M. A. (2009). Human natural killer cell development. *Natural Killer Cells: Basic Science and Clinical Application*, *214*, 113–122. https://doi.org/10.1016/B978-0-12-370454-2.00008-9

Brumbaugh, K. M., Binstadt, B. A., & Leibson, P. J. (1998). *Signal Transduction During NK Cell Activation: Balancing Opposing Forces BT - Specificity, Function, and Development of NK Cells: NK Cells: The Effector Arm of Innate Immunity* (K. Kärre & M. Colonna, Eds.; pp. 103–122). Springer Berlin Heidelberg. https://doi.org/10.1007/978-3-642-46859-9_8

Bryceson, Y. T., March, M. E., Ljunggren, H.-G., & Long, E. O. (2006). Synergy among receptors on resting NK cells for the activation of natural cytotoxicity and cytokine secretion. *Blood*, *107*(1), 159–166. https://doi.org/10.1182/blood-2005-04-1351

Burnet, F. M. (1970). The concept of immunological surveillance. *Progress in Experimental Tumor Research*, *13*, 1–27. https://doi.org/10.1159/000386035

Caligiuri, M. A., Murray, C., Robertson, M. J., Wang, E., Cochran, K., Cameron, C., Schow, P., Ross, M. E., Klumpp, T. R., & Soiffer, R. J. (1993). Selective modulation of human natural killer cells in vivo after prolonged infusion of low dose recombinant interleukin 2. *The Journal of Clinical Investigation*, *91*(1), 123–132.

Caligiuri, M. A., Zmuidzinas, A., Manley, T. J., Levine, H., Smith, K. A., & Ritz, J. (1990). Functional consequences of interleukin 2 receptor expression on resting human lymphocytes. Identification of a novel natural killer cell

subset with high affinity receptors. *Journal of Experimental Medicine*, *171*(5), 1509–1526. https://doi.org/10.1084/jem.171.5.1509

Campbell, K. S. (2010). *Natural Killer Cell Protocols: Cellular and Molecular Methods*.

Capuano, C., Pighi, C., Battella, S., De Federicis, D., Galandrini, R., & Palmieri, G. (2021). Harnessing cd16-mediated nk cell functions to enhance therapeutic efficacy of tumor-targeting mabs. *Cancers*, *13*(10), 1–24. https://doi.org/10.3390/cancers13102500

Carlsten, M., Baumann, B. C., Simonsson, M., Jädersten, M., Forsblom, A.-M., Hammarstedt, C., Bryceson, Y. T., Ljunggren, H.-G., Hellström-Lindberg, E., & Malmberg, K.-J. (2010). Reduced DNAM-1 expression on bone marrow NK cells associated with impaired killing of CD34+ blasts in myelodysplastic syndrome. *Leukemia*, *24*(9), 1607–1616. https://doi.org/10.1038/leu.2010.149

Chandhok, N. S., Boddu, P. C., Gore, S. D., & Prebet, T. (2019). What are the most promising new agents in myelodysplastic syndromes? *Current Opinion in Hematology*, *26*(2), 77–87. https://doi.org/10.1097/MOH.0000000000000483

Chang, C.-H., Qiu, J., O'Sullivan, D., Buck, M. D., Noguchi, T., Curtis, J. D., Chen, Q., Gindin, M., Gubin, M. M., van der Windt, G. J. W., Tonc, E., Schreiber, R. D., Pearce, E. J., & Pearce, E. L. (2015). Metabolic Competition in the Tumor Microenvironment Is a Driver of Cancer Progression. *Cell*, *162*(6), 1229–1241. https://doi.org/https://doi.org/10.1016/j.cell.2015.08.016

Chattopadhyay, P. K., Betts, M. R., Price, D. A., Gostick, E., Horton, H., Roederer, M., & De Rosa, S. C. (2009). The cytolytic enzymes granyzme A, granzyme B, and perforin: expression patterns, cell distribution, and their relationship to cell maturity and bright CD57 expression. *Journal of Leukocyte Biology*, *85*(1), 88–97. https://doi.org/10.1189/jlb.0208107

Chauveau, A., Aucher, A., Eissmann, P., Vivier, E., & Davis, D. M. (2010). Membrane nanotubes facilitate long-distance interactions between natural killer cells and target cells. *Proceedings of the National Academy of Sciences of the United States of America*, *107*(12), 5545–5550. https://doi.org/10.1073/pnas.0910074107

Chen, X., Eksioglu, E. A., Zhou, J., Zhang, L., Djeu, J., Fortenbery, N., Epling-Burnette, P., Van Bijnen, S., Dolstra, H., Cannon, J., Youn, J. I., Donatelli, S. S., Qin, D., De Witte, T., Tao, J., Wang, H., Cheng, P., Gabrilovich, D. I., List, A., & Wei, S. (2013). Induction of myelodysplasia by myeloid-derived suppressor cells. *Journal of Clinical Investigation*, *123*(11), 4595–4611. https://doi.org/10.1172/JCI67580

Choi, P. J., & Mitchison, T. J. (2013). Imaging burst kinetics and spatial coordination during serial killing by single natural killer cells. *Proceedings of the National Academy of Sciences of the United States of America*, *110*(16), 6488–6493. https://doi.org/10.1073/pnas.1221312110

Chong, A. S.-F., Boussy, I. A., Jiang, X. L., Lamas, M., & Graf Jr, L. H. (1994). CD54/ICAM-1 is a costimulator of NK cell-mediated cytotoxicity. *Cellular Immunology*, *157*(1), 92–105.

Chouaib, S., Noman, M. Z., Kosmatopoulos, K., & Curran, M. A. (2017). Hypoxic stress: obstacles and opportunities for innovative immunotherapy of cancer. *Oncogene*, *36*(4), 439–445. https://doi.org/10.1038/onc.2016.225

Cichicki, F., Schlums, H., Theorell, J., Tesi, B., Miller, J. S., Ljunggren, H.-G., & Bryceson, Y. T. (2016). Diversification and Functional Specialization of Human NK Cell Subsets. *Current Topics in Microbiology and Immunology*, *395*, 63–94. https://doi.org/10.1007/82_2015_487

Cichocki, F., Grzywacz, B., & Miller, J. S. (2019). Human NK cell development: One road or many? *Frontiers in Immunology*, *10*(AUG), 1–10. https://doi.org/10.3389/fimmu.2019.02078

Cichocki, F., Wu, C. Y., Zhang, B., Felices, M., Tesi, B., Tuininga, K., Dougherty, P., Taras, E., Hinderlie, P., Blazar, B. R., Bryceson, Y. T., & Miller, J. S. (2018). ARID5B regulates metabolic programming in human adaptive NK cells. *Journal of Experimental Medicine*, *215*(9), 2379–2395. https://doi.org/10.1084/jem.20172168

Ciurea, S. O., Schafer, J. R., Bassett, R., Denman, C. J., Cao, K., Willis, D., Rondon, G., Chen, J., Soebbing, D., Kaur, I., Gulbis, A., Ahmed, S., Rezvani, K., Shpall, E. J., Lee, D. A., & Champlin, R. E. (2017). Phase 1 clinical trial using mbIL21 ex vivo–expanded donor-derived NK cells after haploidentical transplantation. *Blood*, *130*(16), 1857–1868. https://doi.org/10.1182/blood-2017-05-785659

Classen, C. F., Falk, C. S., Friesen, C., Fulda, S., Herr, I., & Debatin, K.-M. (2003). Natural killer resistance of a drug-resistant leukemia cell line, mediated by up-regulation of HLA class I expression. *Haematologica*, *88*(5), 509–521.

Claus, M., Wingert, S., & Watzl, C. (2016). Modulation of natural killer cell functions by interactions between 2B4 and CD48 in cis and in trans. *Open Biology*, *6*(5). https://doi.org/10.1098/rsob.160010

Coca, S., Perez-Piqueras, J., Martinez, D., Colmenarejo, A., Saez, M. A., Vallejo, C., Martos, J. A., & Moreno, M. (1997). The prognostic significance of intratumoral natural killer cells in patients with colorectal

carcinoma. *Cancer*, *79*(12), 2320–2328. https://doi.org/10.1002/(sici)1097-0142(19970615)79:12<2320::aid-cncr5>3.0.co;2-p

Colonna, M., & Samaridis, J. (1995). Cloning of immunoglobulin-superfamily members associated with HLA-C and HLA-B recognition by human natural killer cells. *Science (New York, N.Y.)*, *268*(5209), 405–408. https://doi.org/10.1126/science.7716543

Comerci, C. J., Mace, E. M., Banerjee, P. P., & Orange, J. S. (2012). CD2 Promotes Human Natural Killer Cell Membrane Nanotube Formation. *PLoS ONE*, *7*(10). https://doi.org/10.1371/journal.pone.0047664

Cooley, S., He, F., Bachanova, V., Vercellotti, G. M., Defor, T. E., Curtsinger, J. M., Robertson, P., Grzywacz, B., Conlon, K. C., Waldmann, T. A., Mckenna, D. H., Blazar, B. R., Weisdorf, D. J., & Miller, J. S. (2019). First-in-human trial of rhIL-15 and haploidentical natural killer cell therapy for advanced acute myeloid leukemia. *Blood Advances*, *3*. https://doi.org/10.1182/bloodadvances.2018028332

Cooper, M. A., Elliott, J. M., Keyel, P. A., Yang, L., Carrero, J. A., & Yokoyama, W. M. (2009). *Cytokine-induced memory-like natural killer cells*. *106*(6), 1915–1919.

Cooper, M. A., Fehniger, T. A., & Caligiuri, M. A. (2001). The biology of human natural killer-cell subsets. *Trends in Immunology*, *22*(11), 633–640.

Corey, S. J., Minden, M. D., Barber, D. L., Kantarjian, H., Wang, J. C. Y., & Schimmer, A. D. (2007). Myelodysplastic syndromes: The complexity of stem-cell diseases. *Nature Reviews Cancer*, *7*(2), 118–129. https://doi.org/10.1038/nrc2047

Corradi, G., Baldazzi, C., Očadlíková, D., Marconi, G., Parisi, S., Testoni, N., Finelli, C., Cavo, M., Curti, A., & Ciciarello, M. (2018). Mesenchymal stromal cells from myelodysplastic and acute myeloid leukemia patients display in vitro reduced proliferative potential and similar capacity to support leukemia cell survival. *Stem Cell Research and Therapy*, *9*(1). https://doi.org/10.1186/s13287-018-1013-z

Costello, R. T., Sivori, S., Marcenaro, E., Lafage-Pochitaloff, M., Mozziconacci, M.-J., Reviron, D., Gastaut, J.-A., Pende, D., Olive, D., & Moretta, A. (2002). Defective expression and function of natural killer cell–triggering receptors in patients with acute myeloid leukemia. *Blood*, *99*(10), 3661–3667. https://doi.org/10.1182/blood.V99.10.3661

Curti, A., Ruggeri, L., D'Addio, A., Bontadini, A., Dan, E., Motta, M. R., Trabanelli, S., Giudice, V., Urbani, E., Martinelli, G., Paolini, S., Fruet, F., Isidori, A., Parisi, S., Bandini, G., Baccarani, M., Velardi, A., & Lemoli, R.

M. (2011). Successful transfer of alloreactive haploidentical KIR ligand-mismatched natural killer cells after infusion in elderly high risk acute myeloid leukemia patients. *Blood*, *118*(12), 3273–3279. https://doi.org/10.1182/blood-2011-01-329508

Dąbrowska, A., Grubba, M., Balihodzic, A., Szot, O., Sobocki, B. K., & Perdyan, A. (2023). The Role of Regulatory T Cells in Cancer Treatment Resistance. In *International Journal of Molecular Sciences* (Vol. 24, Issue 18). https://doi.org/10.3390/ijms241814114

Dalle, J.-H., Menezes, J., Wagner, E., Blagdon, M., Champagne, J., Champagne, M. A., & Duval, M. (2005). Characterization of cord blood natural killer cells: implications for transplantation and neonatal infections. *Pediatric Research*, *57*(5 Pt 1), 649–655. https://doi.org/10.1203/01.PDR.0000156501.55431.20

Damoiseaux, J. (2020). The IL-2 – IL-2 receptor pathway in health and disease: The role of the soluble IL-2 receptor. *Clinical Immunology*, *218*(June), 108515. https://doi.org/10.1016/j.clim.2020.108515

D'Andrea, A., Chang, C., Franz-Bacon, K., McClanahan, T., Phillips, J. H., & Lanier, L. L. (1995). Molecular cloning of NKB1. A natural killer cell receptor for HLA-B allotypes. *Journal of Immunology (Baltimore, Md.: 1950)*, *155*(5), 2306–2310.

Dauguet, N., Récher, C., Demur, C., Fournié, J.-J., Poupot, M., & Poupot, R. (2011). Pre-eminence and persistence of immature natural killer cells in acute myeloid leukemia patients in first complete remission. *American Journal of Hematology*, *86*(2), 209–213. https://doi.org/10.1002/ajh.21906

de Jonge, P. K. J. D., van Hauten, P. M. M., Janssen, L. D., de Goede, A. L., Berrien-Elliott, M. M., van der Meer, J. M. R., Mousset, C. M., Roeven, M. W. H., Foster, M., Blijlevens, N., Hobo, W., Fehniger, T. A., Jansen, J. H., Schaap, N. P. M., & Dolstra, H. (2023). Good manufacturing practice production of CD34+ progenitor-derived NK cells for adoptive immunotherapy in acute myeloid leukemia. *Cancer Immunology, Immunotherapy*, *72*(10), 3323–3335. https://doi.org/10.1007/s00262-023-03492-6

de la Fuente, H., Cruz-Adalia, A., Del Hoyo, G. M., Cibrián-Vera, D., Bonay, P., Pérez-Hernández, D., Vázquez, J., Navarro, P., Gutierrez-Gallego, R., & Ramirez-Huesca, M. (2014). The leukocyte activation receptor CD69 controls T cell differentiation through its interaction with galectin-1. *Molecular and Cellular Biology*.

Deng, W., Gowen, B. G., Zhang, L., Wang, L., Lau, S., Iannello, A., Xu, J., Rovis, T. L., Xiong, N., & Raulet, D. H. (2015). A shed NKG2D ligand that

promotes natural killer cell activation and tumor rejection. *Science*, *348*(6230), 136–139. https://doi.org/10.1126/science.1258867

Denman, C. J., Senyukov, V. v, Somanchi, S. S., Phatarpekar, P. v, Kopp, L. M., Johnson, J. L., Singh, H., Hurton, L., Maiti, S. N., Huls, M. H., Champlin, R. E., Cooper, L. J. N., & Lee, D. A. (2012). Membrane-bound IL-21 promotes sustained ex vivo proliferation of human natural killer cells. *PloS One*, *7*(1), e30264. https://doi.org/10.1371/journal.pone.0030264

Dewan, Md. Z., Terunuma, H., Takada, M., Tanaka, Y., Abe, H., Sata, T., Toi, M., & Yamamoto, N. (2007). Role of natural killer cells in hormone-independent rapid tumor formation and spontaneous metastasis of breast cancer cells in vivo. *Breast Cancer Research and Treatment*, *104*(3), 267–275. https://doi.org/10.1007/s10549-006-9416-4

Dickinson, M., Hamad, N., Bryant, C. E., Borthakur, G., Hosing, C., Shook, D., Tan, J., Rajangam, K., Liu, H., Kennedy, G. A., McSweeney, P. A., & Hill, B. T. (2021). A Phase 1 Study of NKX019, a CD19 Chimeric Antigen Receptor Natural Killer (CAR NK) Cell Therapy, in Subjects with B-Cell Malignancies. *Blood*, *138*(Supplement 1), 3868. https://doi.org/10.1182/blood-2021-146602

Diniz, M. O., Schurich, A., Chinnakannan, S. K., Duriez, M., Stegmann, K. A., Davies, J., Kucykowicz, S., Suveizdyte, K., Amin, O. E., Alcock, F., Cargill, T., Barnes, E., & Maini, M. K. (2022). NK cells limit therapeutic vaccine–induced CD8+T cell immunity in a PD-L1–dependent manner. *Science Translational Medicine*, *14*(640). https://doi.org/10.1126/scitranslmed.abi4670

Döhner, H., Weisdorf, D. J., & Bloomfield, C. D. (2015). Acute Myeloid Leukemia. *New England Journal of Medicine*, *373*(12), 1136–1152. https://doi.org/10.1056/NEJMra1406184

Dong, H., Xie, G., Liang, Y., Dongjoo Ham, J., Vergara, J., Chen, J., Ritz, J., & Romee, R. (2020). Engineered Memory-like NK Cars Targeting a Neoepitope Derived from Intracellular NPM1c Exhibit Potent Activity and Specificity Against Acute Myeloid Leukemia. *Blood*, *136*(Supplement 1), 3–4. https://doi.org/10.1182/BLOOD-2020-134148

Donnelly, R. P., Loftus, R. M., Keating, S. E., Liou, K. T., Biron, C. A., Gardiner, C. M., & Finlay, D. K. (2014). mTORC1-Dependent Metabolic Reprogramming Is a Prerequisite for NK Cell Effector Function. *The Journal of Immunology*, *193*(9), 4477–4484. https://doi.org/10.4049/jimmunol.1401558

Draghi, M., Yawata, N., Gleimer, M., Yawata, M., Valiante, N. M., & Parham, P. (2005). Single-cell analysis of the human NK cell response to missing self

and its inhibition by HLA class I. *Blood*, *105*(5), 2028–2035. https://doi.org/10.1182/blood-2004-08-3174

Dufva, O., Gandolfi, S., Huuhtanen, J., Dashevsky, O., Duàn, H., Saeed, K., Klievink, J., Nygren, P., Bouhlal, J., Lahtela, J., Näätänen, A., Ghimire, B. R., Hannunen, T., Ellonen, P., Lähteenmäki, H., Rumm, P., Theodoropoulos, J., Laajala, E., Härkönen, J., … Mustjoki, S. (2023). Single-cell functional genomics reveals determinants of sensitivity and resistance to natural killer cells in blood cancers. *Immunity*, *56*(12), 2816-2835.e13. https://doi.org/10.1016/j.immuni.2023.11.008

Dunn, G. P., Old, L. J., & Schreiber, R. D. (2004). The immunobiology of cancer immunosurveillance and immunoediting. *Immunity*, *21*(2), 137–148. https://doi.org/10.1016/j.immuni.2004.07.017

Eidenschenk, C., Dunne, J., Jouanguy, E., Fourlinnie, C., Gineau, L., Bacq, D., McMahon, C., Smith, O., Casanova, J.-L., Abel, L., & Feighery, C. (2006). A novel primary immunodeficiency with specific natural-killer cell deficiency maps to the centromeric region of chromosome 8. *American Journal of Human Genetics*, *78*(4), 721–727. https://doi.org/10.1086/503269

Elsa, B., Heinz, T., L., G. P., P., H. R., E., A. O. J., Yasuhito, N., M., D. S., Maria, C., Philippe, P., Lily, M., Gunes, G., S., M.-M. J., Dylan, D., Martin, J., Ulrich, G., Guillermo, S., A., van de L. A., Olivier, K., Y., F. M., … Elli, P. (2022). Molecular International Prognostic Scoring System for Myelodysplastic Syndromes. *NEJM Evidence*, *1*(7), EVIDoa2200008. https://doi.org/10.1056/EVIDoa2200008

Epling-Burnette, P. K., Zhong, B., Salih, H. R., Wei, S., Bai, F., Boulware, D., List, A. F., Painter, J. S., Moscinski, L., Rollison, D. E., Ku, E., Krusch, M., Djeu, J. Y., & Zou, J. (2007). Reduced natural killer (NK) function associated with high-risk myelodysplastic syndrome (MDS) and reduced expression of activating NK receptors. *Blood*, *109*(11), 4816–4824. https://doi.org/10.1182/blood-2006-07-035519

Estey, E., Hasserjian, R. P., & Döhner, H. (2022). Distinguishing AML from MDS: a fixed blast percentage may no longer be optimal. *Blood*, *139*(3), 323–332. https://doi.org/10.1182/blood.2021011304

Evans, R., Patzak, I., Svensson, L., De Filippo, K., Jones, K., McDowall, A., & Hogg, N. (2009). Integrins in immunity. *Journal of Cell Science*, *122*(2), 215–225. https://doi.org/10.1242/jcs.019117

Ewen, E. M., Pahl, J. H. W., Miller, M., Watzl, C., & Cerwenka, A. (2018). KIR downregulation by IL-12/15/18 unleashes human NK cells from KIR/HLA-I inhibition and enhances killing of tumor cells. *European Journal of Immunology*, *48*(2), 355–365. https://doi.org/10.1002/eji.201747128

Falschlehner, C., Schaefer, U., & Walczak, H. (2009). Following TRAIL's path in the immune system. *Immunology*, *127*(2), 145–154. https://doi.org/https://doi.org/10.1111/j.1365-2567.2009.03058.x

Fauriat, C., Long, E. O., Ljunggren, H.-G., & Bryceson, Y. T. (2010). Regulation of human NK-cell cytokine and chemokine production by target cell recognition. *Blood*, *115*(11), 2167–2176. https://doi.org/10.1182/blood-2009-08-238469

Fehniger, T. A., Cai, S. F., Cao, X., Bredemeyer, A. J., Presti, R. M., French, A. R. R., & Ley, T. J. (2007). Acquisition of Murine NK Cell Cytotoxicity Requires the Translation of a Pre-existing Pool of Granzyme B and Perforin mRNAs. *Immunity*, *26*(6), 798–811. https://doi.org/10.1016/j.immuni.2007.04.010

Fehniger, T. A., Miller, J. S., Stuart, R. K., Cooley, S., Salhotra, A., Curtsinger, J., Westervelt, P., DiPersio, J. F., Hillman, T. M., Silver, N., Szarek, M., Gorelik, L., Lowdell, M. W., & Rowinsky, E. (2018). A Phase 1 Trial of CNDO-109–Activated Natural Killer Cells in Patients with High-Risk Acute Myeloid Leukemia. *Biology of Blood and Marrow Transplantation*, *24*(8), 1581–1589. https://doi.org/10.1016/j.bbmt.2018.03.019

Felices, M., Sarhan, D., Brandt, L., Guldevall, K., McElmurry, R., Lenvik, A., Chu, S., Tolar, J., Taras, E., Spellman, S. R., Warlick, E. D., Verneris, M. R., Cooley, S., Weisdorf, D., Blazar, B. R., Onfelt, B., Vallera, D., & Miller, J. S. (2016). CD16-IL15-CD33 Trispecific Killer Engager (TriKE) Overcomes Cancer-Induced Immune Suppression and Induces Natural Killer Cell-Mediated Control of MDS and AML Via Enhanced Killing Kinetics. *Blood*, *128*(22), 4291. https://doi.org/10.1182/blood.V128.22.4291.4291

Ferlazzo, G., & Moretta, L. (2014). Dendritic cell editing by natural killer cells. *Critical Reviews in Oncogenesis*, *19*(1–2), 67–75. https://doi.org/10.1615/critrevoncog.2014010827

Ferrini, S., Miescher, S., Zocchi, M. R., von Fliedner, V., & Moretta, A. (1987). Phenotypic and functional characterization of recombinant interleukin 2 (rIL 2)-induced activated killer cells: analysis at the population and clonal levels. *The Journal of Immunology*, *138*(4), 1297–1302. https://doi.org/10.4049/jimmunol.138.4.1297

Fischer, U., Jänicke, R. U., & Schulze-Osthoff, K. (2003). Many cuts to ruin: a comprehensive update of caspase substrates. *Cell Death & Differentiation*, *10*(1), 76–100. https://doi.org/10.1038/sj.cdd.4401160

Focosi, D., Bestagno, M., Burrone, O., & Petrini, M. (2010). CD57+ T lymphocytes and functional immune deficiency. *Journal of Leukocyte*

Biology, *87*(1), 107–116. https://doi.org/https://doi.org/10.1189/jlb.0809566

Foley, B., Cooley, S., Verneris, M. R., Pitt, M., Curtsinger, J., Luo, X., Lopez-Vergès, S., Lanier, L. L., Weisdorf, D., & Miller, J. S. (2012). Cytomegalovirus reactivation after allogeneic transplantation promotes a lasting increase in educated NKG2C+ natural killer cells with potent function. *Blood*, *119*(11), 2665–2674. https://doi.org/10.1182/blood-2011-10-386995

Frank, C., Zhang, B., Felice, M., Blazar, B. R., & Miller, J. S. (2015). mTORC1 Signaling and Metabolism Are Dynamically Regulated during Human NK Cell Maturation and in Adaptive NK Cell Responses to Viral Infection. *Blood*, *126*(23), 209–209. https://doi.org/10.1182/blood.v126.23.209.209

Frederick, M., Grimm, E., Krohn, E., Smid, C., & Yu, T.-K. (1997). Cytokine-Induced Cytotoxic Function Expressed by Lymphocytes of the Innate Immune System: Distinguishing Characteristics of NK and LAK Based on Functional and Molecular Markers. *Journal of Interferon & Cytokine Research*, *17*(8), 435–447. https://doi.org/10.1089/jir.1997.17.435

Frias, A. M., Porada, C. D., Crapnell, K. B., Cabral, J. M. S., Zanjani, E. D., & Almeida-Porada, G. (2008). Generation of functional natural killer and dendritic cells in a human stromal-based serum-free culture system designed for cord blood expansion. *Experimental Hematology*, *36*(1), 61–68. https://doi.org/10.1016/j.exphem.2007.08.031

Froelich, C. J., Orth, K., Turbov, J., Seth, P., Gottlieb, R., Babior, B., Shah, G. M., Bleackley, R. C., Dixit, V. M., & Hanna, W. (1996). New paradigm for lymphocyte granule-mediated cytotoxicity. Target cells bind and internalize granzyme B, but an endosomolytic agent is necessary for cytosolic delivery and subsequent apoptosis. *The Journal of Biological Chemistry*, *271*(46), 29073–29079. https://doi.org/10.1074/jbc.271.46.29073

Frumento, G., Rotondo, R., Tonetti, M., Damonte, G., Benatti, U., & Ferrara, G. B. (2002). Tryptophan-derived catabolites are responsible for inhibition of T and natural killer cell proliferation induced by indoleamine 2,3-dioxygenase. *The Journal of Experimental Medicine*, *196*(4), 459–468. https://doi.org/10.1084/jem.20020121

Fujii, R., Jochems, C., Tritsch, S. R., Wong, H. C., Schlom, J., & Hodge, J. W. (2018). An IL-15 superagonist/IL-15Rα fusion complex protects and rescues NK cell-cytotoxic function from TGF-β1-mediated immunosuppression. *Cancer Immunology, Immunotherapy*, *67*(4), 675–689. https://doi.org/10.1007/s00262-018-2121-4

Fujisaki, H., Kakuda, H., Imai, C., Mullighan, C. G., & Campana, D. (2009). Replicative potential of human natural killer cells. *British Journal of Haematology*, *145*(5), 606–613. https://doi.org/10.1111/j.1365-2141.2009.07667.x

Fujisaki, H., Kakuda, H., Shimasaki, N., Imai, C., Ma, J., Lockey, T., Eldridge, P., Leung, W. H., & Campana, D. (2009a). Expansion of highly cytotoxic human natural killer cells for cancer cell therapy. *Cancer Research*, *69*(9), 4010–4017. https://doi.org/10.1158/0008-5472.CAN-08-3712

Fujisaki, H., Kakuda, H., Shimasaki, N., Imai, C., Ma, J., Lockey, T., Eldridge, P., Leung, W. H., & Campana, D. (2009b). Expansion of highly cytotoxic human natural killer cells for cancer cell therapy. *Cancer Research*, *69*(9), 4010–4017. https://doi.org/10.1158/0008-5472.CAN-08-3712

Gabrilovich, D. I., Chen, H. L., Girgis, K. R., Cunningham, H. T., Meny, G. M., Nadaf, S., Kavanaugh, D., & Carbone, D. P. (1996). Production of vascular endothelial growth factor by human tumors inhibits the functional maturation of dendritic cells. *Nature Medicine*, *2*(10), 1096–1103. https://doi.org/10.1038/nm1096-1096

Gasteiger, G., Hemmers, S., Firth, M. A., Le Floc'h, A., Huse, M., Sun, J. C., & Rudensky, A. Y. (2013). IL-2–dependent tuning of NK cell sensitivity for target cells is controlled by regulatory T cells. *Journal of Experimental Medicine*, *210*(6), 1167–1178. https://doi.org/10.1084/jem.20122462

Gati, A., Da Rocha, S., Guerra, N., Escudier, B., Moretta, A., Chouaib, S., Angevin, E., & Caignard, A. (2004). Analysis of the natural killer mediated immune response in metastatic renal cell carcinoma patients. *International Journal of Cancer*, *109*(3), 393–401. https://doi.org/https://doi.org/10.1002/ijc.11730

Germing, U., Strupp, C., Kuendgen, A., Isa, S., Knipp, S., Hildebrandt, B., Giagounidis, A., Aul, C., Gattermann, N., & Haas, R. (2006). Prospective validation of the WHO proposals for the classification of myelodysplastic syndromes. *Haematologica*, *91*(12), 1596–1604. https://doi.org/10.1016/j.leukres.2005.11.015

Geyh, S., Öz, S., Cadeddu, R. P., Fröbel, J., Brückner, B., Kündgen, A., Fenk, R., Bruns, I., Zilkens, C., Hermsen, D., Gattermann, N., Kobbe, G., Germing, U., Lyko, F., Haas, R., & Schroeder, T. (2013). Insufficient stromal support in MDS results from molecular and functional deficits of mesenchymal stromal cells. *Leukemia*, *27*(9), 1841–1851. https://doi.org/10.1038/leu.2013.193

Geyh, S., Rodríguez-Paredes, M., Jäger, P., Koch, A., Bormann, F., Gutekunst, J., Zilkens, C., Germing, U., Kobbe, G., Lyko, F., Haas, R., & Schroeder, T. (2018). Transforming growth factor β1-mediated functional inhibition of

mesenchymal stromal cells in myelodysplastic syndromes and acute myeloid leukemia. *Haematologica*, *103*(9), 1462–1471. https://doi.org/10.3324/haematol.2017.186734

Ghiringhelli, F., Ménard, C., Terme, M., Flament, C., Taieb, J., Chaput, N., Puig, P. E., Novault, S., Escudier, B., Vivier, E., Lecesne, A., Robert, C., Blay, J.-Y., Bernard, J., Caillat-Zucman, S., Freitas, A., Tursz, T., Wagner-Ballon, O., Capron, C., … Zitvogel, L. (2005). CD4+CD25+ regulatory T cells inhibit natural killer cell functions in a transforming growth factor–β–dependent manner . *Journal of Experimental Medicine*, *202*(8), 1075–1085. https://doi.org/10.1084/jem.20051511

Gleason, M. K., Ross, J. A., Warlick, E. D., Lund, T. C., Verneris, M. R., Wiernik, A., Spellman, S., Haagenson, M. D., Lenvik, A. J., Litzow, M. R., Epling-Burnette, P. K., Blazar, B. R., Weiner, L. M., Weisdorf, D. J., Vallera, D. A., & Miller, J. S. (2014). CD16xCD33 bispecific killer cell engager (BiKE) activates NK cells against primary MDS and MDSC CD33+ targets. *Blood*, *123*(19), 3016–3026. https://doi.org/10.1182/blood-2013-10-533398

Golden-Mason, L., McMahan, R. H., Strong, M., Reisdorph, R., Mahaffey, S., Palmer, B. E., Cheng, L., Kulesza, C., Hirashima, M., Niki, T., & Rosen, H. R. (2013). Galectin-9 functionally impairs natural killer cells in humans and mice. *Journal of Virology*, *87*(9), 4835–4845. https://doi.org/10.1128/JVI.01085-12

Gonçalves, A. C., Cortesão, E., Oliveiros, B., Alves, V., Espadana, A. I., Rito, L., Magalhães, E., Lobão, M. J., Pereira, A., Nascimento Costa, J. M., Mota-Vieira, L., & Sarmento-Ribeiro, A. B. (2015). Oxidative stress and mitochondrial dysfunction play a role in myelodysplastic syndrome development, diagnosis, and prognosis: A pilot study. *Free Radical Research*, *49*(9), 1081–1094. https://doi.org/10.3109/10715762.2015.1035268

Gotthardt, D., Putz, E. M., Straka, E., Kudweis, P., Biaggio, M., Poli, V., Strobl, B., Müller, M., & Sexl, V. (2014). Loss of STAT3 in murine NK cells enhances NK cell–dependent tumor surveillance. *Blood*, *124*(15), 2370–2379. https://doi.org/10.1182/blood-2014-03-564450

Greenberg, P., Cox, C., LeBeau, M. M., Fenaux, P., Morel, P., Sanz, G., Sanz, M., Vallespi, T., Hamblin, T., Oscier, D., Ohyashiki, K., Toyama, K., Aul, C., Mufti, G., & Bennett, J. (1997). International scoring system for evaluating prognosis in myelodysplastic syndromes. *Blood*, *89*(6), 2079–2088.

Grégoire, C., Chasson, L., Luci, C., Tomasello, E., Geissmann, F., Vivier, E., & Walzer, T. (2007). The trafficking of natural killer cells. *Immunological*

Reviews, *220*(1), 169–182. https://doi.org/10.1111/j.1600-065X.2007.00563.x

Grzywacz, B., Kataria, N., & Verneris, M. (2007). CD56dimCD16+ NK cells downregulate CD16 following target cell induced activation of matrix metalloproteinases. *Leukemia*, *21*(2), 356–359.

Gumá, M., Budt, M., Sáez, A., Brckalo, T., Hengel, H., Angulo, A., & López-Botet, M. (2006). Expansion of CD94/NKG2C+ NK cells in response to human cytomegalovirus-infected fibroblasts. *Blood*, *107*(9), 3624–3631. https://doi.org/10.1182/blood-2005-09-3682

Gurney, M., O'dwyer, M., Fracchiolla, S., & Onida, F. (2021). *Realizing Innate Potential: CAR-NK Cell Therapies for Acute Myeloid Leukemia*. https://doi.org/10.3390/cancers

Gurney, M., Stikvoort, A., Nolan, E., Kirkham-McCarthy, L., Khoruzhenko, S., Shivakumar, R., Zweegman, S., van de Donk, N. W. C. J., Mutis, T., Szegezdi, E., Sarkar, S., & O'Dwyer, M. (2022). CD38 knockout natural killer cells expressing an affinity optimized CD38 chimeric antigen receptor successfully target acute myeloid leukemia with reduced effector cell fratricide. *Haematologica*, *107*(2), 437–445. https://doi.org/10.3324/haematol.2020.271908

Hammer, Q., Rückert, T., Borst, E. M., Dunst, J., Haubner, A., Durek, P., Heinrich, F., Gasparoni, G., Babic, M., Tomic, A., Pietra, G., Nienen, M., Blau, I. W., Hofmann, J., Na, I. K., Prinz, I., Koenecke, C., Hemmati, P., Babel, N., … Romagnani, C. (2018). Peptide-specific recognition of human cytomegalovirus strains controls adaptive natural killer cells article. *Nature Immunology*, *19*(5), 453–463. https://doi.org/10.1038/s41590-018-0082-6

Hanahan, D. (2022). Hallmarks of Cancer: New Dimensions. *Cancer Discovery*, *12*(1), 31–46. https://doi.org/10.1158/2159-8290.CD-21-1059

Hanahan, D., & Weinberg, R. A. (2011). Hallmarks of cancer: The next generation. *Cell*, *144*(5), 646–674. https://doi.org/10.1016/J.CELL.2011.02.013

Harrison, D., Phillips, J. H., & Lanier, L. L. (1991). Involvement of a metalloprotease in spontaneous and phorbol ester-induced release of natural killer cell-associated Fc gamma RIII (CD16-II). *The Journal of Immunology*, *147*(10), 3459–3465. https://doi.org/10.4049/jimmunol.147.10.3459

Hashemi, E., & Malarkannan, S. (2020). Tissue-Resident NK Cells: Development, Maturation, and Clinical Relevance. *Cancers*, *12*(6), 1553. https://doi.org/10.3390/cancers12061553

Haubner, S., Perna, F., Köhnke, T., Schmidt, C., Berman, S., Augsberger, C., Schnorfeil, F. M., Krupka, C., Lichtenegger, F. S., Liu, X., Kerbs, P., Schneider, S., Metzeler, K. H., Spiekermann, K., Hiddemann, W., Greif, P. A., Herold, T., Sadelain, M., & Subklewe, M. (2019). Coexpression profile of leukemic stem cell markers for combinatorial targeted therapy in AML. *Leukemia*, *33*(1), 64–74. https://doi.org/10.1038/s41375-018-0180-3

Hayden, M. S., & Ghosh, S. (2014). Regulation of NF-κB by TNF family cytokines. *Seminars in Immunology*, *26*(3), 253–266. https://doi.org/10.1016/j.smim.2014.05.004

Hejazi, M., Manser, A. R., Fröbel, J., Kündgen, A., Zhao, X., Schönberg, K., Germing, U., Haas, R., Gattermann, N., & Uhrberg, M. (2015). Impaired cytotoxicity associated with defective natural killer cell differentiation in myelodysplastic syndromes. *Haematologica*, *100*(5), 643–652. https://doi.org/10.3324/haematol.2014.118679

Herberman, R. B., Nunn, M. E., Holden, H. T., & Lavrin, D. H. (1975). Natural cytotoxic reactivity of mouse lymphoid cells against syngeneic and allogeneic tumors. II. Characterization of effector cells. *International Journal of Cancer*, *16*(2), 230–239. https://doi.org/https://doi.org/10.1002/ijc.2910160205

Herberman, R. B., Nunn, M. E., & Lavrin, D. H. (1975). Natural cytotoxic reactivity of mouse lymphoid cells against syngeneic and allogeneic tumors. I. Distribution of reactivity and specificity. *International Journal of Cancer*, *16*(2), 216–229. https://doi.org/10.1002/ijc.2910160204

Hood, S. P., Foulds, G. A., Imrie, H., Reeder, S., McArdle, S. E. B., Khan, M., & Pockley, A. G. (2019). Phenotype and function of activated natural killer cells from patients with prostate cancer: Patient-dependent responses to priming and IL-2 activation. *Frontiers in Immunology*, *10*(JAN), 1–20. https://doi.org/10.3389/fimmu.2018.03169

Horikawa, N., Abiko, K., Matsumura, N., Hamanishi, J., Baba, T., Yamaguchi, K., Yoshioka, Y., Koshiyama, M., & Konishi, I. (2017). Expression of Vascular Endothelial Growth Factor in Ovarian Cancer Inhibits Tumor Immunity through the Accumulation of Myeloid-Derived Suppressor Cells. *Clinical Cancer Research : An Official Journal of the American Association for Cancer Research*, *23*(2), 587–599. https://doi.org/10.1158/1078-0432.CCR-16-0387

Horng, T., Bezbradica, J. S., & Medzhitov, R. (2007). NKG2D signaling is coupled to the interleukin 15 receptor signaling pathway. *Nature Immunology*, *8*(12), 1345–1352. https://doi.org/10.1038/ni1524

Horowitz, A., Strauss-Albee, D. M., Leipold, M., Kubo, J., Nemat-Gorgani, N., Dogan, O. C., Dekker, C. L., Mackey, S., Maecker, H., Swan, G. E., Davis,

M. M., Norman, P. J., Guethlein, L. A., Desai, M., Parham, P., & Blish, C. A. (2013). Genetic and environmental determinants of human NK cell diversity revealed by mass cytometry. *Science Translational Medicine*, *5*(208), 1–12. https://doi.org/10.1126/scitranslmed.3006702

Hoskin, D. W., Stankova, J., Anderson, S. K., & Roder, J. C. (1989). A functional and phenotypic comparison of murine natural killer (NK) cells and lymphokine-activated killer (LAK) cells. *International Journal of Cancer*, *43*(5), 940–948. https://doi.org/https://doi.org/10.1002/ijc.2910430536

Hsu, J., Hodgins, J. J., Marathe, M., Nicolai, C. J., Bourgeois-Daigneault, M.-C., Trevino, T. N., Azimi, C. S., Scheer, A. K., Randolph, H. E., Thompson, T. W., Zhang, L., Iannello, A., Mathur, N., Jardine, K. E., Kirn, G. A., Bell, J. C., McBurney, M. W., Raulet, D. H., & Ardolino, M. (2018). Contribution of NK cells to immunotherapy mediated by PD-1/PD-L1 blockade. *The Journal of Clinical Investigation*, *128*(10), 4654–4668. https://doi.org/10.1172/JCI99317

Huntington, N. D., Tabarias, H., Fairfax, K., Brady, J., Hayakawa, Y., Degli-Esposti, M. A., Smyth, M. J., Tarlinton, D. M., & Nutt, S. L. (2007). NK Cell Maturation and Peripheral Homeostasis Is Associated with KLRG1 Up-Regulation. *The Journal of Immunology*, *178*(8), 4764–4770. https://doi.org/10.4049/jimmunol.178.8.4764

Imai, C., Iwamoto, S., & Campana, D. (2005). Genetic modification of primary natural killer cells overcomes inhibitory signals and induces specific killing of leukemic cells. *Blood*, *106*(1), 376–383. https://doi.org/10.1182/blood-2004-12-4797

Imai, K., Matsuyama, S., Miyake, S., Suga, K., & Nakachi, K. (2000). Natural cytotoxic activity of peripheral-blood lymphocytes and cancer incidence: an 11-year follow-up study of a general population. *The Lancet*, *356*(9244), 1795–1799. https://doi.org/https://doi.org/10.1016/S0140-6736(00)03231-1

Invernizzi, R., Travaglino, E., Della Porta, M. G., Malcovati, L., Gallì, A., Bastia, R., Ciola, M., Ambaglio, I., Boveri, E., Rosti, V., & Cazzola, M. (2017). Vascular endothelial growth factor overexpression in myelodysplastic syndrome bone marrow cells: biological and clinical implications. *Leukemia and Lymphoma*, *58*(7), 1711–1720. https://doi.org/10.1080/10428194.2016.1262030

Ishigami, S., Natsugoe, S., Tokuda, K., Nakajo, A., Che, X., Iwashige, H., Aridome, K., Hokita, S., & Aikou, T. (2000). Prognostic value of intratumoral natural killer cells in gastric carcinoma. *Cancer*, *88*(3), 577–583.

Jacobs, R., Hintzen, G., Kemper, A., Beul, K., Kempf, S., Behrens, G., Sykora, K. W., & Schmidt, R. E. (2001). CD56bright cells differ in their KIR repertoire and cytotoxic features from CD56dim NK cells. *European Journal of Immunology*, *31*(10), 3121–3127. https://doi.org/10.1002/1521-4141(2001010)31:10<3121::aid-immu3121>3.0.co;2-4

Jensen, H., Potempa, M., Gotthardt, D., & Lanier, L. L. (2017). Cutting Edge: IL-2–Induced Expression of the Amino Acid Transporters SLC1A5 and CD98 Is a Prerequisite for NKG2D-Mediated Activation of Human NK Cells. *The Journal of Immunology*, *199*(6), 1967–1972. https://doi.org/10.4049/jimmunol.1700497

Jiang, H. J., Fu, R., Wang, H. Q., Li, L. J., Qu, W., Liang, Y., Wang, G. J., Wang, X. M., Wu, Y. H., Liu, H., Song, J., Guan, J., Xing, L. M., Ruan, E. B., & Shao, Z. H. (2013). Increased circulating of myeloid-derived suppressor cells in myelodysplastic syndrome. *Chinese Medical Journal*, *126*(13), 2582–2584. https://doi.org/10.3760/cma.j.issn.0366-6999.20121794

Judge, S. J., Murphy, W. J., & Canter, R. J. (2020). Characterizing the Dysfunctional NK Cell: Assessing the Clinical Relevance of Exhaustion, Anergy, and Senescence. *Frontiers in Cellular and Infection Microbiology*, *10*(February). https://doi.org/10.3389/fcimb.2020.00049

Juelke, K., Killig, M., Luetke-eversloh, M., Parente, E., Gruen, J., Morandi, B., Ferlazzo, G., Thiel, A., Schmitt-knosalla, I., & Romagnani, C. (2010). CD62L expression identifies a unique subset of polyfunctional CD56 dim NK cells. *Blood*, *116*(8), 1299–1307. https://doi.org/10.1182/blood-2009-11-253286.

Kagoya, Y., Yoshimi, A., Kataoka, K., Nakagawa, M., Kumano, K., Arai, S., Kobayashi, H., Saito, T., Iwakura, Y., & Kurokawa, M. (2014). Positive feedback between NF-κB and TNF-α promotes leukemia-initiating cell capacity. *The Journal of Clinical Investigation*, *124*(2), 528–542. https://doi.org/10.1172/JCI68101

Kalathil, S. G., & Thanavala, Y. (2021). Importance of myeloid derived suppressor cells in cancer from a biomarker perspective. *Cellular Immunology*, *361*, 104280. https://doi.org/10.1016/j.cellimm.2020.104280

Kared, H., Martelli, S., Tan, S. W., Simoni, Y., Chong, M. L., Yap, S. H., Newell, E. W., Pender, S. L. F., Kamarulzaman, A., Rajasuriar, R., & Larbi, A. (2018). Adaptive NKG2C+CD57+ natural killer cell and Tim-3 expression during viral infections. *Frontiers in Immunology*, *9*(APR), 1–21. https://doi.org/10.3389/fimmu.2018.00686

Karlhofer, F. M., Ribaudo, R. K., & Yokoyama, W. M. (1992). MHC class I alloantigen specificity of Ly-49+ IL-2-activated natural killer cells. *Nature*, *358*(6381), 66–70. https://doi.org/10.1038/358066a0

Kärre, K., Ljunggren, H. G., Piontek, G., & Kiessling, R. (1986). Selective rejection of H–2-deficient lymphoma variants suggests alternative immune defence strategy. *Nature*, *319*(6055), 675–678. https://doi.org/10.1038/319675a0

Katodritou, E., Terpos, E., North, J., Kottaridis, P., Verrou, E., Gastari, V., Chadjiaggelidou, C., Sivakumaran, S., Jide-Banwo, S., Tsirogianni, M., Kapetanos, D., Zervas, K., & Lowdell, M. W. (2011). Tumor-primed natural killer cells from patients with multiple myeloma lyse autologous, NK-resistant, bone marrow-derived malignant plasma cells. *American Journal of Hematology*, *86*(12), 967–973. https://doi.org/10.1002/ajh.22163

Ke, N., Wang, X., Xu, X., & Abassi, Y. A. (2011). *The xCELLigence System for Real-Time and Label-Free Monitoring of Cell Viability BT - Mammalian Cell Viability: Methods and Protocols* (M. J. Stoddart, Ed.; pp. 33–43). Humana Press. https://doi.org/10.1007/978-1-61779-108-6_6

Keating, S. E., Zaiatz-Bittencourt, V., Loftus, R. M., Keane, C., Brennan, K., Finlay, D. K., & Gardiner, C. M. (2016). Metabolic Reprogramming Supports IFN-γ Production by CD56bright NK Cells. *The Journal of Immunology*, *196*(6), 2552–2560. https://doi.org/10.4049/jimmunol.1501783

Keppel, M. P., Saucier, N., Mah, A. Y., Vogel, T. P., & Cooper, M. A. (2015). Activation-specific metabolic requirements for NK Cell IFN-γ production. *The Journal of Immunology*, *194*(4), 1954–1962.

Kerbauy, D. B., & Deeg, H. J. (2007). Apoptosis and antiapoptotic mechanisms in the progression of myelodysplastic syndrome. *Experimental Hematology*, *35*(11), 1739–1746. https://doi.org/10.1016/j.exphem.2007.09.007

Kiessling, R., Klein, E., Pross, H., & Wigzell, H. (1975). „Natural" killer cells in the mouse. II. Cytotoxic cells with specificity for mouse Moloney leukemia cells. Characteristics of the killer cell. *European Journal of Immunology*, *5*(2), 117–121. https://doi.org/https://doi.org/10.1002/eji.1830050209

Kiessling, R., Klein, E., & Wigzell, H. (1975). „Natural" killer cells in the mouse. I. Cytotoxic cells with specificity for mouse Moloney leukemia cells. Specificity and distribution according to genotype. *European Journal of Immunology*, *5*(2), 112–117. https://doi.org/10.1002/eji.1830050208

Kiessling, R., Wasserman, K., Horiguchi, S., Kono, K., Sjöberg, J., Pisa, P., & Petersson, M. (1999). Tumor-induced immune dysfunction. *Cancer*

Immunology, Immunotherapy, *48*(7), 353–362. https://doi.org/10.1007/s002620050586

Kiladjian, J.-J., Bourgeois, E., Lobe, I., Braun, T., Visentin, G., Bourhis, J.-H., Fenaux, P., Chouaib, S., & Caignard, A. (2006). Cytolytic function and survival of natural killer cells are severely altered in myelodysplastic syndromes. *Leukemia*, *20*(3), 463–470. https://doi.org/10.1038/sj.leu.2404080

Kim, M., Kim, T. J., Kim, H. M., Doh, J., & Lee, K. M. (2017). Multi-cellular natural killer (NK) cell clusters enhance NK cell activation through localizing IL-2 within the cluster. *Scientific Reports*, *7*(January), 1–8. https://doi.org/10.1038/srep40623

Kim, T.-J., Kim, M., Kim, H. M., Lim, S. A., Kim, E.-O., Kim, K., Song, K. H., Kim, J., Kumar, V., Yee, C., Doh, J., & Lee, K.-M. (2014). *Homotypic NK cell-to-cell communication controls cytokine responsiveness of innate immune NK cells*. https://doi.org/10.1038/srep07157

Kottaridis, P. D., North, J., Tsirogianni, M., Marden, C., Samuel, E. R., Jide-Banwo, S., Grace, S., & Lowdell, M. W. (2015). Two-stage priming of allogeneic natural killer cells for the treatment of patients with acute myeloid leukemia: A phase I trial. *PLoS ONE*, *10*(6), 1–19. https://doi.org/10.1371/journal.pone.0123416

Kouidhi, S., Noman, M. Z., Kieda, C., Elgaaied, A. B., & Chouaib, S. (2016). Intrinsic and tumor microenvironment-induced metabolism adaptations of T cells and impact on their differentiation and function. *Frontiers in Immunology*, *7*(MAR). https://doi.org/10.3389/fimmu.2016.00114

Krzewski, K., & Coligan, J. E. (2012). *Human NK cell lytic granules and regulation of their exocytosis*. *3*(November), 1–16. https://doi.org/10.3389/fimmu.2012.00335

Kuett, A., Rieger, C., Perathoner, D., Herold, T., Wagner, M., Sironi, S., Sotlar, K., Horny, H. P., Deniffel, C., Drolle, H., & Fiegl, M. (2015). IL-8 as mediator in the microenvironment-leukaemia network in acute myeloid leukaemia. *Scientific Reports*, *5*(July), 1–11. https://doi.org/10.1038/srep18411

Lanier, L. L., Le, A. M., Phillips, J. H., Warner, N. L., & Babcock, G. F. (1983). Subpopulations of human natural killer cells defined by expression of the Leu-7 (HNK-1) and Leu-11 (NK-15) antigens. *Journal of Immunology (Baltimore, Md.: 1950)*, *131*(4), 1789–1796.

Lash, G. E., Schiessl, B., Kirkley, M., Innes, B. A., Cooper, A., Searle, R. F., Robson, S. C., & Bulmer, J. N. (2006). Expression of angiogenic growth

factors by uterine natural killer cells during early pregnancy. *Journal of Leukocyte Biology*, *80*(3), 572–580. https://doi.org/10.1189/jlb.0406250

Lau, C. M., Wiedemann, G. M., & Sun, J. C. (2022). Epigenetic regulation of natural killer cell memory. *Immunological Reviews*, *305*(1), 90–110. https://doi.org/10.1111/imr.13031

Le Priol, Y., Puthier, D., Lécureuil, C., Combadière, C., Debré, P., Nguyen, C., & Combadière, B. (2006). High cytotoxic and specific migratory potencies of senescent CD8+ CD57+ cells in HIV-infected and uninfected individuals. *Journal of Immunology (Baltimore, Md. : 1950)*, *177*(8), 5145–5154. https://doi.org/10.4049/jimmunol.177.8.5145

Lee, J., Walsh, M. C., Hoehn, K. L., James, D. E., Wherry, E. J., & Choi, Y. (2014). Regulator of Fatty Acid Metabolism, Acetyl Coenzyme A Carboxylase 1, Controls T Cell Immunity. *The Journal of Immunology*, *192*(7), 3190–3199. https://doi.org/10.4049/jimmunol.1302985

Lee, J., Zhang, T., Hwang, I., Kim, A., Nitschke, L., Kim, M. J., Scott, J. M., Kamimura, Y., Lanier, L. L., & Kim, S. (2015). Epigenetic modification and antibody-dependent expansion of memory-like NK cells in human cytomegalovirus-infected individuals. *Immunity*, *42*(3), 431–442. https://doi.org/10.1016/j.immuni.2015.02.013

Lee, K. M., Forman, J. P., McNerney, M. E., Stepp, S., Kuppireddi, S., Guzior, D., Latchman, Y. E., Sayegh, M. H., Yagita, H., Park, C. K., Seog, B. O., Wülfing, C., Schatzle, J., Mathew, P. A., Sharpe, A. H., & Kumar, V. (2006). Requirement of homotypic NK-cell interactions through 2B4(CD244)/CD48 in the generation of NK effector functions. *Blood*, *107*(8), 3181–3188. https://doi.org/10.1182/blood-2005-01-0185

Lee, S.-H., Fragoso, M. F., & Biron, C. A. (2012). Cutting Edge: A Novel Mechanism Bridging Innate and Adaptive Immunity: IL-12 Induction of CD25 To Form High-Affinity IL-2 Receptors on NK Cells. *The Journal of Immunology*, *189*(6), 2712–2716. https://doi.org/10.4049/jimmunol.1201528

Leong, J. W., Chase, J. M., Romee, R., Schneider, S. E., Sullivan, R. P., Cooper, M. A., & Fehniger, T. A. (2014). Preactivation with IL-12, IL-15, and IL-18 induces CD25 and a functional high-affinity IL-2 receptor on human cytokine-induced memory-like natural killer cells. *Biology of Blood and Marrow Transplantation : Journal of the American Society for Blood and Marrow Transplantation*, *20*(4), 463–473. https://doi.org/10.1016/j.bbmt.2014.01.006

Leung, C., Hodel, A. W., Brennan, A. J., Lukoyanova, N., Tran, S., House, C. M., Kondos, S. C., Whisstock, J. C., Dunstone, M. A., Trapani, J. A., Voskoboinik, I., Saibil, H. R., & Hoogenboom, B. W. (2017). Real-time

visualization of perforin nanopore assembly. *Nature Nanotechnology*, *12*(5), 467–473. https://doi.org/10.1038/nnano.2016.303

Liu, E., Tong, Y., Dotti, G., Shaim, H., Savoldo, B., Mukherjee, M., Orange, J., Wan, X., Lu, X., Reynolds, A., Gagea, M., Banerjee, P., Cai, R., Bdaiwi, M. H., Basar, R., Muftuoglu, M., Li, L., Marin, D., Wierda, W., … Rezvani, K. (2018). Cord blood NK cells engineered to express IL-15 and a CD19-targeted CAR show long-term persistence and potent antitumor activity. *Leukemia*, *32*(2), 520–531. https://doi.org/10.1038/leu.2017.226

Liu, L. L., Landskron, J., Ask, E. H., Trowsdale, J., Liu, L. L., Landskron, J., Ask, E. H., Enqvist, M., Sohlberg, E., & Traherne, J. A. (2016). *Critical Role of CD2 Co-stimulation in Adaptive Natural Killer Cell Responses Revealed in NKG2C- Article Critical Role of CD2 Co-stimulation in Adaptive Natural Killer Cell Responses Revealed in NKG2C-Deficient Humans*. 1088–1099. https://doi.org/10.1016/j.celrep.2016.04.005

Liu, Y., Beyer, A., & Aebersold, R. (2016). On the Dependency of Cellular Protein Levels on mRNA Abundance. *Cell*, *165*(3), 535–550. https://doi.org/https://doi.org/10.1016/j.cell.2016.03.014

Ljunggren, H.-G., & Kärre, K. (1990). In search of the 'missing self': MHC molecules and NK cell recognition. *Immunology Today*, *11*, 237–244. https://doi.org/10.1016/0167-5699(90)90097-S

Lo, D. J., Weaver, T. A., Stempora, L., Mehta, A. K., Ford, M. L., Larsen, C. P., & Kirk, A. D. (2011). Selective Targeting of Human Alloresponsive CD8+ Effector Memory T Cells Based on CD2 Expression. *American Journal of Transplantation*, *11*(1), 22–33. https://doi.org/10.1111/j.1600-6143.2010.03317.x

Lopes, M. R., Pereira, J. K. N., de Melo Campos, P., Machado-Neto, J. A., Traina, F., Saad, S. T. O., & Favaro, P. (2017). De novo AML exhibits greater microenvironment dysregulation compared to AML with myelodysplasia-related changes. *Scientific Reports*, *7*(1), 40707. https://doi.org/10.1038/srep40707

Lopez, J. A., Susanto, O., Jenkins, M. R., Lukoyanova, N., Sutton, V. R., Law, R. H. P., Johnston, A., Bird, C. H., Bird, P. I., Whisstock, J. C., Trapani, J. A., Saibil, H. R., & Voskoboinik, I. (2013). Perforin forms transient pores on the target cell plasma membrane to facilitate rapid access of granzymes during killer cell attack. *Blood*, *121*(14), 2659–2668. https://doi.org/10.1182/blood-2012-07-446146

Lopez-Vergès, S., Milush, J. M., Pandey, S., York, V. A., Arakawa-Hoyt, J., Pircher, H., Norris, P. J., Nixon, D. F., & Lanier, L. L. (2010). CD57 defines a functionally distinct population of mature NK cells in the

human CD56dimCD16+ NK-cell subset. *Blood*, *116*(19), 3865–3874. https://doi.org/10.1182/blood-2010-04-282301

Lopez-Vergès, S., Milush, J. M., Schwartz, B. S., Pando, M. J., Jarjoura, J., York, V. A., Houchins, J. P., Miller, S., Kang, S. M., Norris, P. J., Nixon, D. F., & Lanier, L. L. (2011a). Expansion of a unique CD57 +NKG2C hi natural killer cell subset during acute human cytomegalovirus infection. *Proceedings of the National Academy of Sciences of the United States of America*, *108*(36), 14725–14732. https://doi.org/10.1073/pnas.1110900108

Lopez-Vergès, S., Milush, J. M., Schwartz, B. S., Pando, M. J., Jarjoura, J., York, V. A., Houchins, J. P., Miller, S., Kang, S. M., Norris, P. J., Nixon, D. F., & Lanier, L. L. (2011b). Expansion of a unique CD57 +NKG2C hi natural killer cell subset during acute human cytomegalovirus infection. *Proceedings of the National Academy of Sciences of the United States of America*, *108*(36), 14725–14732. https://doi.org/10.1073/pnas.1110900108

Lorenzi, L., Tabellini, G., Vermi, W., Moratto, D., Porta, F., Notarangelo, L. D., Patrizi, O., Sozzani, S., de Saint Basile, G., Latour, S., Pace, D., Lonardi, S., Facchetti, F., Badolato, R., & Parolini, S. (2013). Occurrence of nodular lymphocyte-predominant hodgkin lymphoma in hermansky-pudlak type 2 syndrome is associated to natural killer and natural killer T cell defects. *PloS One*, *8*(11), e80131. https://doi.org/10.1371/journal.pone.0080131

Lowdell, M. W., Craston, R., Samuel, D., Wood, M. E., O'Neill, E., Saha, V., & Prentice, H. G. (2002). Evidence that continued remission in patients treated for acute leukaemia is dependent upon autologous natural killer cells. *British Journal of Haematology*, *117*(4), 821–827. https://doi.org/10.1046/j.1365-2141.2002.03495.x

Lucas, M., Schachterle, W., Oberle, K., Aichele, P., & Diefenbach, A. (2007). Dendritic Cells Prime Natural Killer Cells by trans-Presenting Interleukin 15. *Immunity*, *26*(4), 503–517. https://doi.org/10.1016/j.immuni.2007.03.006

Luetke-Eversloh, M., Hammer, Q., Durek, P., Nordström, K., Gasparoni, G., Pink, M., Hamann, A., Walter, J., Chang, H. D., Dong, J., & Romagnani, C. (2014). Human Cytomegalovirus Drives Epigenetic Imprinting of the IFNG Locus in NKG2Chi Natural Killer Cells. *PLoS Pathogens*, *10*(10). https://doi.org/10.1371/journal.ppat.1004441

Lupo, K. B., Moon, J.-I., Chambers, A. M., & Matosevic, S. (2021). Differentiation of natural killer cells from induced pluripotent stem cells under defined, serum- and feeder-free conditions. *Cytotherapy*, *23*(10), 939–952. https://doi.org/10.1016/j.jcyt.2021.05.001

Lv, M., Wang, K., & Huang, X. (2019). Myeloid-derived suppressor cells in hematological malignancies: friends or foes. *Journal of Hematology & Oncology*, *12*(1), 105. https://doi.org/10.1186/s13045-019-0797-3

Ma, S., Caligiuri, M. A., & Yu, J. (2022). Harnessing IL-15 signaling to potentiate NK cell-mediated cancer immunotherapy. *Trends in Immunology*, *43*(10), 833–847. https://doi.org/https://doi.org/10.1016/j.it.2022.08.004

Mace, E. M., Dongre, P., Hsu, H. T., Sinha, P., James, A. M., Mann, S. S., Forbes, L. R., Watkin, L. B., & Orange, J. S. (2014). Cell biological steps and checkpoints in accessing NK cell cytotoxicity. *Immunology and Cell Biology*, *92*(3), 245–255. https://doi.org/10.1038/icb.2013.96

Mace, E. M., Monkley, S. J., Critchley, D. R., & Takei, F. (2009). A Dual Role for Talin in NK Cell Cytotoxicity: Activation of LFA-1-Mediated Cell Adhesion and Polarization of NK Cells. *The Journal of Immunology*, *182*(2), 948 LP – 956. https://doi.org/10.4049/jimmunol.182.2.948

Mace, E. M., Zhang, J., Siminovitch, K. A., & Takei, F. (2010). Elucidation of the integrin LFA-1–mediated signaling pathway of actin polarization in natural killer cells. *Blood*, *116*(8), 1272–1279. https://doi.org/10.1182/blood-2009-12-261487

Mandal, R., Şenbabaoğlu, Y., Desrichard, A., Havel, J. J., Dalin, M. G., Riaz, N., Lee, K. W., Ganly, I., Hakimi, A. A., Chan, T. A., & Morris, L. G. T. (2016). The head and neck cancer immune landscape and its immunotherapeutic implications. *JCI Insight*, *1*(17), 1–18. https://doi.org/10.1172/jci.insight.89829

Marin, D., Li, Y., Basar, R., Rafei, H., Daher, M., Dou, J., Mohanty, V., Dede, M., Nieto, Y., Uprety, N., Acharya, S., Liu, E., Wilson, J., Banerjee, P., Macapinlac, H. A., Ganesh, C., Thall, P. F., Bassett, R., Ammari, M., … Rezvani, K. (2024). Safety, efficacy and determinants of response of allogeneic CD19-specific CAR-NK cells in CD19+ B cell tumors: a phase 1/2 trial. *Nature Medicine*, *9*. https://doi.org/10.1038/s41591-023-02785-8

Markasz, L., Stuber, G., Vanherberghen, B., Flaberg, E., Olah, E., Carbone, E., Eksborg, S., Klein, E., Skribek, H., & Szekely, L. (2007). Effect of frequently used chemotherapeutic drugs on the cytotoxic activity of human natural killer cells. *Molecular Cancer Therapeutics*, *6*(2), 644–654. https://doi.org/10.1158/1535-7163.MCT-06-0358

Martrus, G., Kautz, T., Lunemann, S., Richert, L., Glau, L., Salzberger, W., Goebels, H., Langeneckert, A., Hess, L., Poch, T., Schramm, C., Oldhafer, K. J., Koch, M., Tolosa, E., Nashan, B., & Altfeld, M. (2017). Proliferative capacity exhibited by human liver-resident CD49a+CD25+ NK cells. *PloS One*, *12*(8), e0182532. https://doi.org/10.1371/journal.pone.0182532

Masala, E., Valencia-Martinez, A., Pillozzi, S., Rondelli, T., Brogi, A., Sanna, A., Gozzini, A., Arcangeli, A., Sbarba, P. Dello, & Santini, V. (2018). Severe hypoxia selects hematopoietic progenitors with stem cell potential from primary Myelodysplastic syndrome bone marrow cell cultures. *Oncotarget*, *9*(12), 10561–10571. https://doi.org/10.18632/oncotarget.24302

Matson, BrookeC., & Caron, KathleenM. (2014). Uterine natural killer cells as modulators of the maternal-fetal vasculature. *The International Journal of Developmental Biology*, *58*(2-3–4), 199–204. https://doi.org/10.1387/ijdb.140032kc

McCann, F. E., Eissmann, P., Önfelt, B., Leung, R., & Davis, D. M. (2007). The Activating NKG2D Ligand MHC Class I-Related Chain A Transfers from Target Cells to NK Cells in a Manner That Allows Functional Consequences. *The Journal of Immunology*, *178*(6), 3418–3426. https://doi.org/10.4049/jimmunol.178.6.3418

Mellqvist, U. H., Brune, M., Dahlgren, C., & Hellstrand, K. (2000). Natural killer cell dysfunction and apoptosis induced by CML cells: Role of reactive oxygen species and regulation by histamine. *Blood*, *96*(11 PART I), 1961–1968.

Mentlik, A. N., Sanborn, K. B., Holzbaur, E. L., & Orange, J. S. (2010). Rapid lytic granule convergence to the MTOC in natural killer cells is dependent on dynein but not cytolytic commitment. *Molecular Biology of the Cell*, *21*(13), 2241–2256. https://doi.org/10.1091/mbc.e09-11-0930

Merino, A. M., Kim, H., Miller, J. S., & Cichocki, F. (2020). Unraveling exhaustion in adaptive and conventional NK cells. *Journal of Leukocyte Biology*, *108*(4), 1361–1368. https://doi.org/10.1002/JLB.4MR0620-091R

Merino, J., Martinez-Gonzalez, M. A., Rubio, M., Inoges, S., Sanchez-Ibarrola, A., & Subira, M. L. (1998). Progressive decrease of CD8high+ CD28+ CD57− cells with ageing. *Clinical & Experimental Immunology*, *112*(1), 48–51.

Meyaard, L., Adema, G. J., Chang, C., Woollatt, E., Sutherland, G. R., Lanier, L. L., & Phillips, J. H. (1997). LAIR-1, a novel inhibitory receptor expressed on human mononuclear leukocytes. *Immunity*, *7*(2), 283–290. https://doi.org/10.1016/s1074-7613(00)80530-0

Miller, J. S., & McCullar, V. (2001). Human natural killer cells with polyclonal lectin and immunoglobulinlike receptors develop from single hematopoietic stem cells with preferential expression of NKG2A and KIR2DL2/L3/S2. *Blood*, *98*(3), 705–713. https://doi.org/10.1182/blood.V98.3.705

Miller, J. S., Soignier, Y., Panoskaltsis-Mortari, A., McNearney, S. A., Yun, G. H., Fautsch, S. K., McKenna, D., Le, C., Defor, T. E., Burns, L. J., Orchard, P. J., Blazar, B. R., Wagner, J. E., Slungaard, A., Weisdorf, D. J., Okazaki, I. J., & McGlave, P. B. (2005). Successful adoptive transfer and in vivo expansion of human haploidentical NK cells in patients with cancer. *Blood*, *105*(8), 3051–3057. https://doi.org/10.1182/blood-2004-07-2974

Miller, J. S., Verfaillie, C., & McGlave, P. (1992). The generation of human natural killer cells from CD34+/DR- primitive progenitors in long-term bone marrow culture. *Blood*, *80*(9), 2182–2187.

Miller, J. S., Warlick, E. D., Wangen, R., Zorko, N., Hinderlie, P., Lewis, D., Vallera, D. A., & Felices, M. (2021). 965MO GTB-3550 tri-specific killer engager safely activates and delivers IL-15 to NK cells, but not T-cells, in immune suppressed patients with advanced myeloid malignancies, a novel paradigm exportable to solid tumors expressing Her2 or B7H3. *Annals of Oncology*, *32*, S834. https://doi.org/10.1016/j.annonc.2021.08.1350

Minami, Y., Kana, T., Miyazaki, T., & Taniguchi, T. (1993). THE IL-2 RECEPTOR COMPLEX: Its Structure, Function, and Target Genes. *Annual Review of Immunology*.

Mistry, A. R., & O'Callaghan, C. A. (2007). Regulation of ligands for the activating receptor NKG2D. *Immunology*, *121*(4), 439–447. https://doi.org/10.1111/j.1365-2567.2007.02652.x

Miyazaki, T., Dierich, A., Benoist, C., & Mathis, D. (1996). Independent Modes of Natural Killing Distinguished in Mice Lacking Lag3. *Science*, *272*(5260), 405–408. https://doi.org/10.1126/science.272.5260.405

Montes, P., Bernal, M., Campo, L. N., González-Ramírez, A. R., Jiménez, P., Garrido, P., Jurado, M., Garrido, F., Ruiz-Cabello, F., & Hernández, F. (2019). Tumor genetic alterations and features of the immune microenvironment drive myelodysplastic syndrome escape and progression. *Cancer Immunology, Immunotherapy*, *68*(12), 2015–2027. https://doi.org/10.1007/s00262-019-02420-x

Moretta, A. (2002). Natural killer cells and dendritic cells: rendezvous in abused tissues. *Nature Reviews Immunology*, *2*(12), 957–965. https://doi.org/10.1038/nri956

Moretta, A., Bottino, C., Vitale, M., Pende, D., Biassoni, R., Mingari, M. C., & Moretta, L. (1996). Receptors for HLA class-I molecules in human natural killer cells. *Annual Review of Immunology*, *14*, 619–648. https://doi.org/10.1146/annurev.immunol.14.1.619

Moretta, A., Sivori, S., Vitale, M., Pende, D., Morelli, L., Augugliaro, R., Bottino, C., & Moretta, L. (1995). Existence of both inhibitory (p58) and activatory (p50) receptors for HLA-C molecules in human natural killer cells. *The Journal of Experimental Medicine*, *182*(3), 875–884. https://doi.org/10.1084/jem.182.3.875

Morisot, N., Wadsworth, S., Davis, T., Dailey, N., Hansen, K., Gonzalez, D., Rahman, N., Aronov, A., Fan, Y., Guo, C., Buren, L., Vohra, A., Jamboretz, K., Leman, H., Lazetic, S., Chan, I., Trager, J., & Tan, J. (2020). 127 Preclinical evaluation of NKX019, a CD19-targeting CAR NK Cell. *Journal for ImmunoTherapy of Cancer*, *8*(Suppl 3), A78 LP-A78. https://doi.org/10.1136/jitc-2020-SITC2020.0127

Mortier, E., Advincula, R., Kim, L., Chmura, S., Barrera, J., Reizis, B., Malynn, B. A., & Ma, A. (2009). Macrophage- and Dendritic-Cell-Derived Interleukin-15 Receptor Alpha Supports Homeostasis of Distinct CD8+ T Cell Subsets. *Immunity*, *31*(5), 811–822. https://doi.org/https://doi.org/10.1016/j.immuni.2009.09.017

Mylonis, I., Simos, G., & Paraskeva, E. (2019). Hypoxia-inducible factors and the regulation of lipid metabolism. *Cells*, *8*(3), 1–16. https://doi.org/10.3390/cells8030214

Nachtkamp, K., Kündgen, A., Strupp, C., Giagounidis, A., Kobbe, G., Gattermann, N., Haas, R., & Germing, U. (2009). Impact on survival of different treatments for myelodysplastic syndromes (MDS). *Leukemia Research*, *33*(8), 1024–1028. https://doi.org/https://doi.org/10.1016/j.leukres.2008.12.019

Nagler, A., Lanier, L. L., Cwirla, S., & Phillips, J. H. (1989). Comparative studies of human FcRIII-positive and negative natural killer cells. *Journal of Immunology (Baltimore, Md.: 1950)*, *143*(10), 3183–3191.

Najima, Y., Yoshida, C., Iriyama, N., Fujisawa, S., Wakita, H., Chiba, S., Okamoto, S., Kawakami, K., Takezako, N., Kumagai, T., Ohyashiki, K., Taguchi, J., Yano, S., Igarashi, T., Kouzai, Y., Morita, S., Sakamoto, J., Sakamaki, H., & Inokuchi, K. (2018). Regulatory T cell inhibition by dasatinib is associated with natural killer cell differentiation and a favorable molecular response—The final results of the D-first study. *Leukemia Research*, *66*, 66–72. https://doi.org/10.1016/j.leukres.2018.01.010

Nakamura, K., Nakayama, M., Kawano, M., Amagai, R., Ishii, T., Harigae, H., & Ogasawara, K. (2013). Fratricide of natural killer cells dressed with tumor-derived NKG2D ligand. *Proceedings of the National Academy of Sciences of the United States of America*, *110*(23), 9421–9426. https://doi.org/10.1073/pnas.1300140110

Narni-Mancinelli, E., Vivier, E., & Kerdiles, Y. M. (2011). The ‘T-cell-ness’’ of NK cells: unexpected similarities between NK cells and T cells.’ *International Immunology*, *23*(7), 427–431. https://doi.org/10.1093/intimm/dxr035

Ni, J., Hölsken, O., Miller, M., Hammer, Q., Luetke-Eversloh, M., Romagnani, C., & Cerwenka, A. (2016). Adoptively transferred natural killer cells maintain long-term antitumor activity by epigenetic imprinting and CD4+ T cell help. *OncoImmunology*, *5*(9), 1–12. https://doi.org/10.1080/2162402X.2016.1219009

Nielsen, C. M., White, M. J., Goodier, M. R., & Riley, E. M. (2013). Functional significance of CD57 expression on human NK cells and relevance to disease. *Frontiers in Immunology*, *4*(DEC). https://doi.org/10.3389/FIMMU.2013.00422/ABSTRACT

North, J., Bakhsh, I., Marden, C., Pittman, H., Addison, E., Navarrete, C., Anderson, R., & Lowdell, M. W. (2007). Tumor-Primed Human Natural Killer Cells Lyse NK-Resistant Tumor Targets: Evidence of a Two-Stage Process in Resting NK Cell Activation. *The Journal of Immunology*, *178*(1), 85–94. https://doi.org/10.4049/jimmunol.178.1.85

O’Brien, K. L., & Finlay, D. K. (2019). Immunometabolism and natural killer cell responses. *Nature Reviews. Immunology*, *19*(5), 282–290. https://doi.org/10.1038/s41577-019-0139-2

Ochoa, M. C., Minute, L., Rodriguez, I., Garasa, S., Perez-Ruiz, E., Inogés, S., Melero, I., & Berraondo, P. (2017). Antibody-dependent cell cytotoxicity: immunotherapy strategies enhancing effector NK cells. *Immunology & Cell Biology*, *95*(4), 347–355. https://doi.org/https://doi.org/10.1038/icb.2017.6

O’Connor, G. M., Hart, O. M., & Gardiner, C. M. (2006). Putting the natural killer cell in its place. *Immunology*, *117*(1), 1–10. https://doi.org/10.1111/j.1365-2567.2005.02256.x

Oh, J. S., Ali, A. K., Kim, S., Corsi, D. J., Cooper, C. L., & Lee, S. H. (2016). NK cells lacking FcεRIγ are associated with reduced liver damage in chronic hepatitis C virus infection. *European Journal of Immunology*, *46*(4), 1020–1029. https://doi.org/10.1002/eji.201546009

O’Leary, J. G., Goodarzi, M., Drayton, D. L., & von Andrian, U. H. (2006). T cell- and B cell-independent adaptive immunity mediated by natural killer cells. *Nature Immunology*, *7*(5), 507–516. https://doi.org/10.1038/ni1332

Olofsson, P. E., Forslund, E., Vanherberghen, B., Chechet, K., Mickelin, O., Ahlin, A. R., Everhorn, T., & Önfelt, B. (2014). Distinct migration and contact dynamics of resting and IL-2-activated human natural killer cells.

Frontiers in Immunology, *5*(MAR), 1–10. https://doi.org/10.3389/fimmu.2014.00080

Olson, T. A., Mohanraj, D., Carson, L. F., & Ramakrishnan, S. (1994). Vascular permeability factor gene expression in normal and neoplastic human ovaries. *Cancer Research*, *54*(1), 276–280.

Orange, J. S. (2006). Human natural killer cell deficiencies. *Current Opinion in Allergy and Clinical Immunology*, *6*(6), 399–409.

Orange, J. S. (2013). Natural killer cell deficiency. *The Journal of Allergy and Clinical Immunology*, *132*(3), 515–525. https://doi.org/10.1016/j.jaci.2013.07.020

Orange, J. S., Harris, K. E., Andzelm, M. M., Valter, M. M., Geha, R. S., & Strominger, J. L. (2003). The mature activating natural killer cell immunologic synapse is formed in distinct stages. *Proceedings of the National Academy of Sciences of the United States of America*, *100*(SUPPL. 2), 14151–14156. https://doi.org/10.1073/pnas.1835830100

Ortaldo, J. R., Wiltrout, R. H., & Reynolds, C. W. (2014). Natural killer activity: early days, advances, and seminal observations. *Critical Reviews in Oncogenesis*, *19*(1–2), 1–13. https://doi.org/10.1615/critrevoncog.2014011125

O'Sullivan, D., van der Windt, G. J. W., Huang, S. C.-C., Curtis, J. D., Chang, C.-H., Buck, M. D., Qiu, J., Smith, A. M., Lam, W. Y., DiPlato, L. M., Hsu, F.-F., Birnbaum, M. J., Pearce, E. J., & Pearce, E. L. (2014). Memory CD8(+) T cells use cell-intrinsic lipolysis to support the metabolic programming necessary for development. *Immunity*, *41*(1), 75–88. https://doi.org/10.1016/j.immuni.2014.06.005

Pahl, J. H. W., Cerwenka, A., & Ni, J. (2018). Memory-Like NK cells: Remembering a previous activation by cytokines and NK cell receptors. *Frontiers in Immunology*, *9*(NOV), 1–9. https://doi.org/10.3389/fimmu.2018.02796

Pal, M., Schwab, L., Yermakova, A., Mace, E. M., Claus, R., Krahl, A. C., Woiterski, J., Hartwig, U. F., Orange, J. S., Handgretinger, R., & André, M. C. (2017). Tumor-priming converts NK cells to memory-like NK cells. *OncoImmunology*, *6*(6), 1–13. https://doi.org/10.1080/2162402X.2017.1317411

Palumbo, G. A., Parrinello, N. L., Giallongo, C., D'Amico, E., Zanghì, A., Puglisi, F., Conticello, C., Chiarenza, A., Tibullo, D., Raimondo, F. Di, & Romano, A. (2019). Monocytic Myeloid Derived Suppressor Cells in Hematological Malignancies. *International Journal of Molecular Sciences*, *20*(21), 5459. https://doi.org/10.3390/ijms20215459

Parker, R. A., & Berman, N. G. (2003). Sample Size. *The American Statistician*, *57*(3), 166–170. https://doi.org/10.1198/0003130031919

Paust, S., Senman, B., & Von Andrian, U. H. (2010). Adaptive immune responses mediated by natural killer cells. *Immunological Reviews*, *235*(1), 286–296. https://doi.org/10.1111/j.0105-2896.2010.00906.x

Peddie, C. M., Wolf, C. R., McLellan, L. I., Collins, A. R., & Bowen, D. T. (1997). Oxidative DNA damage in CD34+ myelodysplastic cells is associated with intracellular redox changes and elevated plasma tumour necrosis factor-alpha concentration. *British Journal of Haematology*, *99*(3), 625–631. https://doi.org/10.1046/j.1365-2141.1997.4373247.x

Penack, O., Gentilini, C., Fischer, L., Asemissen, A. M., Scheibenbogen, C., Thiel, E., & Uharek, L. (2005). CD56dimCD16neg cells are responsible for natural cytotoxicity against tumor targets. *Leukemia*, *19*(5), 835–840. https://doi.org/10.1038/sj.leu.2403704

Pennock, N. D., White, J. T., Cross, E. W., Cheney, E. E., Tamburini, B. A., & Kedl, R. M. (2013). T cell responses: Naïve to memory and everything in between. *American Journal of Physiology - Advances in Physiology Education*, *37*(4), 273–283. https://doi.org/10.1152/advan.00066.2013

Peppa, D., Pedroza-Pacheco, I., Pellegrino, P., Williams, I., Maini, M. K., & Borrow, P. (2018). Adaptive reconfiguration of natural killer cells in HIV-1 infection. *Frontiers in Immunology*, *9*(MAR), 1–13. https://doi.org/10.3389/fimmu.2018.00474

Peter, M. E., & Krammer, P. H. (2003). The CD95(APO-1/Fas) DISC and beyond. *Cell Death and Differentiation*, *10*(1), 26–35. https://doi.org/10.1038/sj.cdd.4401186

Picou, F., Vignon, C., Debeissat, C., Lachot, S., Kosmider, O., Gallay, N., Foucault, A., Estienne, M. H., Ravalet, N., Bene, M. C., Domenech, J., Gyan, E., Fontenay, M., & Herault, O. (2019). Bone marrow oxidative stress and specific antioxidant signatures in myelodysplastic syndromes. *Blood Advances*, *3*(24), 4271–4279. https://doi.org/10.1182/bloodadvances.2019000677

Pinton, P., Giorgi, C., Siviero, R., Zecchini, E., & Rizzuto, R. (2008). Calcium and apoptosis: ER-mitochondria Ca2+ transfer in the control of apoptosis. *Oncogene*, *27*(50), 6407–6418. https://doi.org/10.1038/onc.2008.308

Prager, I., Liesche, C., Ooijen, H. Van, Urlaub, D., Verron, Q., Sandstr, N., Fasbender, F., Claus, M., & Eils, R. (2019). *NK cells switch from granzyme B to death receptor – mediated cytotoxicity during serial killing*. *216*(9), 2113–2127.

Racanelli, V., & Rehermann, B. (2006). The Liver as an Immunological Organ. *Hepatology*, *43*. https://journals.lww.com/hep/fulltext/2006/02001/the_liver_as_an_immunological_organ.4.aspx

Raulet, D. H., Gasser, S., Gowen, B. G., Deng, W., & Jung, H. (2013). Regulation of ligands for the NKG2D activating receptor. *Annual Review of Immunology*, *31*, 413–441. https://doi.org/10.1146/annurev-immunol-032712-095951

Roe, K. (2022). NK-cell exhaustion, B-cell exhaustion and T-cell exhaustion—the differences and similarities. *Immunology*, *166*(2), 155–168. https://doi.org/10.1111/imm.13464

Romee, R., Foley, B., Lenvik, T., Wang, Y., Zhang, B., Ankarlo, D., Luo, X., Cooley, S., Verneris, M., Walcheck, B., & Miller, J. (2013). NK cell CD16 surface expression and function is regulated by a disintegrin and metalloprotease-17 (ADAM17). *Blood*, *121*(18), 3599–3608. https://doi.org/10.1182/blood-2012-04-425397

Romee, R., Rosario, M., Berrien-Elliott, M. M., Wagner, J. A., Jewell, B. A., Schappe, T., Leong, J. W., Abdel-Latif, S., Schneider, S. E., Willey, S., Neal, C. C., Yu, L., Oh, S. T., Lee, Y. S., Mulder, A., Claas, F., Cooper, M. A., & Fehniger, T. A. (2016). Cytokine-induced memory-like natural killer cells exhibit enhanced responses against myeloid leukemia. *Science Translational Medicine*, *8*(357), 357ra123. https://doi.org/10.1126/scitranslmed.aaf2341

Romee, R., Schneider, S. E., Leong, J. W., Chase, J. M., Keppel, C. R., Sullivan, R. P., Cooper, M. A., & Fehniger, T. A. (2012). Cytokine activation induces human memory-like NK cells. *Blood*, *120*(24), 4751–4760. https://doi.org/10.1182/blood-2012-04-419283

Rosenberg, S. A., Lotze, M. T., Muul, L. M., Chang, A. E., Avis, F. P., Leitman, S., Linehan, W. M., Robertson, C. N., Lee, R. E., & Rubin, J. T. (1987). A progress report on the treatment of 157 patients with advanced cancer using lymphokine-activated killer cells and interleukin-2 or high-dose interleukin-2 alone. *The New England Journal of Medicine*, *316*(15), 889–897. https://doi.org/10.1056/NEJM198704093161501

Rubnitz, J. E., Inaba, H., Ribeiro, R. C., Pounds, S., Rooney, B., Bell, T., Pui, C. H., & Leung, W. (2010). NKAML: A pilot study to determine the safety and feasibility of haploidentical natural killer cell transplantation in childhood acute myeloid leukemia. *Journal of Clinical Oncology*, *28*(6), 955–959. https://doi.org/10.1200/JCO.2009.24.4590

Rückert, T., Lareau, C. A., Mashreghi, M. F., Ludwig, L. S., & Romagnani, C. (2022). Clonal expansion and epigenetic inheritance of long-lasting NK

cell memory. *Nature Immunology*, *23*(11), 1551–1563. https://doi.org/10.1038/s41590-022-01327-7

Ruggeri, L., Capanni, M., Urbani, E., Perruccio, K., Shlomchik, W. D., Tosti, A., Posati, S., Rogaia, D., Frassoni, F., Aversa, F., Martelli, M. F., & Velardi, A. (2002). Effectiveness of Donor Natural Killer Cell Alloreactivity in Mismatched Hematopoietic Transplants. *Science*, *295*(5562), 2097–2100. https://doi.org/10.1126/science.1068440

Sabry, M., & Lowdell, M. W. (2013). Tumor-primed NK cells: Waiting for the green light. *Frontiers in Immunology*, *4*(NOV), 1–7. https://doi.org/10.3389/fimmu.2013.00408

Sabry, M., & Lowdell, M. W. (2020). Killers at the crossroads: The use of innate immune cells in adoptive cellular therapy of cancer. *Stem Cells Translational Medicine*, *9*(9), 974–984. https://doi.org/10.1002/sctm.19-0423

Sabry, M., Tsirogianni, M., Bakhsh, I. A., North, J., Sivakumaran, J., Giannopoulos, K., Anderson, R., Mackinnon, S., & Lowdell, M. W. (2011). Leukemic Priming of Resting NK Cells Is Killer Ig-like Receptor Independent but Requires CD15-Mediated CD2 Ligation and Natural Cytotoxicity Receptors. *The Journal of Immunology*, *187*(12), 6227–6234. https://doi.org/10.4049/jimmunol.1101640

Sabry, M., Zubiak, A., Hood, S. P., Simmonds, P., Arellano-Ballestero, H., Cournoyer, E., Mashar, M., Pockley, A. G., & Lowdell, M. W. (2019). Tumor- and cytokine-primed human natural killer cells exhibit distinct phenotypic and transcriptional signatures. *PloS One*, *14*(6), e0218674. https://doi.org/10.1371/journal.pone.0218674

Salcedo, T. W., Azzoni, L., Wolf, S. F., & Perussia, B. (1993). Modulation of perforin and granzyme messenger RNA expression in human natural killer cells. *Journal of Immunology (Baltimore, Md. : 1950)*, *151*(5), 2511–2520.

Sarhan, D., Brandt, L., Felices, M., Guldevall, K., Lenvik, T., Hinderlie, P., Curtsinger, J., Warlick, E., Spellman, S. R., Blazar, B. R., Weisdorf, D. J., Cooley, S., Vallera, D. A., Onfelt, B., & Miller, J. S. (2018). 161533 TriKE stimulates NK-cell function to overcome myeloid-derived suppressor cells in MDS. *Blood Advances*, *2*(12), 1459–1469. https://doi.org/10.1182/bloodadvances.2017012369

Schall, T. J., Bacon, K., Camp, R. D. R., Kaspari, J. W., & Goeddel, D. V. (1993). Human macrophage inflammatory protein α (MIP-1α) and MIP-1β chemokines attract distinct populations of lymphocytes. *Journal of Experimental Medicine*, *177*(6), 1821–1826.

Schimmer, S., Mittermüller, D., Werner, T., Görs, P. E., Meckelmann, S. W., Finlay, D. K., Dittmer, U., & Littwitz-Salomon, E. (2023). Fatty acids are crucial to fuel NK cells upon acute retrovirus infection. *Frontiers in Immunology*, *14*(November), 1–14. https://doi.org/10.3389/fimmu.2023.1296355

Schinke, C., Giricz, O., Li, W., Shastri, A., Gordon, S., Barreyro, L., Bhagat, T., Bhattacharyya, S., Ramachandra, N., Bartenstein, M., Pellagatti, A., Boultwood, J., Wickrema, A., Yu, Y., Will, B., Wei, S., Steidl, U., & Verma, A. (2015). IL8-CXCR2 pathway inhibition as a therapeutic strategy against MDS and AML stem cells. *Blood*, *125*(20), 3144–3152. https://doi.org/10.1182/blood-2015-01-621631

Schlums, H., Cichocki, F., Tesi, B., Theorell, J., Beziat, V., Holmes, T. D., Han, H., Chiang, S. C. C., Foley, B., Mattsson, K., Larsson, S., Schaffer, M., Malmberg, K. J., Ljunggren, H. G., Miller, J. S., & Bryceson, Y. T. (2015). Cytomegalovirus infection drives adaptive epigenetic diversification of NK cells with altered signaling and effector function. *Immunity*, *42*(3), 443–456. https://doi.org/10.1016/j.immuni.2015.02.008

Schönberg, K., Sribar, M., Enczmann, J., Fischer, J. C., & Uhrberg, M. (2011). Analyses of HLA-C-specific KIR repertoires in donors with group a and B haplotypes suggest a ligand-instructed model of NK cell receptor acquisition. *Blood*, *117*(1), 98–107. https://doi.org/10.1182/blood-2010-03-273656

Schweier, O., Hofmann, M., & Pircher, H. (2014). KLRG1 activity is regulated by association with the transferrin receptor. *European Journal of Immunology*, *44*(6), 1851–1856. https://doi.org/10.1002/eji.201344234

Scoville, S. D., Freud, A. G., & Caligiuri, M. A. (2017). Modeling human natural killer cell development in the era of innate lymphoid cells. *Frontiers in Immunology*, *8*(MAR), 4–11. https://doi.org/10.3389/fimmu.2017.00360

Selvaraj, P., Plunkett, M. L., Dustin, M., Sanders, M. E., Shaw, S., & Springer, T. A. (1987). The T lymphocyte glycoprotein CD2 binds the cell surface ligand LFA-3. *Nature*, *326*(6111), 400–403. https://doi.org/10.1038/326400a0

Shannon, M. J., & Mace, E. M. (2021). Natural Killer Cell Integrins and Their Functions in Tissue Residency . In *Frontiers in Immunology* (Vol. 12). https://www.frontiersin.org/article/10.3389/fimmu.2021.647358

Shapiro, R. M., Birch, G. C., Hu, G., Vergara Cadavid, J., Nikiforow, S., Baginska, J., Ali, A. K., Tarannum, M., Sheffer, M., Abdulhamid, Y. Z., Rambaldi, B., Arihara, Y., Reynolds, C., Halpern, M. S., Rodig, S. J., Cullen, N., Wolff, J. O., Pfaff, K. L., Lane, A. A., … Romee, R. (2022). Expansion, persistence, and efficacy of donor memory-like NK cells

infused for posttransplant relapse. *The Journal of Clinical Investigation*, *132*(11). https://doi.org/10.1172/JCI154334

Sheppard, S., Srpan, K., Lin, W., Lee, M., Delconte, R. B., Owyong, M., Carmeliet, P., Davis, D. M., Xavier, J. B., Hsu, K. C., & Sun, J. C. (2024). Fatty acid oxidation fuels natural killer cell responses against infection and cancer. *Proceedings of the National Academy of Sciences*, *121*(11), 2017. https://doi.org/10.1073/pnas.2319254121

Sheppard, S., & Sun, J. C. (2021). Virus-specific NK cell memory. *Journal of Experimental Medicine*, *218*(4), 1–10. https://doi.org/10.1084/jem.20201731

Shibuya, A., Campbell, D., Hannum, C., Yssel, H., Franz-Bacon, K., McClanahan, T., Kitamura, T., Nicholl, J., Sutherland, G. R., Lanier, L. L., & Phillips, J. H. (1996). DNAM-1, a novel adhesion molecule involved in the cytolytic function of T lymphocytes. *Immunity*, *4*(6), 573–581. https://doi.org/10.1016/s1074-7613(00)70060-4

Sinha, C., Seth, A., Kahali, B., & Cunningham, L. (2017). Development and Evaluation of NK-CD123 CAR Against High Risk Acute Myeloid Leukemia. *Biology of Blood and Marrow Transplantation*, *23*(3), S253. https://doi.org/10.1016/j.bbmt.2016.12.423

Sivori, S., Della Chiesa, M., Carlomagno, S., Quatrini, L., Munari, E., Vacca, P., Tumino, N., Mariotti, F. R., Mingari, M. C., Pende, D., & Moretta, L. (2020). Inhibitory Receptors and Checkpoints in Human NK Cells, Implications for the Immunotherapy of Cancer. *Frontiers in Immunology*, *11*(September), 1–10. https://doi.org/10.3389/fimmu.2020.02156

Sivori, S., Parolini, S., Falco, M., Marcenaro, E., Biassoni, R., Bottino, C., Moretta, L., & Moretta, A. (2000). 2B4 functions as a co-receptor in human NK cell activation. *European Journal of Immunology*, *30*(3), 787–793. https://doi.org/10.1002/1521-4141(200003)30:3<787::AID-IMMU787>3.0.CO;2-I

Sivori, S., Vacca, P., Del Zotto, G., Munari, E., Mingari, M. C., & Moretta, L. (2019). Human NK cells: surface receptors, inhibitory checkpoints, and translational applications. *Cellular and Molecular Immunology*, *16*(5), 430–441. https://doi.org/10.1038/s41423-019-0206-4

Spanholtz, J., Tordoir, M., Eissens, D., Preijers, F., van der Meer, A., Joosten, I., Schaap, N., de Witte, T. M., & Dolstra, H. (2010). High log-scale expansion of functional human natural killer cells from umbilical cord blood CD34-positive cells for adoptive cancer immunotherapy. *PloS One*, *5*(2), e9221. https://doi.org/10.1371/journal.pone.0009221

Spinner, M. A., Sanchez, L. A., Hsu, A. P., Shaw, P. A., Zerbe, C. S., Calvo, K. R., Arthur, D. C., Gu, W., Gould, C. M., Brewer, C. C., Cowen, E. W., Freeman, A. F., Olivier, K. N., Uzel, G., Zelazny, A. M., Daub, J. R., Spalding, C. D., Claypool, R. J., Giri, N. K., … Holland, S. M. (2014). GATA2 deficiency: a protean disorder of hematopoiesis, lymphatics, and immunity. *Blood*, *123*(6), 809–821. https://doi.org/10.1182/blood-2013-07-515528

Spits, H., Artis, D., Colonna, M., Diefenbach, A., di Santo, J. P., Eberl, G., Koyasu, S., Locksley, R. M., McKenzie, A. N. J., Mebius, R. E., Powrie, F., & Vivier, E. (2013). Innate lymphoid cells--a proposal for uniform nomenclature. *Nature Reviews. Immunology*, *13*(2), 145–149. https://doi.org/10.1038/nri3365

Srpan, K., Ambrose, A., Karampatzakis, A., Saeed, M., Cartwright, A. N. R., Guldevall, K., De Matos, G. D. S. C., Önfelt, B., & Davis, D. M. (2018). Shedding of CD16 disassembles the NK cell immune synapse and boosts serial engagement of target cells. *Journal of Cell Biology*, *217*(9), 3267–3283. https://doi.org/10.1083/jcb.201712085

Storey, J. D., & Tibshirani, R. (2003). Statistical significance for genomewide studies. *Proceedings of the National Academy of Sciences of the United States of America*, *100*(16), 9440–9445. https://doi.org/10.1073/pnas.1530509100

Storkus, W. J., Alexander, J., Payne, J. A., Dawson, J. R., & Cresswell, P. (1989). Reversal of natural killing susceptibility in target cells expressing transfected class I HLA genes. *Proceedings of the National Academy of Sciences*, *86*(7), 2361–2364. https://doi.org/10.1073/pnas.86.7.2361

Sun, J. C., Beilke, J. N., & Lanier, L. L. (2009). Adaptive immune features of natural killer cells. *Nature*, *457*(7229), 557–561. https://doi.org/10.1038/nature07665

Sun, J. C., & Lanier, L. L. (2011). NK cell development, homeostasis and function: parallels with $CD8^+$ T cells. *Nature Reviews. Immunology*, *11*(10), 645–657. https://doi.org/10.1038/nri3044

Sun, L., He, C., Nair, L., Yeung, J., & Egwuagu, C. E. (2015). Cytokine Interleukin 12 (IL-12) family cytokines : Role in immune pathogenesis and treatment of CNS autoimmune disease. *Cytokine*, *75*(2), 249–255. https://doi.org/10.1016/j.cyto.2015.01.030

Surace, L., Doisne, J. M., Escoll, P., Marie, S., Dardalhon, V., Croft, C., Thaller, A., Topazio, D., Sparaneo, A., Cama, A., Musumeci, O., d'Ecclesia, A., Buchrieser, C., Taylor, N., & Di Santo, J. P. (2021). Polarized mitochondria as guardians of NK cell fitness. *Blood Advances*, *5*(1), 26–38. https://doi.org/10.1182/bloodadvances.2020003458

Sutton, V. R., Davis, J. E., Cancilla, M., Johnstone, R. W., Ruefli, A. A., Sedelies, K., Browne, K. A., & Trapani, J. A. (2000). Initiation of apoptosis by granzyme B requires direct cleavage of bid, but not direct granzyme B-mediated caspase activation. *The Journal of Experimental Medicine*, *192*(10), 1403–1414. https://doi.org/10.1084/jem.192.10.1403

Szczepanski, M. J., Szajnik, M., Czystowska, M., Mandapathil, M., Strauss, L., Welsh, A., Foon, K. A., Whiteside, T. L., & Boyiadzis, M. (2009). Increased frequency and suppression by regulatory T cells in patients with acute myelogenous leukemia. *Clinical Cancer Research : An Official Journal of the American Association for Cancer Research*, *15*(10), 3325–3332. https://doi.org/10.1158/1078-0432.CCR-08-3010

Sze, D. M., Giesajtis, G., Brown, R. D., Raitakari, M., Gibson, J., Ho, J., Baxter, A. G., Fazekas de St Groth, B., Basten, A., & Joshua, D. E. (2001). Clonal cytotoxic T cells are expanded in myeloma and reside in the CD8(+)CD57(+)CD28(-) compartment. *Blood*, *98*(9), 2817–2827. https://doi.org/10.1182/blood.v98.9.2817

Szmania, S., Lapteva, N., Garg, T., Greenway, A., Lingo, J., Nair, B., Stone, K., Woods, E., Khan, J., Stivers, J., Panozzo, S., Campana, D., Bellamy, W. T., Robbins, M., Epstein, J., Yaccoby, S., Waheed, S., Gee, A., Cottler-Fox, M., … van Rhee, F. (2015). Ex vivo-expanded natural killer cells demonstrate robust proliferation in vivo in high-risk relapsed multiple myeloma patients. *Journal of Immunotherapy (Hagerstown, Md. : 1997)*, *38*(1), 24–36. https://doi.org/10.1097/CJI.0000000000000059

Tang, X., Yang, L., Li, Z., Nalin, A. P., Dai, H., Xu, T., Yin, J., You, F., Zhu, M., Shen, W., Chen, G., Zhu, X., Wu, D., & Yu, J. (2018). First-in-man clinical trial of CAR NK-92 cells: safety test of CD33-CAR NK-92 cells in patients with relapsed and refractory acute myeloid leukemia. *American Journal of Cancer Research*, *8*(9), 1899. http://www.ncbi.nlm.nih.gov/pubmed/30323981%0Ahttp://www.pubmedcentral.nih.gov/articlerender.fcgi?artid=PMC6176185

Terme, M., Tartour, E., & Taieb, J. (2013). VEGFA/VEGFR2-targeted therapies prevent the VEGFA-induced proliferation of regulatory T cells in cancer. *Oncoimmunology*, *2*(8), e25156. https://doi.org/10.4161/onci.25156

Terrén, I., Orrantia, A., Astarloa-Pando, G., Amarilla-Irusta, A., Zenarruzabeitia, O., & Borrego, F. (2022). Cytokine-Induced Memory-Like NK Cells: From the Basics to Clinical Applications. *Frontiers in Immunology*, *13*(May), 1–8. https://doi.org/10.3389/fimmu.2022.884648

Terrén, I., Orrantia, A., Mosteiro, A., Vitallé, J., Zenarruzabeitia, O., & Borrego, F. (2021). Metabolic changes of Interleukin-12/15/18-stimulated human

NK cells. *Scientific Reports*, *11*(1), 1–15. https://doi.org/10.1038/s41598-021-85960-6

Thiery, J., Keefe, D., Boulant, S., Boucrot, E., Walch, M., Martinvalet, D., Goping, I. S., Bleackley, R. C., Kirchhausen, T., & Lieberman, J. (2011). Perforin pores in the endosomal membrane trigger the release of endocytosed granzyme B into the cytosol of target cells. *Nature Immunology*, *12*(8), 770–777. https://doi.org/10.1038/ni.2050

Tian, Z., & Wei, H. (2017). *Developmental and Functional Control of Natural Killer Cells by Cytokines*. *8*(August). https://doi.org/10.3389/fimmu.2017.00930

Tilden, A. B., Grossi, C. E., Itoh, K., Cloud, G. A., Dougherty, P. A., & Balch, C. M. (1986). Subpopulation analysis of human granular lymphocytes: associations with age, gender and cytotoxic activity. *Natural Immunity and Cell Growth Regulation*, *5*(2), 90–99.

Tong, L., Jiménez-Cortegana, C., Tay, A. H. M., Wickström, S., Galluzzi, L., & Lundqvist, A. (2022). NK cells and solid tumors: therapeutic potential and persisting obstacles. *Molecular Cancer*, *21*(1), 1–18. https://doi.org/10.1186/s12943-022-01672-z

Torres, N., Regge, M. V., Secchiari, F., Friedrich, A. D., Spallanzani, R. G., Raffo Iraolagoitia, X. L., Núñez, S. Y., Sierra, J. M., Ziblat, A., Santilli, M. C., Gilio, N., Almada, E., Lauche, C., Pardo, R., Domaica, C. I., Fuertes, M. B., Madauss, K. P., Hance, K. W., Gloger, I. S., … Zwirner, N. W. (2020). Restoration of antitumor immunity through anti-MICA antibodies elicited with a chimeric protein. *Journal for Immunotherapy of Cancer*, *8*(1). https://doi.org/10.1136/jitc-2019-000233

Tsirogianni, M., Grigoriou, E., Kapsimalli, V., Dagla, K., Stamouli, M., Gkirkas, K., Konsta, E., Karagiannidou, A., Gkodopoulos, K., Stavroulaki, G., Pappa, V., Angelopoulou, M., Lowdell, M., & Tsirigotis, P. (2019). Natural killer cell cytotoxicity is a predictor of outcome for patients with high risk myelodysplastic syndrome and oligoblastic acute myeloid leukemia treated with azacytidine. *Leukemia and Lymphoma*, *60*(10), 2457–2463. https://doi.org/10.1080/10428194.2019.1581935

Valés-Gómez, M., Reyburn, H. T., Erskine, R. A., López-Botet, M., & Strominger, J. L. (1999). Kinetics and peptide dependency of the binding of the inhibitory NK receptor CD94/NKG2-A and the activating receptor CD94/NKG2-C to HLA-E. *The EMBO Journal*, *18*(15), 4250–4260. https://doi.org/10.1093/emboj/18.15.4250

van den Bosch, G., Preijers, F., Vreugdenhil, A., Hendriks, J., Maas, F., & De Witte, T. (1995). Granulocyte-macrophage colony-stimulating factor (GM-CSF) counteracts the inhibiting effect of monocytes on natural killer (NK)

cells. *Clinical and Experimental Immunology*, *101*(3), 515–520. https://doi.org/10.1111/j.1365-2249.1995.tb03143.x

Van der Maaten, L., & Hinton, G. (2008). Visualizing data using t-SNE. *Journal of Machine Learning Research*, *9*(11).

van der Windt, G. J. W., Everts, B., Chang, C.-H., Curtis, J. D., Freitas, T. C., Amiel, E., Pearce, E. J., & Pearce, E. L. (2012). Mitochondrial Respiratory Capacity Is a Critical Regulator of CD8+ T Cell Memory Development. *Immunity*, *36*(1), 68–78. https://doi.org/https://doi.org/10.1016/j.immuni.2011.12.007

van der Windt, G. J. W., O'Sullivan, D., Everts, B., Huang, S. C.-C., Buck, M. D., Curtis, J. D., Chang, C.-H., Smith, A. M., Ai, T., Faubert, B., Jones, R. G., Pearce, E. J., & Pearce, E. L. (2013). CD8 memory T cells have a bioenergetic advantage that underlies their rapid recall ability. *Proceedings of the National Academy of Sciences*, *110*(35), 14336–14341. https://doi.org/10.1073/pnas.1221740110

Vanherberghen, B., Olofsson, P. E., Forslund, E., Sternberg-Simon, M., Khorshidi, M. A., Pacouret, S., Guldevall, K., Enqvist, M., Malmberg, K. J., Mehr, R., & Önfelt, B. (2013). Classification of human natural killer cells based on migration behavior and cytotoxic response. *Blood*, *121*(8), 1326–1334. https://doi.org/10.1182/blood-2012-06-439851

Vasu, S., Bhatnagar, B., Blachly, J. S., Szuminski, N., O'Donnell, L., & Lee, D. A. (2020). A Phase I Clinical Trial Testing the Safety of IL-21-Expanded, Off-the-Shelf, Third-Party Natural Killer Cells for Relapsed/Refractory Acute Myeloid Leukemia and Myelodysplastic Syndrome. *Blood*, *136*(Supplement 1), 44–44. https://doi.org/10.1182/blood-2020-139170

Vela, M., Corral, D., Carrasco, P., Fernández, L., Valentín, J., González, B., Escudero, A., Balas, A., de Paz, R., Torres, J., Leivas, A., Martinez-Lopez, J., & Pérez-Martínez, A. (2018). Haploidentical IL-15/41BBL activated and expanded natural killer cell infusion therapy after salvage chemotherapy in children with relapsed and refractory leukemia. *Cancer Letters*, *422*, 107–117. https://doi.org/https://doi.org/10.1016/j.canlet.2018.02.033

Verron, Q., Forslund, E., Brandt, L., Leino, M., Frisk, T. W., Olofsson, P. E., & Önfelt, B. (2021). NK cells integrate signals over large areas when building immune synapses but require local stimuli for degranulation. *Science Signaling*, *14*(684). https://doi.org/10.1126/scisignal.abe2740

Vetter, C. S., Lieb, W., Bröcker, E.-B., & Becker, J. C. (2004). Loss of nonclassical MHC molecules MIC-A/B expression during progression of uveal melanoma. *British Journal of Cancer*, *91*(8), 1495–1499. https://doi.org/10.1038/sj.bjc.6602123

Vey, N., Bourhis, J.-H., Boissel, N., Bordessoule, D., Prebet, T., Charbonnier, A., Etienne, A., Andre, P., Romagne, F., Benson, D., Dombret, H., & Olive, D. (2012). A phase 1 trial of the anti-inhibitory KIR mAb IPH2101 for AML in complete remission. *Blood*, *120*(22), 4317–4323. https://doi.org/10.1182/blood-2012-06-437558

Vey, N., Dumas, P.-Y., Recher, C., Gastaud, L., Lioure, B., Bulabois, C.-E., Pautas, C., Marolleau, J.-P., Lepretre, S., Raffoux, E., Thomas, X., Hicheri, Y., Bonmati, C., Quesnel, B., Rousselot, P., Castaigne, S., Jourdan, E., Malfuson, J., Guillerm, G., & Dombret, H. (2017). Randomized Phase 2 Trial of Lirilumab (anti-KIR monoclonal antibody, mAb) As Maintenance Treatment in Elderly Patients (pts) with Acute Myeloid Leukemia (AML): Results of the Effikir Trial. *Blood*, *130*, 889. https://doi.org/10.1182/blood.V130.Suppl_1.889.889

Viel, S., Marçais, A., Guimaraes, F. S. F., Loftus, R., Rabilloud, J., Grau, M., Degouve, S., Djebali, S., Sanlaville, A., Charrier, E., Bienvenu, J., Marie, J. C., Caux, C., Marvel, J., Town, L., Huntington, N. D., Bartholin, L., Finlay, D., Smyth, M. J., & Walzer, T. (2016). TGF-β inhibits the activation and functions of NK cells by repressing the mTOR pathway. *Science Signaling*, *9*(415), 1–14. https://doi.org/10.1126/scisignal.aad1884

Villegas, F. R., Coca, S., Villarrubia, V. G., Jiménez, R., Chillón, M. J., Jareño, J., Zuil, M., & Callol, L. (2002). Prognostic significance of tumor infiltrating natural killer cells subset CD57 in patients with squamous cell lung cancer. *Lung Cancer (Amsterdam, Netherlands)*, *35*(1), 23–28. https://doi.org/10.1016/s0169-5002(01)00292-6

Vitale, M., Falco, M., Castriconi, R., Parolini, S., Zambello, R., Semenzato, G., Biassoni, R., Bottino, C., Moretta, L., & Moretta, A. (2001). Identification of NKp80, a novel triggering molecule expressed by human NK cells. *European Journal of Immunology*, *31*(1), 233–242. https://doi.org/10.1002/1521-4141(200101)31:1<233::AID-IMMU233>3.0.CO;2-4

von Karstedt, S., Montinaro, A., & Walczak, H. (2017). Exploring the TRAILs less travelled: TRAIL in cancer biology and therapy. *Nature Reviews. Cancer*, *17*(6), 352–366. https://doi.org/10.1038/nrc.2017.28

Wagtmann, N., Biassoni, R., Cantoni, C., Verdiani, S., Malnati, M. S., Vitale, M., Bottino, C., Moretta, L., Moretta, A., & Long, E. O. (1995). Molecular clones of the p58 NK cell receptor reveal immunoglobulin-related molecules with diversity in both the extra- and intracellular domains. *Immunity*, *2*(5), 439–449. https://doi.org/10.1016/1074-7613(95)90025-x

Waldhauer, I., & Steinle, A. (2008). NK cells and cancer immunosurveillance. *Oncogene*, *27*(45), 5932–5943. https://doi.org/10.1038/onc.2008.267

Wang, Z., Guan, D., Wang, S., Chai, L. Y. A., Xu, S., & Lam, K.-P. (2020). Glycolysis and Oxidative Phosphorylation Play Critical Roles in Natural Killer Cell Receptor-Mediated Natural Killer Cell Functions. *Frontiers in Immunology*, *11*, 202. https://doi.org/10.3389/fimmu.2020.00202

Warren, H. S., Altin, J. G., Waldron, J. C., Kinnear, B. F., & Parish, C. R. (1996). A carbohydrate structure associated with CD15 (Lewis x) on myeloid cells is a novel ligand for human CD2. *Journal of Immunology (Baltimore, Md. : 1950)*, *156*(8), 2866–2873.

Wee, H., Oh, H.-M., Jo, J.-H., & Jun, C.-D. (2009). ICAM-1/LFA-1 interaction contributes to the induction of endothelial cell-cell separation: implication for enhanced leukocyte diapedesis. *Experimental & Molecular Medicine*, *41*(5), 341–348. https://doi.org/10.3858/emm.2009.41.5.038

Wherry, E. J. (2011). T cell exhaustion. *Nature Immunology*, *12*(6), 492–499. https://doi.org/10.1038/ni.2035

Wiley, S. R., Schooley, K., Smolak, P. J., Din, W. S., Huang, C.-P., Nicholl, J. K., Sutherland, G. R., Smith, T. D., Rauch, C., Smith, C. A., & Goodwin, R. G. (1995). Identification and characterization of a new member of the TNF family that induces apoptosis. *Immunity*, *3*(6), 673–682. https://doi.org/https://doi.org/10.1016/1074-7613(95)90057-8

Wülfing, C., Purtic, B., Klem, J., & Schatzle, J. D. (2003). Stepwise cytoskeletal polarization as a series of checkpoints in innate but not adaptive cytolytic killing. *Proceedings of the National Academy of Sciences of the United States of America*, *100*(13), 7767–7772. https://doi.org/10.1073/pnas.1336920100

Xiao, Z., Wang, R., Wang, X., Yang, H., Dong, J., He, X., Yang, Y., Guo, J., Cui, J., & Zhou, Z. (2023). Impaired function of dendritic cells within the tumor microenvironment. *Frontiers in Immunology*, *14*(June), 1–13. https://doi.org/10.3389/fimmu.2023.1213629

Xu, K., & Hansen, E. (2021). Novel agents for myelodysplastic syndromes. *Journal of Oncology Pharmacy Practice*, *27*(8), 1982–1992. https://doi.org/10.1177/10781552211037993

Yang, C., Siebert, J. R., Burns, R., Gerbec, Z. J., Bonacci, B., Rymaszewski, A., Rau, M., Riese, M. J., Rao, S., Carlson, K. S., Routes, J. M., Verbsky, J. W., Thakar, M. S., & Malarkannan, S. (2019). Heterogeneity of human bone marrow and blood natural killer cells defined by single-cell transcriptome. *Nature Communications*, *10*(1). https://doi.org/10.1038/s41467-019-11947-7

Yang, Y., & Lundqvist, A. (2020). Immunomodulatory E ff ects of IL-2 and IL-15; Implications for Cancer Immunotherapy. *Cancers*, *2*, 1–20. https://doi.org/10.3390/cancers12123586

Young, A., Ngiow, S. F., Gao, Y., Patch, A.-M., Barkauskas, D. S., Messaoudene, M., Lin, G., Coudert, J. D., Stannard, K. A., Zitvogel, L., Degli-Esposti, M. A., Vivier, E., Waddell, N., Linden, J., Huntington, N. D., Souza-Fonseca-Guimaraes, F., & Smyth, M. J. (2018). A2AR Adenosine Signaling Suppresses Natural Killer Cell Maturation in the Tumor Microenvironment. *Cancer Research*, *78*(4), 1003–1016. https://doi.org/10.1158/0008-5472.CAN-17-2826

Yu, H., Fehniger, T. A., Fuchshuber, P., Thiel, K. S., Vivier, E., Carson, W. E., & Caligiuri, M. A. (1998). Flt3 ligand promotes the generation of a distinct CD34(+) human natural killer cell progenitor that responds to interleukin-15. *Blood*, *92*(10), 3647–3657.

Yu, J., Freud, A. G., & Caligiuri, M. A. (2013). Location and cellular stages of natural killer cell development. *Trends in Immunology*, *34*(12), 573–582. https://doi.org/10.1016/j.it.2013.07.005

Zeng, W., Miyazato, A., Chen, G., Kajigaya, S., Young, N. S., & Maciejewski, J. P. (2006). Interferon-gamma-induced gene expression in CD34 cells: identification of pathologic cytokine-specific signature profiles. *Blood*, *107*(1), 167–175. https://doi.org/10.1182/blood-2005-05-1884

Zhang, L., Meng, Y., Feng, X., & Han, Z. (2022). CAR-NK cells for cancer immunotherapy: from bench to bedside. *Biomarker Research*, *10*(1), 1–19. https://doi.org/10.1186/s40364-022-00364-6

Zhang, Q., Bi, J., Zheng, X., Chen, Y., Wang, H., Wu, W., Wang, Z., Wu, Q., Peng, H., Wei, H., Sun, R., & Tian, Z. (2018). Blockade of the checkpoint receptor TIGIT prevents NK cell exhaustion and elicits potent anti-tumor immunity. *Nature Immunology*, *19*(7), 723–732. https://doi.org/10.1038/s41590-018-0132-0

Zhao, X., Weinhold, S., Brands, J., Hejazi, M., Degistirici, Ö., Kögler, G., Meisel, R., & Uhrberg, M. (2018). NK cell development in a human stem cell niche: KIR expression occurs independently of the presence of HLA class i ligands. *Blood Advances*, *2*(19), 2452–2461. https://doi.org/10.1182/bloodadvances.2018019059

Zhou, J., Amran, F. S., Kramski, M., Angelovich, T. A., Elliott, J., Hearps, A. C., Price, P., & Jaworowski, A. (2015). An NK Cell Population Lacking FcRγ Is Expanded in Chronically Infected HIV Patients. *The Journal of Immunology*, *194*(10), 4688–4697. https://doi.org/10.4049/jimmunol.1402448

Zhou, J., Peng, H., Li, K., Qu, K., Wang, B., Wu, Y., Ye, L., Dong, Z., Wei, H., Sun, R., & Tian, Z. (2019). Liver-Resident NK Cells Control Antiviral Activity of Hepatic T Cells via the PD-1-PD-L1 Axis. *Immunity*, *50*(2), 403-417.e4. https://doi.org/10.1016/j.immuni.2018.12.024

Zhou, L., Nguyen, A. N., Sohal, D., Ying Ma, J., Pahanish, P., Gundabolu, K., Hayman, J., Chubak, A., Mo, Y., Bhagat, T. D., Das, B., Kapoun, A. M., Navas, T. A., Parmar, S., Kambhampati, S., Pellagatti, A., Braunchweig, I., Zhang, Y., Wickrema, A., … Verma, A. (2008). Inhibition of the TGF-beta receptor I kinase promotes hematopoiesis in MDS. *Blood*, *112*(8), 3434–3443. https://doi.org/10.1182/blood-2008-02-139824

Zhou, X.-M., Li, W.-Q., Wu, Y.-H., Han, L., Cao, X.-G., Yang, X.-M., Wang, H.-F., Zhao, W.-S., Zhai, W.-J., Qi, Y.-M., & Gao, Y.-F. (2018). Intrinsic Expression of Immune Checkpoint Molecule TIGIT Could Help Tumor Growth in vivo by Suppressing the Function of NK and CD8(+) T Cells. *Frontiers in Immunology*, *9*, 2821. https://doi.org/10.3389/fimmu.2018.02821

Zhu, D.-M., Dustin, M. L., Cairo, C. W., Thatte, H. S., & Golan, D. E. (2006). Mechanisms of Cellular Avidity Regulation in CD2–CD58-Mediated T Cell Adhesion. *ACS Chemical Biology*, *1*(10), 649–658. https://doi.org/10.1021/cb6002515

Zhu, H., & Kaufman, D. S. (2019). An Improved Method to Produce Clinical-Scale Natural Killer Cells from Human Pluripotent Stem Cells. *Methods in Molecular Biology (Clifton, N.J.)*, *2048*, 107–119. https://doi.org/10.1007/978-1-4939-9728-2_12

Author contribution statement

Some data included in this thesis are part of collaborative projects and were kindly provided by other lab members or study collaborators. Datasets that are not generated by me are listed below:

- Chapter 3:
    - Data on the proteomics study of the different types of stimulated NK cells was provided and analysed by Byognosys AG
- Chapter 4:
    - Data on the data for different cytotoxic capacity of TpNK cells against different targets (Figure 4.2) were provided as follows: SKOV3 and OVCAR data were provided by Xenia Charalambous (Lowdell lab, UCL); 786O and ACHN data were provided by Robert Torrance and Trinity Eales (Lowdell lab, UCL)
    - Data on the cytokine secretion of TpNK cells (Figure 4.2) were provided by Agnieszka Zubiak (Lowdell lab, UCL)
    - Data on the cytotoxicity of TpNK and CIML-NK against SKOV3 (3 out of 7 donors) (Figure 4.3) were provided by Melina Michael (Lowdell lab, UCL)
    - Data on the cytotoxicity of TpNK and CIML-NK against DU145 (Figure 4.4) were provided by Benjamin Hammond (Lowdell lab, UCL)
    - Data on the glycolysis and mitochondrial respiration of TpNK and CIML-NK cells (Figure 4.9 and Figure 4.10) were provided by Aljawharah Alrubayyi (Peppa lab, University of Oxford)
- Chapter 6:
    - The processing of samples and data analysis from the clinical trial samples was carried out by both Agnieszka Zubiak (Lowdell lab, UCL) and myself

Appendix

Conventional flow cytometry panels to immunophenotype NK cell receptors

COMMON MARKERS IN ALL PANELS

MARKER	Fluorochrome	Source	Clone	Cell Location
ZOMBIE VIABILITY DYE	Pacific Orange	BioLegend	N/A	N/A
CD56	APC/Cy7	BioLegend	HCD56	Surface
CD3	BV650	BD Biosciences	SK7	Surface

PANEL 1

MARKER	Fluorochrome	Source	Clone	Cell Location
CD16	VioBlue	Miltenyi Biotec	VEP13	Surface
NKP80	FITC	Miltenyi Biotec	4A4.D10	Surface
NKP44	PE	invitrogen	44.189	Surface
DNAM1	PE/Dazle 594	BioLegend	11A8	Surface
CD25	PE/Cy5	BioLegend	BC96	Surface
KLRG1	PE/Cy7	BioLegend	2F1	Surface
NKG2A	APC	Miltenyi Biotec	REA110	Surface

PANEL 2

MARKER	Fluorochrome	Source	Clone	Cell Location
NKP46	eFluor 450	invitrogen	9E2	Surface
PD1	BV605	BD Biosciences	EH12.1	Surface
CD57	FITC	invitrogen	TB01	Surface
NKG2D	PE	BioLegend	1D11	Surface
NKG2C	PE/Vio 615	Miltenyi Biotec	REA205	Surface
CD69	PE/Cy5	BioLegend	FN50	Surface
NKP30	PE/Cy7	BioLegend	P30-15	Surface
KIR2DS4	AF647	BD Bioscience	179315	Surface

PANEL 3

MARKER	Fluorochrome	Source	Clone	Cell Location
CXCR6	BV421	BioLegend	K041E5	Surface
TIGIT	BV605	BioLegend	A15153G	Surface
ICAM-1	FITC	ThermoFisher	RR1/1	Surface
CD62-L	PE	BioLegend	DREG-56	Surface
2B4	PE/Vio 615	Miltenyi Biotec	REA112	Surface
TIM3	PE/Cy5	BioLegend	F38-2E2	Surface
CD161	PE/Cy7	BioLegend	HP-3G10	Surface
CXCR4	APC	BioLegend	12G5	Surface

PANEL 4

MARKER	Fluorochrome	Source	Clone	Cell Location
KIR3DL1	BV421	BioLegend	DX9	Surface
LAG3	BV605	BD Biosciences	T47-530	Surface
KIR2DL3	AF488	R&D	180701	Surface
KIR2DL2/L3/S2	PE	Beckman Coulter	GL183	Surface
KIR3DL2	AF594	R&D	539304	Surface
CD94	PE/Vio 770	Miltenyi Biotec	REA113	Surface
KIR2DL1	APC	R&D	143211	Surface

Table 7.1. Conventional flow cytometry panels for NK cell phenotyping in Novocyte (Agilent)

Spectral flow cytometry panel to immunophenotype NK cell receptors

MARKER	FLUOROCHROME	SOURCE	CLONE	CELL LOCATION
LIVE/DEAD BLUE	N/A	ThermoFischer	N/A	N/A
DNAM1	BUV563	BD Biosciences	DX11	Surface
CD25	BUV661	BD Biosciences	2A3	Surface
NKP30	BV650	BD Biosciences	p30-15	Surface
CD62L	BUV805	BD Biosciences	DREG-56	Surface
NKP80	APC-Vio 770	Miltenyi Biotec	REA845	Surface
NKP44	BV786	BD Biosciences	p44-8	Surface
ICAM1	PerCP	Invitrogen	1h4	Surface
NKG2C	PE	R&D systems	134591	Surface
KIR2DL1/KIR2DS5	APC	R&D systems	143211	Surface
KIR3DL2/CD158K	APC	R&D systems	539304	Surface
GRANZYME B	Alexa Fluor 700	BD Biosciences	GB11	Intracellular
LAG3	eFluor506	Invitrogen	3D5223H	Surface
CD45RA	BUV395	BD Biosciences	5H9	Surface
CD16	BUV496	BD Biosciences	3G8	Surface
NKG2D	FITC	Biolegend	1D11	Surface
CD56	BUV737	BD Biosciences	NCAM16.2	Surface
NKP46	Pacific Blue	Biolegend	9E2	Surface
CD2	BV480	BD Biosciences	S5.2	Surface
CD3	BV510	Biolegend	SK7	Surface
CD57	BV605	BD Biosciences	NK-1	Surface
HLA-DR	BV570	Biolegend	L243	Surface
TIM-3	BV711	Biolegend	F38-2E2	Surface
LAIR-1	PerCp Cy5.5	Biolegend	NKTA25S	Surface
KLRG1	PerCp e-Fluor710	eBioscience	13F12F2	Surface
TIGIT	PE-Dazzle 594	Biolegend	A15153G	Surface
CD161	Alexa Fluor594	R&D	594	Surface
CD69	PE-Cy5	Biolegend	FN50	Surface
PDL-1	PE/Fire810	Biolegend	29E.2A3	Surface
CD38	PE/Fire700	Biolegend	517015A	Surface
HLA-DR	BUV570	Biolegend	L243	Surface
TRAIL	BV421	BD Biosciences	RIK-2	Surface

Table 7.2. Spectral flow cytometry panel for NK cell phenotyping in Aurora (Cytek)

Panel for immunophenotyping of NK cell ligands in cancer cells

MARKER	FLUOROCHROME	SOURCE	CLONE	CELL LOCATION
CD155	PE	Miltenyi Biotec	PV404.19	Surface
B7-H6	PE	R&D	875001	Surface
HLA-C	PE	BD	DT-9	Surface
PD1	BV421	Biolegend	EH12.2H7	Surface
TRAIL	BV421	BD	RIK-2	Surface
HLA-E	PE	Biolegend	3D12	Surface
ULBP1	PE	R&D	170818	Surface
ULBP3	PE	R&D	166510	Surface
ULBP2/5/6	APC	R&D	165903	Surface
CD15	PE	Biolegend	HI98	Surface
TRAIL-R1	PE	R&D	69036	Surface
TRAIL-R2	PE	R&D	71908	Surface
TRAIL-R3	PE	Biolegend	DJR3	Surface
CD122	BV421	Biolegend	TU27	Surface
LFA3	PE	Biolegend	TS2/9	Surface
HLA-A/B/C	FITC	Biolegned	W6/32	Surface
MICA/B	PE	R&D	159207	Surface

Table 7.3. Conventional flow cytometry panel for phenotyping of NK cell ligands in cancer cells in Novocyte (Agilent)

List of abstracts

Tumour-priming induces memory-like properties on NK cells: characterisation of the proteomic and receptor profile. **The 20th Meeting of the Society for Natural Immunity NK2023**; Oslo (Norway) 2023 – oral presentation

NK cell immunotherapy for cancer. **UCL Cancer Institute Annual Conference**; London (UK) 2023 – oral presentation

In Vivo Generation of Memory-like NK Cells for the Treatment of AML and Myelodysplastic Syndrome; Early Clinical Applications of INKmune™. **The American Society for Hematology conference**; New Orleans (USA) 2022 – poster presentation

In vivo tumour-induced memory-like Natural Killer cells: A phase I trial of INKmune™. **The 19th Meeting of the Society for Natural Immunity NK2022**; Florida (USA) 2022 – poster presentation

Tumour-priming generates memory-like natural killer cells with universal anti-tumour functions. **The British Society for Immunology conference**; Edinburgh (UK) 2021 – poster presentation

Tumour-priming induces human natural killer cell anti-tumoral functions through mechanisms that enhance NK cell degranulation, proliferation and motility. **The British Society for Immunology conference**; Liverpool (UK) 2019 – poster presentation